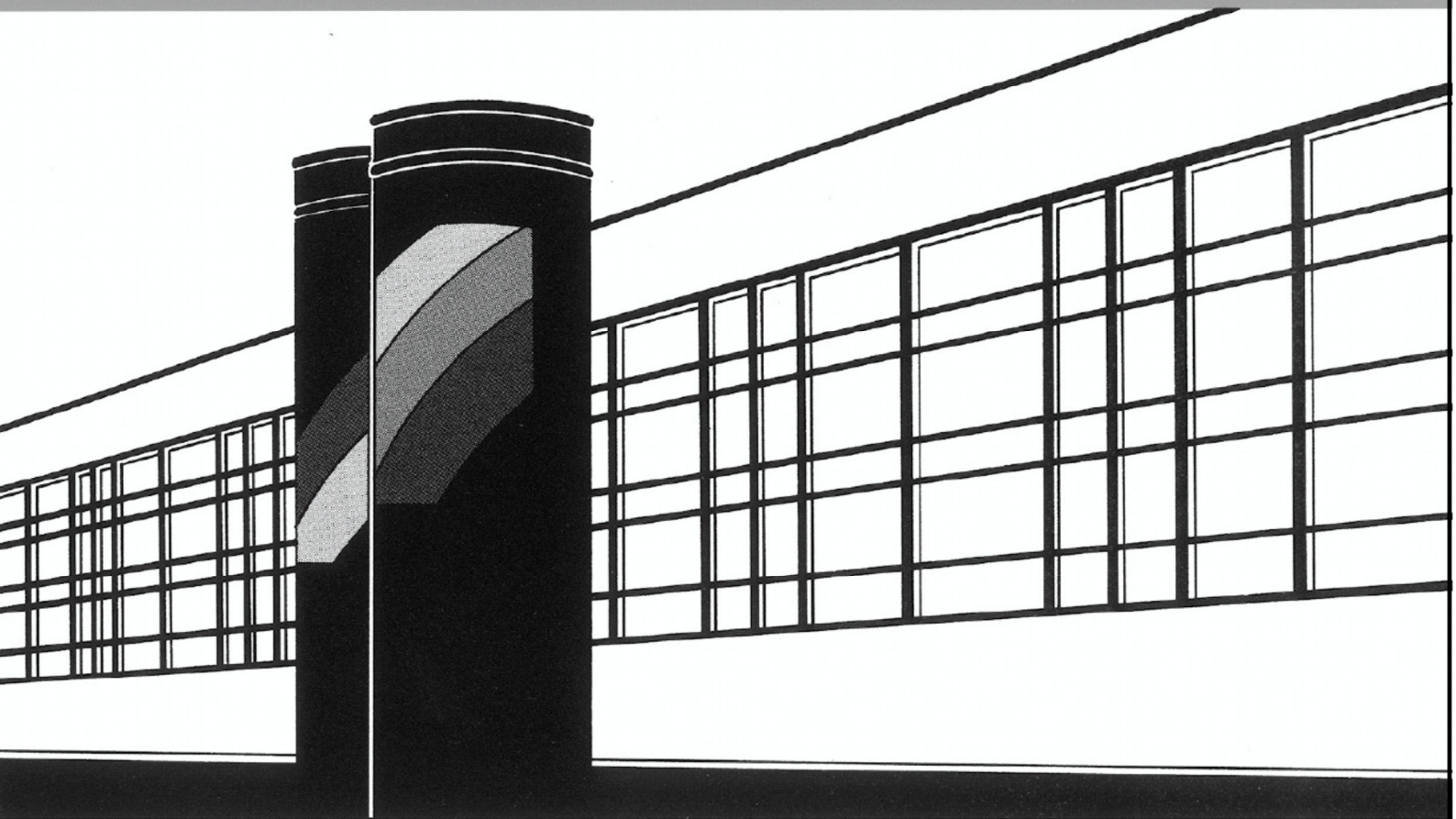


Universität Stuttgart



Institut für Wasser- und Umweltsystemmodellierung

Mitteilungen



Heft 295 Stefan Haun

Advanced Methods for a
Sustainable Sediment
Management of Reservoirs

Heft 295 **Advanced Methods for a
Sustainable Sediment
Management of Reservoirs**

von
Privatdozent
Stefan Haun, PhD

Eigenverlag des Instituts für Wasser- und Umweltsystemmodellierung
der Universität Stuttgart

D93 Advanced Methods for a Sustainable Sediment Management of Reservoirs

Habilitationsschrift, Fakultät für Bau- und Umweltingenieurwissenschaften der Universität Stuttgart

Hauptberichter: Prof. Dr.-Ing. Silke Wieprecht

Mitberichter: Prof. Nils Rüther, PhD

Prof. Dr. Robert Boes

Tag des Habilitationskolloquiums: 20. Juli 2022

Bibliografische Information der Deutschen Nationalbibliothek

Die Deutsche Nationalbibliothek verzeichnet diese Publikation in der Deutschen Nationalbibliografie; detaillierte bibliografische Daten sind im Internet über <http://www.d-nb.de> abrufbar

Haun, Stefan:

Advanced Methods for a Sustainable Sediment Management of Reservoirs,
Universität Stuttgart. - Stuttgart: Institut für Wasser- und
Umweltsystemmodellierung, 2022

(Mitteilungen Institut für Wasser- und Umweltsystemmodellierung, Universität
Stuttgart: H. 295)

Zugl.: Stuttgart, Univ., Habil., 2022

ISBN 978-3-942036-99-3

NE: Institut für Wasser- und Umweltsystemmodellierung <Stuttgart>: Mitteilungen

Gegen Vervielfältigung und Übersetzung bestehen keine Einwände, es wird lediglich um Quellenangabe gebeten.

Herausgegeben 2022 vom Eigenverlag des Instituts für Wasser- und Umweltsystemmodellierung

Druck: DCC Kästl e.K., Ostfildern

Acknowledgments

The presented scientific work gives an overview of recent developments to investigate hydro-morphological processes in reservoirs. At the same time, this work incorporates a fundamental part of my academic work during the recent years.

First of all, I would like to express my greatest appreciation to Prof. Silke Wieprecht, chair of the Department of Hydraulic Engineering and Water Resources Management. Prof. Wieprecht guided me to the University of Stuttgart to become the head of the work group Hydromorphology in 2014. This was an honor and also a huge step in my career. In 2019 I became the head of the Hydraulic laboratory at her department, which was a huge privilege. Within the last years, we have worked together in more than 20 smaller and larger research projects. I am very grateful for her valuable guidance and her support throughout these years.

Furthermore, I would like to extend my sincere thanks to Prof. Robert Boes, Director of the Laboratory for Hydraulics, Hydrology and Glaciology (VAW) at the Eidgenössische Technische Hochschule Zürich (ETH) and Prof. Nils Rüter from the Chair of Hydraulic Engineering at the Technical University of Munich (TUM), for serving as committee of my habilitation thesis. Prof. Boes and Prof. Rüter are both experts in the field of hydraulic engineering and reservoir management and have a very high reputation internationally. Hence, I am honored that they are part of the committee.

I owe particular thanks to the team of the Department of Hydraulic Engineering and Water Resources Management, which has accompanied me throughout the last years. These are in particular the colleagues from the work group Hydromorphology, led by Markus Noack and later by Sebastian Schwindt, and the colleagues from the Hydraulic Laboratory, led by Gerhard Schmid and Henning Eickhoff. Many of the presented studies have been conducted by this magnificent team. Even deeper in my memories are the discussions we had together, and which I also do not want to miss. These are (names in alphabetic order):

Alexander Bäßler, Felix Beckers, Ruslan Biserov, Margot Doucet, Steffen Hägele, Alexander Kikillus, Kaan Koca, Maximilian Kunz, Assem Mayar, Benedikt Mester, Kilian Mouris, Beatriz Negreiros, Maria Ponce, Najibullah Sadid, Marko Schmitt, Federica Scolari, Lydia Seitz, Vahid Shoarinezhad, Bojan Skodic, James Nodwell Taylor and Kristina Terheiden.

My very special thanks goes to Maria Costa Jornet, the good soul of our department and the person who has helped me to improve my language skills during the writing process.

A large part of this scientific work has been written during the projects CHARM (CHALLENGES of Reservoir Management - Meeting Environmental and Social Requirements), DIRT-X (Evaluating sediment Delivery Impacts on Reservoirs in changing climaTe and society across scales and sectors) and AMSTEL (Akkumulation von Mikroplastik in Speichern und

Stauhaltungen - Eine unterschätzte Gefahr? -). Therefore, I would like to thank the Ministry of Science, Research, and Art of the federal state of Baden-Württemberg, Germany (CHARM), the European Union, funder of AXIS, an ERA-NET initiated by JPI Climate (DIRT-X), and the Baden-Württemberg Stiftung through the Eliteprogramme for Postdocs (AMSTEL) for their financial support.

My deepest gratitude goes to my family and friends for their persistent support and encouragement throughout my academic career.

Stefan Haun,
October 3, 2021
Stuttgart, Germany

Contents

- 1 Introduction..... 1
 - 1.1 Reservoirs as backbone for a sustainable development..... 1
 - 1.2 Reservoirs as multipurpose structures – multi-stakeholder involvement 5
 - 1.3 Reservoirs from a local to a global scale 9
 - 1.4 Reservoirs as elements to disturb the continuity of watercourses..... 10
- 2 Sediments - From large scale to small scale processes 12
 - 2.1 Production zone (catchment)..... 13
 - 2.2 Transfer zone (rivers) 17
 - 2.3 Depositional zone (oceans/reservoirs)..... 19
- 3 Mechanisms of sediment transport and river morphology 24
 - 3.1 Erosion..... 25
 - 3.2 Transport 30
 - 3.2.1 Bed load transport..... 31
 - 3.2.2 Suspended load transport 32
 - 3.2.3 Factors influencing the sediment transport..... 34
 - 3.3 Deposition 36
 - 3.4 Consolidation..... 37
- 4 Reservoir sedimentation 39
 - 4.1 Loss of storage capacity..... 39
 - 4.2 The effects upstream..... 41
 - 4.3 The effects on the reservoir 43
 - 4.3.1 Reservoir management and operation 43
 - 4.3.2 A sink for pollutants and micoplastics..... 44
 - 4.4 The effects downstream..... 48
- 5 Sediment management strategies for reservoirs..... 51
 - 5.1 Accepting reservoir sedimentation 54
 - 5.2 A reduction of the quantity of inflowing sediments 55
 - 5.2.1 Ecological and structural conversation measures..... 56
 - 5.2.2 Pre- and check dams 58
 - 5.3 Avoiding settling of sediments within the reservoir 60
 - 5.3.1 Routing sediments through the reservoir 60
 - 5.3.2 Bypassing sediments around the reservoir 61

5.4	Removing accumulated sediments	63
5.4.1	Conventional mechanic dredging.....	63
5.4.2	Hydraulic dredging	65
5.4.3	Reservoir flushing	66
5.5	Increase of storage volume	72
6	Hydro-morphodynamic measurements.....	73
6.1	Bed level measurements.....	73
6.2	Bed material measurements.....	76
6.2.1	Critical shear stress measurements	79
6.3	Sediment transport measurements	84
6.3.1	Suspended sediment transport measurements.....	85
6.3.2	Bed load transport measurements.....	95
6.3.3	Direct measurement methods	96
6.3.4	Indirect measurement methods.....	98
6.3.5	Particle tracers.....	101
7	Hydro-morphodynamic numerical models	102
7.1	Basics in hydrodynamic modeling	102
7.2	Dimensionality in hydrodynamic modeling.....	106
7.2.1	2D Shallow water equations.....	106
7.2.2	1D Saint-Venant equations.....	107
7.3	Discretization in numerical modeling.....	108
7.3.1	Spatial discretization	108
7.3.2	Temporal discretization.....	109
7.4	Basics in hydro-morphodynamic modeling.....	111
7.4.1	Erosion and re-suspension of particles	111
7.4.2	Sediment transport modeling	114
7.4.3	Bed level changes within the hydro-morphodynamic model	117
8	Measurements as basis for setting up hydro-morphodynamic prediction Models.....	119
8.1	Choice of a model.....	119
8.1.1	Commercial models and models available for free.....	120
8.1.2	Based on the dimension of the model (1D – 3D)	121
8.1.3	Based on the available algorithms for hydro-morphodynamic simulations	125
8.2	Basic steps in setting up a hydro-morphodynamic prediction model.....	126

8.3	Model setup	127
8.3.1	Geometrical data (topographic and bathymetric data) and their implementation in numerical models with different dimensions	128
8.3.2	Hydraulic structures in numerical models.....	134
8.3.3	Boundary conditions for hydrodynamic and hydro-morphodynamic modeling	135
8.4	Calibration and validation	140
8.4.1	Hydrodynamic calibration and validation of numerical models	142
8.4.2	Hydro-morphodynamic calibration and validation of the numerical models	147
8.5	Sensitivity analysis.....	150
9	Hydro-morphodynamic models as basis for implementing reliable measurements	156
9.1	Selection of measurement and monitoring parameters based on sensitive domain-specific parameters	157
9.2	Selection of a spatial resolution of measurements based on results from hydro-morphodynamic numerical models	164
9.3	Selection of a temporal resolution of measurements based on results from hydro-morphodynamic numerical models	167
10	Summary and Conclusions	175
	Deutschsprachige Zusammenfassung	181
	Bibliography.....	190

List of Figures

Fig. 1: Percentage of population with access to basic drinking water services in 2015 (WHO and UNICEF, 2017).....	2
Fig. 2: Predicted changes in precipitation intensity (a) of three SRES, globally averaged (land only) for the length of the 21st century; (b) as spatial patterns of multi-model averages of changes at the end of the 20th century (adapted from Tebaldi et al., 2006).	3
Fig. 3: Maximum number of consecutive dry days (a) of three SRES, globally averaged (land only) for the length of the 21st century; (b) as spatial patterns of multi-model averages of changes at the end of the 20th century (adapted from Tebaldi et al., 2006).	3
Fig. 4: Existing hydropower dams and outlook for dams under construction or planned on a global scale (Zarfl et al., 2015; modified; Lehner et al., 2011a).....	4
Fig. 5: (a) river Isar at Krün in 2012 (photo courtesy: Daniel Skublics); (b) impounded Sylvenstein reservoir, used for recreation purposes, in 2021; (c) the former parish of Fall during the lowering of the reservoir in 2015; (d) dam heightening measures at the Sylvenstein reservoir in 2001.....	7
Fig. 6: The Kleine Kinzig reservoir, located in the Black Forest, Germany.	9
Fig. 7: Global distribution of 6,862 reservoirs with a total storage capacity of 6,197 km ³ (GRanD database; Lehner et al., 2011b).....	10
Fig. 8: Different kind of disturbances of the continuity of the watercourse as result of the construction of reservoirs (a) diversion hydropower plant in the Austrian Alps; (b) lock Eckersmühlen at the Main-Donau-waterway, Germany; (c) technical fish elevator at the weir Runserau, Austria; (d) sedimentation in a small reservoir in the Austrian Alps.	11
Fig. 9: Spatial distribution of sediment production, sediment transfer and sediment depositions in an undisturbed system (Thornberry-Ehrlich, 2020; modified).	12
Fig. 10: Global distribution of the sediment yield based on case study basin regions (Morgan, 2005).	14
Fig. 11: Tributary of the El General river in Costa Rica (a) before; (b) after a sand slide occurred; (c) reservoir sedimentation in the El General reservoir as a result of the sand slide; (d) outflow from the reservoir after the sand slide (photo courtesy: Alberto Jimenez).	15
Fig. 12: Pictures from a cross section of the Peñas Blancas, Costa Rica on (a) November 28, 2013; (b) December 19, 2013.	16
Fig. 13: Changes in the annual runoff, annual suspended sediment yield and the cumulative annual suspended sediment yield for (a) the Dnestr river, Ukraine; (b) the Kolyma River, W. Siberia as a result of anthropogenic interventions (Walling and Fang, 2003).	17
Fig. 14: Figurative example for possible river bed changes (aggradation and degradation) as function of the boundary resistance and the stream power (Blum and Törnqvist, 2000; modified).	18
Fig. 15: (a) sediment transport paths for the river Rhine (Frings et al. 2014a); (b) identified sources and sinks of sediments for the reach of the river Rhine between km 640–865 (Frings et al. 2014b)..	19
Fig. 16: (a) schematic overview of the sedimentation processes in a reservoir (Dargahi, 2012); (b) Gilbert-type delta at the reservoir of Wasserfallboden, in Austria.....	20
Fig. 17: Periodically surveyed longitudinal sections of the Solis reservoir, Switzerland (Auel and Boes, 2011).....	21

Fig. 18: Numerical model results from a physical model study with the aim to investigate the deposition mechanism of a sediment mixture. Horizontal velocities are presented for different time steps (Rashid, 2020; modified).....	23
Fig. 19: The Erosion, Transport, Deposition and Consolidation (ETDC) processes within water bodies (Klassen, 2017, modified).	24
Fig. 20: Forces acting on a single grain.....	25
Fig. 21: The Shields diagram correlating the dimensionless critical shear stress with the grain Reynolds number (Shields, 1936).....	26
Fig. 22: Relation between the dimensionless grain size and the mean velocity in accordance to Hjulström (1935, modified by Yang et al., 2019).....	27
Fig. 23: (a) principle of hiding and exposure processes, where smaller particles hide behind larger ones; (b) natural sediment mixture with a broad spectrum of different sediment sizes at the river Inn, Germany; (c) principle of river bed armoring, where an armor layer is formed out of the available bed material; (d) river bed armoring at the river Inn, Germany; (e) steps of river bed clogging with an infiltration of fine sediments in voids of the gravel bed of the river; (f) picture of outer colmation at the river Inn, Germany.	29
Fig. 24: Sketch of particle movement forms during bed load transport (Rheinheimer and Yarnell, 2017).....	32
Fig. 25: Suspended sediment load as function of the flow velocity and the sediment concentration over depth.	33
Fig. 26: Dimensionless plot of suspended load distribution (Rouse, 1937).	33
Fig. 27: Principles of flow and sediment transport in a channel bend (Rüther, 2006).	34
Fig. 28: Bed form types in alluvial channels (Simons and Richardson, 1966).	35
Fig. 29: Influence of bed roughness on the bed shear stress (Engelund and Hansen, 1967, modified).	35
Fig. 30: (a) picture of flocs, taken by the In-Line microscope Aello 7000; (b) post processed image after subsequent analysis by an image recognition software (Klassen, 2017).	37
Fig. 31: (a) pore space of uniform sediment depositions, depending on the packing arrangement of the spheres; (b) sorting coefficients for sediment mixtures, calculated based on the <i>phi</i> unit.	38
Fig. 32: Reservoir flushing operation at the Cachí reservoir, Costa Rica, in 2011 (a) during drawdown of the water level; (b) emptied reservoir during free flow conditions.	40
Fig. 33: (a) operation of the Sylvenstein reservoir during the flood event in 2005 (European Working Group on Dams and Floods, 2010); (b) annual peak discharges of the Isar River at the gauging station in Munich (European Working Group on Dams and Floods, 2010).	42
Fig. 34: Management of a year-to-year storage reservoir (Gebler et al., 2014).....	43
Fig. 35: (a) invert abrasion at Palagnedra sediment bypass tunnel in Switzerland (Boes et al., 2014; photo courtesy: Christian Auel); (b) turbine abrasion on the buckets of the Twin-Pelton turbines after release of around 15,000 tons of sediments from the Gepatsch reservoir (photo courtesy: Martin Schletterer).....	44
Fig. 36: (a) micro- and macroplastic particles sampled at the river Danube in Austria (Liedermann et al., 2018); (b) HCB contamination of sediments in the Marckolsheim reservoir at the river Rhine in Germany (Keller, 2008).	47
Fig. 37: Carbon dioxide and methane pathways in a freshwater reservoir with an anoxic hypolimnion (Kumar et al., 2011; adapted from Guerin, 2006).....	48

Fig. 38: Predicted river bed erosion downstream of the planned Stiegler’s Gorge dam, USA (Lysne et al., 2003; modified)	49
Fig. 39: (a) sediment feeding at the river Rhine downstream of the Iffezheim reservoir, Germany; (b) sediment replenishment at the river Inn in Bavaria, Germany.....	50
Fig. 40: Classification of possible sediment management strategies for reservoirs (modified after Kondolf et al., 2014).	52
Fig. 41: Reservoir sediment management measures implemented in different reservoirs with different relative reservoir size (CAP/MAF) and different relative amounts of inflowing sediments (CAP/MAS) (Annandale, 2013).	54
Fig. 42: (a) Finstertal reservoir in Austria during an operational draw down; (b) Schwarzenbach reservoir in Germany with lowered water level as a result of pump storage operation.....	55
Fig. 43: Conceptual overview of soil conservation measures within a catchment.	56
Fig. 44: (a) local deforestation in Manaus, Brazil, resulting in higher surface runoff and subsequent soil erosion; (b) ongoing soil erosion as consequence of precipitation and a limited soil cover.....	57
Fig. 45: (a) Orchard terraces for farming on La Gomera Island, Spain; (b) hillslope with developed rill network at Gramsh, Albania, in 2021.....	57
Fig. 46: Pre-dam of the Kleine Kinzig reservoir, Germany (a) view from downstream; (b) view into the pre-dam.	59
Fig. 47: Check-dam of the Schallerbach, Austria (a) view from downstream (photo courtesy: Silke Wieprecht); (b) view into the check-dam (photo courtesy: Kilian Mouris).	59
Fig. 48: (a) Angostura reservoir in Costa Rica with a lowered water level for routing sediments coming from the upstream located Cachí reservoir in (view from the dam upstream); (b) sketch of a turbidity current, travelling along the bed of the reservoir (Chamoun et al., 2016).	61
Fig. 49: (a) sketch of a sediment bypass tunnel system with the tunnel intake at the head of the reservoir (Auel & Boes, 2011); (b) outlet of the Solis sediment bypass tunnel, Switzerland (photo courtesy: Christian Auel).	62
Fig. 50: (a) bucket dredge in operation at the Schönau reservoir in Austria in front of the turbine inlets (Harb, 2013); (b) dry excavation at El General reservoir, Costa Rica (photo courtesy: Alberto Jimenez).....	65
Fig. 51: Cutter suction dredge, installed at the Peñas Blancas reservoir in Costa Rica.	66
Fig. 52: (a) suction head used for syphoning (photo courtesy: Sedicon AS); (b) slurry pipe of the syphon dredge over the spillway crest at El General, Costa Rica (photo courtesy: Sedicon AS).....	66
Fig. 53: Flushing with full drawdown at the Angostura reservoir, Costa Rica in 2010 (a) view from upstream to the intake, bottom outlet and spillways; (b) view from the dam in upstream direction.	67
Fig. 54: Coordinated flushing of the Dashidaira and the Unazuki reservoirs in the Kurobe river in 2006 (a) precipitation; (b, c) inflow and outflow hydrographs and reservoir stage for Dashidaira and the Unazuki reservoirs, respectively; (d) suspended sediment concentrations downstream of both reservoirs (Kondolf et al., 2014).	69
Fig. 55: Flushing with partial drawdown at the Peñas Blancas reservoir, Costa Rica in 2013 (a) view from the spillway upstream; (b) view from the head of the reservoir towards the dam.	70
Fig. 56: (a) monitoring of the downstream suspended sediment concentrations during the flushing of the Fischeing reservoir, Austria, in 2012; (b) ecological monitoring downstream of the Peñas Blancas reservoir during flushing with partial drawdown in 2013.....	71

Fig. 57: Dam heightening at the Sylvenstein reservoir also as preventative measure against possible impacts of climate change (a) view from upstream; (b) view from downstream.....	72
Fig. 58: Bathymetric survey of the Angostura reservoir (a) on September 22, 2010 before the flushing; (b) on November 17, 2010 after the flushing.....	74
Fig. 59: (a) bathymetric survey of the Wasserfallboden reservoir in 2010; (b) measurement points of the bed levels of the Angostura reservoir, obtained by sonar measurements in 2010.....	75
Fig. 60: (a) Van Veen grabber used at the Geesthacht reservoir at the river Elbe, Germany, in April 2013; (b) sampling with an excavator at the Peñas Blancas reservoir, Costa Rica, in 2014; (c) freeze-core sampling in the residual stretch of the the Brixentaler Ache, Austria, in 2015; (d) core sampling with the Frahm-lot at lake Brombach in 2017.	78
Fig. 61: (a) Vane shear (Geonor Inc., 2021) and Torvane Soiltest (Humboldt, 2021) instruments (photo courtesy: Bojan Skodic); (b) the straight benthic flow through flume “EROMOB”, developed at the University of Stuttgart (photo courtesy: Bojan Skodic).	80
Fig. 62: Schematic view of (a) the gamma-ray densitometer; (b) the SETEG flume, constructed at the University of Stuttgart (Beckers et al., 2018).	83
Fig. 63: (a) subdivision of the investigated area of a sediment core, obtained from the Schwarzenbach reservoir in Germany into regions of interest (ROIs) for 3 investigated layers; (b) mean sediment deepening for a subdivision of 4 ROIs for 3 investigated layers (4cm, 8cm, 12cm).	84
Fig. 64: (a) taking a gravimetric sample downstream of the Fischening reservoir, Austria, during a reservoir flushing operation in 2012 by using a bucket sampler; (b) acoustic backscatter signal distribution along a transect at the Peñas Blancas reservoir, Costa Rica.	86
Fig. 65: (a) recommended distribution of single measurements over the cross section for an acquisition of the suspended sediment matter in rivers; (b) P61 A1 suspended sediment sampler, which enables an isokinetic correct sampling of single point samples, operated during the reservoir drawdown of the Gepatsch reservoir in Austria in 2016 (Hauer et al., 2017).	87
Fig. 66: (a) USD-49 depth integrated sampler downstream of the Peñas Blancas reservoir in Costa Rica during reservoir flushing in 2013; (b) depth integrated sampler “Cuxi” at the Geesthacht reservoir at the river Elbe, Germany in 2013.	88
Fig. 67: (a) water sampler with horizontally located in- and outflow, used at the Bächental reservoir in Austria in 2016; (b) water sampler with vertically located in- and outflow (type Kemmerer, photo courtesy: Bojan Skodic).	89
Fig. 68: (a) Malvern Mastersizer 2000 (Malvern Instruments Ltd, 2021) to obtain PSD for sediments in the range of 0.01 – 10,000 μm (photo courtesy: Bojan Skodic); (b) “Imhoff-cone” samples taken downstream of the Bächental reservoir in Austria in 2015.	89
Fig. 69: (a) OBS-3 sensor with automatic wiper to prevent from biofouling (photo courtesy: Bojan Skodic); (b) OBS-3 sensor installed downstream of the Bächental reservoir in Austria in 2015.	91
Fig. 70: (a) LISST-ST sensor, used for obtaining suspended sediment concentrations from a sample taken from the Angostura reservoir after a flood event in 2012; (b) LISST-SL applied at the Sandillal reservoir in Costa Rica in 2013.	92
Fig. 71: Measured ABS by a RDI RiverRay for a transect in the Peñas Blancas reservoir in Costa Rica on (a) November 28, 2013; (b) December 19, 2013.....	94
Fig. 72: Vibrating Tube Density Meter installed in the powerhouse of (a) the Fieschertal hydropower plant in 2015 (photo courtesy: David Felix); (b) the Kaunertal hydropower plant in 2016 (photo courtesy: Martin Schletterer).	95

Fig. 73: (a) pit trap installed at the Schöttlbach, Austria to collect sediments and to determine bed load transport (photo courtesy: Gabriele Harb); (b) bed load trap at the Schöttlbach, Austria, placed downstream of an artificially built cross section (photo courtesy: Gabriele Harb).	97
Fig. 74: (a) Helley-Smith sampler used to sample bed load transport at the head of the Bodendorf reservoir, Austria (photo courtesy: Gabriele Harb); (b) bed load trap array at the Riedbach in Switzerland (Schneider et al., 2016).	98
Fig. 75: (a) moving ADCP measurements at the Bodendorf reservoir in Austria in 2010 with a Sontek M9 ADCP; (b) with a clear indication of bed load transport.	99
Fig. 76: steel plates, equipped with a geophone installed at the Schöttlbach, Austria, with an installed bed load trap (photo courtesy: Gabriele Harb) (a) view in downstream direction; (b) view in upstream direction.	100
Fig. 77: (a) tracer stones used at the river Rhone to investigate the occurring bed shear stress and bed load transport during a eco-friendly flushing in 2017; (b) remote Frequency Identification (RFID) transponder inserted into a tracer stone, implemented at the Schöttlbach in Austria (photo courtesy: Gabriele Harb).	101
Fig. 78: Overview on the discretization procedure for time dependent calculations with an (a) explicit time discretization; (b) implicit time discretization.	111
Fig. 79: Simulated bed level changes in the Gebidem reservoir, Switzerland, for the 2015 calibration season (June to September), by using monthly-averaged water levels. Bed level changes and maximum bed levels, which evolved in the simulations, are shaded in grey (Ehrbar et al., 2018).	122
Fig. 80: Comparison of the simulation results of a reservoir flushing operation conducted in the Bodendorf reservoir in 2004, with the obtained digital terrain model.....	123
Fig. 81: Flushing simulation of the Angostura reservoir in Costa Rica (a) initial grid for the flushing simulations in close vicinity of the dam, spillways and the intake; (b) adaptive grid during the full drawdown stage of the flushing with a formed flushing channel; (c) simulated bed levels at the end of the flushing simulation (Haun et al., 2012a).	125
Fig. 82: Terrestrial survey along the Bodendorf reservoir, Austria, in 2010 (a) total station located at a fixed point on a bridge; (b) rover for taking points along the shore of the reservoir.....	129
Fig. 83: Point cloud of a lake, obtained with a RIEGL VQ-840-G Laser Measurement Systems and displayed by <i>Potree</i> , a viewer for LIDAR data sets (RIEGL, 2020; Schuetz, 2020).	129
Fig. 84: Survey of the Murgtalsperre Kirschbaumwasen by an UAS in 2013 and a subsequent analysis with SfM (photo courtesy: I AM HYDRO).	130
Fig. 85: Bathymetry of the Schwarzenbach reservoir, located in the Black Forest in Germany, obtained by single beam echo sounder in 2016.	131
Fig. 86: Point cloud of a lake, obtained with a RIEGL VQ-840-G Laser Measurement System and displayed by <i>Potree</i> , a viewer for LIDAR data sets (RIEGL, 2020; Schuetz, 2020).	131
Fig. 87: (a) cross section of a Wadi in the United Arab Emirates, implemented in the model <i>Basement</i> ; (b) sketch of the orthogonal, structured and non-adaptive grid, used in <i>Flow-3D</i> . (Haun et al., 2011); (c) sketch of the non-orthogonal, unstructured and adaptive grid of the Schwarzenbach reservoir, setup in <i>SSIIM</i> (Mouris et al., 2018).	133
Fig. 88: (a) geometrically correctly implemented Zollhaus weir, located at the river Saalach, into the 2D hydro-morphological model <i>Hydro_FT</i> ; (b) 2D computational grid in <i>Basement</i> , with an implemented inner boundary condition at the weir (Vetsch et al., 2011).	135

Fig. 89: Overview on different hydrological and sedimentological boundary conditions for numerical modeling of hydro-morphodynamics (Haun and Wieprecht, 2017).....	136
Fig. 90: (a) gauging station at the Reventazòn river in Costa Rica, upstream of the Angostura reservoir; (b) inflow time series for the numerical simulation of reservoir sedimentation (weekly averaged values for discharge and water levels); (c) concentration-discharge relationship developed for the Reventazòn river in Costa Rica, upstream of the Angostura reservoir; (d) suspended sediment sampling at the Reventazòn river in Costa Rica, downstream of the Angostura reservoir.	137
Fig. 91: (a) bed material sample obtained from the bed surface of the Angostura reservoir in Costa Rica in 2010; (b) Van Veen grabber for obtaining bed surface samples; (c) Vane shear measurements of critical bed shear stresses of the cohesive bed material; (d) results of the sieve analysis of eight samples, taken along the thalweg of the Angostura reservoir.	139
Fig. 92: (a) water level fixations at the intake of the Peñas Blancas reservoir in Costa Rica during pressure flushing; (b) outflow of the Peñas Blancas reservoir in Costa Rica through the bottom outlets; (c) water level and outflow of the Bodendorf reservoir in Austria during the flushing operation in 2004.	140
Fig. 93: Flood inundation map from calibration simulations of the 1987 Goldersbach flood (center), including important hydraulic structures of the implemented flood retention reservoir (Doucet et al., 2018; modified).	143
Fig. 94: Flow velocities within the reservoir of the Leoben run-of river power plant (Austria) based on (a) ADCP measurements; (b) the numerical simulation with <i>Telemac-2D</i> for the same discharge (Harb et al., 2012).....	145
Fig. 95: Simulated depth averaged flow velocities in the Schwarzenbach reservoir in Germany, simulated with the numerical program <i>SSIIM 2</i> by (a) using a first order upwind scheme (power law scheme); (b) a second order upwind scheme (Mouris et al., 2018).	146
Fig. 96: Simulated depth averaged flow velocities in the Schwarzenbach reservoir in Germany with the numerical program <i>SSIIM 2</i> by (a) using a first order upwind scheme (power law scheme); (b) the same upwind scheme, but taking wind forces into account (Mouris et al., 2018).	147
Fig. 97: (a) grid for the flushing simulation of the Bodendorf reservoir with 15,358 cells at the beginning of the flushing simulation; (b) bed geometry of the reservoir after the flushing (measured); (c) bed geometry of the reservoir after the flushing (simulated); (d) measured and simulated bed level changes with different bed-load transport formulae in a cross section of the reservoir.	149
Fig. 98: Depth averaged suspended sediment concentrations at the Angostura reservoir in Costa Rica (a) simulated with the numerical model <i>SSIIM 2</i> ; (b) measured with a LISST-SL device at discrete points (Haun et al., 2013a).	150
Fig. 99: Final bed levels of the experiments (left) compared to the simulation results (right) for (a) the lozenge-shaped reservoir; (b) the hexagonal-shaped reservoir; all dimensions are given in meters (Shoarinezhad et al., 2021).....	152
Fig. 100: Final bed levels of experiments and the numerical simulations at four cross sections along the shallow reservoir for different fall velocities (Purnomo, 2018).....	154
Fig. 101: Evolution volume difference of the reference simulation subtracted by the outcomes of the respective parameter variations for model-specific parameters (left) and domain-specific parameters (right) (Beckers et al., 2020b; modified).	159
Fig. 102: Suspended sediment distribution of the finest grain fraction $d = 5.09 \mu\text{m}$ as function of the water level and the inflowing water volume (Mouris et al., 2018).....	160

Fig. 103: Sediment thicknesses after the simulated flushing operations with different drawdown targets of the water level (a) maximum operational level; (b) minimum operation level; (c) free flow conditions (Saam et al. 2019).	161
Fig. 104: Occurring geotechnical bank failure during the drawdown of the Bodendorf reservoir, simulated by the 3D hydro-morphodynamic model <i>SSIIM 2</i> (Olsen and Haun, 2018).	163
Fig. 105: Range of possible morphodynamic bed level changes along a longitudinal section of the river Saalach, as a result of a combination of sensitive parameters (Beckers et al., 2016).	165
Fig. 106: Simulated bed level changes (bed movements) as a result of the flushing operation with full drawdown (erosion in red and depositions in green) as well as four recommended spots for further field investigations (red circles).	166
Fig. 107: Geotechnical bank failure (blue) and subsequent depositions (red) during the flushing of the Bodendorf reservoir in Austria for a simulation with (a) default values; (b) a decrease of the cohesion from 1,000 Pa to 500 Pa; (c) an increase of the cohesion from 1,000 Pa to 10,000 Pa (Olsen and Haun, 2020; modified).	167
Fig. 108: (a) selected hydrograph from 2005 considering different threshold discharges to investigate the initiation of bed load transport (Beckers et al., 2016); (b) bed load transport rates for a linearly increasing flow hydrograph at six different river sections along the river Saalach (Beckers et al., 2016).	170
Fig. 109: Simulated cumulated sediment outflow from the Schwarzenbach reservoir during a reservoir flushing with full drawdown for different varied parameters.	172
Fig. 110: (a) measured bed levels of the Bodendorf reservoir in Austria in 2006 after the flushing operation (Badura, 2007); (b) measured thalweg of the Bodendorf reservoir for the years 1980, 1994, 1996, 1999 and 2002.	174

List of Tables

Table 1: Mean annual sedimentation rates depending on the region of the reservoirs.....	40
Table 2: Boundary conditions for Meyer-Peter-Müller's and van Rijn's bed load transport equations (U.S. Army Corps of Engineers, 1998).	116
Table 3: Overview on terrain parameters and their impact on modelled water levels when changing the Strickler coefficients by increments of $1 \text{ m}^{1/3}/\text{s}$	151
Table 4: List of selected parameters and their sensitivity on the model results, investigated during a sensitivity analysis.	153
Table 5: Overview of parameters investigated during the sensitivity analysis as well as reference values of the parameters and varied ranges during the sensitivity analysis.	158
Table 6: Sensitivity analysis of parameters related to the properties of bed sediments and the inflow discharge during the flushing simulation (domain-specific parameters).....	162
Table 7: Sensitivity analysis of soil mechanic parameters used in the model to calculate the lowering of the embankment, as a result of geotechnical bank failures (selected parameters).	164

Abbreviations

Abbreviation	Denotation
1D	one-dimensional
2D	two-dimensional
3D	three-dimensional
ABS	acoustic backscatter signal
ADCP	acoustic Doppler current profile
ADV	acoustic Doppler velocimetry
BS	corrected backscatter signal
C-factor	ground cover condition factor
CAP	reservoir volume
CCD	charge-coupled device
CEC	cation exchange capacity
CFD	computational fluid dynamics
CHL-a	chlorophyll-a
DEM	digital elevation model
DGPS	differential global positioning system
DI	directivity index (equipment)
DNS	direct numerical simulations
DT	detection Threshold (equipment)
E	32-element data vector
E-modulus	coefficient of elasticity
GHG	greenhouse gases
GML	Gauss-Marquardt-Levenberg
GPS	global positioning system
GR	total roughness
G-modulus	shear modulus
HPP	hydro power plant
ICOLD	International Commission On Large Dams
K	scattering property kernel matrix
K-factor	erodibility factor
KR	grain roughness
LDA	laser Doppler anemometer
LES	large eddy simulations
LIDAR	light detection and ranging
LISST	Laser In-Situ Scattering and Transmissometry instrument
LS-factor	combined slope length and gradient factor
MAF	mean annual flow into the reservoir
MAS	mean annual volume of sediment flowing
MPM	Meyer-Peter and Müller bed load equation
MPP	microplastic particles
N	volume distribution
NL	noise Level (medium, equipment)
OBS	optical backscatter signal
P- factor	conservation practice factor
PAL	active layer thickness
PEST	parameter estimation tool
PHOTOSED	PHOTOgrammetric Sediment Erosion Detection
PSD	particle size distribution

R-factor	rainfall-runoff factor
RANS	Reynolds-averaged Navier Stokes equations
RFID	Remote frequency identification
ROI	region of interest
RTK	real time kinetic
RUSLE	Revised Universal Soil Loss Equation
SCFG	acceleration factor
SETEG	Stroemungskanal zur Ermittlung der tiefenabhaengigen Erosionsstabilitaet von Gewaessersedimenten
SfM	structure from motion
SL	stream lined
SLE	source level (equipment)
SNR	signal-to-noise ratio
Sonar	sound navigation and ranging
SRES	The Special Report on Emissions Scenarios Particle Size Distribution
SSC	suspended sediment concentrations
SSIIM	Sediment Simulation In Intakes with Multiblock option
SWE	shallow water equations
TL	transmission loss (medium)
TOC	total organic carbon
TS	target strength (target)
UAS	Unmanned Aircraft System
UN	United Nations
USLE	Universal Soil Loss Equation
VOF	Volume of Fluid method
WC	water content

Nomenclature

Symbol	Definition	Dimension
a	height of the center of the bed cell	[m]
C	Courant number	[-]
$C_{bed,i}$	concentration of the suspended load at the bed for the i^{th} fraction	[kg/m ³]
C_{max}	maximum Courant number	[-]
C_S	sediment concentration	[kg/m ³]
C_{Si}	sediment concentration for the i^{th} sediment fraction	[kg/m ³]
c_1	a proportionality constant equal to 0.19	[-]
d	diameter of a particle (grain-size)	[m]
d_i	particle diameter of the i^{th} sediment fraction	[m]
d_{50}	particle diameter representing the 50% cumulative percentile value	[m]
d_{80}	particle diameter representing the 80% cumulative percentile value	[m]
d_{90}	particle diameter representing the 90% cumulative percentile value	[m]
g	acceleration of gravity	[m/s ²]
h	water depth	[m]
k	turbulent kinetic energy	[m ² /s ²]
k_s	total roughness	[m]
k_{St}	Manning-Strickler coefficient	[m ^{1/3} /s]
l	path length	[m]
N	number of particle size fractions of the non-uniform sediment mixture	[-]
n	spatial dimension	[-]
n_p	bed porosity	[%]
m	a constant and equal to 0.6	[-]
P	dynamic pressure	[N/m ²]
p	instantaneous pressure	[N/m ²]
Q	discharge	[m ³ /s]
q	the x- component of specific flow	[m ³ /s]
$q_{b,i}$	transport rate of the total bed load per unit width	[kg/s]
r	the y- component of specific flow	[m ³ /s]
Re_*	grain Reynolds number	[-]
S	friction slope (gravity term)	[m/m]
S_f	slope of the bed (friction term)	[m/m]
t	time	[s]
u^*	shear velocity	[m/s]
v	flow velocity	[m/s]
v_{bed}	velocity in the bed cell	[m/s]
v_c	critical flow velocity	[m/s]
v_i	averaged velocity	[m/s]
v_x	flow velocity in x-direction	[m/s]
v_y	flow velocity in y-direction	[m/s]
v_z	flow velocity in z-direction	[m/s]
\bar{v}	mean component of the flow velocity	[m/s]
v'	velocity fluctuation component	[m/s]
w_s	settling velocity of a particle	[m/s]
$w_{s,i}$	settling velocity of the specific particle size	[m/s]
y	distance between the bed cell and the wall	[m]
z_b	bottom elevation	[m]
A	water flow direction	[°]

α	angle between the flow direction and a line normal to the bed plane	[°]
δ_{ij}	Kronecker delta	[-]
Δ	bed-form height	[m]
Δt	time step	[s]
ε	diffusion coefficient	[m ² /s]
η_i	correction factor	[-]
θ	an empirical factor	[-]
κ	Von Kármán constant	[-]
μ	dynamic viscosity	[N*s/m ²]
ϑ_t	turbulent viscosity (eddy viscosity)	[m ² /s]
ρ	fluid density	[kg/m ³]
ρ_s	density of sediment particles	[kg/m ³]
ρ_w	density of water	[kg/m ³]
τ_0	actual shear stress (on the bed)	[N/m ²]
τ_c	critical shear stress	[N/m ²]
$\tau_{c,i}$	critical shear stress for d_i ,	[N/m ²]
τ_{ii}	turbulent normal stresses	[N/m ²]
τ_{ij}	turbulent shear stresses	[N/m ²]
τ_*	dimensionless critical shear stress	[-]
τ'	bed shear stresses as result of skin friction	[N/m ²]
τ''	bed shear stresses as result of the bed forms	[N/m ²]
ϕ	function of the angle of the slope perpendicular to the water flow direction	[°]
ρ	slope angle	[°]
ω	specific rate of dissipation	[m ² /s]

1 INTRODUCTION

Within this chapter an overview on the importance of reservoirs for providing water and energy, but also as structures to enable the further development of our society, is given. A special focus is thereby set on the expected global change, which needs to be taken into account for a sustainable development of resources in the future. However, also insight into problems, connected with the construction and the management of reservoirs, is given within this chapter. Besides that, a brief overview on the spatial distribution of reservoirs and an overview on the use and operation purposes of reservoirs is presented.

1.1 *Reservoirs as backbone for a sustainable development*

The world's population is growing and is projected to reach 9.8 billion in 2050 and 11.2 billion in 2100, according to the United Nations (UN; 2017). It is expected that half of this population growth will happen in only nine countries, namely: India, Nigeria, the Democratic Republic of the Congo, Pakistan, Ethiopia, the United Republic of Tanzania, the United States of America, Uganda and Indonesia (United Nations, 2017).

This population growth represents a huge challenge to governments in implementing the Agenda for Sustainable Development launched by the UN. Among the 17 goals set by the United Nations to transform our world in a way to achieve a better and more sustainable future for all, the points clean water, sanitation, zero hunger as well as affordable and clean energy are listed (United Nations, 2017). This shows the importance of water for human life, human health and human wealth.

However, the availability of water is not uniformly distributed around the world and in many countries water in general and clean water in particular is not available on demand. Figure 1 gives an overview on the percentage of population with access to basic drinking water services (WHO and UNICEF, 2017). The figure shows that especially regions in Africa and South-East Asia are affected by a shortage of fresh water. The storage of water in reservoirs is as a consequence an important aspect and often the only way to secure a sustainable supply of drinking water, for the production of food and generation of clean energy. A study presented by the International Energy Agency (IEA) in 2007 assumed that worldwide around 20 % of the cultivated land is irrigated and approx. 17 % of the total electricity production is coming from hydropower. As a result of the climate change or the decision of many governments around the world to increase the amount of "green" energy, these numbers will increase in the future. The importance of reservoirs for a sustainable water supply is also shown by Mankin et al. (2015), who analyzed data from 97 river basins. Within these basins around 2 billion people depend on water from snow melt, which is stored in reservoirs, to ensure a sustainable fresh water supply also during the dry season.

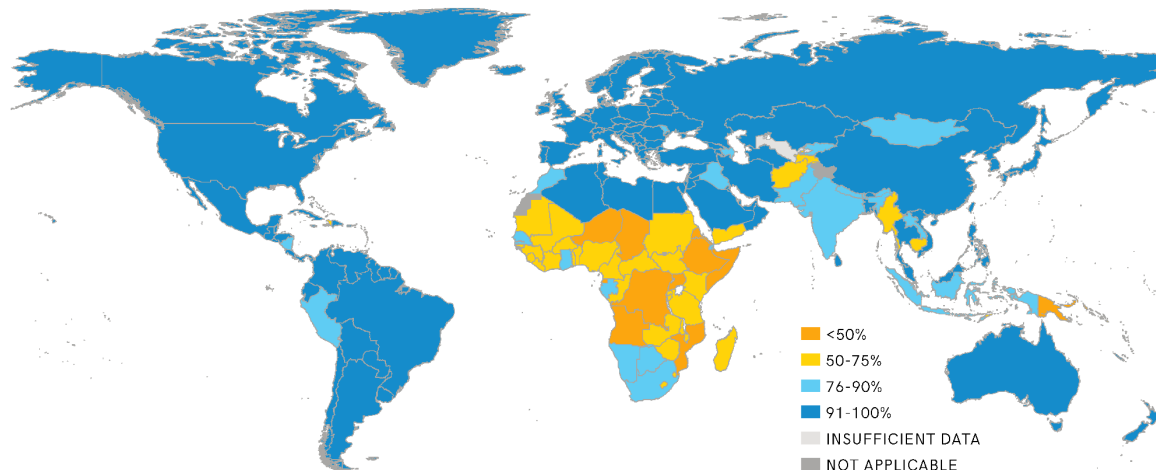


Fig. 1: Percentage of population with access to basic drinking water services in 2015 (WHO and UNICEF, 2017).

Many indicators show that our climate will alter within the next decades. Tebaldi et al. (2006) analyzed in their work historical and future simulations of ten different indicators, which were derived from an ensemble of nine atmosphere-ocean global general circulation models under a range of different emission scenarios. Two examples are presented in this thesis, namely the predicted changes in precipitation intensity and the maximum number of consecutive dry days. Precipitation, and especially the precipitation intensity, is an important factor regarding water resources management, but also regarding soil erosion and the production of sediments. The maximum number of consecutive dry days, on the other side, is an indicator for the necessity to store water on a daily, monthly, seasonal or even a year-to-year basis, to ensure fresh water supply also during dry periods.

Figure 2a shows the predicted future trend for the precipitation intensity (globally averaged and land only) based on three future SRES emission scenarios: A2 (higher), A1B (mid-range) and B1 (lower) (The Special Report on Emissions Scenarios; Nakicenovic and Swart, 2000). Even if the nine global general circulation models show differences in predictions of future precipitation intensities, a clear increase can be seen for all models and for all modelled scenarios (Tebaldi et al., 2006), which is in accordance to the findings of the Intergovernmental Panel on Climate Change (IPCC, 2007) and a study published by Plate (1993). Changes in the spatial patterns of rain, as a result of multi-model averages of change under A1B (represents mid-range changes) and as difference between two 20-year averages (2080–2099 minus 1980–1999) are presented in figure 2b (adapted from Tebaldi et al., 2006). The figure illustrates that increases in precipitation intensities are globally predicted, but with different magnitudes for different regions.

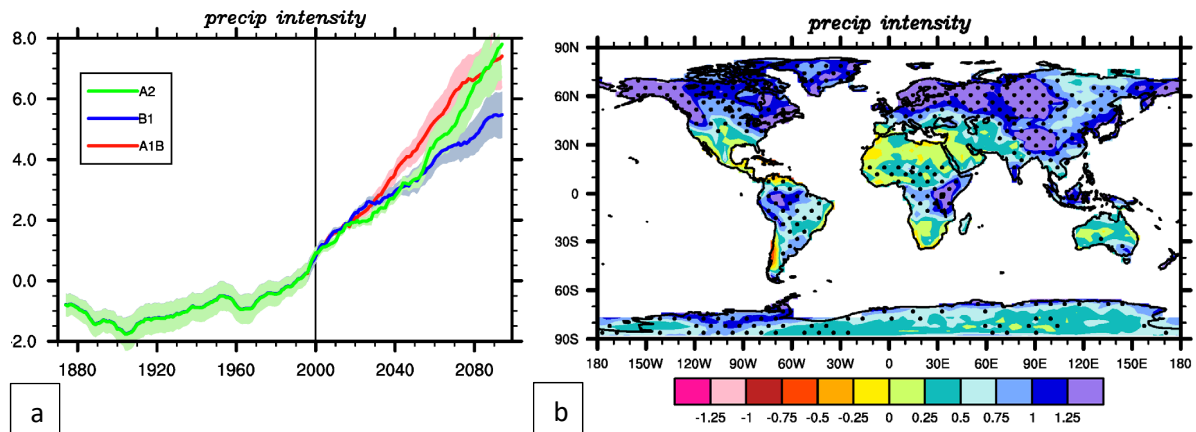


Fig. 2: Predicted changes in precipitation intensity (a) of three SRES, globally averaged (land only) for the length of the 21st century; (b) as spatial patterns of multi-model averages of changes at the end of the 20th century (adapted from Tebaldi et al., 2006).

Figure 3a shows the predicted maximum number of consecutive dry days (globally averaged and land only) based on three SRES (The Special Report on Emissions Scenarios; Nakicenovic and Swart, 2000). An increasing trend can be seen for all models, even if scenario B1 (lower scenario) shows only a small increase. Figure 3b shows again non-uniform changes in the spatial distribution of the maximum number of consecutive dry days (Tebaldi et al., 2006).

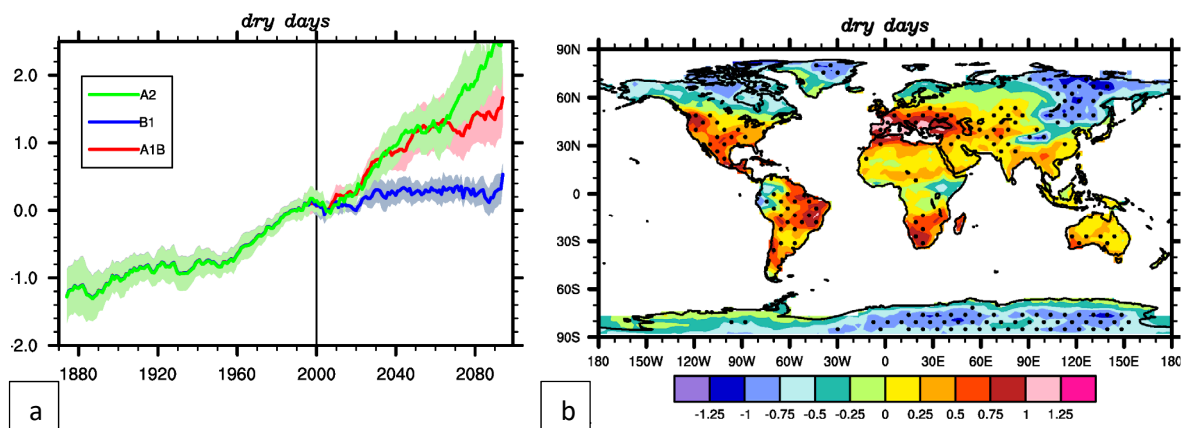


Fig. 3: Maximum number of consecutive dry days (a) of three SRES, globally averaged (land only) for the length of the 21st century; (b) as spatial patterns of multi-model averages of changes at the end of the 20th century (adapted from Tebaldi et al., 2006).

Due to the unequal occurrence of water, the irregularly distributed population growth and changes in the climate within the next years, water availability will be a stressor in several regions in the world, but especially in Africa and South-East Asia, where a major part of the population has no direct access to basic drinking water services (see figure 1). As a consequence, several research projects try to assess the impact of global climate change on reservoirs to optimize their future management. An example is the project DIRT-X (Evaluating sediment Delivery Impacts on Reservoirs in changing climate and society across scales and sectors). DIRT-X addresses the question of how the changing climate and socioeconomic

conditions influence water reservoirs and the services they provide through integration of existing climate services, shared socioeconomic pathways framework, impact models, and close cooperation with stakeholders from the relevant sectors (Bartosova et al., 2021).

Although reservoirs are already important technical structures in many countries of the world, they may become even more important during the next decades. Consequently, reservoirs are the backbone of a sustainable development of our society.

As a direct result of the challenges we face, the decreasing trend in constructing reservoirs has stopped (Gleick, 2003) and almost a boom in the construction of new reservoirs has started. Figure 4 gives an overview on the recent trend in reservoir construction and the number of reservoirs in the process of planning (Zarfl et al., 2015).

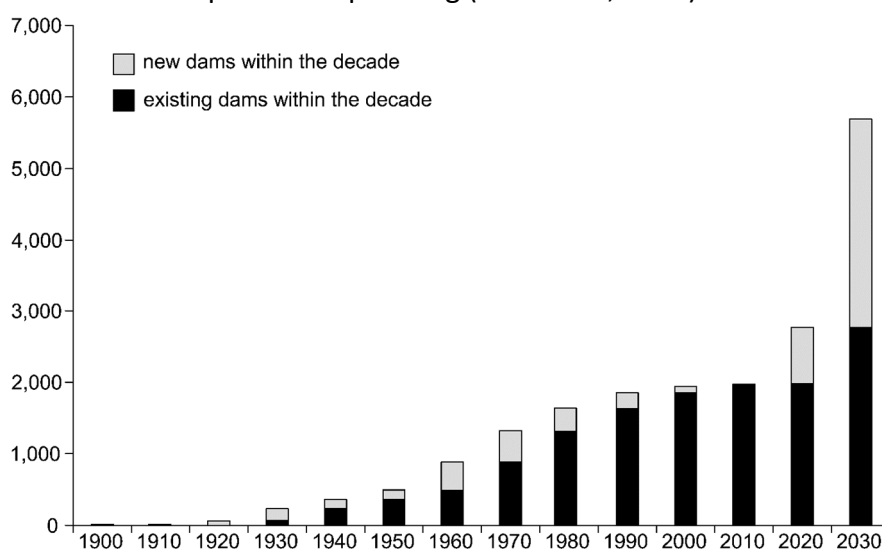


Fig. 4: Existing hydropower dams and outlook for dams under construction or planned on a global scale (Zarfl et al., 2015; modified; Lehner et al., 2011a).

To ensure the required amount of storage capacity for the future, not only the construction of new reservoirs is required, but also a reliable, efficient and flexible management of already existing reservoirs is essential for a sustainable development (IAHS, 1998). Reliable in a way that a secure water supply is guaranteed throughout, efficient in a way that the life-time of the reservoir can be prolonged, and flexible in a way that the reservoir operation can be changed in long, medium but also short term.

When planning and operating reservoirs several aspects are important, such as the technical point of view (construction, maintenance, safety, sediment management), economics, the impact on the society and one of the most important aspects, the effects on the environment. All these aspects have to be taken into account in an early stage of the design phase have to be monitored and may be adapted during the life-time of the reservoir for a safe and sustainable reservoir operation.

Within this thesis the focus is set on the influence of reservoir sedimentation as a limitation factor for a sustainable reservoir management. To implement sediment management strategies in a sustainable way, an understanding of hydromorphology in reservoirs,

possibilities to measure and monitor sediment transport and reservoir sedimentation, knowledge on capabilities to model these processes and the possibility to predict the success and the consequences of management strategies are necessary. The thesis is structured in a way that first a general introduction on reservoirs and the need for a sustainable reservoir management is presented in chapter one. Chapter two explains the origin of sediments and the transport paths from the production zone to the depositional zone. Chapter two describes processes on a large scale, while chapter three gives a brief overview on the mechanisms of sediment transport on a small scale. In chapter four the challenges associated with the construction of reservoirs and subsequent sediment depositions are described, followed by a description of management strategies, to obtain a sustainable sediment management in reservoirs, in chapter five. These management solutions can be implemented as standalone solutions or in combination. Even if the engineering point of view is set as focus of this thesis, also a brief overview on related topics, such as environmental aspects, will be given. In chapter six and seven the topics sediment transport measurements and numerical methods are covered, where different measurement methods as well as modeling approaches are presented. Finally, a hybrid modeling approach is presented (numerical modeling in combination with in-situ measurements), which may provide the reservoir designer and later the operator with a method to understand ongoing processes, to investigate reservoir sedimentation and to obtain sustainable management strategies. On one side, a special focus is set on the question of how sediment-related measurements can support hydro-morphological models, and on the other side how measurements can be planned and optimized, based on the results of numerical models. Finally, conclusions and an outlook are drawn.

1.2 *Reservoirs as multipurpose structures – multi-stakeholder involvement*

Dams are human-made structures with the aim to use the associated artificial lakes (reservoirs) to serve for one or more purposes. The construction of dams has a long history. In Europe the oldest and still active reservoirs are the Cornalbo, Proserpina and El Belcial reservoirs in Spain, which were built in the 2nd century (EEA, 2018). Compared to these old reservoirs, especially during the last two centuries, the size with respect to height of the dam and the storage volume has increased. In addition, the number of constructed reservoirs increased. There are currently about 7,000 large dams and thousands of smaller dams in operation, in Europe only (EEA, 2018), whereas Spain is the country with most large dams (approx. 1,000) (ICOLD, 2020).

These reservoirs provide important, but also vulnerable services such as:

- (i) Drinking water supply,
- (ii) irrigation of agricultural land,
- (iii) flood protection and drought mitigation,
- (iv) groundwater enrichment,
- (v) stabilization of stream and river beds,
- (vi) production of hydroelectricity,
- (vii) making water bodies navigable,
- (viii) sedimentation basins,
- (ix) recreation and leisure (e.g., bathing or fishing).

Regarding ICOLD (2009) the main share of reservoirs serves for irrigation (approx. 47 %), hydropower (approx. 22 %), drinking water (approx. 12 %) and flood protection (approx. 9 %). However, in many cases reservoirs are multipurpose structures, serving for several objectives. Examples for multipurpose dams are manifold. Within this thesis one example, the Sylvenstein reservoir in Bavaria, Germany, was selected to show the combination of different objectives. In addition, this example illustrates the impact on the society as well as historical changes in operation plans, which were adapted during the lifetime of the reservoir several times.

The river Isar (figure 5a), with a catchment area of 8,964.57 km², originates in the Hinterautal, Austria, and drains after 292.26 km into the Danube, five kilometers south of Deggendorf, Germany (Bayerisches Landesamt für Umwelt, 2016). Due to the planned construction of water transition ways to the Walchensee power plant in Germany and the Achensee power plant in Austria, approved by the US American occupant forces in 1948, fears appeared that the discharge of the river Isar would drop, resulting in dried out river beds during the summer (Wasserwirtschaftsamt Weilheim, 2009). The legislative assembly of the Bavarian state (Bayerischer Landtag) claimed as a consequence a minimum flow (residual flow) within the river Isar valley to avoid such problems during the summer. This was the starting point of the Sylvenstein reservoir project, which should guarantee a minimum flow (Wasserwirtschaftsamt Weilheim, 2009) within the river Isar. Further, it was requested that the reservoir should also act as a flood protection structure for the downstream Isar valley (Isartal) with the two main cities of Bad Tölz and Munich. An additional demand was the incorporation of a small hydropower plant to generate peak-hydroelectricity in winter (Winterspitzenstrom). Hence, the reservoir volume was designed based on flood protection purposes, residual flow issues, hydropower production as well as based on sediment transport issues, which were already taken into account during the planning phase (Wasserwirtschaftsamt Weilheim, 2009). Finally, it was also pointed out that an additional focus had to be set on homeland and nature protection.

A first document regarding the Sylvenstein reservoir project was already available in 1949, including 16 different pre-feasibility studies. The selected project alternative, which was built between 1954 and 1959, had a dam height of 45 meters, a reservoir area at maximum operation level of 6 km², a reservoir volume of 104 Mm³, where 40 Mm³ would be used for residual flow purposes, 59 Mm³ for flood protection purposes and 5 Mm³ as dead storage for reservoir sedimentation, and a catchment area of approx. 1,100 km² (Lang & Overhoff, 2018). In 1959 also the first hydro power plant started its operation. Modifications of the hydraulic structures in 1970 made it possible to produce in average yearly 18,000 MWh of electricity with a maximum discharge of 15 m³/s (Wasserwirtschaftsamt Weilheim, 2009).

The Sylvenstein reservoir serves nowadays also as one of the most beautiful recreation areas in Bavaria, used by locals as well as by tourists (figure 5b). The municipality of Lenggries, where the Sylvenstein reservoir is located, published in its statistics a number of overnight stays in 2016 of 184,463 (Bayerisches Landesamt für Statistik, 2017).

The construction of the Sylvenstein reservoir shows also the societal impact through the construction of the reservoir. The parish of Fall was completely impounded and had to be re-settled during the construction of the reservoir in 1957 (Wasserwirtschaftsamt Weilheim, 2009). Around 20 houses, including custom office, police station, smithy, forestry office, chapel and school were removed before the impoundment (figure 5c).



Fig. 5: (a) river Isar at Krün in 2012 (photo courtesy: Daniel Skublics); (b) impounded Sylvenstein reservoir, used for recreation purposes, in 2021; (c) the former parish of Fall during the lowering of the reservoir in 2015; (d) dam heightening measures at the Sylvenstein reservoir in 2001.

Several retrofitting measures were conducted at the Sylvenstein dam and reservoir between 1994 and 2001, such as the enhancement of the old spillways, the implementation of an underground sealing via a new grout curtain or a new monitoring system for the dam. The dam itself was heightened by 3 m to further increase the flood protection of the Isar valley (Lang & Overhoff, 2018; figure 5d). The additionally constructed 20 Mm³ are also used by a new implemented hydropower plant, which has been in operation since 2000 and increases the total standard production capacity to a value of 25,000 MWh/year (Wasserwirtschaftsamt Weilheim, 2009).

Usually, the different aspects and objectives of a reservoir are already taken into account when a new reservoir is being planned, as it was also the case of the Sylvenstein reservoir in Germany. However, several planned and constructed projects in many countries in the world show that the construction of reservoirs leads to tensions between people and even states and may result even to a launch of threats (Dahir, 2018; Wein, 2017). There are two main reasons for such circumstances. The first reason is that water is stored in the reservoir and will be abstracted from the river for other purposes, such as agriculture, and will be no longer released to the downstream river section in a natural way. An example is the construction of the Grand Ethiopian Renaissance Dam at the Blue Nile in Ethiopia, resulting in an escalating dispute between Egypt, Sudan and Ethiopia (Water Technology, 2018). The second reason are disparate views of different stakeholder groups, especially when decisions are based on economic interests only. But also the plan to change the operation/main use of an already existing reservoir, or to increase its capacity, either by refurbishment or by construction of an additional reservoir, as example for pump storage operation, may lead to such protests of single stakeholder groups. An example is the development of the pump storage power plant Atdorf, Germany, where the project was stopped after an evaluation of the results of a public hearing. The energy provider Energie Baden-Württemberg AG (EnBW) stated that even if the public hearing did not raise concerns regarding the project's prospects of receiving approval, the in-depth examination revealed that the subsequent stages of the project would require significant cost- and time-intensive work, especially a comprehensive examination of the ecological mapping and the environmental compensation concept (EnBW, 2017).

Within socio-science many studies exist regarding the construction of reservoirs dealing with stakeholder and conflict analysis. An extended study with the title: "Multipurpose water uses of hydropower reservoirs: The SHARE concept" was presented by Branche (2017). The focus within this study is set on multipurpose hydropower reservoirs, which are designed to provide services beyond electricity generation. Therefore, the objectives water quantity management, ecosystem services, economic growth and local livelihoods are taken into account. Such a broad spectrum of objectives leads inevitably to tensions and conflicts, even if they are often complementary. Within the study by Branche (2017) the questions: (i) how competition among multipurpose water uses of hydropower reservoirs can be minimized as well as (ii) how

appropriate governance could be set to allow coordinated and integrated water uses management are covered. Within the concept a sustainable approach for all users, higher efficiency among all sectors, adaptability for all solutions, river basin perspectives as well as engaging all stakeholders are incorporated. Hence, a multi-stakeholder approach with governments, banks, non-governmental organizations (NGOs), international organizations, hydropower utilities, and other sectors was implemented, taking in total twelve case studies into account.

1.3 *Reservoirs from a local to a global scale*

The number of reservoirs constructed in the federal state of Baden-Württemberg, Germany, was determined within the CHARM project (CHALLENGES of Reservoir Management) during the years 2016-2021. Within Baden-Württemberg a total number of 247 reservoirs, with a volume of more than 0.1 Mio m³, were recorded, where most of the reservoirs were built for flood protection (206) and hydropower production (20). However, several of them serve as multipurpose structures, such as the Kleine Kinzig reservoir, which serves for drinking water supply, flood protection, release of minimum flow and the production of hydroelectricity (Zweckverband Wasserversorgung Kleine Kinzig, 2018; figure 6).



Fig. 6: The Kleine Kinzig reservoir, located in the Black Forest, Germany.

Such a detailed investigation does not exist for most countries. It is therefore not possible to give an exact number of dams and reservoirs worldwide, especially due to the fact that a multitude of reservoirs are “small” reservoirs and are not recorded in existing databases. One goal of the International Commission On Large Dams (ICOLD) was to setup the so called *World Register of Dams*, where detailed information of dams, submitted by the member states, is incorporated. Within this register, more than 58,000 dams are included (ICOLD, 2020). By definition of ICOLD: large dams are dams with a height of more than 15 meters or dams with a height of 5-15 meters, but only if they impound more than 3 Mm³. Based on the definition of large dams, drawn by ICOLD, 64 large dams exist in the federal state of Baden-Württemberg, Germany. Another free database is presented by Lehner et al. (2011b), including 6,862 records of reservoirs with a storage capacity of more than 100 Mm³. Within

the GRanD database, dams are geospatially referenced. Figure 7 presents reservoirs having a total storage volume of 6,197 km³.

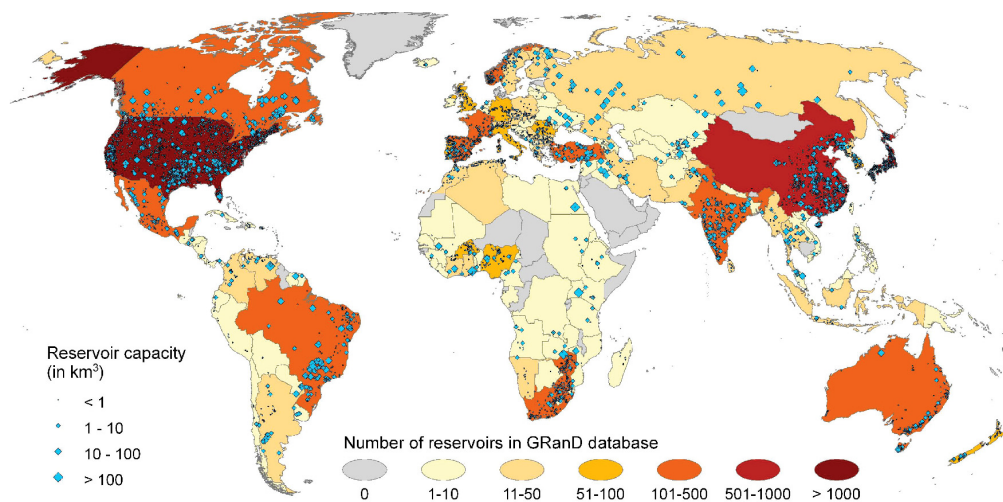


Fig. 7: Global distribution of 6,862 reservoirs with a total storage capacity of 6,197 km³ (GRanD database; Lehner et al., 2011b).

1.4 *Reservoirs as elements to disturb the continuity of watercourses*

Although the construction of reservoirs has a large number of positive effects for our society, it has to be mentioned that the construction of reservoirs is an anthropogenic intervention in the natural river course and leads inevitably to a disturbance of the watercourse continuity. This disturbance happens in terms of:

- (i) water, e.g., in case of diversion hydropower plants where only a residual flow is left in the origin river bed (figure 8a),
- (ii) navigation, where special technical measures, such as locks, have to be constructed to make the waterway navigable for vessels (figure 8b),
- (iii) ecological consistency, where special measures, such as fish ladders or fish elevators, are necessary to enable fish migration (figure 8c) and
- (iv) sediment transport, with negative effects on the up- and downstream river reach (figure 8d).

Depending on the location of the reservoir some points have a higher importance compared to others. For instance, in headwater reservoirs navigation is not a problem.

Although each of the mentioned disturbances would be worth to be discussed by itself. In this work the focus is set only on the disturbance of the sediment continuity (figure 8d), as a result of the construction of reservoirs. Small and large reservoirs will be taken into account because reservoir sedimentation may create problems for both, independently if they are located at the main stream (run-of river) or in higher altitudes to store water on e.g., a year-to-year basis.



Fig. 8: Different kind of disturbances of the continuity of the watercourse as result of the construction of reservoirs (a) diversion hydropower plant in the Austrian Alps; (b) lock Eckersmühlen at the Main-Donau-waterway, Germany; (c) technical fish elevator at the weir Runserau, Austria; (d) sedimentation in a small reservoir in the Austrian Alps.

Sediments are usually transported by rivers to the oceans and will start to descent as a result of the changes in the hydraulic boundaries and will finally deposit. When a river discharges into a reservoir a similar settling of the transported particles occurs as a result of a decrease in flow velocities, bed shear stresses and turbulences. Based on different factors, such as the shape of the reservoir, the hydrology, the quantity and quality of sediments, reservoir sedimentation will occur. Vörösmarty et al. (1997) and Vörösmarty et al. (2003) estimated that around 40 % of the global river discharge is intercepted by large reservoirs. By taking the theoretical sediment trapping efficiency into account, this will lead to the assumption that 25-30 % of the yearly occurring sediment flux is trapped behind dams (4 to 5 Gt of sediment per year). Syvitski et al. (2005) estimated that 20 % of sediments on a global scale and 12 % of sediments on an European scale are being retained in reservoirs. Uncertainties in these estimations are a result of the lack of measured data, where gaps exist especially for smaller rivers and creeks.

2 SEDIMENTS - FROM LARGE SCALE TO SMALL SCALE PROCESSES

*Reservoir sedimentation is often called “a symptom” of a sick patient; in this case a disturbed system. Hence, many researchers state that reservoir management is only a task to treat the symptom, but not the sickness. To understand the interlinkages between the sickness and the symptoms first an overview about the origin of sediments, sediment transport in water bodies and sediments in reservoirs (based on a river scaling concept) is given within this chapter. On the basis of this overview it is further possible to identify locations where countermeasures can be conducted to deal with the sickness of a disturbed river course and the symptom of reservoir sedimentation. For a more detailed overview and to gain deeper insight the book *Understanding Earth (8th Edition)* by Grotzinger and Jordan (2020) is recommended literature.*

To understand reservoir sedimentation and the processes behind it, it is important to have a holistic overview on sediment production, sediment transfer and deposition processes in reservoirs, which is only possible by looking on the processes on a catchment scale. In literature this spatial distribution is often called “sediment cycle”. However, this wording is not correct because sediments do not follow a cycle, such as the “hydrological cycle”. The reason is that sediments, which have deposited in the ocean, have reached their final destination. However, in general it is possible to distinguish between three zones: the production zone, the transfer zone and the depositional zone (figure 9). To investigate these different zones in detail researchers from the fields of geology and hydrology, geography, hydraulic engineering as well as oceanography are necessary due to the different involved processes and the different time scales, which have to be taken into account.

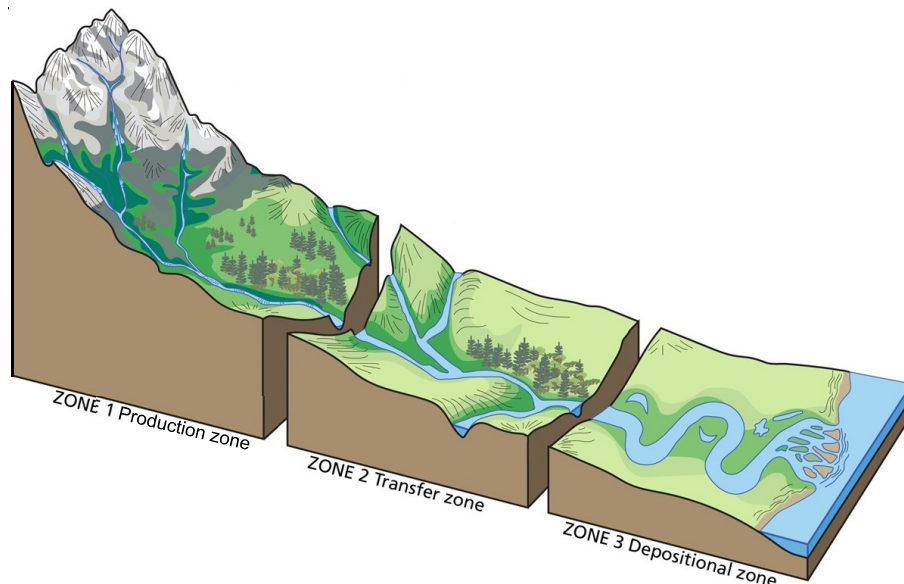


Fig. 9: Spatial distribution of sediment production, sediment transfer and sediment depositions in an undisturbed system (Thornberry-Ehrlich, 2020; modified).

2.1 *Production zone (catchment)*

Sediments are produced in the catchment by denudation processes, which are long-term processes, leading to a reduction in elevation as well as changes in landforms and landscapes. Denudation includes mechanical, biological and chemical processes of weathering, erosion and mass wasting. Within this chapter the focus is set on erosion processes within the catchment.

Erosion processes can be subdivided by the driving factors of the process, such as erosion by water (fluvial system), ice (glacial system), wind (aeolian system) and by the sea in coastal areas (littoral system). It has to be considered that for fluvial systems erosion can be distinguished between stream erosion, which results in a deepening of river beds and which is mostly linear, and erosion in terms of denudation processes within the catchment, which is understood as aerial erosion (soil erosion). This chapter focuses on the second type, erosion as result of denudation processes. Erosion types are sheet, rill and gully erosion, where gully erosion is often an extent from rill erosion.

The most important factors for erosion are geology, topography, soil characteristics and soil cover (degree and type of vegetation), human impacts (land use practice and land use changes) as well as hydrological and climatic conditions (White and Bettess, 1984). To classify a catchment with respect to the production of sediments, the sediment yield is often used as an indicator. The sediment yield, with the unit $t/km^2/yr$, is defined as the amount of sediments measured at the intersection to the transfer zone and divided by the catchment area given on a yearly basis. However, when using the sediment yield as number to characterize the catchment, attention has to be drawn on how the number for the sediment yield is estimated as well as on the fact that the sediment yield is often influenced by a high spatial but also temporal variation (e.g., due to dry and wet years or a production of sediments in pulses, such as sand slides). In addition, the sediment yield may be different from the amount of sediments, which are produced by surface erosion within the catchment, as not all mobilized sediments actually reach the basin outlet because parts of the eroded sediments will deposit in intermediate areas as soon as gravity and drag forces are no longer sufficient to move these sediments. This fact has to be taken into account when the sediment yield ratio is obtained, which describes the amount of sediments, which are produced by denudation processes, compared to the sediment yield, means the sediments, which reach the outflow of the catchment. The denudation rate and the sediment yield are in small and steep catchments almost equal, while in large catchments, with gentle slopes, a larger amount of sediments deposit and the numbers may differ from each other (e.g., Lu et al., 2005; Walling and Webb, 1983).

Due to the multitude of influencing factors, the sediment yield is not uniformly distributed around the world and depends strongly on the given boundary conditions of the region. Figure 10 gives an overview on the worldwide distribution of the sediment yield. The data were

obtained by Walling and Webb (1983) and adapted by Morgan (2005). However, such large scale maps have to be treated with care, as in most cases such maps are generated by interpolation of measurements from single catchments.



Fig. 10: Global distribution of the sediment yield based on case study basin regions (Morgan, 2005).

Although Figure 10 gives an indication on the global distribution of sediment yield, at this point it has to be mentioned that sediment yield may vary strongly, means in an order of magnitude, from basin to basin, even if catchments are located in close vicinity. Morris and Fan (1998) presented for instance values ranging from 100 up to 2,000 t/km²/y in tropical countries like Costa Rica or Puerto Rico. Attention should be given to the fact that the number for the sediment yield is given on an annual basis. Especially in regions with a distinctive wet and dry season (also monsoon season) the main sediment production may happen only within a few months of the year. Also processes like mass wasting or sand slides may change the sediment yield by several orders of magnitude. Figure 11 shows two pictures from the El General river, located at the Atlantic side of Costa Rica. A large landslide, as a result of heavy precipitation, caused a sudden increase in the sediment yield. The amount of sediments produced as a result of this slide is in the range of approximately 15 times the annual sediment load, resulting in a negative effect on the further downstream located El General hydropower plant, located in Sarapiquí, Costa Rica (Alberto Jimenez, personal communication, January 19, 2020).

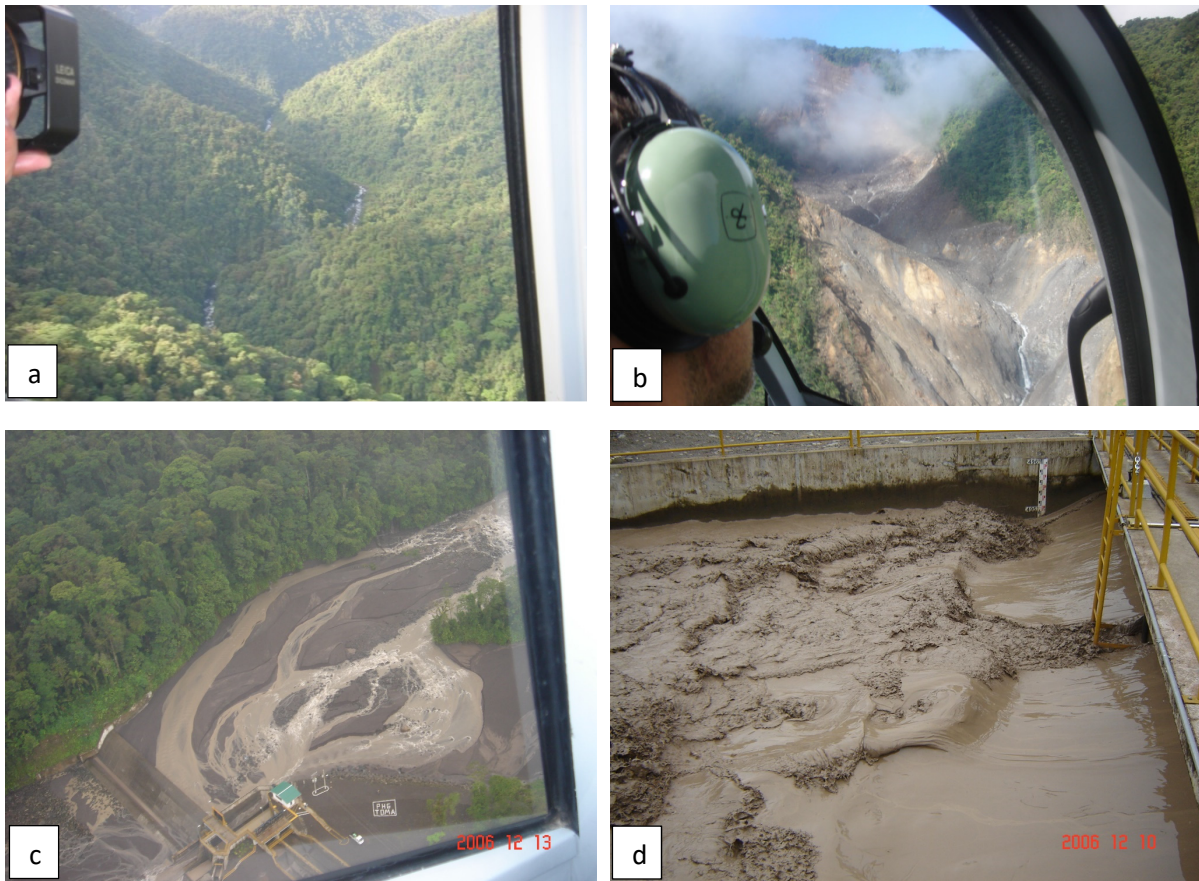


Fig. 11: Tributary of the El General river in Costa Rica (a) before; (b) after a sand slide occurred; (c) reservoir sedimentation in the El General reservoir as a result of the sand slide; (d) outflow from the reservoir after the sand slide (photo courtesy: Alberto Jimenez).

Another important point are the measurements of the sediment outflow from the catchment, used to obtain the sediment yield. Not only events, such as landslides, change the magnitude of sediment loads, but also historical, inter-annual (i.e., effects of seasonality and floods) and over annual timescales (i.e., differences between dry and wet years) are important to consider (e.g., Pomázi & Baranya, 2020; Mead et al., 2012; Mossa, 1996). In addition, it has to be taken into account that during the rising limb of flood events higher concentrations of sediment transport occur, as a result of the clockwise hysteresis effect (Bogen, 1980). Figure 12 shows two pictures of the same cross section of the Peñas Blancas reservoir in Costa Rica, which was investigated several times during field investigations in 2013 and 2014 (Haun and Lizano, 2018; 2014). The fluxes of suspended sediments within this cross section, located almost at the head of the reservoir, were evaluated at the end of the rainy season in 2013 (Haun and Lizano, 2016; 2015). On November 28, 2013, a discharge of $142 \text{ m}^3/\text{s}$ and a subsequent suspended sediment flux of $41.23 \text{ kg}/\text{s}$ was measured (Figure 12a), whereas on December 19, 2013, a discharge of $24 \text{ m}^3/\text{s}$ and a subsequent suspended sediment transport of $0.93 \text{ kg}/\text{s}$ was evaluated (Figure 12b). These values show that the suspended sediment fluxes even during a small flood event were 40 times higher as during low flow conditions.

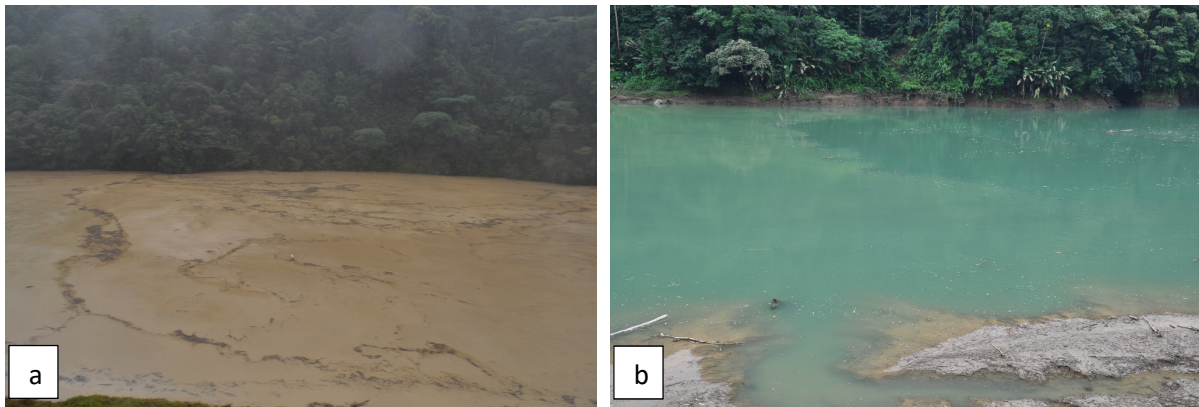


Fig. 12: Pictures from a cross section of the Peñas Blancas, Costa Rica on (a) November 28, 2013; (b) December 19, 2013.

In addition, climate change and human interactions may change the sediment yield on a long term. Precipitation events will occur more frequently and with a higher intensity (see figure 2a), which will necessarily lead to an increase in the production of sediments in the catchment due to soil erosion and will consequently lead to high sediment laden flows in rivers (Zheng et al., 2014).

However, climate change may lead into shifts in the hydrological parameters as well as in changes in growth rates and subsequently in changes in sediment delivery (e.g., Plate, 1993; Walling and Fang, 2003). On the other side, the predicted population growth will result in severe anthropogenic influences within the catchments, such as deforestation to gain resources and to increase the areas of farmland for food production. Walling and Webb (1989) illustrated the influence of anthropogenic measures within the catchment with changing numbers for soil erosion. Based on this study the annual loss in agricultural land due to soil erosion is 3 million hectares and the annual loss in soil is approximately 33 billion tons, which represent 0.7 percent of the available soil resources. Morris and Fan (1998) presented values for the erosion rates of forest, croplands and harvested forest of 8, 1,680 and 4,200 t/km²/y, respectively, just to get an impression on the impacts of land use changes. Walling and Fang (2003) presented in a study an increase in annual runoff and measured annual suspended sediment yield for the Dnestr river at Sambur in the Ukraine (1950-1983), as a result of forest clearance in the headwaters of the catchment during the mid to late 1960s (figure 13a) and the resulting expansion of agriculture. Another example, also presented by Walling and Fang (2003), is the Kolyma River at Ust Srednekansk, W. Siberia (1941-1988), where an increase in the annual suspended sediment yield can be discovered as a result of land disturbance (widespread gold mining) within the basin, although the annual runoff remains almost constant (figure 13b).

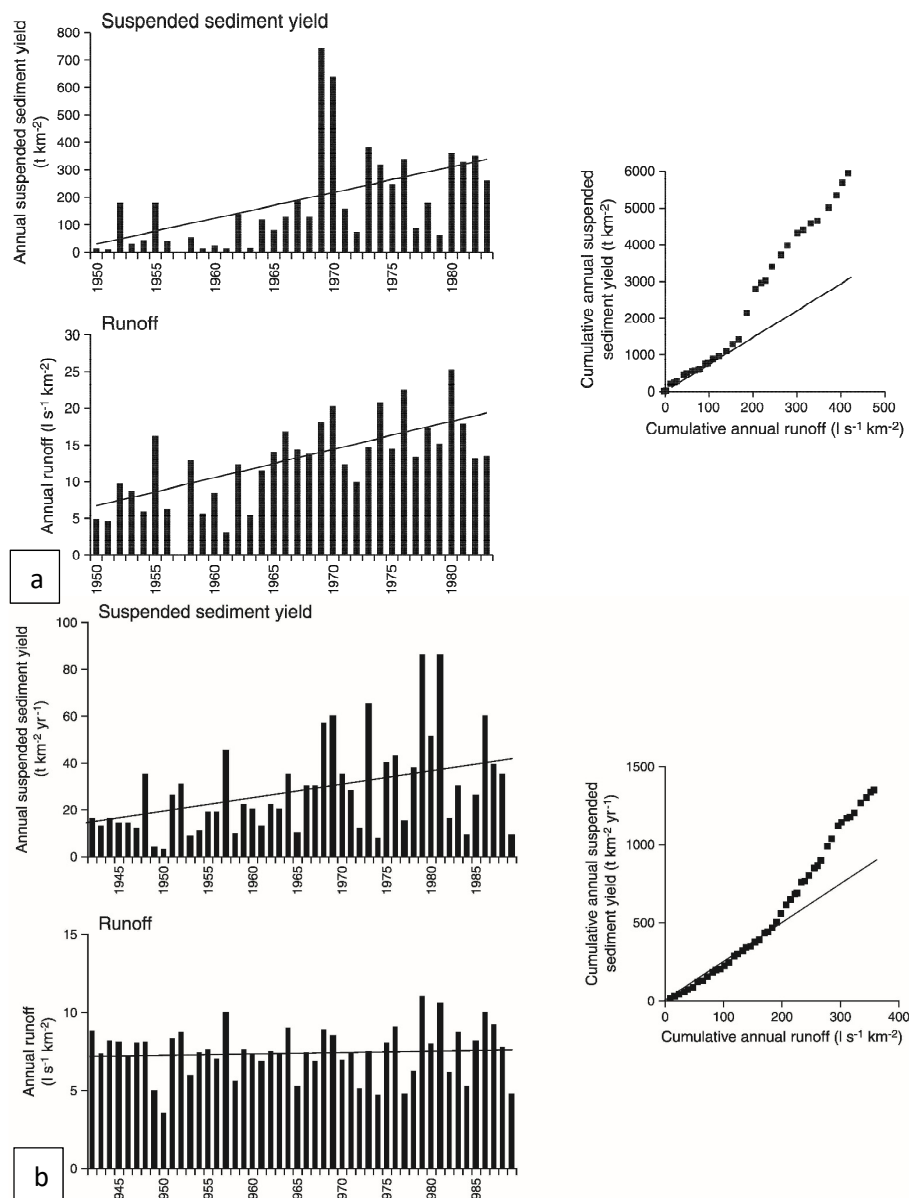


Fig. 13: Changes in the annual runoff, annual suspended sediment yield and the cumulative annual suspended sediment yield for (a) the Dnestr river, Ukraine; (b) the Kolyma River, W. Siberia as a result of anthropogenic interventions (Walling and Fang, 2003).

2.2 Transfer zone (rivers)

In a second stage, sediments produced within the basin are transported by rivers towards the oceans. It is assumed that around 20×10^9 tons of sediments are transported in rivers per year, 80 - 90 % of which are transported in suspension (Milliman and Syvitski, 1992; Walling and Webb, 1996; Milliman and Farnsworth, 2011). It has to be noted that this value is only an assumption due to a lack in monitoring of suspended sediment as well as bed load transport, which are missing for most of the rivers worldwide. In addition, it should also be mentioned here, that this value is an average for all rivers and streams worldwide. Rivers in Scandinavia for instance do not transport high amounts of sediments due to strong bedrock formations

and due to the fact that the last ice age removed in large parts the upper soil cover. On the contrary high sediment-laden flows may occur, as it is e.g. the case in the main stream of the Yellow River, with measured sediment transport of up to 941 kg/m^3 and about $1,500 \text{ kg/m}^3$ in the tributaries (Fan and Morris, 1992).

From a morphological point of view natural rivers are characterized by a long-term balance between sedimentation and erosion processes (dynamic equilibrium), which means that degradation and aggradation processes may occur on a short term, but without changing the long-term equilibrium conditions of the river. These temporal changes are a result of the stream power (often also known as the transport capacity) of the river on one side and on the other side by the provided boundary resistance. The stream power of the river depends mainly on the discharge and the slope of the river, whereas provided boundary resistance is a result of the sediment supply and the sediment size (Lane, 1955). Figure 14 shows figurative the interaction between stream power and boundary resistance.

In case a river is not in dynamic equilibrium conditions anymore, a distinction can be made between supply-limited-systems, where the sediment supply is smaller than the transport capacity of the river, and transport-limited-systems, where the sediment supply exceeds the transport capacity of the watercourse. In case of a supply-limited-system bed degradation will occur, where in cases of a transport-limited-system, river bed aggradation will happen.

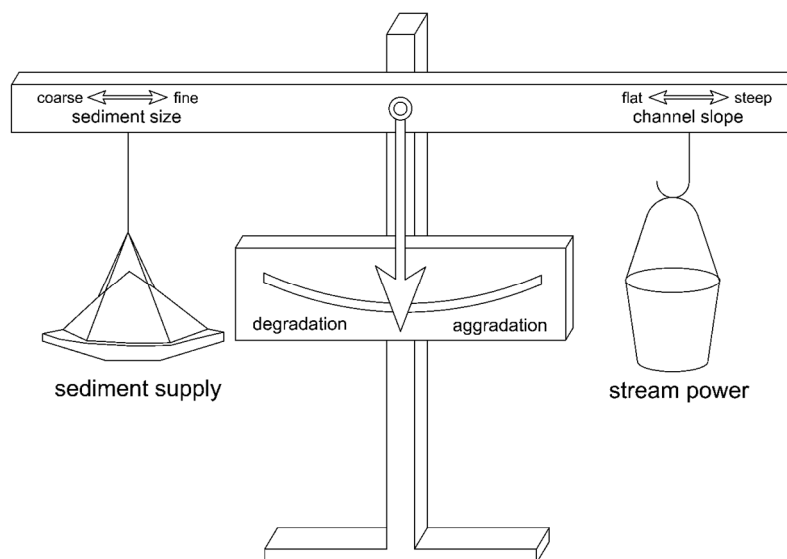


Fig. 14: Figurative example for possible river bed changes (aggradation and degradation) as function of the boundary resistance and the stream power (Blum and Törnqvist, 2000; modified).

To get insight into the long-term behavior of a river, with respect to the morphodynamics, and to see if a dynamic equilibrium occurs, long term investigation should be performed for the river or a selected river reach. Frings et al. (2014a, 2014b) collected all available values and numbers to give an overview for the river Rhine in Germany. Due to a unique dataset it was possible to quantify fluxes of clay, silt, sand, gravel and cobbles along a more than 200 km long part of the river Rhine for the period between 1991 and 2010. All sediment transport paths

were taken into account to identify the sources and sinks of sediments in the investigated river reach (figure 15a). Frings et al. (2014a, 2014b) used in their study data sets of bed level measurements, thousands of sediment transport measurements along the investigated river stretch, information on sediment supply from tributaries and took into account depositions in groin fields and flooded areas as well as abrasion and anthropogenic measures, such as dredged sediments. The final result is an overview for the study area between Rhine-km 640 and 866 (figure 15b). The results show for instance a transfer of sand, gravel and cobbles of $0.66 \text{ Mt/a} \pm 26\%$ from the hinterland towards the delta. In addition, a long-term bed degradation for the study area in the range of 3 mm/a for the period between 1991 to 2010 was discovered (Frings et al., 2014b). However, such a detailed study, as it was conducted for the River Rhine, is strongly depending on the existing data, which are not available for most of the rivers worldwide.

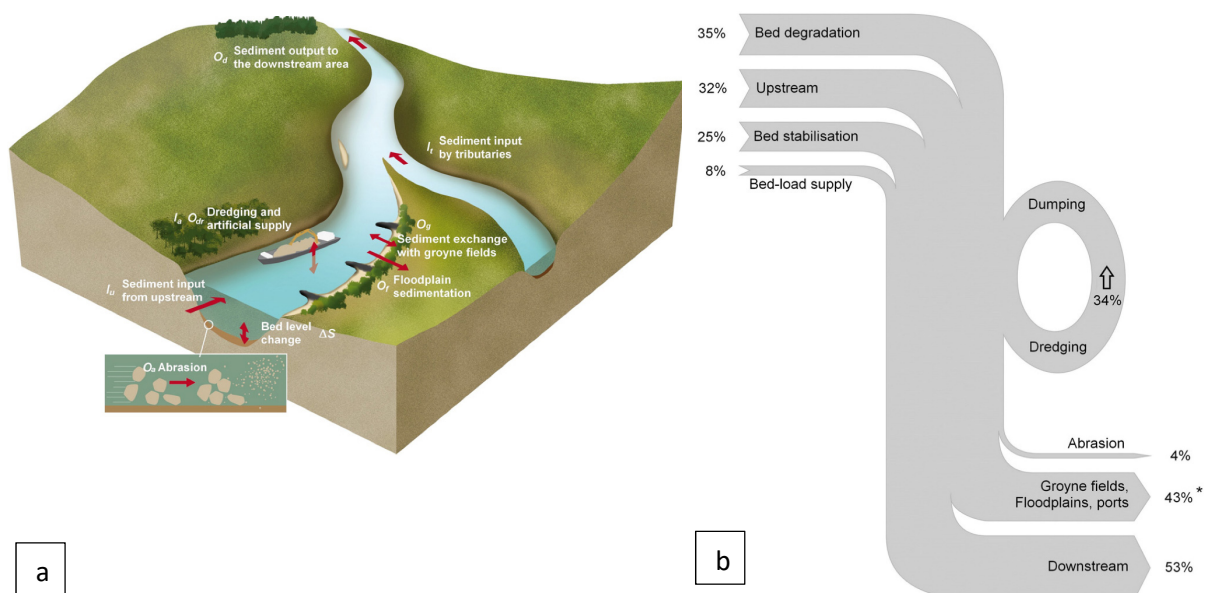


Fig. 15: (a) sediment transport paths for the river Rhine (Frings et al. 2014a); (b) identified sources and sinks of sediments for the reach of the river Rhine between km 640–865 (Frings et al. 2014b).

2.3 Depositional zone (oceans/reservoirs)

Usually, most sediments are transported by rivers directly to the ocean and deposit at the mouth of the river. The factors, which influence the formation of the river mouth are the river itself, waves and tides. Depending on the dominating factors river mouths can be subdivided in deltas and estuaries. Deltas are usually river and wave dominated mouths, whereas estuaries are tidal-dominated river mouths with a high tidal range.

However, the construction of artificial structures in rivers changes the natural balance of the system and leads to a reduced amount of sediments reaching the ocean due to a trapping of sediments within the reservoirs. When a river discharges into a reservoir, flow velocities, bed

shear stresses and turbulences decrease and a natural settling effect occurs. Several parameters may influence reservoir sedimentation with respect to quantity of settled sediments and the resulting sedimentation pattern. Badura (2007) categorized these parameters into three groups, namely:

- (i) Catchment specific parameters, such as: geology, topography, vegetation cover, hydrology and climate,
- (ii) reservoir specific parameters, such as: geometry, size, slope and sedimentological parameters,
- (iii) human impacts, such as: land use, trapping of sediments in upstream, desiltation of upstream located reservoirs.

Although sedimentation processes are strongly depending on the above mentioned parameters, reservoir sedimentation itself follows generally a pre-defined pattern. Morris and Fan (1998) introduced three zones along the longitudinal section of the reservoir, namely the topset bed, foreset bed and bottomset bed (see figure 16a). Within the topset bed sediments start to settle as the stabilizing forces exceed the moments of the driving forces and a delta is formed. Usually coarser sediments settle first and finer sediments are further transported into the reservoir (gradation). However, depending on the morphology and the hydraulic conditions, as a result of the boundaries of the reservoir, finer sediments can also be found in this area (Harb, 2013). Such a delta formation can be seen e.g., during low water levels in the Wasserfallboden reservoir in Austria (figure 16b), where a Gilbert-type delta formed at the head of the reservoir.

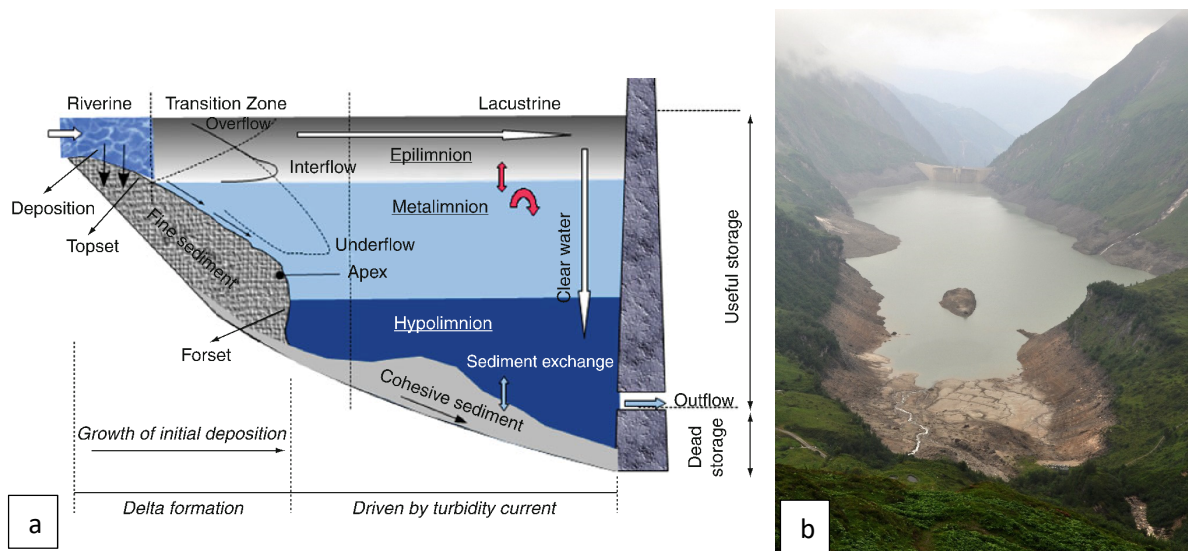


Fig. 16: (a) schematic overview of the sedimentation processes in a reservoir (Dargahi, 2012); (b) Gilbert-type delta at the reservoir of Wasserfallboden, in Austria.

As foreset bed the head of the delta is defined, which is characterized by decreasing grain-sizes. The formed front of the delta is moving successively towards the dam. Figure 17 shows

the tendency of a moving delta through periodically surveyed longitudinal sections, obtained from measurements of the Solis reservoir in Switzerland (Auel and Boes, 2011)

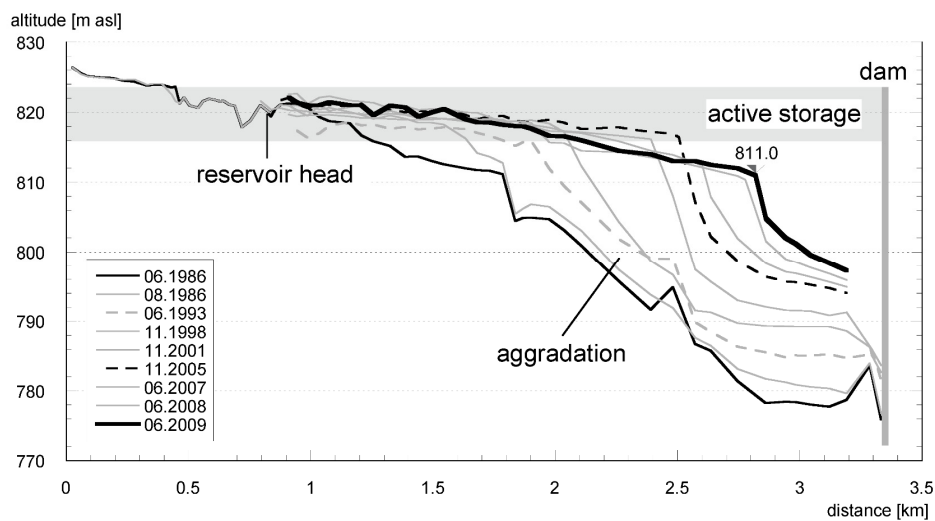


Fig. 17: Periodically surveyed longitudinal sections of the Solis reservoir, Switzerland (Auel and Boes, 2011).

The finest particles are transported in suspension further to the dam (bottomset bed), and will settle in this area. These particles are deposited either by stochastic transport processes or by stratified flows (Harb, 2013).

In reservoirs, currents often occur due to differences in the density of the inflowing and the stored water as result of the temperature, the sediment content and/or due to salinity (Morris and Fan, 1998). The influence of salinity in freshwater reservoirs can generally be neglected. However, currents as a result of temperature differences (stratified flow) occur regularly, e.g., when inflowing water is colder than the warm water in the reservoir. Usually the cold water of the river will mix only slowly with the warm water stored in the reservoir.

Currents with a difference in density, resulting from the sediment content (high sediment concentrations in the inflowing water), are called turbidity currents. This type of current is driven by the differences in density and by gravity (Batuca and Jordan, 2000). Each current is characterized by a plunge point, where it can visually be seen that the high sediment laden flow moves to the bottom of the reservoir (underflow; USBR, 2006), as result of different densities. These currents can transport a large amount of sediments and are also characterized by considerable speed towards the dam, where flow velocities up to 0.5 to 0.8 m/s can be reached with a maximum transported sediment diameter between 0.01 and 0.03 mm (Morris and Fan, 1998). Depending on the shape of the reservoir and the already deposited sediments, turbidity currents may be able to re-mobilize sediments, as a result of their high flow velocities. As a consequence of further increasing density, the turbidity density accelerates towards the dam (Parker et al., 1986; De Cesare, 2006), where the current transforms into a muddy lake (e.g., De Cesare, 2006; Schneider et al., 2012a). However, it can

also happen that coarser sediment starts to deposit, and as a result the current might dissipate and may often not reach the dam (USBR, 2006). The occurring processes are therefore similar to a snow avalanche moving downhill the slope of a mountain (Harb, 2013).

Figure 18 shows results of a three-dimensional numerical model, where the deposition mechanism of a sediment mixture was investigated based on a physical model study obtained by Toniolo et al. (2007). In the figure the horizontal velocities are presented for different time steps. It shows the inflowing water, with higher density, plunges at the entrance and moves with high flow velocities along the bed toward the dam (Rashid, 2020).

Especially in high altitude regions, a clear distinction between stratified flow, as result of temperature differences or as result of the sediment concentration is not feasible as both processes may mix with each other (Batuca and Jordan, 2000). An example are heavy precipitation events in summer, where cold water with high sediment loads enters reservoirs with warmer water.

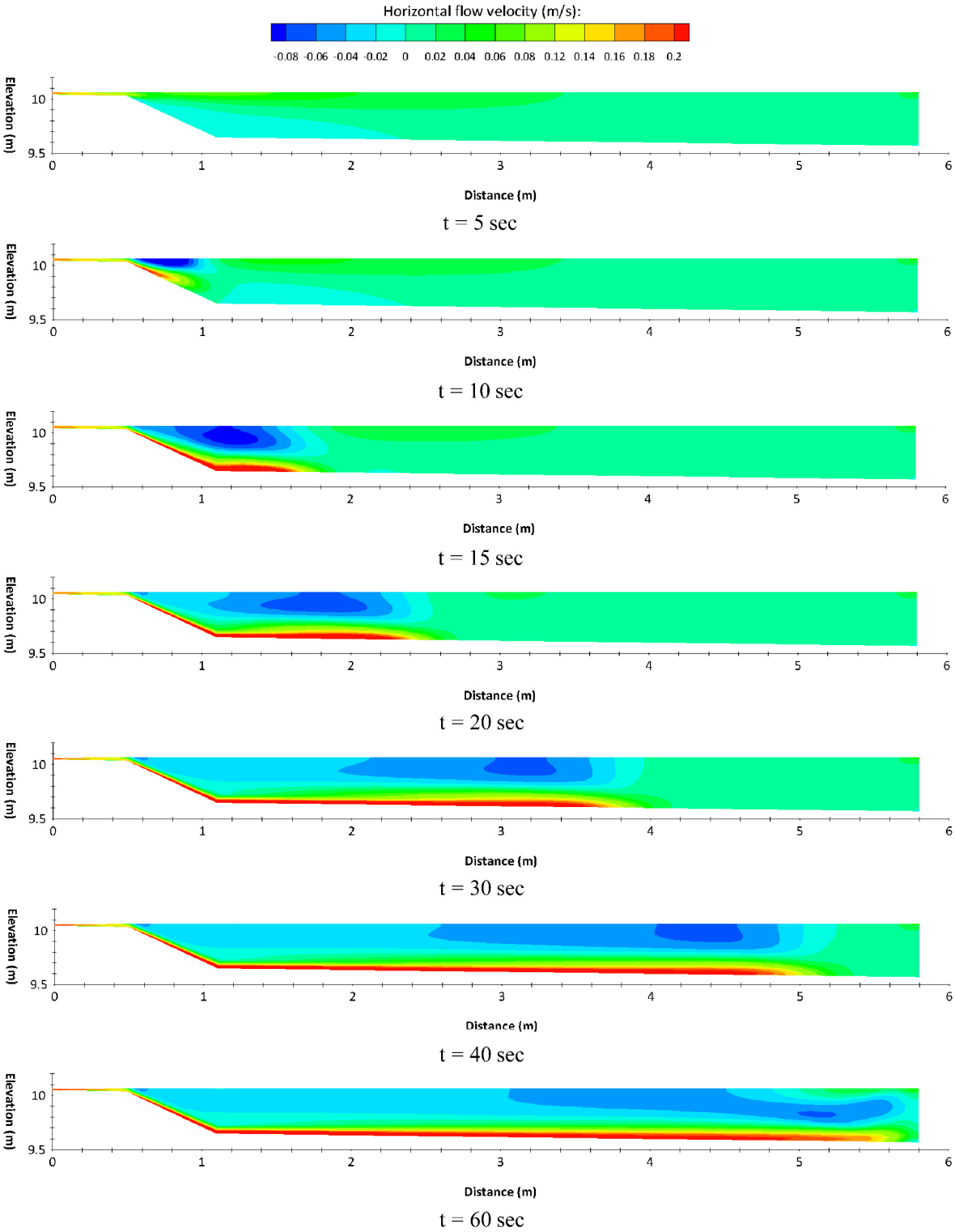


Fig. 18: Numerical model results from a physical model study with the aim to investigate the deposition mechanism of a sediment mixture. Horizontal velocities are presented for different time steps (Rashid, 2020; modified).

3 MECHANISMS OF SEDIMENT TRANSPORT AND RIVER MORPHOLOGY

Erosion, Transport, Deposition and Consolidation (ETDC) are the main processes that control sediment transport as well as the river morphology. Within this chapter a brief overview of the ETDC processes is given, explaining the most important processes, but also showing gaps in knowledge. These processes are the basis for planning measurements, setting up a monitoring program or for running hydro-morphodynamic numerical models. For a more detailed overview and to gain deeper insight, the ASCE Manuals and Reports on Engineering Practice No. 54 and No. 110 by Vanoni (1975) and Garcia (2007), respectively, are recommended literature.

To predict reservoir sedimentation and to obtain a sustainable reservoir management an understanding on governing processes of sediment transport and morphological processes is necessary. In general, the mechanisms of sediment transport can be subdivided into four principles, namely erosion, transport, deposition and consolidation (ETDC processes; Maggi, 2005). Figure 19 gives an overview on these four processes. However, within the ETDC processes not all the physical processes, and especially interactions between the processes, are fully discovered yet and analytical approaches are not available to describe most of these processes. Two of these so far unrevealed processes can be seen in figure 19, namely the flocculation process on one hand and the remobilization of cohesive fine sediment particles from the bed on the other hand. One reason is that within the flocculation process as well as in the erosion process of cohesive sediments sediment-related parameters (physical parameters), such as the granulometry, but also biological and chemical parameters are involved and have to be taken into account.

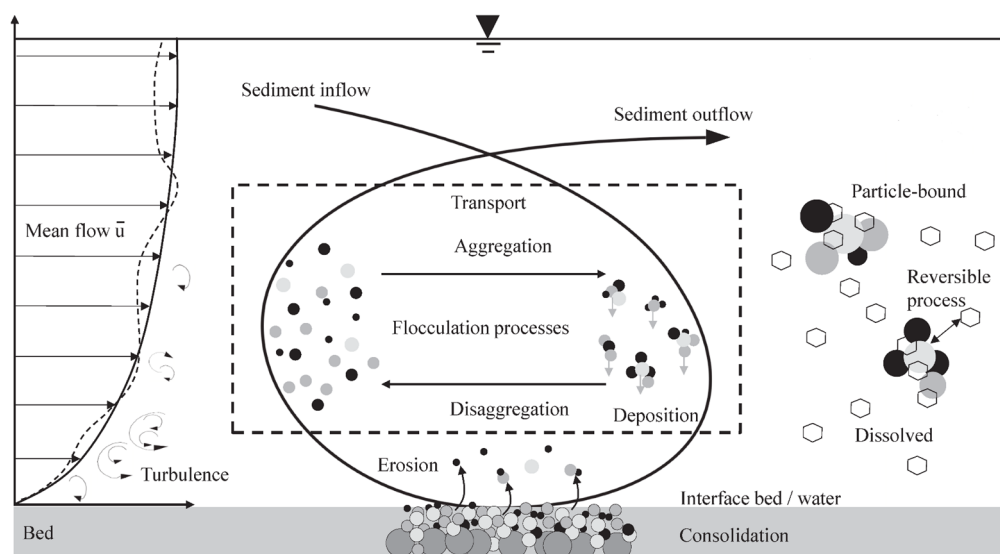


Fig. 19: The Erosion, Transport, Deposition and Consolidation (ETDC) processes within water bodies (Klassen, 2017, modified).

3.1 Erosion

Gravity force, drag force, lift force, buoyancy force and friction are the five main forces acting on a sediment particle (figure 20). The movement of a single grain (cohesionless) may be described by the sum of these forces. If the moments of the driving forces (turbulence and shear stress) become larger than the moments of the stabilizing forces (weight, fall velocity and friction), motion of a particle starts. In the opposite way, if the stabilizing forces exceed the moments of the driving forces a settling is the consequence (Yalin, 1977).

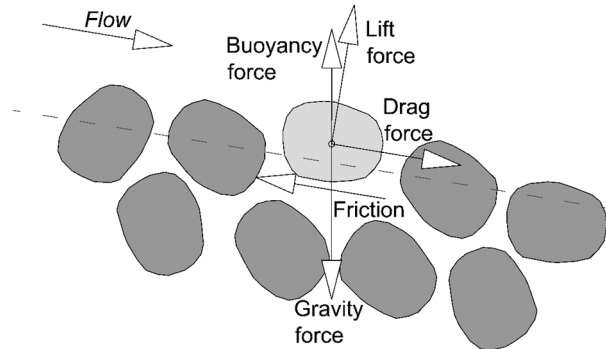


Fig. 20: Forces acting on a single grain.

Under natural conditions, in rivers and reservoirs, all above mentioned forces, except the gravity force, are highly variable in space and time. This is a result of the turbulent flow characteristics in natural systems, of sediment mixtures of which the river and reservoir beds exist as well as the subsequent interactions between the sediment particles.

Consequently, the description of single particle movement, as shown in figure 20, is unrewarding for practical engineering purposes (e.g., Wiberg and Smith, 1987; Kirchner et al., 1990; Komar and Carling, 1991). In hydromorphological studies the Shields diagram is therefore often used to evaluate whether particles start to move or not, based on the occurring hydraulic conditions (figure 21; Shields, 1936). Shields developed this diagram in 1936 based on experimental observations for non-cohesive sediments (particles $>62.5 \mu\text{m}$). In the Shields diagram the dimensionless critical shear stress (τ_* ; Eq. 1) is correlated with the grain Reynolds number (Re_* ; Eq. 2).

$$\tau_* = \frac{\tau_c}{g(\rho_s - \rho_w)d_i} \quad (\text{Eq. 1})$$

where τ_c is the critical shear stress, g is the acceleration of gravity, ρ_s is the density of the sediment particle, ρ_w is the density of water and d_i is the particle diameter of the i^{th} fraction of the particles.

$$R_* = \frac{u_* d_i}{\nu} = \frac{d_i \sqrt{\tau_0}}{\nu \sqrt{\rho_s}} \tag{Eq. 2}$$

where u_* is the shear velocity, d_i is the particle diameter of the i^{th} fraction of the particles, ν is the viscosity of the fluid, τ_0 is the actual shear stress on the bed and ρ_s is the density of the sediment particle.

The actual shear stress at the river bed, used in Eq. 2, is calculated with respect to the occurring hydraulic conditions for a certain flow regime. As grain diameter, used to obtain the grain Reynolds number, the particle diameter of a grain fraction of interest or a representative grain fraction is used. In practice the incipient of motion of sediment mixtures is often captured by using a characteristic grain diameter of the bulk mixture (Lamb et al., 2008). Different authors report here different diameters (see Zanke, 1982); for instance, Stelczer (1981) used a particle size corresponding to d_{80} , whereas the use of d_{50} is often recommended in case that a uniform sediment distribution occurs (Booth, 2006). However, Wilcock et al. (2001) show in their study that it is difficult to quantify the critical shear stress for sediment mixtures of different grain-sizes.

The points above the curve in the Shields diagram (figure 21) indicate a motion of particles, whereas the points below the curve indicate no sediment movement. For most natural rivers, with turbulent flow conditions, only the part of the Shields diagram is relevant, where the dimensionless critical shear stress is constant ($Re^* > 70$). However, in some large lowland rivers the conditions with $Re^* < 70$ may occur, which is representative for fine grains, partly hidden in the laminar sublayer and requiring a larger critical shear stress relative to their size (Booth, 2006).

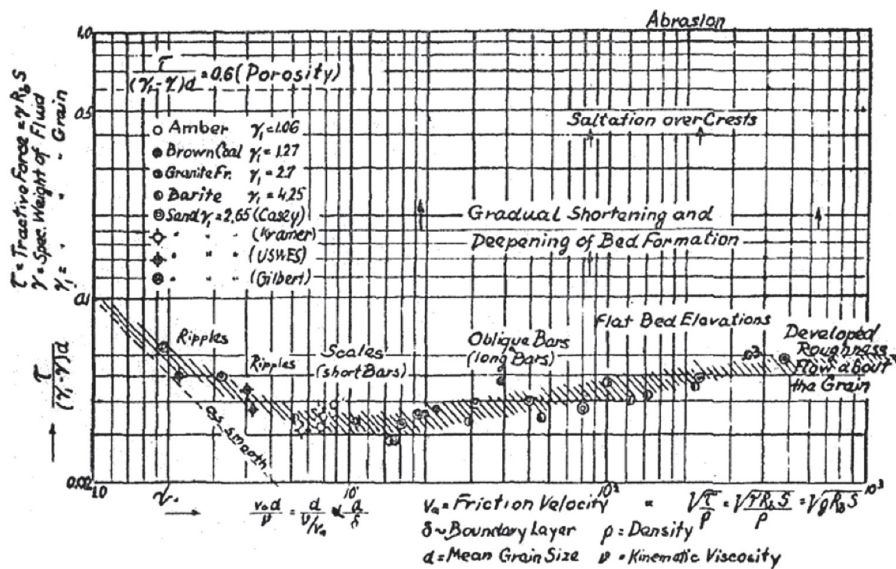


Fig. 21: The Shields diagram correlating the dimensionless critical shear stress with the grain Reynolds number (Shields, 1936).

Other researchers correlated the condition of a particle, with respect to movement, with different factors, such as the critical specific discharge, which is a function of the bed slope and a characteristic grain diameter (Schoklitsch, 1935), the stream power, used by Yang (1984), or the critical velocity v_c , used by Hjulström (1935).

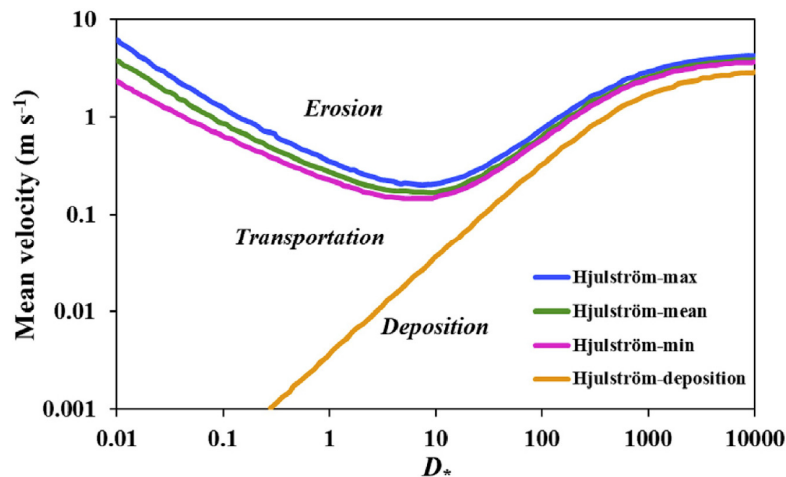


Fig. 22: Relation between the dimensionless grain size and the mean velocity in accordance to Hjulström (1935, modified by Yang et al., 2019).

A correlation of the bed shear stress and the sediment transport is discussed in several books and articles, e.g., Zanke (1982) or van Rijn (1993). By only considering the critical shear stress, it can be assumed that in sediment mixtures smaller particles would erode earlier compared to coarse particles (e.g., Andrews, 1983; Lenzi et al., 2006). However, several studies have shown that in case of sediment movement coarse as well as fine sediments are transported more simultaneously, as result of hiding and exposure effects (Stelczer, 1981; Parker et al., 1982; Wiberg and Smith, 1987; Parker, 1990). Hiding and exposure describe the ability of small particles to hide behind larger particles, which minimizes the exposure of these particles to the flow (figure 23a). As a consequence, smaller particles will not be eroded, even if the driving forces are larger than the stabilizing forces of a single particle. Figure 23b shows a picture of sediments at the river Inn, Germany, where a broad spectrum of different sediment sizes can be seen, with smaller sediments in between larger stones.

Another phenomenon is bed armoring or river bed pavement, which plays an important role in river environments, because the critical threshold for erosion is for armored river beds much higher compared to a fully mixed river bed with similar grain-size composition. Figure 23c shows a sketch of bed armoring of a river bed, where coarse sediments form a layer similar to roof tiles at the surface of the bed. The sublayer still contains the full range of available sediments. Figure 23d presents an armored river bed at the river Inn in Germany. The difference between the two processes of armoring and river bed pavement is that bed armoring is associated with an immobile river bed, whereas river bed pavement is associated with a mobile bed (Jain, 1990; Parker et al., 1982). Pavement occurs often in graded rivers

with poorly sorted gravel (Parker et al., 1982), whereas armoring can be found in gravel bed rivers with a wide range in grain-sizes (Harb, 2013).

A third process, which influences the stability of river and reservoir beds is colmation. Colmation, or river bed clogging, describes the process of infiltration and accumulation of fine sediments in pores of gravel bed rivers (figure 23 e; Einstein, 1968). The governing processes of colmation are highly complex and are characterized by a high spatial and temporal variability. Colmation is often related to environmental issues as it influences the hydraulic conductivity and influences the exchange process between surface and sub-surface flow (e.g., Schaelchli 1993; Heywood and Walling, 2007). However, river bed clogging leads to a solidification of the bed and subsequently influences the erosion stability. Colmation and the solidification is strongly influenced by biological and physico-chemical parameters, especially when infiltrated sediments have a high silt and clay content. In general, colmation can be subdivided into outer colmation (figure 23f) and inner colmation; Schaelchli (2002) further divided the inner colmation in five stages, namely: no colmation, weak colmation, medium colmation, strong colmation and fully clogged. Nevertheless, the investigation of colmation is still a challenge as objective methods to measure and investigate colmation are still under development (Seitz et al. 2017, 2018; Holzapfel et al. 2020). So far, the most used method is a large-scale mapping Schaelchli (2002) and sediment sampling to investigate the amount of fine sediment particles, usually <1 mm or <2 mm. However, recent studies have shown that these methods are not sufficient to investigate the occurrence and the influence of colmation completely (Seitz et al., 2019; Hauer et al., 2020a).

Finally, it should be noted that all the above mentioned processes are natural processes, but may be influenced by human interventions. Colmation for instance is as result of fine sediment transport and happens especially during low flow conditions, where fine particles may settle and infiltrate. In a natural system decolmation processes happen regularly in case of morphological bed changes, e.g., during flood events. Nevertheless, in case of human interventions, where e.g., flood peaks are cut off as a result of flood protection structures or water extraction is performed, the number of decolmation processes decrease and the impact of colmation may increase. As a result, a shift of interstitial habitats of benthic organisms may be seen (e.g., Gayraud and Phillipe, 2003) as well as an altering process of the reproduction habitats of gravel-spawning fish (e.g., Noack et al. 2017).

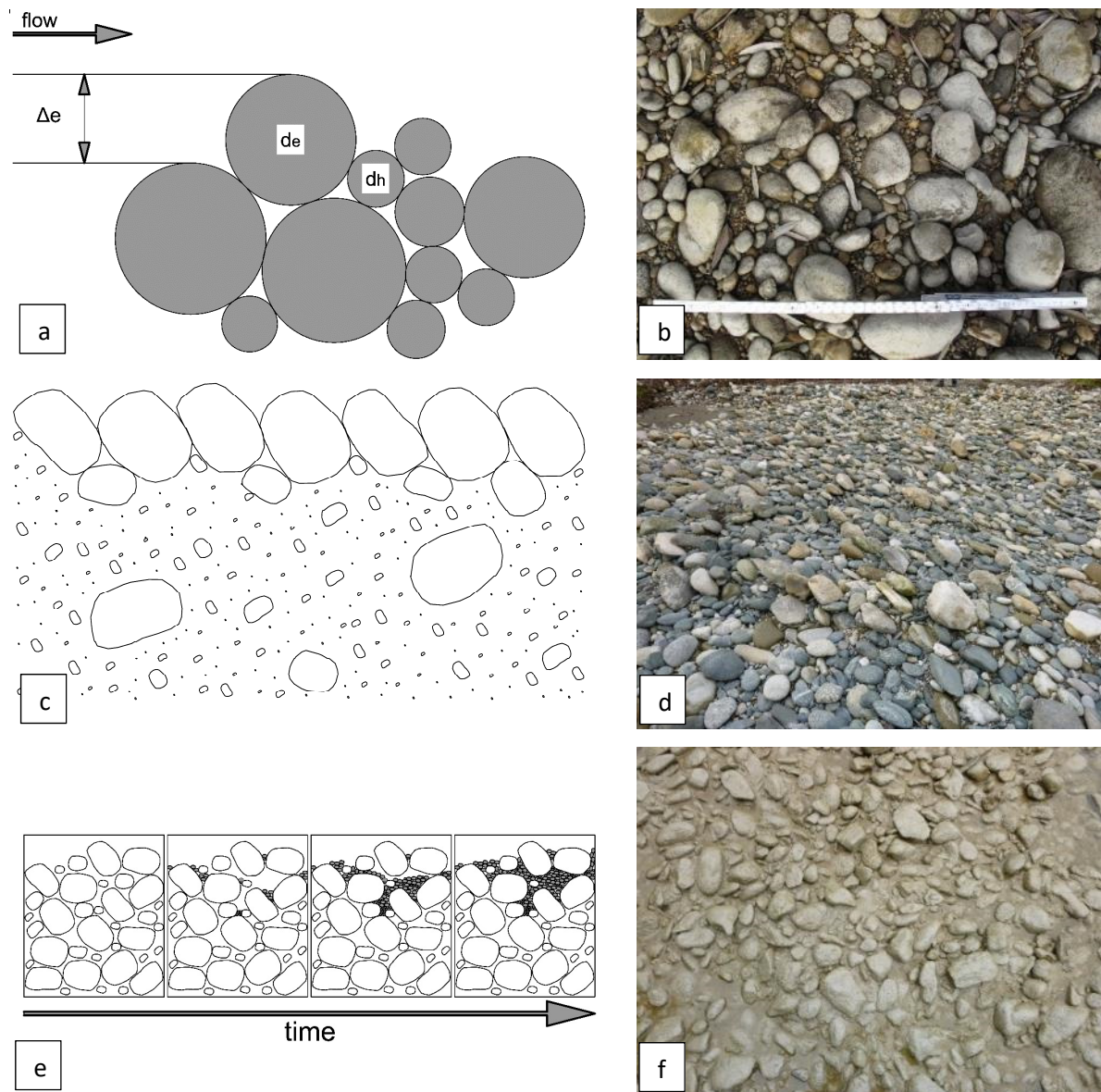


Fig. 23: (a) principle of hiding and exposure processes, where smaller particles hide behind larger ones; (b) natural sediment mixture with a broad spectrum of different sediment sizes at the river Inn, Germany; (c) principle of river bed armoring, where an armor layer is formed out of the available bed material; (d) river bed armoring at the river Inn, Germany; (e) steps of river bed clogging with an infiltration of fine sediments in voids of the gravel bed of the river; (f) picture of outer colmation at the river Inn, Germany.

The erosion behavior of fine particles (particles $<62.5 \mu\text{m}$) differs significantly from that of non-cohesive sediments and remains in contrast to coarse sediments largely unpredictable, since their incipient motion, erosion and post-entrainment is a result of complex biological and physico-chemical interactions. Clay, silt and mud particles have high surface loadings (interparticulate binding forces; known as cohesion) that are strengthened by biological interactions (adhesion), such as organic substances and microorganisms permeating the void spaces to bridge and interlock single grains (known as adhesion; e.g., Black et al., 2002; Gerbersdorf et al., 2007; 2008; Righetti and Lucarelli, 2010). As a result of these factors, the

critical shear stress of fine sediments may be up to 50 times larger compared to particles of similar arithmetic mean sizes without cohesion and adhesion forces (Kothyari and Jain, 2008). Van Rijn (1993) reports that sediment mixtures with clay content of 10 % or higher have already significant cohesive properties. However, available knowledge regarding the resuspension of cohesive sediments is mostly obtained by a few experiments in the laboratory and - to an even lesser extent - by field surveys (e.g., by Kamphuis and Hall, 1983; Mehta et al., 1989, Berlamont et al., 1993; Gerbersdorf et al., 2007; Kothyari and Jain, 2008, 2010; Noack et al., 2015; Rodrigues Silva et al., 2018 or Beckers et al., 2020). As a result, there is still no general analytical theory for cohesive sediment resuspension available yet (Black et al., 2002; Gerbersdorf et al. 2007; Haun and Olsen 2012a; Haun et al. 2013a; Rodrigues Silva et al., 2018). Especially for reservoir sediments further investigations and the identification of key parameters, which govern resuspension processes, are indispensable to increase the understanding of the behavior of fine sediment accumulations with respect to their erosion stability. Rodrigues Silva et al. (2018) made an attempt to investigate governing parameters by using a fuzzy-logical approach, where the critical bed shear stresses of undisturbed sediment cores from run-of river reservoirs were correlated with physico-chemical and biological parameters of the sediments to unravel such key parameters.

Finally, it should be mentioned that erosion is a result of different factors, which are for non-cohesive sediments e.g., the randomness of particle sizes and their shape and for cohesive sediments the content of clay, water and other physico-chemical and biological parameters. The initiation of motion is therefore not only a deterministic process but a stochastic process (van Rijn, 1993; Harb, 2013). To successfully predict erosion processes it is inevitable to characterize sediment depositions to gain comprehensive knowledge of the physical, chemical and biological properties as well as of the erosion stability of sediment depositions (Wieprecht et al., 2020). However, the characteristic of sediment depositions shows a high temporal and spatial heterogeneity within reservoirs, also as a result of the deposition pattern within a reservoir (see chapter 2.3 *Depositional zone (oceans/reservoirs)*). This should be considered when selecting spots for investigating reservoir sediments.

3.2 *Transport*

If sediment motion occurs, particles may be transported in form of bed load along the river/reservoir bed or in suspension as suspended sediment load (figure 24). Morris and Fan (1998) assumed that the bed load constitutes only around 15 % of the total sediment load. Also Booth (2006) assumed a similar range, giving a value between 5 and 20 %. However, this value is with regard to hydraulics and sediment characteristics strongly site-dependent. Maddock & Borland (1950) made an attempt to distinguish between rivers with a high suspended sediment load and (i) sand as bed material and (ii) gravel or rock as bed material, where values between 10-20 % and 2-8 % of the total load were reported, respectively.

However, to specify a sharp threshold between the two transport mechanisms is often not possible due to the involved hydraulic forces (e.g., bed shear stress, turbulences) and sediment parameters (e.g., grain-size, grain forms).

3.2.1 *Bed load transport*

When the effective bed shear stress is close to the critical shear stress, the transport of sediment particles occurs in form of sliding, whereas with increasing shear stresses and turbulences a rolling or even saltation of the particles occurs. First studies in this field were conducted by Bagnold before World War II based on sand transported by wind forces (Bagnold, 1973). Einstein et al. (1940) characterized the transport as bed load transport when particles move in form of sliding but also rolling along the bed, whereas van Rijn (1984) took, based on Bagnold studies, also jumping of particles into account (see figure 24). However, all the authors indicate that during bed load transport a continuous contact to the river bed must be given to consider the transport form as bed load transport. As a consequence, it is a challenge to measure bed load transport accurately as well as to predict and calculate the exact amount of particles transported as bed load. Hence, a large number of empirically developed bed load transport formulae exist. However, each of them was developed for certain conditions. These bed load transport formulae are not based on the force balance approach, explained earlier in *chapter 3.1 Erosion*, which means that also other effects, such as hiding and exposure are partly taken into account, even if their share cannot be quantified. The development of these equations is based on the relation between sediment transport rates with values describing the hydraulic conditions, such as discharge or bed shear stress and the physical sediment characteristics, such as geometry or grain diameter (Booth, 2006). In general, these empirical bed load transport formulae can be divided into three general types and are based on:

(i) *Exceeded shear stress*: These bed load formulae describe the difference between the effective bed shear stress at the bed and the critical bed shear stress of the bed material. Examples are the formula by Meyer-Peter and Müller (1948), which refers to a large number of flume experiments with uniform, graded and lightweight materials, or the formula developed by Parker (1990), based on data from the Oak Creek in Oregon, United States of America. However, many more formulae are available (e.g., Graf and Acaroglu, 1968; van Rijn, 1984a; Parker, 1990; Hunziker, 1995 or Wu et al., 2000), where each of them was developed under different conditions, such as different grain-sizes or slopes of the river bed. This fact has to be considered when choosing an appropriate formula.

(ii) *The stream power*: Bagnold (1966) proposed that the bed load transport rate can also be predicted on the basis of the mean value of the stream power per unit bed area. Within this equation the rate of loss of potential energy, as water flows downhill, is quantified and consequently the potentially available energy for morphological changes is used (Ferguson,

2005). Bagnold's approach was only used by a few researchers for further investigations (e.g., by Yang, 1984).

(iii) *Stochastics*: This probabilistic approach was developed by Einstein (1950) and is based on sand bed rivers in the Mississippi basin. The equation expresses an equilibrium condition of the exchange of particles between the bed layer and the bed, which means that grains may leave or enter a unit area in a unit period of time, where for each unit of time and of bed area the same number of a given type and size of particles must be deposited and scoured from the bed. Several statistic laws are incorporated in this approach, such as the probability of the movement of a single sediment particle, which is dependent on the particle size, shape and weight as well as on the near bed flow pattern. This approach was also used by Yalin in 1977.

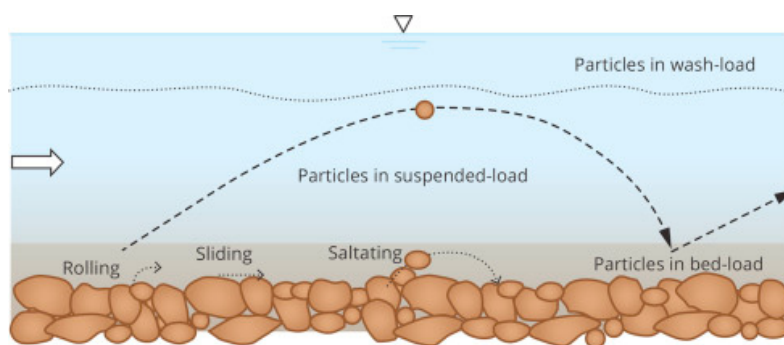


Fig. 24: Sketch of particle movement forms during bed load transport (Rheinheimer and Yarnell, 2017).

3.2.2 *Suspended load transport*

In case that the upward component of the hydraulic turbulence is larger than the settling velocity of the particle, sediments are kept in suspension and will be transported as suspended sediment load (Rouse, 1937; van Rijn, 1984b). The total suspended sediment transport (sediment flux) in the water body is a function of the occurring flow velocities and the suspended sediment concentrations. Figure 25 shows, beside the logarithmic velocity profile for turbulent flow, also the sediment concentration profile with highest concentrations close to the bed.

Frequently, also the term wash load can be found in literature. Wash load is defined as sediments, which are transported in suspension, and without any interaction with the bed. An important point is that wash load does not originate from the bed material of the river. Often the origin of wash load is eroded soil from the catchment and is transported through the fluvial system (Harb, 2013). Therefore, wash load occurs mainly during flood events and will not settle in rivers and reservoirs, also as result of the occurring lower density of the particles and the higher flow velocities and turbulences during high discharge periods.

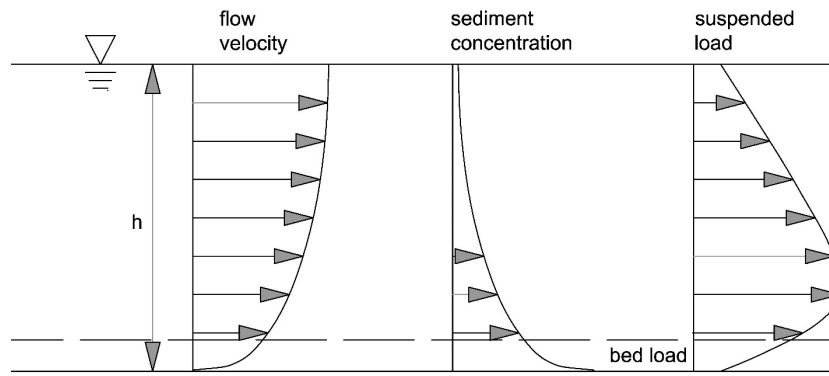


Fig. 25: Suspended sediment load as function of the flow velocity and the sediment concentration over depth.

Rouse introduced in 1937 a dimensionless number for determining the vertical distribution (concentration profile) of the suspended sediments, which is nowadays often used to define the form of sediment transport (suspended sediment transport or bed load transport). The Rouse number is the ratio between the occurring shear velocity u_* , the settling velocity of a particle w_s and the upwards velocity of the grain, which is the product of the shear velocity and the Von Kármán constant (κ ; figure 26). If the Rouse number is above 2.5, bed load transport occurs; for a number between 0.8 and 1.2 suspended sediment transport happens and for a value smaller 0.8 wash load is transported.

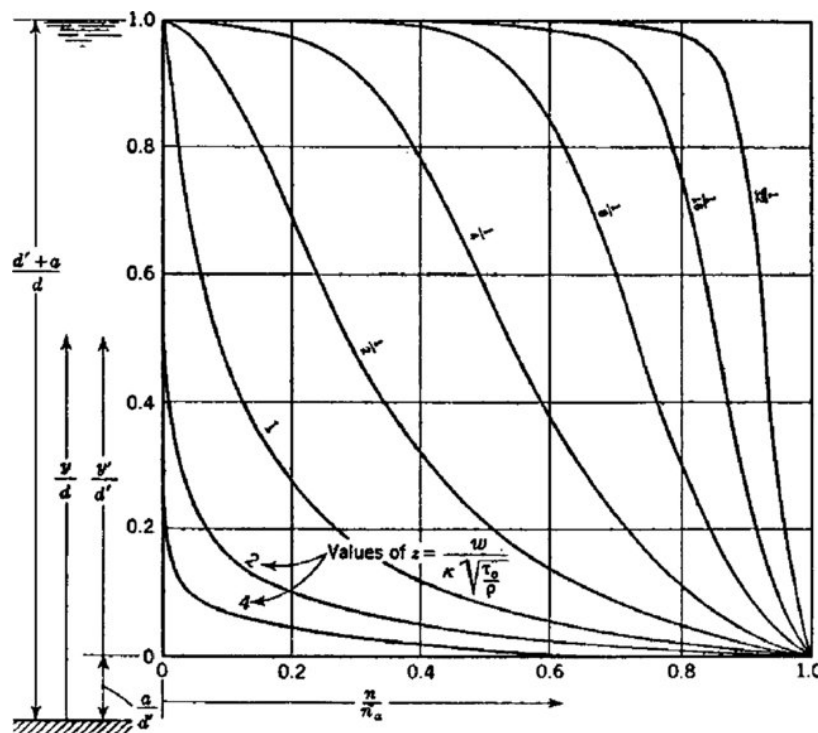


Fig. 26: Dimensionless plot of suspended load distribution (Rouse, 1937).

Other researchers used the ratio between the occurring shear velocity u_* and the settling velocity of a particle w_s to distinguish between suspended and bed load transport. Graf (1971)

for instance indicated that numbers above 0.1 indicate the beginning of bed load transport and values larger than 0.4 indicate suspended sediment transport. Engelund (1965) and Bagnold (1966) used a value of 1.0 to indicate suspended sediment transport.

3.2.3 Factors influencing the sediment transport

The flow as well as the sediment transport in river and reservoir bends are influenced by helical flow. Especially secondary currents (the lateral component of the helical flow) may dominate the sediment transport within these sections. As a result, sediments are eroded at the outer side of the bend and transported to the inner side where subsequently deposition happens. Additionally, the changing transversal slope of the bed results in a change of the transport direction of a particle. The transport path is no longer influenced by the direction of the flow only, but also by the movement direction of the particle as result of the gravity force on the transversal slope, also called influence of a sloping bed (Rüther, 2006; figure 27).

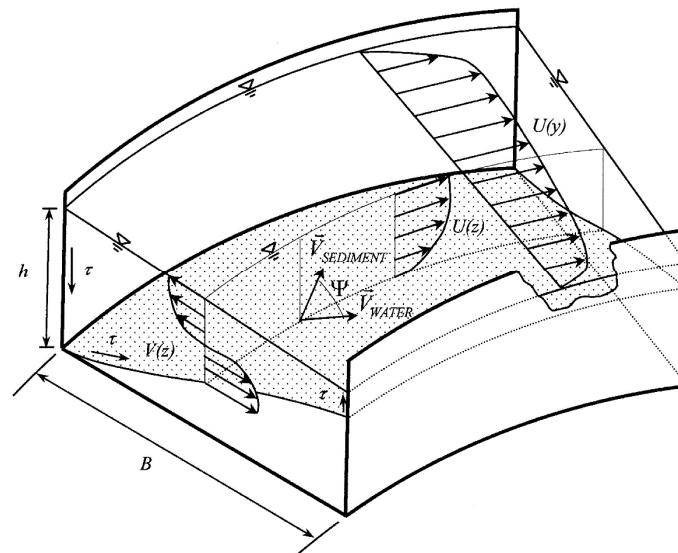


Fig. 27: Principles of flow and sediment transport in a channel bend (Rüther, 2006).

Another factor influencing the sediment transport is the hydromorphology. The hydromorphology describes the interaction of water and sediments in water bodies on spatial as well as on temporal scales. Erosion, transport and deposition are vital processes and play an important role in the evolution of the highly dynamic hydromorphological fluvial systems, also resulting in morphological structures, the so-called bed forms (Yalin, 1977).

The resulting natural structures such as ripples, dunes, antidunes (small-scale) or chutes and pools (large-scale) represent dynamic structures, which are highly variable in space and time due to the alternating relationship with the hydraulic flow processes. In general bed forms can be subdivided into structures of the lower flow regime (left side in figure 28), such as ripples, dunes, ripples on dunes, and washed out dunes as well as structures of the upper flow regime (right side in figure 28), such as plane bed, antidunes and chutes and pools.

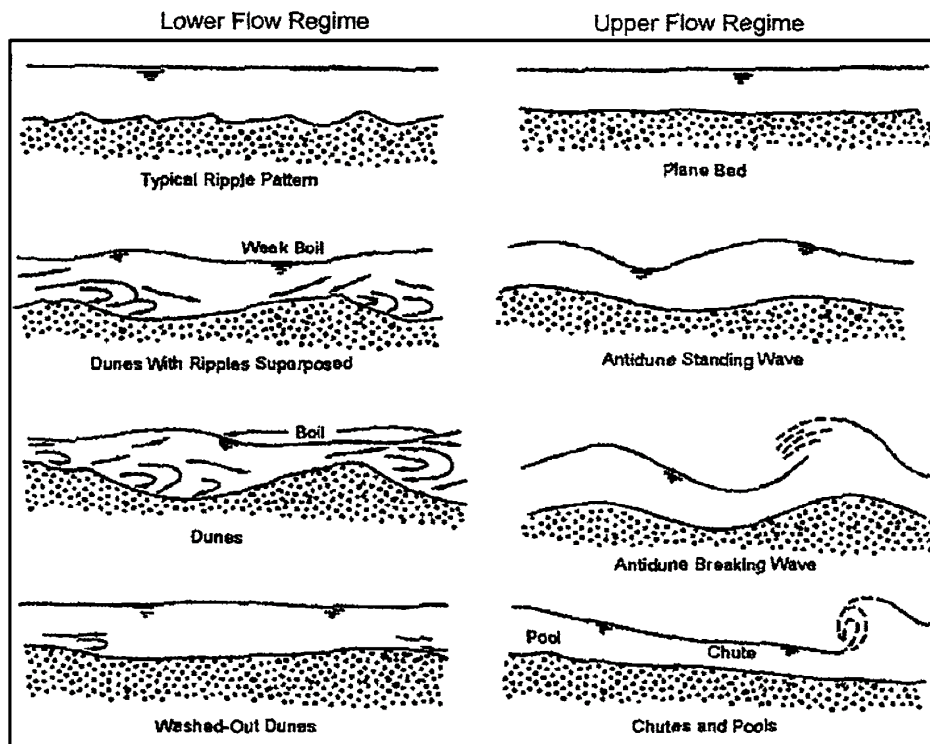


Fig. 28: Bed form types in alluvial channels (Simons and Richardson, 1966).

The formation of bed forms may be essential for the sediment transport, because changes in the bed roughness will occur and consequently changes in the bed shear stress are a direct result. An overview on the influence of bed roughness (bed forms) on sediment transport is given by Einstein and Barbossa (1952) and Engelund and Hansen (1967). In figure 29 the flow velocity v is plotted against the occurring bed shear stress τ_0 . The figure illustrates that partly large differences in the bed shear stresses occur, as result of the bed forms (τ''), compared to the case where only skin friction occurs (τ'), especially for flow regimes where dunes and antidunes develop.

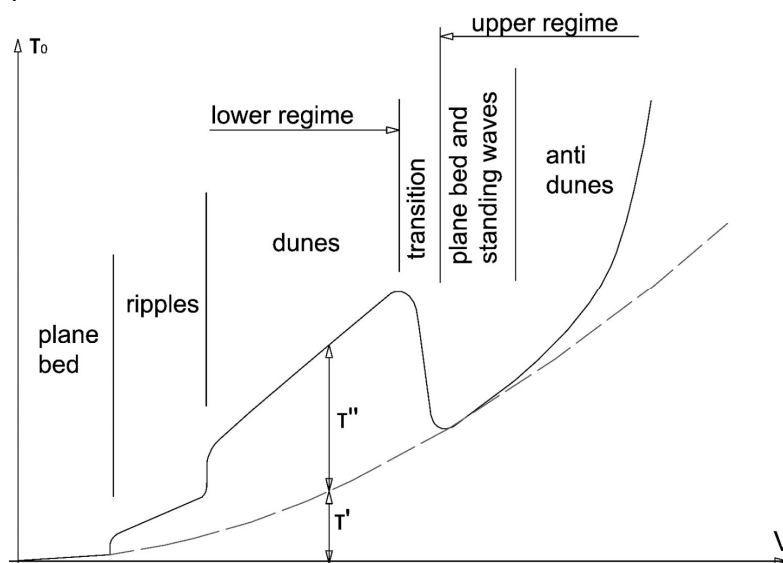


Fig. 29: Influence of bed roughness on the bed shear stress (Engelund and Hansen, 1967, modified).

3.3 *Deposition*

Deposition of non-cohesive sediments (particles $>62.5 \mu\text{m}$) depends strongly on the settling velocity of the sediment particles w_s , which is a function of the submerged weight of the particle, the viscous fluid resistance and inertia effects. In general, it can be observed that smaller particles have a smaller settling velocity compared to larger particles, because the viscous fluid resistance dominates and the inertia effects are negligible, whereas for larger particles inertial forces dominate (Booth, 2006). The formulae most often used to calculate the settling velocity is given by Stokes (Stokes' Law, 1851; Eq. 3), but also other researchers such as Rubey (1933) or Rouse (1937) obtained equations describing the settling velocity of particles. When selecting an appropriate formula, it is important to take into account that most of these formulae were developed for spherical shaped sediments only, and some of them are only valid for conditions with low Reynolds numbers, such as Stokes' Law. For higher Reynolds numbers it is necessary to obtain the drag coefficient by experiments or empirical data.

$$w_s = g \frac{\rho_s - \rho_w}{\rho_w} \frac{1}{18\nu} d^2 \quad (\text{Eq. 3})$$

where w_s is the settling velocity, g is the acceleration of gravity, ρ_s is the density of the sediment particle, ρ_w is the density of water, ν is the kinematic viscosity of the fluid and d is the particle diameter.

However, the settling velocity of a particle depends also on the shape of the particles and on water-related factors, such as salinity and suspended sediment concentration of the fluid (Harb, 2013). Small particles, such as clay and silt, have theoretically very low settling velocities. But due to inter-particle interactions, which are influenced by the pH-value, the salt content of the water (Hillebrand, 2008) or by adhesive forces (originated by extracellular polymeric substances, EPS), aggregation processes occur in the water column, resulting in flocculation (figure 30; Hillebrand et al., 2012; Klassen, 2017). Flocs have compared to single clay and silt particles a larger diameter/area (0.1 - 1 mm), weight and subsequently a larger settling velocity. Hillebrand (2008) showed a significant influence caused by flocculation on the deposition process of sediments, as a result of the cohesive properties of the particles. However, these flocculation processes are still difficult to describe theoretically because of their dependency on cohesive and adhesive forces as well as the stochastic colliding processes. The collided particles can either bond together to flocs, or already existing flocs will break up as a result of the shear stress induced collision (see figure 19; Harb, 2013; Klassen, 2017). Especially in reservoirs, where fine sediment fractions will settle, knowledge regarding flocculation is of high importance to predict reservoir sedimentation accurately (Hillebrand et al., 2017; Olsen and Hillebrand, 2018).

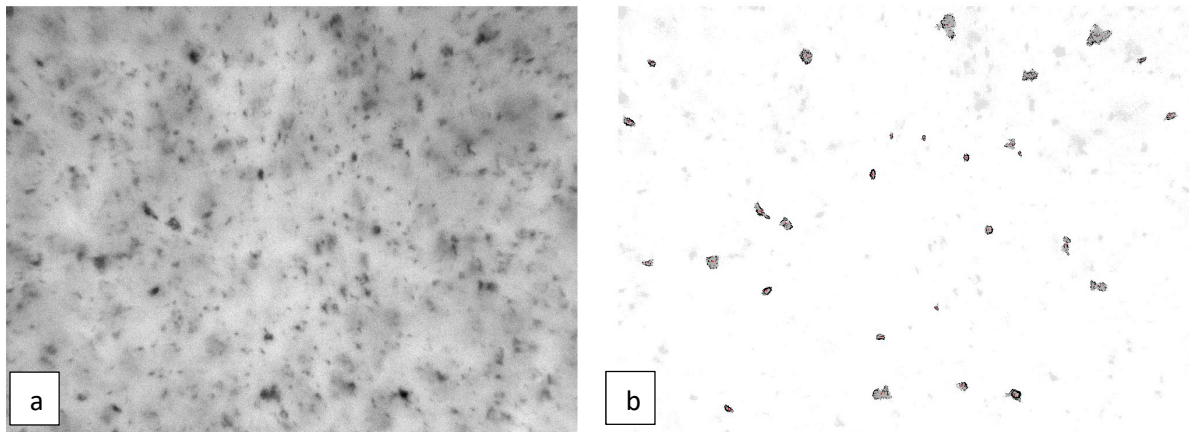


Fig. 30: (a) picture of flocs, taken by the In-Line microscope Aello 7000; (b) post processed image after subsequent analysis by an image recognition software (Klassen, 2017).

3.4 Consolidation

After deposition, a consolidation of particles can appear, as a result of the pressure induced by water and the weight of the particles itself. Especially in reservoirs the water pressure may be much larger compared to other fluvial systems, such as rivers.

In case of uniform non-cohesive sediments, the pore space of deposited particles is in the range between 26 % and 48 %, strongly depending on the packing arrangement of the particles. A cubic packing represents the highest pore space (48 %) and subsequently the lowest bulk density, a theoretical rhombohedral packing represents the closest possible packing (26 %) and subsequently the highest bulk density (figure 31a).

In case of non-uniform sediment mixtures, the sorting coefficient is an important parameter, as it gives information about the heterogeneity of the sediment mixture, which has a direct influence on the available pore space, as smaller particles fill voids in the structure of the coarse sediments. Folk (1966, 1980) introduced the inclusive graphic standard deviation as a possibility to quantify the grain-size variation of a sample by encompassing the largest parts of the size distribution as measured from a cumulative curve (Eq. 4). Based on the equation a high coefficient (>4) is an indicator that the sediment mixture is extremely poor sorted, whereas small numbers represent very well sorted sediments (figure 31b). In the equation the *phi* unit is used, which is a logarithmic transformation of millimeters into whole integers.

$$\sigma_1 = \frac{\phi_{84} - \phi_{16}}{4} + \frac{\phi_{95} - \phi_5}{6.6} \quad (\text{Eq. 4})$$

where σ_1 is the graphic standard deviation, ϕ_5 , ϕ_{16} , ϕ_{84} , ϕ_{95} are the diameters at the 5th, 16th, 84th and 95th percentiles of the sample, respectively (in *phi* scale).

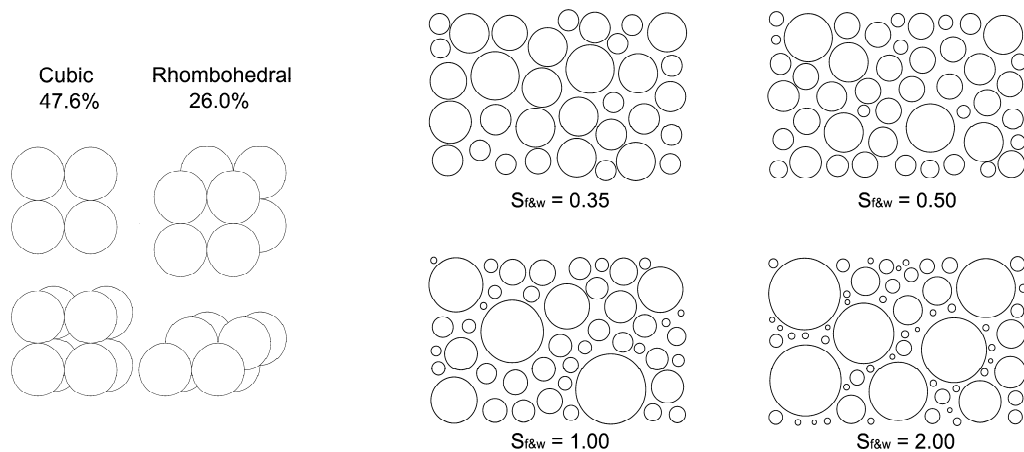


Fig. 31: (a) pore space of uniform sediment depositions, depending on the packing arrangement of the spheres; (b) sorting coefficients for sediment mixtures, calculated based on the ϕ unit.

Albeit the detailed processes of consolidation are not clear yet, consolidation effects may result in much higher shear strength of the sediments (Mehta et al., 1989; Gerbersdorf and Wieprecht, 2015; Rodrigues Silva et al., 2018). Especially for cohesive sediments the consolidation effects are of high importance. Fresh cohesive sediment depositions have a loose texture (especially depositions from flocs), a high water content and subsequently a low density. However, due to consolidation (compression as a result of their own weight and the water pressure) the bulk density of these sediment depositions increases as a result of reducing the pore water content, porosity and permeability (Harb, 2013). The consolidation time itself is strongly depending on the hydraulic boundaries as well as the sediment characteristics.

4 RESERVOIR SEDIMENTATION

Within this chapter the consequences of the construction of reservoirs on river systems are discussed. This is done by taking into account the ongoing processes within the reservoir itself, but also by looking on the surrounding environment. In a first step an overview is given on the loss of storage volume, as a result of progressive reservoir sedimentation due to the disturbance of the sediment continuity, followed by an overview of mainly negative effects on the up- and downstream river stretch. For a more detailed overview the Reservoir Sediment Handbook (1998) by Morris and Fan is recommended literature.

4.1 Loss of storage capacity

A loss of storage volume, as a result of ongoing sedimentation, is for reservoirs used for the production of hydroelectricity equivalent to a monetary loss. However, this loss of storage volume may have an even more drastic effect in case the reservoir is used for drinking water supply or irrigation purposes, where people depend on fresh water during dry periods (Mahmood, 1987; Fan and Morris, 1992; Morris and Fan, 1998). In the event that reservoir sedimentation may even block or affect the operation of hydraulic structures, safety problems can occur, resulting in severe damage, including dam failures with all the subsequent economic damages and in the worst case even the loss of lives.

The ICOLD World Register of Dams (1998) shows that around 25,410 large dams are in use worldwide, with a total storage volume of approx. 6,465 km³. Small reservoirs are not taken into account within this statistic. Vörösmarty et al. (2003) assumed that more than 44,000 smaller reservoirs are in addition to the large dams in operation. However, this number is fairly under-predicted due to the missing data on small reservoirs. Also an exact number of storage loss, resulting from reservoir sedimentation, is difficult to identify, but Mahmood (1987), Yoon (1992) and Bruk (1996) presented a value for the average annual loss of storage volume (worldwide averaged) to be in the range of 1 % of the existing storage volume. By taking into account the uneven distribution of the sediment yield, this value varies drastically depending on the region of the world, the catchment characteristics and the boundaries of the reservoir itself. Table 1 gives an overview on percentages of storage losses for different countries around the world.

But on a smaller scale, even more drastic examples can be found, such as the Wetzman reservoir at the river Gail in Austria, which lost its complete storage volume within one year after commissioning of the dam in 1883 (Cyberski, 1973).

Table 1: Mean annual sedimentation rates depending on the region of the reservoirs.

Location	Sedimentation rate [%]	Literature
United States of America	0.2	Crowder (1987)
India	0.5	Morris (1995)
Morocco	0.7	Abdelhadi (1995)
Turkey	1.2	Morris and Fan (1998)
Tunisia	2.3	Abdelhadi (1995)
China	2.3	Morris and Fan (1998)

The loss of storage volume is also a limiting factor to achieve the goals set by the United Nations in the Agenda for Sustainable Development (United Nations, 2017). An estimate by Palmieri et al. (2003) showed that the costs for restoring the annual losses of storage volume by rebuilding dams would cost approx. US\$ 13 billion per year.

An example for a hydropower reservoir, where sediments would influence the operation, is the Cachí reservoir in Costa Rica (figure 32). The reservoir has a designed volume of approximately 54 Mm³ and has been in operation since 1966. The combination of high precipitation rates (1,500 - 7,000 mm/year) and land cover/land use (55 % tropical forest, 43 % crops and pasture and approximately 2 % urban use) result into a sediment yield of up to 5,000 t/km²/y coming for the catchment (Jansson and Rodriguez, 1992). This represents an annual sediment inflow into the reservoir of around 810,000 tons (Jansson and Rodriguez, 1992). By taking the trapping efficiency of 82 % into account, the calculated storage loss is approximately 0.8 - 1.0 % per year, which would represent a half lifetime of the reservoir of about 50 years without sediment management. As a consequence, a management strategy with a yearly conducted flushing with full drawdown was incorporated to overcome the progressive storage loss.

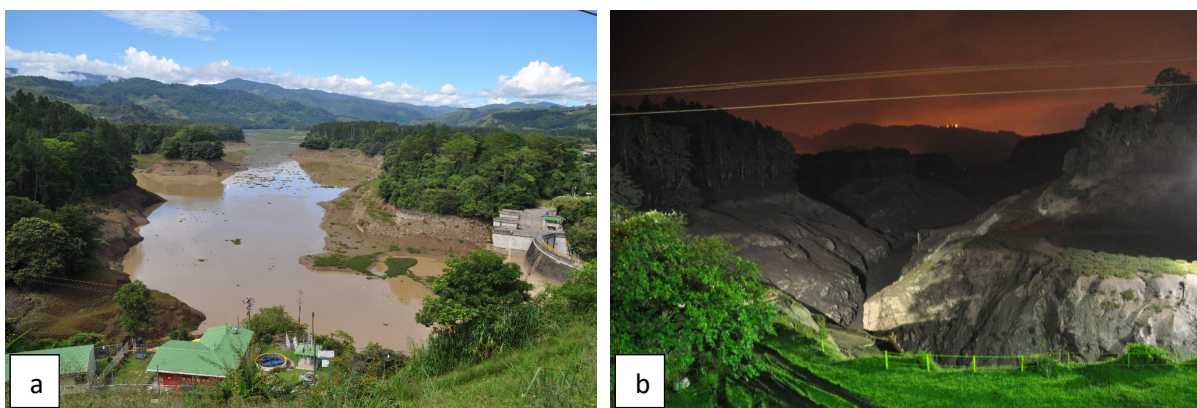


Fig. 32: Reservoir flushing operation at the Cachí reservoir, Costa Rica, in 2011 (a) during drawdown of the water level; (b) emptied reservoir during free flow conditions.

4.2 *The effects upstream*

The influence on flood events

Reservoirs themselves may act as a measure to improve the flood safety of the downstream river reach by storing water during flood events (cutting of the peak discharge) and releasing water after the event with a much smaller peak discharge, but for a longer time interval. Figure 33a shows for instance the operation of the Sylvenstein reservoir, Germany, during a flood event in 2005 (European Working Group on Dams and Floods, 2010). The Sylvenstein reservoir in Germany acts, as described in *chapter 1.2 Reservoirs as multipurpose structures – multi-stakeholder involvement*, as flood protection structure for the downstream located cities of Bad Tölz and Munich. The water level in the reservoir was, based on the flood forecast, lowered before the event to increase the available storage volume. During the flood event the reservoir was filled and only the amount of water was released, which would not result in damages in the downstream located cities of Bad Tölz and Munich (350 m³/s in figure 33a). Finally, water was released after the event to reestablish the normal operation conditions of the reservoir. Figure 33b shows the annual peak discharges at the downstream located gauging station in Munich for the time before and after the impoundment of the Sylvenstein reservoir. It can clearly be seen that the number of years with critical discharges decreased after the impoundment of the reservoir. In addition, the measurements show that for the flood events in 1999 und 2005 a clear decrease of the peak discharges, compared to the predicted ones without the storage volume of the reservoir, was achieved. If the available storage volume is reduced by sedimentation, also the amount of water, which may be stored during a flood event may be limited and may decrease the flood protection of the cities located in the downstream river reach. A reduction of the retention volume due to reservoir sedimentation would result in serious problems for these cities.

Reservoir sedimentation may in addition influence the upstream flood protection security. At the head of the reservoir (topset bed) bed levels successively rise when sediment depositions form a delta. These depositions result in higher water levels during flood events and as a consequence often in extended flood areas (Annandale, 1987). An example is the Lewis and Clark Lake (Gavins Point Dam) at the boarder of Nebraska and South Dakota, United States of America, where an increased flood frequency could be observed after the construction of the dam (Carter, 1991; Army Corps of Engineers Northwestern Division 2006; George, 2016).

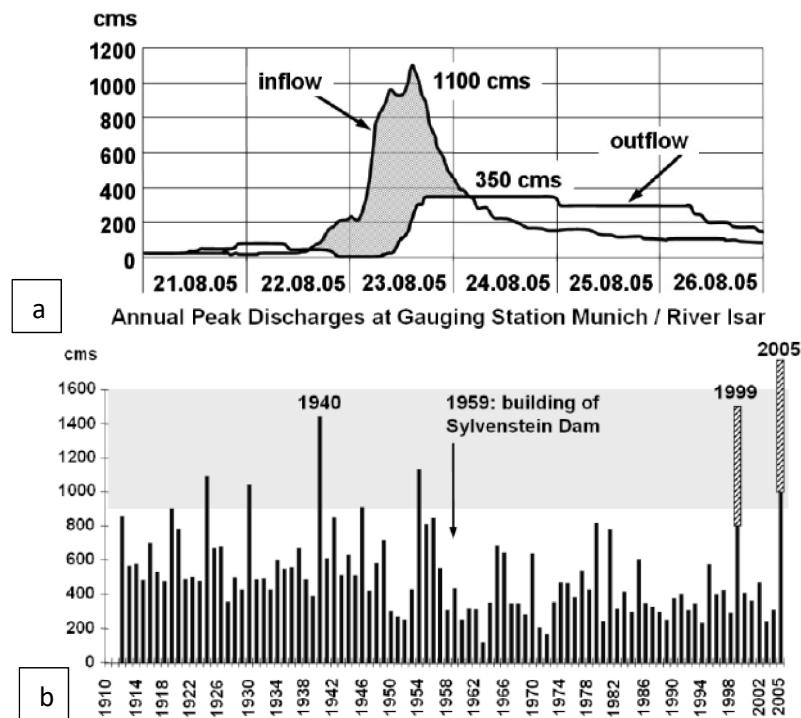


Fig. 33: (a) operation of the Sylvenstein reservoir during the flood event in 2005 (European Working Group on Dams and Floods, 2010); (b) annual peak discharges of the Isar River at the gauging station in Munich (European Working Group on Dams and Floods, 2010).

The influence on groundwater

Every anthropogenic measure within a natural river will have an influence on the surrounding groundwater table. The construction of dams and reservoirs is a distinctive interference of the system and leads to an increase in the water table upstream of the dam due to higher water levels within the reservoir compared to the water level in the origin river. Ashraf et al. (2007) presented in their study two small dams in Pakistan, where an increase in the water tables was observed by several meters. In this case the rise of the groundwater table made it possible for local inhabitants to have an easier access to fresh water and resulted also in a benefit regarding agricultural land use. In a contrary way, the increase of the water table, as a result of the construction of the Gavins Point Dam (Lewis and Clark Lake), led to problems in the upstream located town of Niobrara, Nebraska (Carter, 1991). The heightened groundwater levels flooded basements. As a consequence, the entire town had to be relocated to a higher elevation in the 1970s, which resulted in expenses of US\$ 14.5 million (Carter, 1991). However, such impacts are strongly depending on the connection of the surface water of the impounded reservoir with the connected aquifer, where the ability of infiltration has to be given. Hence, the interactions between surface water and groundwater have to be investigated prior to the construction of a reservoir. Reservoir sedimentation can further increase the heightening of groundwater levels, especially in the upstream part of the reservoir (topset bed), where

aggradation happens, resulting in an increase of the bed levels, the water levels and subsequently the water table.

4.3 The effects on the reservoir

4.3.1 Reservoir management and operation

Every reservoir has a scheduled management and as a consequence an operation plan. The operation is on one side depending on the size of the reservoir compared to the inflow and on the other side on the purpose of the reservoir. The simplest form of management is to fill the reservoir during seasons with high water inflow and release water during drier periods (e.g., drinking water reservoirs and reservoirs used for irrigation; figure 34). Such a reservoir is then operated in a monthly, seasonal, year-to-year or even as a multi-year storage reservoir.

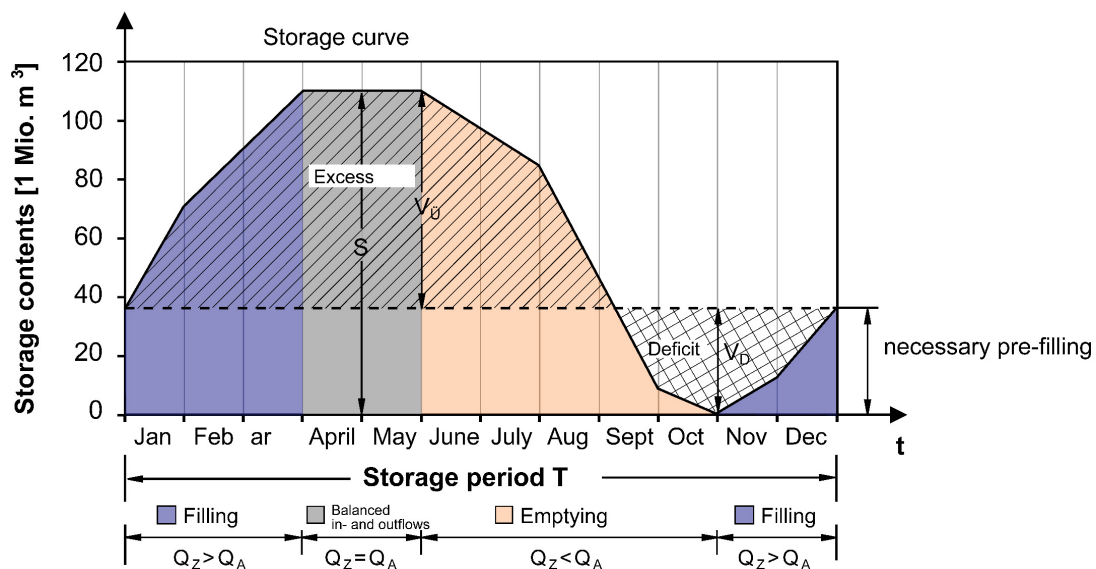


Fig. 34: Management of a year-to-year storage reservoir (Gebler et al., 2014).

As a result of the different purposes of reservoirs the operation and the management strategies may vary and as a consequence in- and outflow conditions may be adapted based on the given boundaries. Many reservoirs are as a result operated in a more flexible manner. For instance, if the reservoir is part of a pump storage hydropower plant, it serves as storage or buffers electrical energy. In case that too much energy is available water will be pumped into the reservoir; this may be the case during periods with a high energy production from wind or solar power plants. On the other side water will be released (turbine operation) during periods with a demand on electricity, which is also known as hydropeaking. In this case reservoirs have no static operation plan anymore and are operated only based on the given external boundaries. In this case the reservoir is managed based on the demand on energy by means of the market price of electric energy at the stock exchange.

If reservoir sedimentation occurs, its available storage capacity will be reduced and the management of the given reservoir has to be adapted. In case of progressive sedimentation of a reservoir and in case that no countermeasures are initiated, planned sediment depositions will increase and may even block the bottom outlets or enter intake structures. If the bottom outlets are blocked due to sedimentation, it is no longer possible to empty the reservoir in a controlled way. Furthermore, a safe operation of the reservoir is not feasible anymore. Consequently, emergency measures have to be initiated to ensure a safe operation of the reservoir. If sediments enter the intakes, the result is in many cases a damage of the hydraulic structures (Fan and Morris, 1992). The influence and damages of sediments on different structures of a hydropower plant can be seen in Figure 35. Figure 35a shows heavy wear of a sediment bypass tunnel in Switzerland (compare also *chapter 5.3.2 Bypassing sediments around the reservoir*). Especially larger sediments, which are transported as bed load, lead to damage of the concrete sealing of the tunnel. Figure 35b shows turbine abrasion due to the sediments coming from the Gepatsch reservoir, Austria, after the release of 15,000 tons of sediments during a controlled drawdown of the reservoir (Fernandes et al., 2016). Several factors influence the abrasion, namely: suspended sediment concentration, particle size distribution, particle shape, mineralogical composition and particle hardness as well as particle solid density (e.g., Duan and Karelin 2002; Felix et al. 2016).

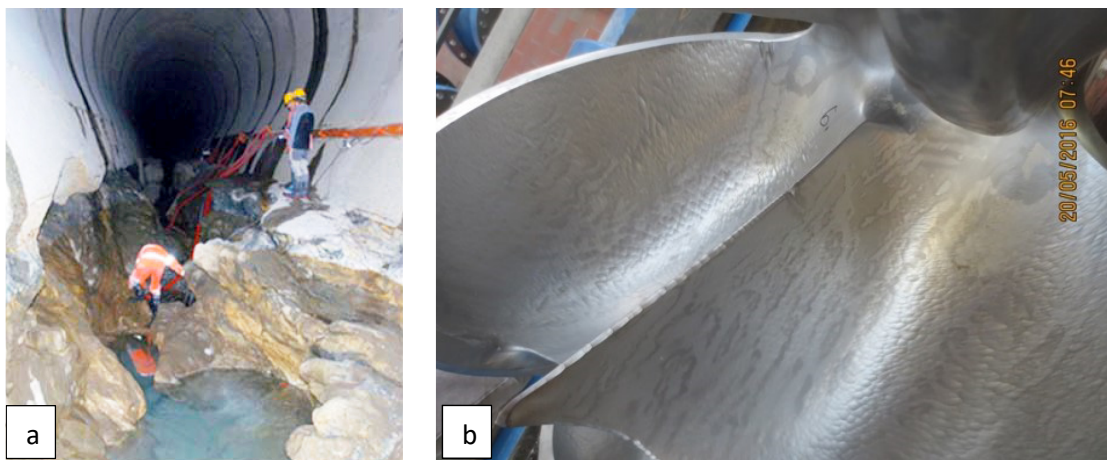


Fig. 35: (a) invert abrasion at Palagnedra sediment bypass tunnel in Switzerland (Boes et al., 2014; photo courtesy: Christian Auel); (b) turbine abrasion on the buckets of the Twin-Pelton turbines after release of around 15,000 tons of sediments from the Gepatsch reservoir (photo courtesy: Martin Schletterer).

4.3.2 A sink for pollutants and microplastics

The transport of fine sediments is probably one of the fastest transport mechanisms for pollutants in water bodies. Martin and Meybeck (1979) estimated that more than 90 % of the flux of phosphorus, nickel, manganese, chromium, plumb, iron and aluminum are transported in a sediment-associated way. Especially fine sediments (<20 μm) with a high surface-to-volume ratio have a high sorption to pollutants. Two of these pollutant groups should be

mentioned, which are emerging more and more in water bodies (the oceans as well as in freshwater) and which are important for water quality, habitat functionality and human health: namely micropollutants and microplastic particles. However, even if only two pollutant groups are mentioned within this chapter, dangerous substances in water bodies are manifold, but are very site specific due to the given boundaries within the catchment (e.g., degree of urbanization and industrialization).

Microplastic: The pollution of the world's oceans by plastic is one of the most formative issue that has moved our society for years. While the problem of macroplastics is becoming more and more visible due to larger accumulations and even the formation of floating islands (Lebreton et al., 2018), microplastic particles (MPP) pose an almost invisible but no lesser threat to our environment. According to the Marine Strategy Framework Directive, plastic particles of less than 5 mm in size, both spherical and fibrous, are referred to as MPP. A distinction is generally made between large MPP (1 - 5 mm) and small MPP (<1 mm). In many studies, however, only plastic particles <1 mm in diameter are referred to as MPP (see Figure 36a; Browne et al., 2008; Moore, 2008). These MPP are increasingly absorbed by organisms and can thus enter the human food cycle (Sanchez et al., 2014). In addition, MPP are often carriers of toxic substances in the environment, which aggravates the problem (Lee et al., 2014).

Microplastic particles in sediments were first reported by Thompson et al. (2004). However, in this study, as well as in Hidalgo-Ruz et al. (2012), the sampling and investigations are limited to microplastic in marine sediments. A study at Lake Ontario, Canada, has shown that microplastic of about 38 years of age can already be found at a sediment depth of 8 cm (Corcoran et al., 2014). First preliminary investigations of sediments in German rivers were carried out by Klein et al. (2015) on the banks of the Rhine and Main rivers, which showed up to 4,000 MPP per kg of sediment. One of the main challenges at the moment is the possibility to take undisturbed sediment samples, especially from large water depths (Liedermann et al., 2018) as well as the possibility to quantify the substance determination e.g., with optical methods (Braun et al., 2018; Scherer et al., 2020).

Reservoirs, which show the largest accumulations of sediments in inland waters, have not been considered so far for investigating the amount and the characteristics of MPP in freshwater systems. However, it is assumed that sediment depositions in reservoirs represent a long-term sink for MPP (Van Cauwenberghe et al., 2015). This leads to the necessity to investigate the essential role of reservoirs in the transport process of MPP in more detail (Nizzetto et al., 2016).

Micropollutants: Meanwhile more than 89 million chemical compounds are registered at the Chemical Abstract Service (Gerbersdorf et al., 2015), with an increasing tendency. This is a direct result of new approaching products of pharmaceuticals as well as personal care

products. In addition, steroid hormones, surfactants, industrial chemicals and pesticides reach the water bodies due to an insufficient treatment of sewage and a missing purification (Luo et al., 2014; Schwarzenbach et al., 2006). A continuous re-supply from diffusive entry paths and point sources leads to an increase in micropollutants, reported e.g., by Benner et al. (2013). Micropollutants may have a great ecological impact on habitat quality and are as a consequence a risk factor for humans, wildlife and the ecosystem functionality.

The prediction of fine sediment transport including attached contaminants is not trivial due to the occurrence of physico-chemical and biological processes, resulting in flocculation (see chapter 3.3 *Deposition*). As a result of the aggregation mechanism, the volume of particles increases resulting in higher settling velocity. Consequently, even fine particles settle in reservoirs. Reservoirs are therefore sinks for sediments and micropollutants. Due to the accumulation of sediments and associated substances even higher concentrations of micropollutants may occur in reservoirs.

Examples of contaminated fine sediment accumulations and associated problems are the reservoirs of the Iffezheim and the Marckolsheim barrages, located at the Upper River Rhine in Germany. As a result of historical industrial emissions of particle-bound micropollutants, sediments in these reservoirs are highly contaminated with hexachlorobenzene (HCB; Figure 36b; Pohlert et al., 2011). Measurements conducted in 2009 and 2001 in the reservoirs of Iffezheim and Marckolsheim showed values for the hexachlorobenzene concentration of 207 μg per kg suspended matter (Breitung, 2009) and 609 μg per kg suspended matter (International Commission for the Protection of the River Rhine (ICPR), 2009), respectively. Especially for the implementation of management strategies and the re-mobilization of sediments this fact is of high importance. In case that sediments will be re-suspended, pollutants will be transferred to the downstream part of the river, and in the worst case with an even higher concentration, as at the time when sediments settled (Gerbersdorf et al., 2011; Wölz et al., 2009). For the Iffezheim reservoir a relocation of the dredged sediments is restricted as a consequence of the high HCB-concentrations.

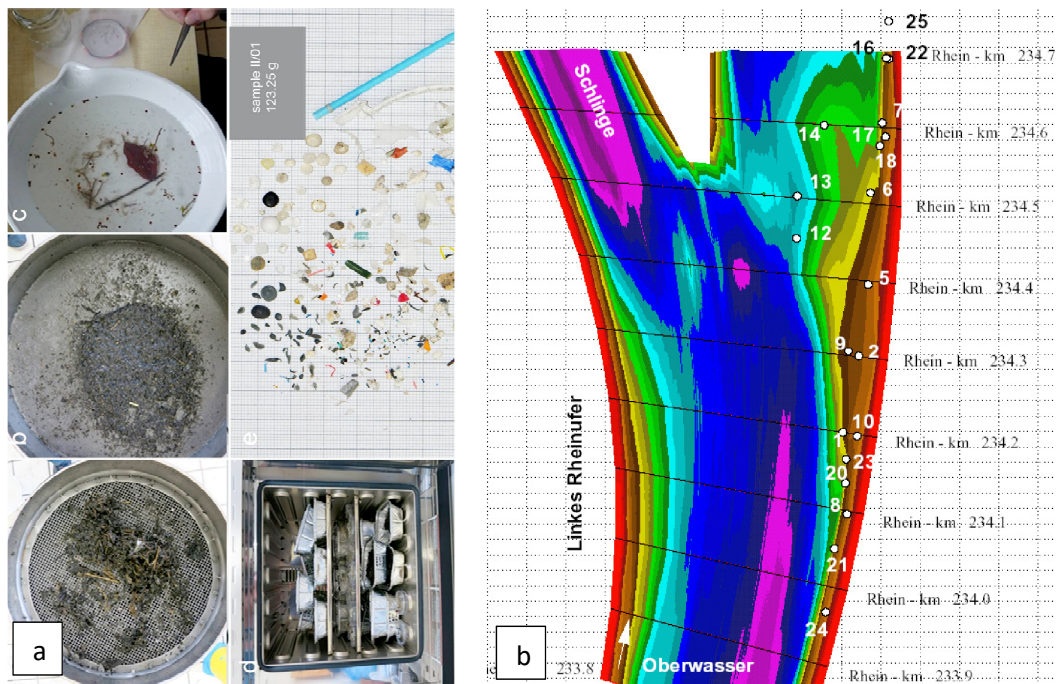


Fig. 36: (a) micro- and macroplastic particles sampled at the river Danube in Austria (Liedermann et al., 2018); (b) HCB contamination of sediments in the Marckolsheim reservoir at the river Rhine in Germany (Keller, 2008).

The production of greenhouse gases (GHG)

The most significant driver of climate change since the mid-20th century has been the greenhouse gases (GHG) produced by humans (IPCC, 2013). However, when analyzing water bodies, it can be seen that also inland waters contribute significantly to the total greenhouse gas budget by producing carbon dioxide (CO_2) and methane (CH_4) (Tremblay et al., 2005; Cole et al., 2007; Bastviken et al., 2011). The main reason therefore is the transport of organic matter within rivers, but also their settlement in lakes and reservoirs (figure 37). However, also domestic sewage, industrial waste and agricultural pollution may enter rivers and reservoirs, resulting in high GHG emissions (Kumar et al., 2011). Around 18 % of the global methane emissions are a result of inland waters, means natural water bodies and large reservoirs (Maeck et al., 2013). This is on the one hand, a result of microbial degradation of organic matter in oxic sediments (CO_2 production) and, on the other hand, a result of anaerobic pathways in e.g., freshwater sediments (CH_4 production). In reservoirs especially high depositional zones are often anoxic (Kennedy and Walker, 1990). However, the quantity and main pathways of emissions from reservoirs are still under debate. Lima et al. (2008) used a theoretical model, bootstrap resampling and data provided by the International Commission On Large Dams to quantify the methane emissions from large dams as renewable energy resources, by considering upstream and downstream CH_4 sources from large dams in Brazil, China and India. Encinas Fernández et al. (2020) presented in their study that the transport of methane-enriched water from shallow water zones is the major source of CH_4 in the open surface water of lakes rather than in-situ methanogenesis linked to algae growth. Maeck et al.

(2013) presented in a study a comparison between riverine and reservoir reaches along the Saar River, containing measurements of diffusive surface emissions, bubble flux emissions, seasonal ebullition measurements and sediment analysis. The results show that the reservoir reaches are the major source of CH₄ emissions. A study conducted by Tremblay et al. (2005) led to the conclusions that reservoirs and natural water systems produce similar levels of CO₂ emissions per unit area within a given region with similar ecological conditions. It could even be seen that natural waters may act as sink for CO₂.

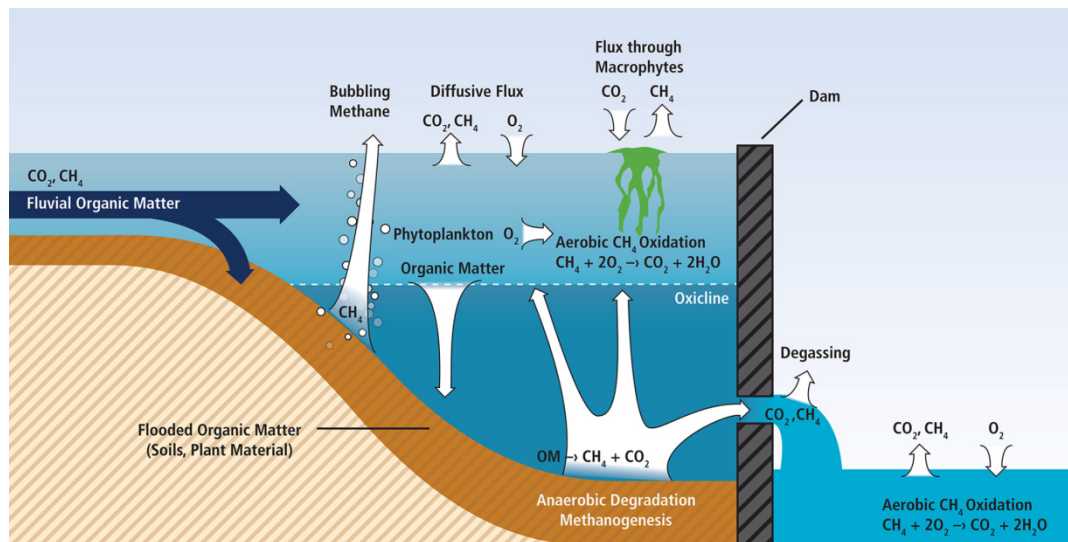


Fig. 37: Carbon dioxide and methane pathways in a freshwater reservoir with an anoxic hypolimnion (Kumar et al., 2011; adapted from Guerin, 2006).

4.4 The effects downstream

River bed degradation

Natural rivers are characterized by a dynamic equilibrium of the river bed (see chapter 2.2 *Transfer zone (rivers)*). However, the construction of reservoirs interrupts the sediment continuity, resulting in a reduction of the sediment supply downstream of the dam. A direct consequence of the missing sediment supply are downstream changes of the river morphology and as a consequence also a change from a stable river bed to a stretch with a progressive erosion tendency. This phenomenon, often called “hungry rivers”, will not only result in river bed erosion, but also in river bank erosion in case the river banks are not secured by river bank fixations. A special focus has also to be set on the scour depth in close vicinity to the dam, due to a possible negative influence on stability of the dam structure (dam failure). Consequently, before new dams and reservoirs are constructed a stable slope of the downstream river reach, depending on the new conditions, has to be calculated to evaluate possible bed degradation downstream of the dam. Figure 38 shows predicted bed degradation for the Stiegler’s Gorge dam in the United States of America as function of time (Lysne et al., 2003). The figure illustrates that the river bed degradation in close vicinity to the dam reaches

several meters and may result in a failure of the hydraulic structure. In addition, it can be seen that the erosion tendency will reach almost 90 km downstream of the dam within 30 years after the dam construction.

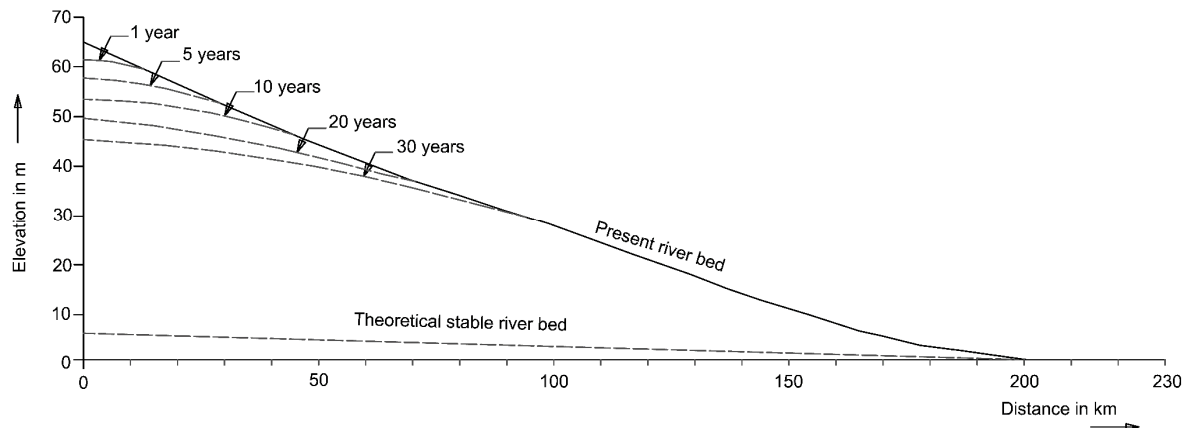


Fig. 38: Predicted river bed erosion downstream of the planned Stiegler's Gorge dam, USA (Lysne et al., 2003; modified)

In case a progressive bed erosion tendency is predicted as a result of the dam construction, certain measures have to be initiated to reduce or in the best case to avoid the ongoing river bed deepening. In principle measures can be subdivided in (i) an increase in the sediment supply from upstream (direct measure) and (ii) a reduction of the transport capacity of the river (indirect measure). In case of the dam construction and an interruption of the sediment continuity, only indirect measures are possible, such as changing the slope or the width of the river or by changing the boundary resistance, means the sediment characteristics within the river stretch downstream. Another and costlier countermeasure represents an artificial sediment supply. An example for this measure is the Iffezheim reservoir at the river Rhine in Germany. Here in average around 180,000 m³ of sediments are yearly artificially supplied downstream of the barrage to avoid ongoing river bed deepening (figure 39a; Weichert et al., 2010). This countermeasure requires accurate knowledge on the hydraulics and subsequently the transport capacity of the river. Often a monitoring program is affiliated to this measure to observe the transport of the artificial supplied sediments and to avoid a supply of too less or too much sediments. Especially in case of too much sediment supply, depositions may create flood protection problems due to higher bed levels. In smaller rivers also a sediment replenishment is possible. An example is the river Saalach, where the construction of the Kibling dam in Germany in 1913 resulted in a sediment deficit downstream of the barrage. As countermeasure sediment feeding was started in 1985. During the years 1985–1999, a total amount of 21,195 m³ of sediments was taken from the reservoir and was fed downstream as sediment replenishment. The sediment feeding has been intensified since 1999 and yearly about 50,000 m³ are dumped downstream of the reservoir into the river (Sadid et al., 2016). Figure 39b shows a sediment replenishment at

the river Inn in Bavaria, Germany, which was conducted within the residual stretch between the weir Jettenbach and the hydropower plant Töging.



Fig. 39: (a) sediment feeding at the river Rhine downstream of the Iffezheim reservoir, Germany; (b) sediment replenishment at the river Inn in Bavaria, Germany.

The influence on groundwater

If water is withdrawn from a reservoir, e.g., for water supply or for a diversion power plant, the released discharge to the downstream river stretch may be reduced, which results in lower water levels in the remaining river bed (residual water stretch). As a direct consequence, also the groundwater table may be influenced. However, the effect is often smaller compared to effect at the upstream part of the reservoir, because changes in the water level will not be that drastic in the downstream river reach compared to the impounded reservoir (Çelik, 2018). Depending on the residual discharge in the downstream river stretch even water logging from the groundwater may be observed, resulting in a loss of water, nutrients and salts of the soil (e.g., Baxter, 1977). A serious problem, often related to reservoir sedimentation, is downstream river bed erosion. In case of ongoing river bed degradation, the water level in the river may drop, resulting in an additional influence on the groundwater table. However, specific studies on this phenomenon are scarce; a general overview can be found in Winter (1998).

5 SEDIMENT MANAGEMENT STRATEGIES FOR RESERVOIRS

To find an appropriate sediment management strategy for a certain reservoir is not a trivial task and depends on several parameters such as the technical feasibility, ecological targets, water resources management as well as on economics. Within this chapter an overview on existing management strategies is given, including an overview of boundary conditions, methods and restrictions. For a more detailed overview the Reservoir Sediment Handbook (1998) by Morris and Fan or Extending the Life of Reservoirs (2016) by Annandale, Morris and Karki is recommended literature.

Reservoirs have a finite lifetime and are traditionally designed and built for a life span of 100 years (Morris and Fan, 1998). To ensure a safe operation of the reservoir, with respect to sedimentation, reservoirs are usually designed with a dead storage volume, where sediments deposit during the life span. Consequently, operation outlets, especially the bottom outlets, are located above this dead storage (see figure 16a) to ensure a safe operation even in case that reservoir sedimentation happens. The dead storage is often planned with a capacity for sediment depositions equal to the amount of sediments, which enter the reservoir within 20 to 40 years (Harb, 2013). Usually, it is assumed that the dead storage is located in the area close to the dam, but in reality often a downstream migrating delta is formed, resulting in sedimentation in the higher-elevation active pool area (see figure 17) and only partially in the dead storage in front of the dam (Morris and Fan, 1998). In such a case care has to be taken that the sedimentation does not result in a negative influence, such as flood problems in the area of the depositions. If the sediment yield or the trapping efficiency was not assumed correctly or in case of changing boundaries (e.g., changes in the sediment yield as a result of climate change) reservoir sedimentation may occupy also the operational storage volume. As a consequence, reservoir sedimentation should already be taken into account during the design phase and a sustainable sediment management strategy should be elaborated.

Countermeasures, implemented before the reservoir is constructed, have the benefit that a broad range of methods can be applied, which may be technically efficient, reduce the environmental impact and reduce finally also the economic losses. Examples are the construction of bottom outlets with sufficient capacity for reservoir flushing, the implementation of pipes into the dam, which can be later employed for hydrosuction or the construction of diversion tunnels, which can be used during the construction of the reservoir for diverting water to ensure a dry construction site and during operation as sediment bypass tunnels.

Since the 1990s more and more guideline documents with the subject of sediment management in reservoirs have been available (e.g., Kondolf et al., 2014; Peteuil, 2018; Sumi, 2006; Sumi, 2000; Batuca & Jordaan, 2000; García et al., 2008; Jenzer-Althaus and De Cesare, 2006; Morris & Fan, 1998; White (2001), Atkinson (1996), among others). The existing

literature shows that in the past most investigations focused mainly on large storage reservoirs with a large ratio between the initial storage volume (CAP) and the annual mean inflow (MAF), also called CAP/MAF-ratio (Harb, 2013). However, meanwhile also studies on small reservoirs, such run-of river reservoirs are more and more in the focus.

The existing literature recommends that investigations before the construction of the reservoir should include detailed information regarding the sediment yield coming from the catchment, the trapping efficiency of the reservoir itself, which depends on the shape, size, different possible operation modes of the reservoir and other factors, such as legal aspects, economic and ecological considerations. Atkinson (1996), Wen Shen (1999) and White (2001) defined in their work additional and more specified parameters, which have to be taken into account when evaluating the feasibility and the efficiency of sediment management methods. With this knowledge, reservoirs can be designed in a way that the expected storage loss does not reduce the lifetime, the operation plans or the safety of the reservoir.

From the perspective of sustaining reservoir capacity three main approaches exist to reduce or, in the best case to avoid the influence of sedimentation on the reservoir (figure 40). Whereas the first two approaches try to reduce the amount of sediment inflow and the depositions within the reservoir, the third approach deals with handling already deposited sediments and recovering of storage volume (Fan and Morris, 1992; Atkinson, 1996; Morris and Fan, 1998; Wen Shen, 1999; Batuca and Jordaan, 2000; White, 2001; Sumi and Kantoush, 2011; Kondolf et al., 2014).

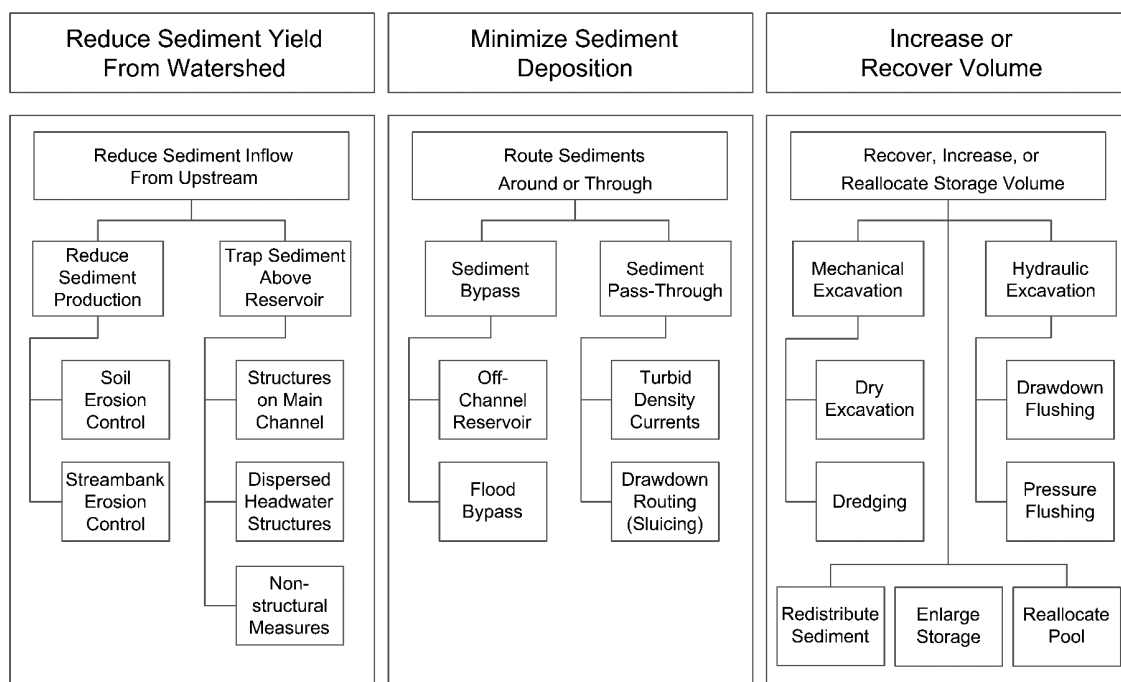


Fig. 40: Classification of possible sediment management strategies for reservoirs (modified after Kondolf et al., 2014).

As already mentioned, due to the different boundary conditions of reservoirs and the associated catchments it is impossible to find a general management strategy, which is the best solution for all reservoirs. Therefore, each reservoir needs a unique management strategy, which is tailored to the given conditions (reservoir and catchment). However, several researchers tried to categorize possible measures in a way that a rough estimation is feasible. As a result, it is possible to at least decide whether different management strategies are feasible or can be neglected. Annandale (2013) for instance evaluated existing sediment management strategies of different reservoirs, with respect to the relative sizes of reservoirs and the relative amount of inflowing sediments (figure 41). The figure shows that the choice of a sediment management measure depends strongly on the relative reservoir size (CAP/MAF) and the relative amount of inflowing sediments (CAP/MAS). The relative reservoir size is similar to the turnover rate of water, means it is the ratio of the reservoir volume (CAP) and the mean annual flow into the reservoir (MAF). The relative amount of inflowing sediments is the ratio between the volume of the reservoir (CAP) and the mean annual volume of sediment flowing into a reservoir (MAS). This number is a clear indicator whether the sediment load can be classified as high, moderate or low. Especially small reservoirs with a high turnover rate (e.g., run-of river reservoirs) and with relatively high sediment loads, are often managed by reservoir flushing with full drawdown (relative size of the reservoirs between 0.0001 and 0.04 times the mean annual inflow). The management strategy for somewhat larger reservoirs and relatively lesser amounts of sediment inflow tend to be flushing with partial draw down, sluicing, bypassing or dredging (relative size of the reservoirs between 0.001 and 0.4 times the mean annual inflow). These are reservoirs in between run-of river reservoirs and carryover storage sizes. For even larger reservoirs and smaller sediment inflow, compared to the initial volume of the reservoir, check dams are often used. In case turbidity currents occur, density current venting is performed as management strategy. Figure 41 shows that not all implemented sediment management strategies of the different reservoirs are sustainable, even if in the design phase an evaluation of the success of the methods was made. In addition, it should be kept in mind that the presented management strategies were just evaluated with respect to their sustainability. A focus on environmental compatibility was not made.

Within the next subchapters an introduction to the different available management strategies is given.

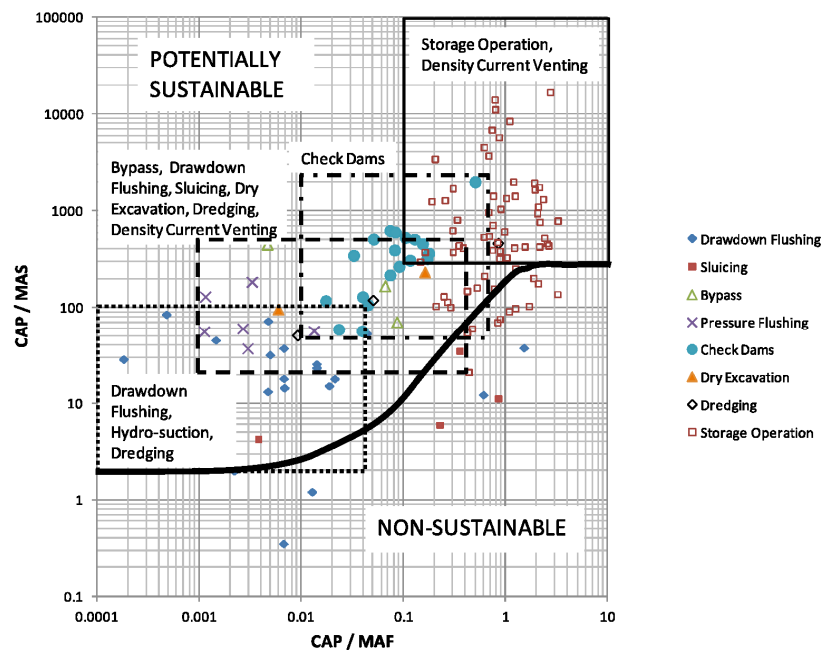


Fig. 41: Reservoir sediment management measures implemented in different reservoirs with different relative reservoir size (CAP/MAF) and different relative amounts of inflowing sediments (CAP/MAS) (Annandale, 2013).

5.1 *Accepting reservoir sedimentation*

In case that the mean annual volume of sediment inflow is small compared to the reservoir volume (high CAP/MAS ratio), the simplest management strategy is to accept reservoir sedimentation (storage operation in figure 41). In this case the dead storage of the reservoir is usually sufficient to store sediments during the lifetime of the reservoir. An example of this is the Finstertal reservoir in Austria with a reservoir volume of 60 mio m³ and relatively small sediment inflow from the catchment, as a result of the small catchment area and the comparative hard bedrock (figure 42a). Owens and Slaymaker (1994) presented sediment yields of only 2 t/km²/yr in small undisturbed alpine catchments as a result of erosion-resistant granitic parent bedrock. Other catchments with a low sediment production and as a consequence small sediment yields are for instance catchments located in the Northern parts of Europe, where glaciers have removed the upper soil layers and the bedrock can be quantified as not erodible due to the hardness of the rock (Haun and Olsen, 2012). The analysis of bathymetric data of the Schwarzenbach reservoir, located in the Black Forrest in Germany (figure 42b), showed a reduction of storage volume between 1926 and 2018 of around 331,382 m³ from the initial reservoir volume of 14.4 mio m³, which represents a sedimentation rate of only 2.3 % within 86 years of operation (Urban et al., 2006; Mouris et al., 2018; Saam et al., 2019). In the case of the Schwarzenbach reservoir this is a result of the small catchment area (only about 50 km²), small gradients and the large area of forest within the catchment, where the erosion rate is generally small. The Schwarzenbach reservoir and the Finstertal reservoir show that beside the soil cover in the catchments also the size of the catchment and

the composition of the rock is of high importance. Especially high head reservoirs have comparably small catchment sizes. However, in case of high head reservoirs care has to be taken if parts of the catchment are partially glaciated, as this may change the sediment production and consequently also the sediment yield (Ehrbar et al., 2017).

An extensive study regarding the production of sediments and the sediment yield was conducted by Jansson (1988), where suspended sediment data from 1,358 gauging stations of tributaries from watersheds with areas between 350 and 10,000 km² were analyzed. The result showed that watersheds with specific sediment yields smaller 50 t/km²/yr represent nearly half of the total land area of the analyzed watersheds. However, it is important to have reliable data and predictions regarding the sediment yield coming from the catchment during the pre-feasibility studies to e.g., optimize the size of the dead storage volume of the reservoir. During these studies also the possibility of occurring unforeseen anthropogenic activities (e.g., land use changes) or natural events (e.g., wildfire or mass wasting) have to be taken into account. Ryan et al. (2011) presented data from changing annual sediment yield from the Little Granite Creek watershed, Wyoming, USA, which was in the first post-fire year five times higher compared to data based on the 13 previous runoff seasons. In addition, also possible effects of the changing climate should be considered to avoid negative consequences on the operation on a long term. Lu et al. (2013) showed in a preliminary study based on data from eight large Chinese reservoirs that a 1 % change in precipitation results in a 2 % change in sediment loads.

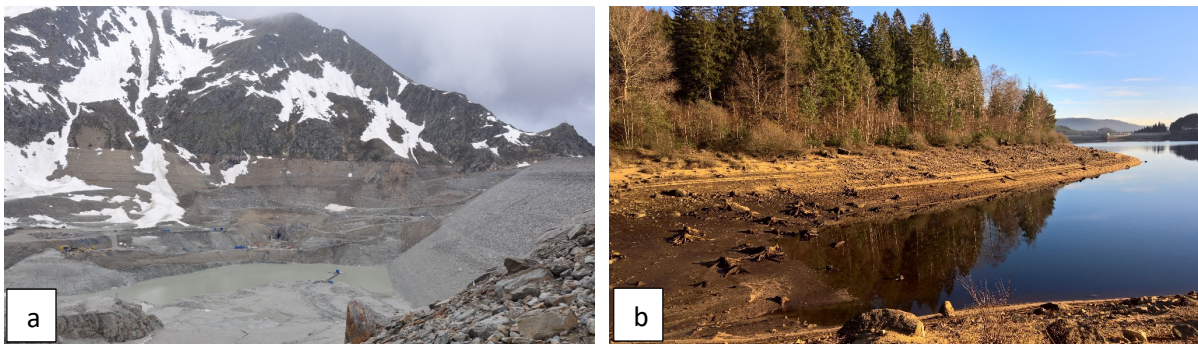


Fig. 42: (a) Finstertal reservoir in Austria during an operational draw down; (b) Schwarzenbach reservoir in Germany with lowered water level as a result of pump storage operation.

5.2 *A reduction of the quantity of inflowing sediments*

In general, two different approaches can be found in the literature for reducing the quantity of inflowing sediments into reservoirs: the application of ecological and structural conservation measures in the catchment, which result in a reduction of the sediment yield coming from the watershed (e.g., by soil erosion control) and the construction of a single or a multiple number of pre- and check dams in the main stream or the tributaries upstream of the reservoir to trap sediments before they reach the reservoir.

5.2.1 Ecological and structural conservation measures

Reservoir sedimentation is often called the symptom of a sick patient, where the patient is in this case the catchment. This statement indicates that only direct measures can make it possible to bring the system back to dynamic long-term equilibrium conditions and to deal with the challenge of reservoir sedimentation in a sustainable way. This would mean that sustainable measures to avoid reservoir sedimentation can only be realized within the catchment itself and not within the water body. Therefore, many researchers have focused their work on management strategies within the catchment to modify the runoff and the inherent hydraulic conditions and subsequently the soil erosion processes. Conservation measures within the catchment can generally be divided into ecological and structural conservation measures (Bureau of Economic Geology, 2020; figure 43).

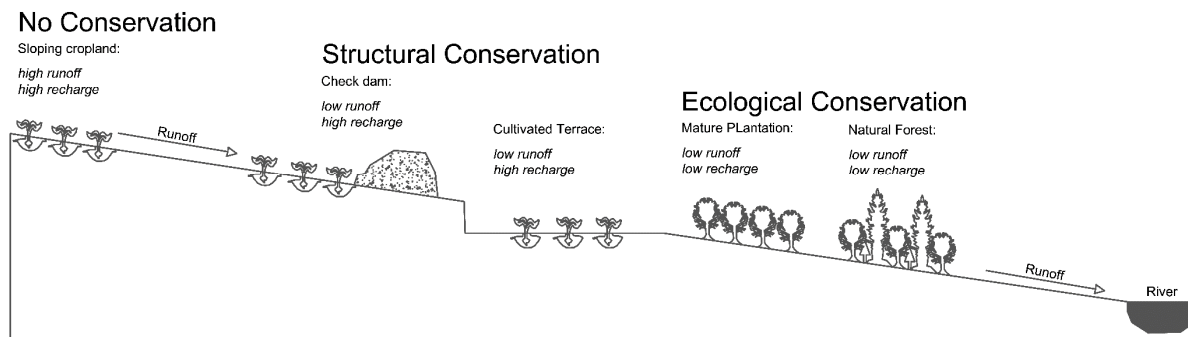


Fig. 43: Conceptual overview of soil conservation measures within a catchment.

Ecological Conservation

An important factor for the production and the transport of sediments within the catchment is vegetation (Blöschl, et al., 2019; Bronstert et al., 2014). The erosion rate of forest is compared to grassland ten times and compared to farmland two hundred times smaller (Morris and Fan, 1998). As a consequence, the most applied management strategies in soil conservation practices (ecological conservation) within the catchment deal with maximizing the vegetation cover to reduce the amount of soil which is prone to erosion (e.g., Chitata et al., 2014). In addition, the vegetation may be adapted or the production of agricultural products changed. The methods often used are the implementing of grassed waterways, riparian buffers in agricultural crop and grazing land as well as afforestation. Especially areas where the land cover changes as a result of human interventions, like deforestation or land clearance for agriculture or as result of wildfire, it is important to recover the vegetation cover to protect the soil against erosion and to avoid an increase in the sediment yield (figure 44a). Figure 44b shows an example for intense erosion, as a consequence of scarce soil cover and high precipitation in the area of Las Médulas, Spain. The disadvantage of ecological measures is that the positive impact on the system will need several years to decades compared to structural measures. However, such measures are necessary to preserve cultivated soils for agriculture and to prevent from mass wasting (Harb, 2013).

Hence, it is often recommended to combine these non-structural soil conservation measures together with other reservoir management methods, which are successful in a short term and can on a long term be reduced based on the observations (e.g., Bechteler, 2006; Batuca and Jordaan, 2000; Morris and Fan, 1998).

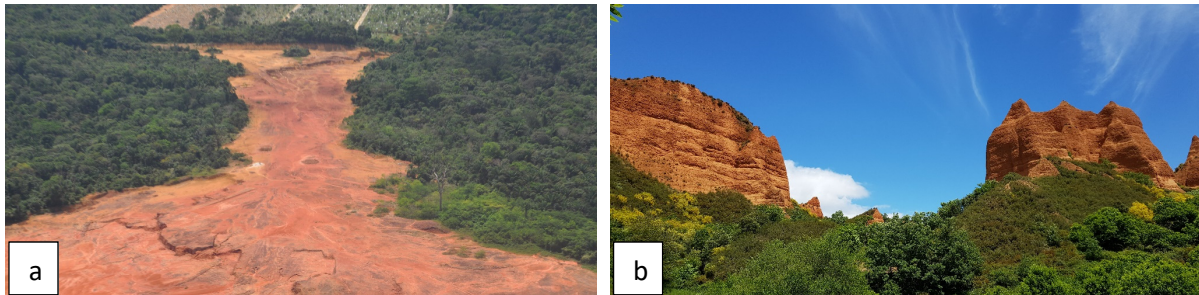


Fig. 44: (a) local deforestation in Manaus, Brazil, resulting in higher surface runoff and subsequent soil erosion; (b) ongoing soil erosion as consequence of precipitation and a limited soil cover.

Structural Conservation

Another approach are structural conservation measures with the goal to reduce the stream power of the surface runoff. An example is the implementation of terraces (figure 45a), which serve as runoff management structures (Foster, 2005). Terraces are topographic modifications of hillslopes, which result in a shortening of the overland flow path length and in reducing the land slope. Consequently, rill and interrill erosion (compare figure 45b) is reduced. As an alternative structural conservation measures are a possibility to stabilize slopes and banks (Bechteler, 2006). Also measures to reduce active streambank erosion in tributaries and rivers is a possibility to reduce the sediment production and as consequence also reservoir sedimentation (Fox et al., 2016).

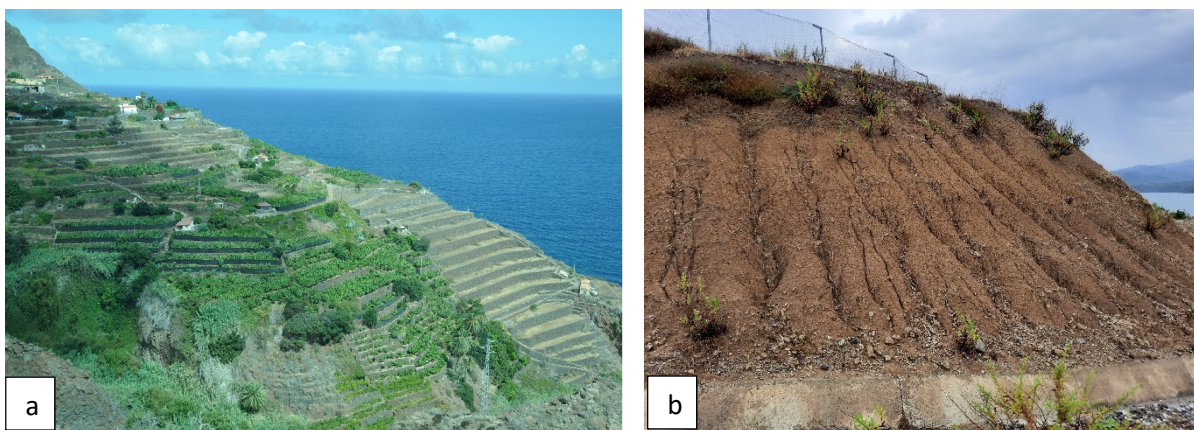


Fig. 45: (a) Orchard terraces for farming on La Gomera Island, Spain; (b) hillslope with developed rill network at Gramsh, Albania, in 2021.

The development of adequate erosion control measures in the catchment is a difficult task and several ineffective case studies have been reported (Morris and Fan, 1998). A method often used to predict the success of such measures is the application of soil erosion models.

The USLE (Universal Soil Loss Equation) model and its successor the Revised Universal Soil Loss Equation (RUSLE) model are widely adopted as the major soil conservation-planning tools, where the components of these equations are the results of extensive analyses of a large number of data, gained mainly in the United States (Renard et al., 2011; Kenneth et al., 1991; Wischmeier and Smith, 1978). The USLE/RUSLE models are basically used to estimate long-term average sheet, rill and interrill upland soil erosion due to raindrop impact and surface runoff on uniform sloped fields. The RUSLE model combines six empirical erosion factors that form a linear relationship with the amount of soil loss. These factors are the erosive power of a rainfall-runoff factor (R-factor), the erodibility factor (K-factor), the combined slope length and gradient factor (LS-factor), the ground cover condition factor (C-factor) and the conservation practice factor (P-factor). In ArcGIS these factors are linked as overlaying raster. The raster, which uses a grid cell representation of landscapes, assumes that each grid cell is a homogenous morphological unit with respect to the above stated factors and enables subsequently an estimation of the average annual soil erosion for any given cell (Kinnel, 2000, 2010). To predict changes in the soil erosion as a result of ecological and structural measures, the conservation practice factor as well as the erodibility factor, the combined slope length and the gradient factor as well as the ground cover condition factor can be adapted.

5.2.2 *Pre- and check dams*

The second approach is an upstream sediment trapping, either by a single structure (pre-dams) in the main steam of the river or a multiple number of smaller structures in the tributaries (check dam). Pre-dams are structures located right upstream of the reservoir with the purpose to trap sediments before they enter the reservoir. In principle these structures act like the reservoir itself, where due to a reduction of flow velocities, turbulences and bed shear stresses a trapping of gravel and in some parts also sand occurs. Figure 46a shows the pre-dam of the Kleine Kinzig reservoir in Germany, seen from downstream and figure 46b shows gravel and mainly sand, trapped within the small reservoir of the pre-dam. The figures illustrate that the depositions in the small upstream located reservoir almost reach the water surface. This example also shows that pre- and check-dams need maintenance during their life-time to fulfil their purpose.

In case that check-dams, located at the tributaries within the catchment, are chosen the number of structures is higher, but they are usually smaller compared to a single pre-dam. Often these structures are also build for protection of people in the surrounding areas from mud flow flooding.

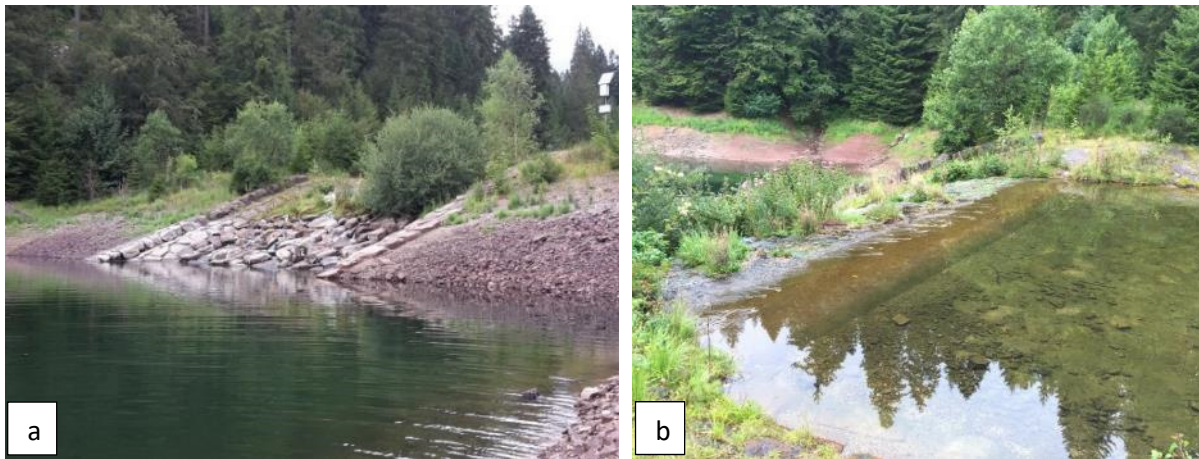


Fig. 46: Pre-dam of the Kleine Kinzig reservoir, Germany (a) view from downstream; (b) view into the pre-dam.

Figures 47a-b shows a check-dam at the Schallerbach creek in Austria, which serves mainly as protection structure. In high altitude areas such structures are constructed to trap mainly coarse sediments; fine sediments will not be trapped. However, sediment inflow into the reservoir can never be avoided completely (Scheuerlein, 1990). Care has to be taken in the case of implementing check-dams regarding the river stretch between the structure and the main reservoir. In case that check-dams are located far upstream of the reservoir, it may happen that these structures reduce the sediment supply. This results in disturbed equilibrium conditions in the upstream section of the river (between the check-dam and the reservoir). Subsequently, the stream power dominates, resulting in the worst case in ongoing river bed erosion, a river pavement and in a deficit of habitat conditions (Hauer et al., 2020a; 2020b).

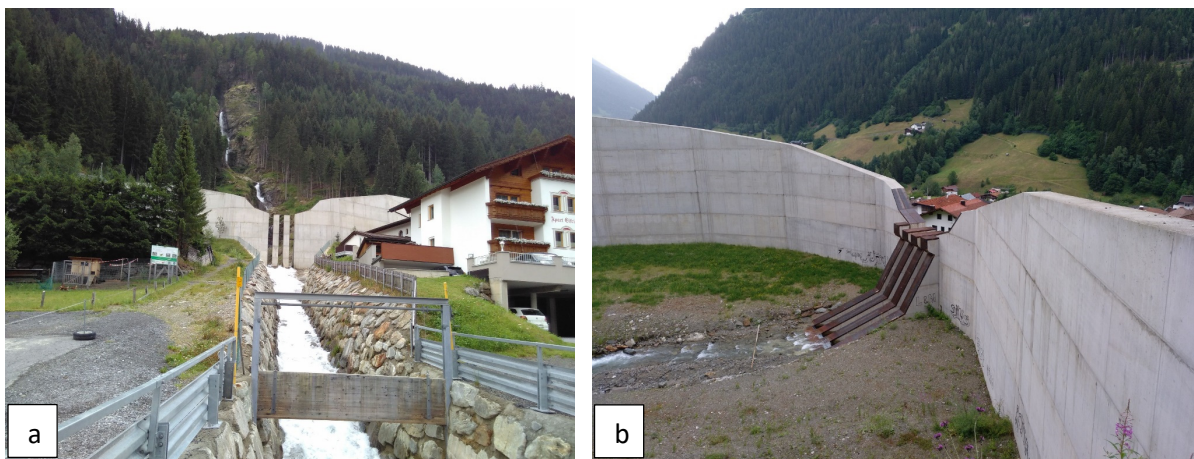


Fig. 47: Check-dam of the Schallerbach, Austria (a) view from downstream (photo courtesy: Silke Wieprecht); (b) view into the check-dam (photo courtesy: Kilian Mouris).

5.3 *Avoiding settling of sediments within the reservoir*

A minimization of sediment depositions in reservoirs can also be achieved by routing sediments through the reservoir or by bypassing sediment laden flows around the reservoir by the use of sediment bypass tunnels. Both methods are particularly suitable in areas with distinctive wet or monsoon seasons, where the majority of sediments enter the reservoir within a short time period. An example is Northern China, where around 80 - 90 % of the annual sediment load is transported by only 25 - 50 % of the annual runoff (Fan and Morris, 1992). The runoff, but also the storage volume and the loss of water are important factors when evaluating the suitability of these management tasks, because a large amount of water will be directly delivered to the downstream region and will not be stored within the reservoir for later use.

5.3.1 *Routing sediments through the reservoir*

When routing sediments through a reservoir a balance has to be found between forces leading to sediment depositions and forces keeping sediments in transport. In most reservoirs this can be achieved by lowering the water level during high discharges and subsequent high sediment laden inflows. By lowering the water level flow velocities as well as turbulences increase compared to normal operation with high water levels. These conditions lead to a reduction of sediment depositions within the reservoir. At the same time the spillway gates (if possible due to their location) and/or the bottom outlets will be opened to release the sediment laden flow from the reservoir. When a chain of power plants is located within a river, sediment management strategies have to be aligned to each other. In case of routing sediments through one reservoir, sediments would otherwise deposit in the downstream located reservoirs, which has to be avoided. An example is the sediment routing through the Angostura reservoir in Costa Rica (Figure 48a). At the same time when the upstream located Cachí reservoir is flushed, the water level in the downstream located Angostura reservoir is lowered and sediments can pass-through the reservoir and will so minimize the expected depositions within the Angostura reservoir.

In case that during the sediment routing the bottom outlets will be opened to release the sediment laden flow, in addition a flushing cone (flushing with partial draw down) may form in front of the bottom outlet (see also *chapter 5.4.3 Reservoir flushing*), means local sediment erosion will occur within the reservoir. However, creating additional erosion is not the main purpose of sediment routing. Morris and Fan (1998) divide this method into three categories, namely:

- (i) Seasonal drawdown (partial or complete),
- (ii) drawdown before floods, based on upstream gauges or hydrological forecast or
- (iii) density current venting.

A special form of sediment routing is density or turbidity current venting (figure 48b). Density currents are stratified flows and are driven by gravity and due to differences in density (see chapter 2.3 *Depositional zone (oceans/reservoirs)*). When sediment laden flow enters the reservoir, the current usually plunges at a certain point and moves near the bottom directly to the low-level outlets, where they transform to a submerged muddy lake (De Cesare, 2006; Schneider et al., 2012a). However, turbidity currents occur suddenly and only rough estimations about their occurrence can be made. An adequate real time monitoring is therefore essential to detect the emergence of a current and to operate the reservoir and the gates immediately. Due to the physical processes, e.g., travelling along the bed, sediments carried by density currents can pass through the reservoir without a drawdown of the water level in the reservoir. Examples for a successful use of this management method were reported by Morris and Fan (1998) for the Lost Creek reservoir in Oregon, United States of America or for the Sanmenxia reservoir in China.

One disadvantage of sediment routing is that sediments are sluiced through the outlet structures. These structures are operated during the measure under pressure conditions. The occurrence of high flow velocities in combination with a high sediment concentration may harm the structure (e.g., the bottom outlets) by abrasion or even by blockage (Auel and Boes, 2011; see chapter 4.3.1 *Reservoir management and operation*). The risk might be smaller if both bottom and upper outlets, such as spillways, are used; however, possible turbine wear or abrasion of the hydraulic structure have to be considered (Auel and Boes, 2011; Schleiss et al., 2010).

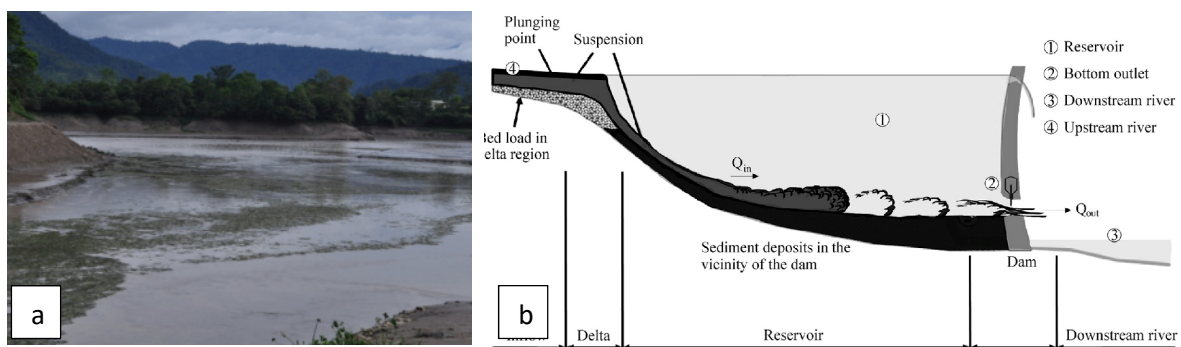


Fig. 48: (a) Angostura reservoir in Costa Rica with a lowered water level for routing sediments coming from the upstream located Cachí reservoir in (view from the dam upstream); (b) sketch of a turbidity current, travelling along the bed of the reservoir (Chamoun et al., 2016).

5.3.2 *Bypassing sediments around the reservoir*

The basic principle of bypassing sediments is that high sediment laden flows, e.g., during flood events, do not enter the reservoir. A sediment bypass system, mostly conducted as sediment bypass tunnel, is a method to route suspended but also bed load around the reservoir and the dam and divert the flow directly into the tailwater. During this period no water will be stored within the reservoir. An alternative form is to route these sediment laden flows into an off-

stream reservoir, where sediments settle and the clear water will be released at a later time. However, this option is conducted very seldom due to the fact that an additional reservoir has to be constructed and maintained.

In general, the intake of the bypass system is located at the head of the reservoir, in a small number of cases also within the reservoir. Most often the intake is constructed together with an upstream located guiding structure or a check dam (Auel & Boes, 2011). Especially the tunnel design is of high importance for the success of a bypass system. Its dimensions depend on the design discharge (up to a 100-year return period; Boes & Reindl 2006), but also on the expected sediment characteristics. Especially for bed load dominated fractions hydro-abrasion of the tunnel invert is reported (see figure 35a) e.g., by Vischer et al. (1997), Sumi et al. (2004) or Auel et al. (2018) and an additional steel lining could be a necessary measure. Downstream of the dam the flow will be diverted back into the river, where in some cases a plunge pool is necessary due to the high flow velocities within the bypass tunnel.

Sediment bypassing can be either scheduled, e.g., during a monsoon period, or operated with a reliable monitoring system. Successful sediment bypass systems have been implemented in Japan at the Nunobiki dam, the Asahi dam, the Miwa dam and the Matsukawa dam as well as in Switzerland at the Palagnedra dam, the Pfaffensprung dam, the Rempen dam and the Runcahez dam (Sumi et al., 2004).

From an ecological point of view sediment bypass systems have the advantage that only sediments from the upstream river stretch will be diverted into the downstream located river and no additional sediment will be eroded from the reservoir bed (Auel & Boes, 2011). However, also for sediment bypass tunnels the ecological impact has to be considered. In case of a diversion power plant with a minimum residual flow, problems may occur when introducing high sediment laden flows to river reaches (Auel et al., 2017).

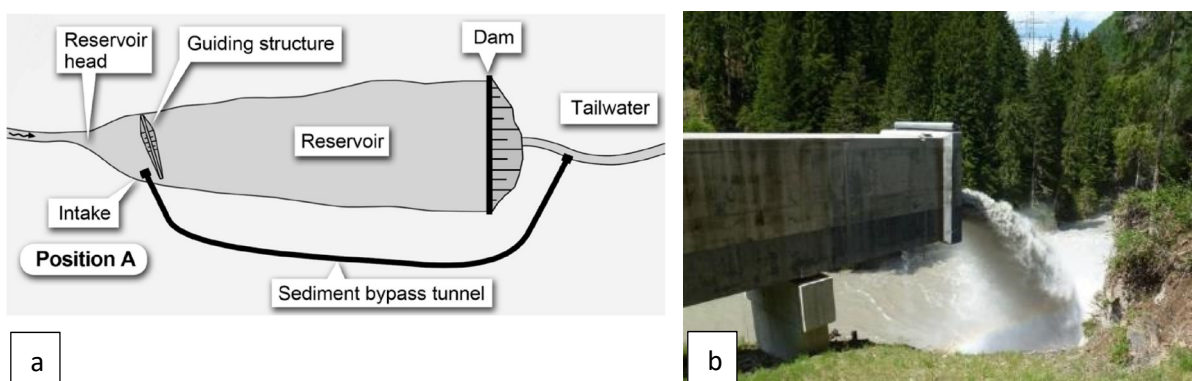


Fig. 49: (a) sketch of a sediment bypass tunnel system with the tunnel intake at the head of the reservoir (Auel & Boes, 2011); (b) outlet of the Solis sediment bypass tunnel, Switzerland (photo courtesy: Christian Auel).

5.4 *Removing accumulated sediments*

In case sediments deposit in the reservoir, which may have a negative influence on the operation or reduce the available storage volume, measures need to be implemented to recover already lost storage volume. However, even if it sounds as an easy task to remove these already accumulated sediments from reservoirs, this management strategy is one of the most difficult ones to implement. The reason therefore is manifold. First of all, it is difficult to predict the technical feasibility and the success of such a measure due to the given conditions, this kind of measure is often expensive and from an environmental point of view high standards are set. From a technical point of view, the challenge is to find a suitable method for the specific reservoir with its specific boundaries. Due to different parameters of the reservoir itself, the hydrological conditions, sediment properties as well as other factors, like clauses given by the authorities, environmental protection issues but also economic considerations the feasibility and efficiency of different sediment management strategies varies. A complete list of influencing parameters is very site specific. However, an overview about the main influencing parameters, in accordance to Atkinson (1996), Wen Shen (1999), White (2001), Haun (2012) and Harb (2013) is given.

- (i) Type, geometry, volume and configuration of the reservoir and the downstream river section,
- (ii) hydrological conditions such as, discharge rating curves as well as duration and magnitude of floods and the possibility of forecasting a flood,
- (iii) hydraulic structure and machinery, including maximum outlet discharge and minimum drawdown of the water level,
- (iv) legal aspects such as duration of the measure, allowed water level lowering per hour, suspended sediment concentrations, minimum oxygen concentration, chemistry, disposal possibilities,
- (v) sediment inflow, sediment properties and state of sedimentation (quantity, grain size distribution, contamination, organic and toxic content).

Existing approaches to remove already accumulated sediments can be subdivided into two categories, namely measures based on mechanical intervention (conventional mechanic dredging and hydraulic dredging) and measures governed by hydraulic forces (drawdown and pressure flushing).

5.4.1 *Conventional mechanic dredging*

Conventional mechanical dredging of sediments is carried out either by the use of bucket dredges, in case the water of the reservoir cannot be released or by dry excavation of the reservoir for cases where it is possible to empty the reservoir completely.

The use of a bucket dredge is more or less for all reservoirs a possible management method. The huge benefit is that there is no need to release water from the reservoir, which will avoid economic losses and will not influence the operation of the reservoir. Figure 50a shows a bucket dredge at the Schönau reservoir in Austria (Harb, 2013). Within this reservoir flood events with a return period larger 10 years carry and deposit sediments in front of the turbine inlets at the orographic right side of the barrage (Harb et al., 2014). These depositions are removed after each event to ensure a safe re-start of the turbines. The use of a bucket dredge is limited to small amounts of sediment depositions and/or to local sedimentation problems (Batuca and Jordaan, 2000). As a consequence, this method is often used in front of intakes, bottom outlets or other hydraulic structures to ensure a safe operation of the hydraulic structure. For large quantities of sediment depositions this method is often economically not sustainable (Wen Shen, 1999). When implementing this measure, it has also to be clarified what happens with the dredged sediments, especially from an environmental point of view. Depending on the composition of the sediments and the national laws, dredged sediments can be either fed back to the river, withdrawn from the reservoir and used as construction material e.g., as aggregate in concrete, or have (see also *chapter 4.3.2 A sink for pollutants and microplastics*) to be disposed or treated in a special way in case that contamination occurs, which increases the costs by an order of magnitude or even more (DWA, 2019).

A very rarely conducted measure is dry excavation of the reservoir (Figure 50b). The main reason is that the reservoir has to be emptied completely so that heavy apparatus can be deployed to remove the sediment depositions from the reservoir. Compared to a bucket dredge a larger amount of sediments can be excavated in a much shorter period. An important point when considering this measure is the volume of the reservoir compared to the annual inflow. Due to the complete release of water this method works better for reservoirs with a small storage capacity compared to the mean annual runoff. However, in smaller reservoirs, with a small CAP/MAF care has to be taken, that the inflow discharge into the reservoir is low during the measure to ensure a safe operation of the apparatus. For large reservoirs the measure has to be evaluated from an economical point of view, where the advantage (new gained storage volume) and disadvantage (loss of stored water) have to be weighed against each other. Bechteler (2006) also concluded that this measure works best in wide shallow-water areas, where other management strategies fail. Another point is the characteristics of deposited sediments. This method works best in cases where coarse sediment particles have settled. The reasons are that the employed heavy apparatus needs a stable underground and that fine sediments contain a fairly large amount of water in their pore space and, compared to coarse sediments, will not dewater that quickly when the water is released from the reservoir.

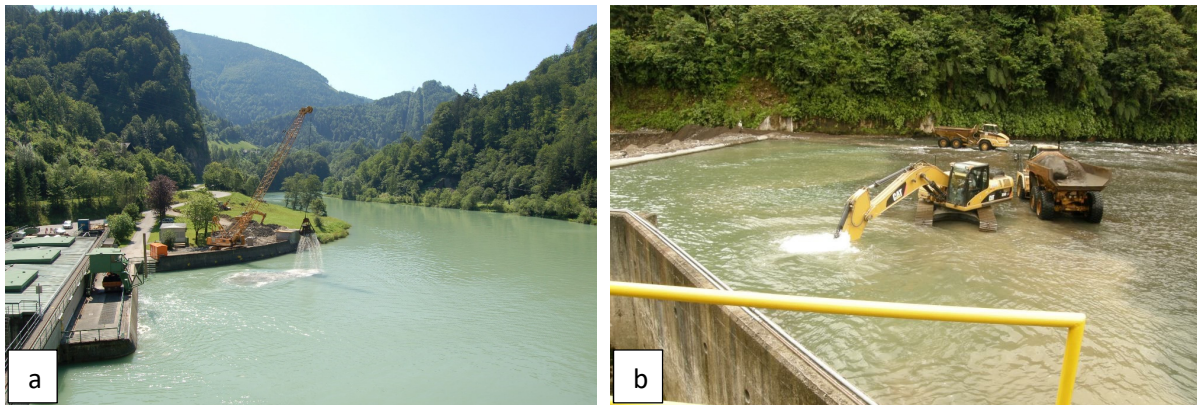


Fig. 50: (a) bucket dredge in operation at the Schönau reservoir in Austria in front of the turbine inlets (Harb, 2013); (b) dry excavation at El General reservoir, Costa Rica (photo courtesy: Alberto Jimenez).

5.4.2 *Hydraulic dredging*

Hydraulic dredging combines different dredging systems to erode sediments from the reservoir bed and transport the emerging mixture of water and sediments through a slurry pipe system either downstream of the dam, on a disposal site or on a vessel for dewatering and further use. In reservoirs either suction dredges are used, often in combination with a water jet, which dredge loose sediments from the reservoir bed (due to the fine sediment depositions used very rarely) or cutter suction dredges, which uses a cutter head to erode compacted sediments (used in most cases). Figure 51 shows a cutter suction dredge with cutter head, installed at the Peñas Blancas reservoir in Costa Rica. During operation the cutter head moves around a spud pole and erodes the deposited sediments (Vlasblom, 2005). The eroded sediments are then sucked away by the device and transported as slurry through a pipeline to the final destination. A special focus should be set on the cutter itself, as its dimensions and the head speed should meet the requirements of the sediments. Cutter suction dredgers are limited to reservoir depths between 25 and 30 m (Vlasblom, 2005). A relocation of the sediments within the reservoir is conducted in case that the storage volume is not the governing parameter. However, the deposited sediments may influence the operation. A prominent example are depositions in front of the water intakes, where sediment entrainment leads for instance to hydro abrasion of the hydraulic structures and turbines (see chapter 4.3.1 *Reservoir management and operation*). In case of pumping the water-sediment slurry downstream of the dam a special focus on the environmental compatibility has to be ensured. When water extraction/diversion happens into the downstream section where only a residual flow occurs, where the entrainment of the slurry can increase the “usual” concentrations in the river by far. In addition, the river has in this part only a limited transport capacity, which may result in strong depositions. If a natural disposal site is chosen, sediments have to be tested first regarding contaminants (DWA, 2019).



Fig. 51: Cutter suction dredge, installed at the Peñas Blancas reservoir in Costa Rica.

A special form of hydraulic dredging is the so called syphoning. This system uses the accelerated pressurized flows, created by the hydraulic head between the reservoir and the downstream river and thus can save energy for pumping the slurry mixture (Jacobsen, 1997; Morris and Fan, 1998). Figure 52a shows a suction head used for syphoning. In principle two types of syphoning schemes can be found in literature: one where the pipeline is led over the crest (figure 52b) of the dam and one where pipeline traverses the dam body. The second scheme is only possible when openings in the dam were already planned in the design phase of the dam. An example is the Banja reservoir in Albania (Sedicon AS, 2013). Nevertheless, the success of syphoning depends strongly on the characteristics of the deposited sediments the consolidation as well as the hydraulic boundaries, such as the hydraulic head. Batuca and Jordaan (2000) reported that due to the limited effectiveness in large reservoirs syphoning is usually only applied locally close to intakes. However, several cases, especially for small reservoirs exist, where syphoning resulted in a good performance of the method (Detering, 2014; Jimenez, 2012).

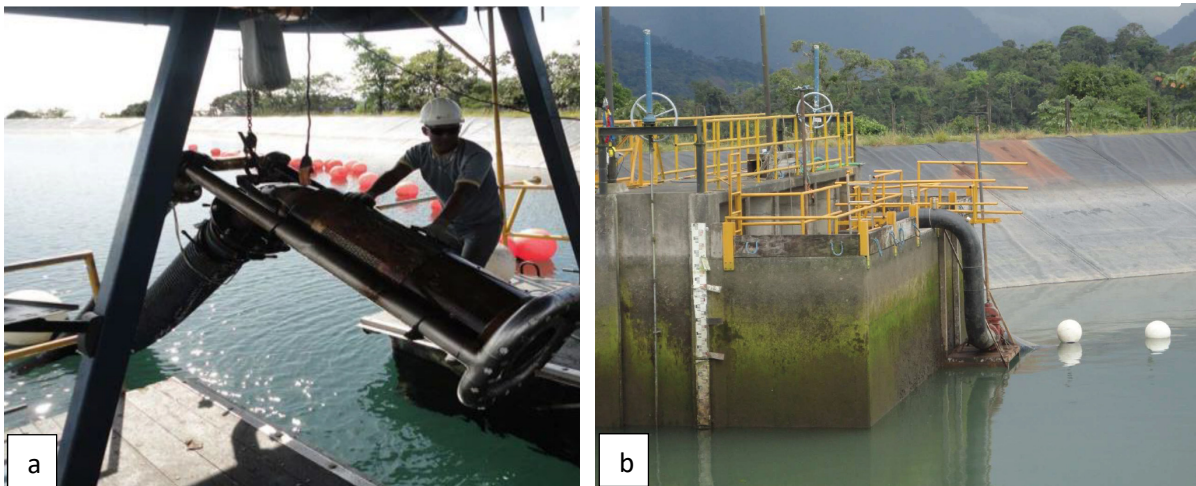


Fig. 52: (a) suction head used for syphoning (photo courtesy: Sedicon AS); (b) slurry pipe of the syphon dredge over the spillway crest at El General, Costa Rica (photo courtesy: Sedicon AS).

5.4.3 Reservoir flushing

Another approach to remove already accumulated sediments from reservoirs is the removal by the use of hydraulic forces, means by reservoir flushing. The basic principle is the lowering

of the water level in the reservoir to increase the bed shear stresses to initiate erosion at the reservoir bed. Due to the higher flow velocities and turbulences within the reservoir the remobilized sediments are kept in suspension and are transported to the low level outlets of the dam, which are opened to facilitate the outflow of the water sediment mixture from the reservoir. Basically, two kinds of flushing scenarios exist, namely pressure flushing, also called flushing with partial draw down, and free flow flushing, also called flushing with full draw down. However, the success of reservoir flushing depends strongly on the given boundary conditions of the reservoir (e.g., shape of the reservoir), the hydrology (e.g., water inflow) and the sediment characteristics (e.g., sediment size, consolidation). Hence, predictions regarding the technical feasibility of this measure are challenging.

Free flow or drawdown flushing

Reservoir flushing with full drawdown is in accordance to literature the most effective way to remove deposited sediments from reservoirs. During drawdown flushing the water level of the reservoir is lowered until free flow conditions occur within the reservoir. This increases the bed shear stress to the conditions in the initial river bed and as a consequence it initiates the erosion process (figure 53a-b). However, flushing with full drawdown is especially in large reservoirs associated with a loss of stored water. In literature several attempts exist to predict the success of reservoir flushing, also with respect to economics, mainly based on the ratio between the storage capacity of the reservoir (CAP) and the mean annual inflow (MAF). Kondolf et al. (2014) investigated the success of a flushing operation of different reservoirs with different boundary conditions and concluded that the ratio between the storage capacity CAP and the mean annual inflow MAF should not exceed 0.04, because conducting free flow flushing in large reservoirs show disadvantages, especially regarding economic considerations (Sumi, 2008).

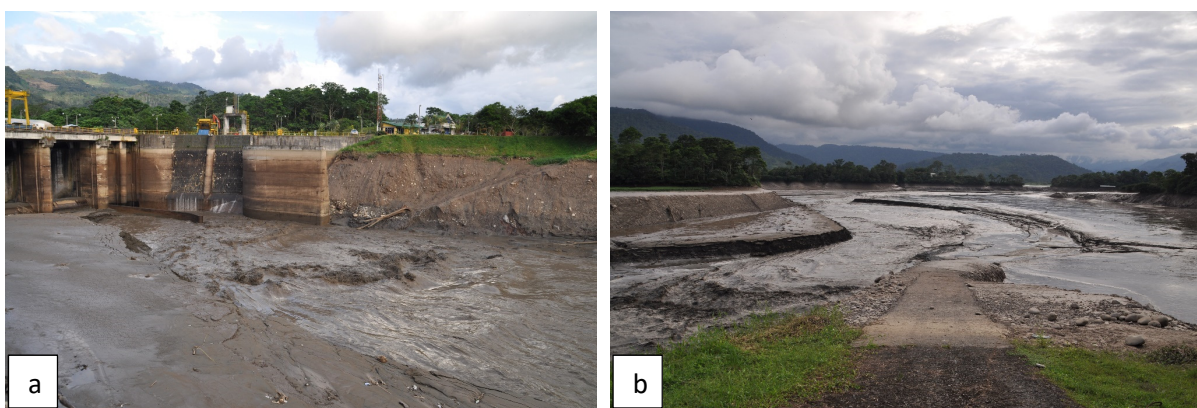


Fig. 53: Flushing with full drawdown at the Angostura reservoir, Costa Rica in 2010 (a) view from upstream to the intake, bottom outlet and spillways; (b) view from the dam in upstream direction.

In general, each flushing with full drawdown follows similar steps, namely:

- (i) *Drawdown of the water level.* The drawdown of the water level is usually conducted by releasing stored water as long as possible through the intakes, so that water can be used for e.g., producing hydroelectricity, followed by the release of water through the spillway gates (if technically possible) and finally through the bottom outlets to initiate free flow conditions in the reservoir. Figure 54 shows a graph of the drawdown flushing of the Dashidaira and the Unazuki reservoirs, located at the Kurobe River in Japan, in 2006. In this case the flushing is first initiated in the downstream located Dashidaira reservoir, followed by the upstream located Unazuki reservoir. This order is important to ensure that the flushed-out sediments from the upstream located reservoir do not settle within the downstream located reservoir. Another important point during the drawdown of the water level is the monitoring of the occurring sediment concentrations in the residual water stretch. Usually the highest concentrations occur during the drawdown of the water level, when bed shear stresses increase. Often also geotechnical failures, such as sand slides, happen along the banks of the reservoir during draw down, resulting in uncontrolled concentration peaks downstream. An example for this is the Bodendorf reservoir in Austria. Here the drawdown has to be stopped when a concentration peak occurred, and the water level was increased until the measured concentrations decrease (Badura, 2007).
- (ii) *Free flow conditions:* At the end of the drawdown the so-called flushing channel forms. This channel has often the geometry of the initial river, which was impounded through the construction of the reservoir (Haun, 2012). Figure 53b shows the flushing channel of the Angostura reservoir in Costa Rica, formed during drawdown flushing in 2010. During free flow conditions the highest bed shear stresses, flow velocities and turbulences occur within the flushing channel. As a result, most sediments are eroded from the reservoir bed. During this phase of the flushing an in-depth monitoring is important as sand slides may happen at the edges of the flushing channel, which has, on one side, the advantage that the narrow flushing channel widens and more sediments can be re-mobilized, but which can also result in further concentration peaks. The width of the flushing channel is an important factor for the success of a flushing; therefore, narrow reservoirs are more suitable for flushing with full drawdown than wide reservoirs, where the ratio between the reservoir width and the width of the flushing channel is relatively high. The duration of the free flow flushing varies depending on the reservoir. As a rule of thumb, it can be said that for smaller reservoirs, which are flushed more frequently this phase is usually shorter than for larger reservoirs. Figure 54 shows that the phase with free flow conditions lasted only for some hours for the Dashidaira and the Unazuki reservoirs, whereas e.g., the Sanmenxia reservoir in China shows a flushing duration of about four months (Atkinson, 1996).

- (iii) *Refill of the reservoir*: The last phase is the refill, where the water level rises until the usual operation of the reservoir is possible again. The start of the reservoir refill can be based on a schedule, e.g., flushing during time slots where no electricity production of the power plant is necessary, based on forecasts of the duration of a flood event or based on downstream measurements of the amount of flushed-out sediments. Due to the formation of a flushing channel usually the efficiency of the flushing, that is the amount of flushed out sediments, decreases over time.

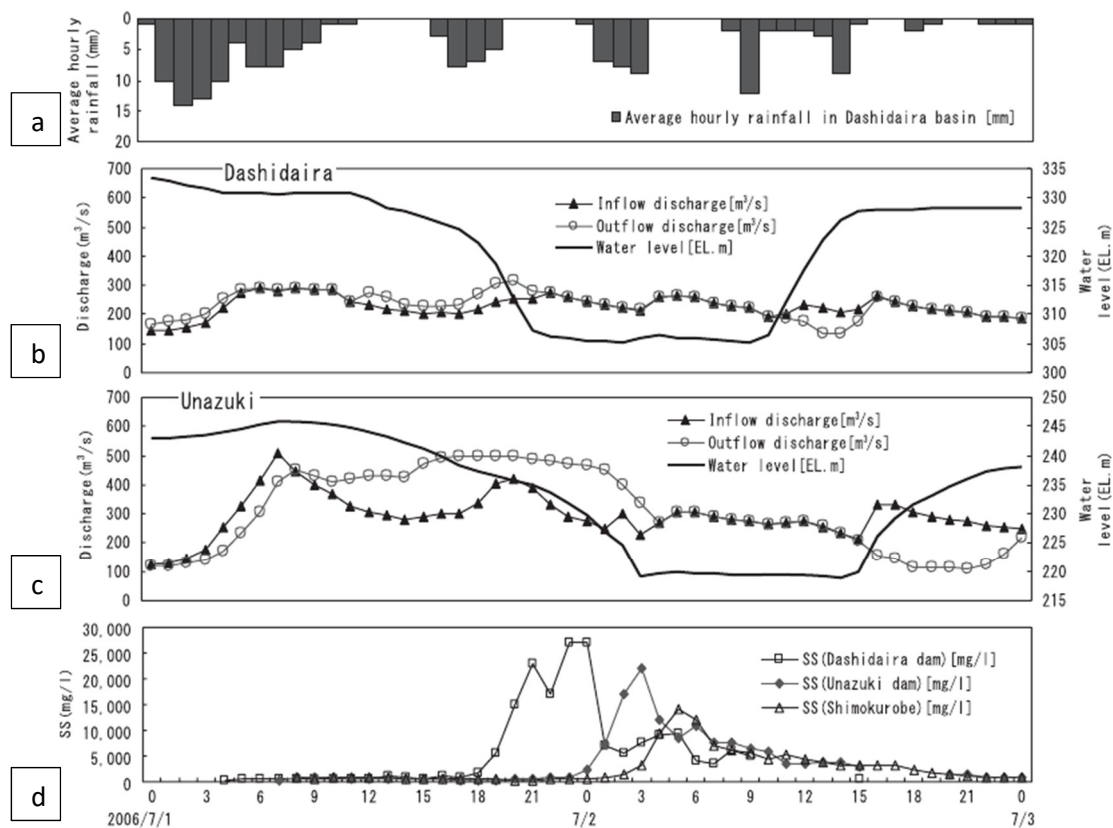


Fig. 54: Coordinated flushing of the Dashidaira and the Unazuki reservoirs in the Kurobe river in 2006 (a) precipitation; (b, c) inflow and outflow hydrographs and reservoir stage for Dashidaira and the Unazuki reservoirs, respectively; (d) suspended sediment concentrations downstream of both reservoirs (Kondolf et al., 2014).

The success of reservoir flushing depends on a variety of parameters and so reservoir flushing is not the best solution for all reservoirs. In addition, in the past many cases of reservoir flushing were reported, which led to environmental problems in the downstream region. Even if drawdown flushing is the most effective way, the erosion is often limited to the flushing channel, which forms during the drawdown. Hence, an in-depth investigation of the success of the measure is necessary before initiating a reservoir flushing operation. An important factor for the technical success of a drawdown flushing are the hydrological conditions during the flushing. A drawdown flushing is most effective when high discharges occur (e.g. during flood events). Therefore, drawdown flushing in areas without a distinctive wet season

depends strongly on an accurate weather and precipitation forecast, which deliver information regarding the peak value of the flood as well as on the duration of the event.

Pressure flushing

During pressure flushing the water level is, compared to a full drawdown flushing, only partially lowered and the low level outlets are opened at the same time to release water and sediments from the reservoir. In many cases the lowering of the water level in the reservoir happens by releasing water through the bottom outlets. When opening the low level outlets bed shear stresses increase in close vicinity to the outlets and a so called flushing cone is formed as a result of the new hydraulic conditions. As this measure only leads to erosion in close vicinity to the outlets, in literature flushing with partial drawdown is often stated as an ineffective measure, even if several examples exist, where pressure flushing has been successfully applied, e.g., at the Peñas Blancas reservoir in Costa Rica. Conducting this measure regularly has the benefit that fine sediments will not consolidate and erosion is possible even with the occurring bed shear stresses. An advantage of flushing with partial drawdown is that a smaller amount of stored water is lost compared to flushing with full drawdown, however, also the ratio of water to sediment of the flushed out mixture is low and thus a negative environmental impact on the downstream river reach can be avoided or reduced. For a partial drawdown, depending on the lowering of the water level and the bathymetry of the reservoir, often only in the most upstream part of the reservoir free flow conditions occur. Figure 55a shows a flushing event with partial drawdown at the Peñas Blancas reservoir in Costa Rica (view from the dam upstream) in 2013. In Figure 55b the upstream part of the reservoir is shown, where free flow conditions and a re-mobilization of sediments happen. When considering this management method, the lowering of the water level has to be performed with care, so that eroded sediments from the upstream part of the reservoir are transported through the reservoir and leave the reservoir through the low level outlets without settling in between or, in worst case, even clog the bottom outlets.

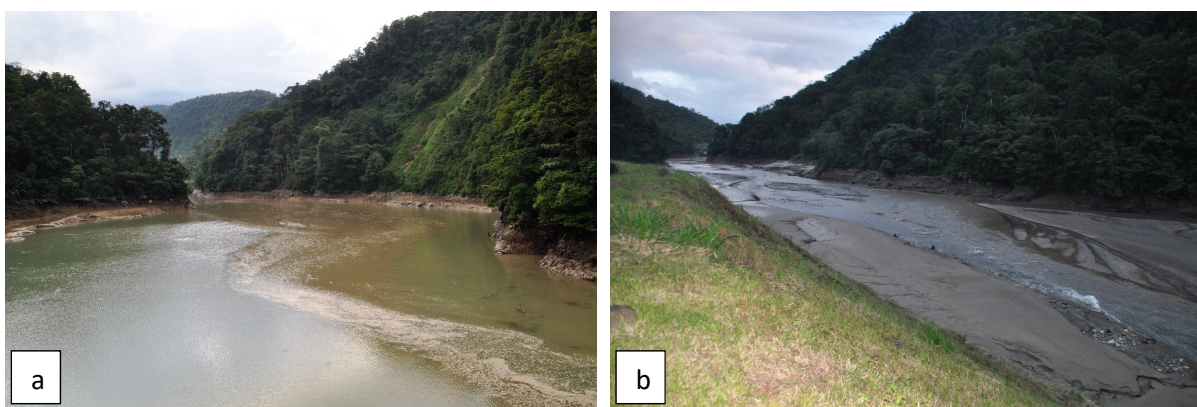


Fig. 55: Flushing with partial drawdown at the Peñas Blancas reservoir, Costa Rica in 2013 (a) view from the spillway upstream; (b) view from the head of the reservoir towards the dam.

From an economical point of view, it has to be taken into account that the reservoir will be partially or completely emptied during reservoir flushing. Especially flushing in larger reservoirs needs to be scheduled ahead, means the management of the reservoir has to be adapted in a way that no shortcomings of water appear during and especially after the measure. In case that a reservoir is used for multiple purposes, such a decision may lead to tensions between the involved stakeholder groups (see chapter 1.2 *Reservoirs as multipurpose structures – multi-stakeholder involvement*). Even if reservoir flushing is technically and economically a possibility, special attention has to be paid to the ecological impact on the downstream river region. During reservoir flushing the suspended sediment concentrations in the downstream region rise suddenly, which may be a stressor for the downstream located ecosystem and the fish habitat. Several examples were reported, where reservoir flushing ended in a disaster for fauna and flora. However, several groups around the world focus on an environmental-friendly flushing, which has been proved to be a good option and result in a successful flushing (Peteuil, 2018). As a result, often standard limits, such as maximum allowed suspended sediment concentrations, minimum oxygen concentrations or chemical parameters are implemented and have to be monitored during the measure. Figures 56a-b show the downstream monitoring during the reservoir flushing operations of the Fischeing reservoir in Austria and the Peñas Blancas reservoir in Costa Rica, respectively. In the Fischeing reservoir in Austria the suspended sediment concentrations were evaluated during the flushing with so-called “Imhoff-cones”. This is a widely used method to evaluate the concentrations in a relatively short time. Often also an ecological monitoring is implemented, as it can be seen from the figure. Here the impact of flushing on fish was evaluated during the flushing of the Peñas Blancas reservoir in 2013.



Fig. 56: (a) monitoring of the downstream suspended sediment concentrations during the flushing of the Fischeing reservoir, Austria, in 2012; (b) ecological monitoring downstream of the Peñas Blancas reservoir during flushing with partial drawdown in 2013.

5.5 *Increase of storage volume*

In case that a recovery of already lost storage volume is not feasible due to the given conditions (technical, economic and environmental reasons) another alternative is to create additional storage volume. For instance, this can be realized by upgrading a dam (e.g., heightening of the crest) or by building a new reservoir. The advantage of an upgrade of a dam is that often the impact on the society is smaller, the work can be conducted in most cases in a shorter period and the ecological impact is smaller compared to a new dam project. Such a heightening of the crest of the dam was for instance conducted at the New Katsurazawa dam, the Yesa dam and the Kasabori dam, both located in Japan (Water and Disaster Management Bureau, 2013). Although the heightening of the crest of the Sylvenstein reservoir in Germany was not performed because of lost storage volume due to sedimentation, the additional storage volume will also counteract the ongoing sedimentation (see chapter 1.2 *Reservoirs as multipurpose structures – multi-stakeholder involvement*; figure 57a-b).

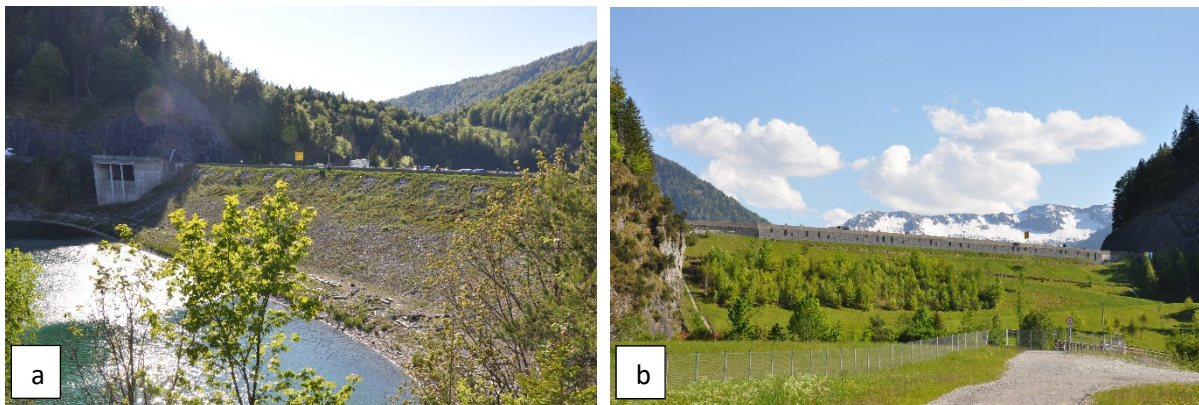


Fig. 57: Dam heightening at the Sylvenstein reservoir also as preventative measure against possible impacts of climate change (a) view from upstream; (b) view from downstream.

6 HYDRO-MORPHODYNAMIC MEASUREMENTS

*Within this chapter an overview is given on methods, which are used to measure bed levels, bed material composition as well as bed load and suspended sediment load transport in open water environments. A focus is thereby set on the measurement principles behind the different measurement methods to understand limitations of the methods and devices. In addition, advantages and disadvantages are highlighted, to show the application possibilities of different measurement methods. For a more detailed overview on sediment transport measurements the book series *Experimental Hydraulics: Methods, Instrumentation, Data Processing and Management (2017) Volume I and Volume II* by Muste et al., and Aberle et al., respectively, is recommended.*

Reliable knowledge on the amount of transported sediments, morphological bed changes and the bed sediment composition in water bodies is an important factor for a sustainable water resources management. Especially for implementing reservoir management strategies are necessary to have accurate information on the quantity and quality of sediments within the river, already before the reservoir is impounded. With this knowledge it is feasible to predict possible reservoir sedimentation and the subsequent storage loss already in an early stage. However, also during operation, a monitoring of the reservoir bed, the composition of the sediment depositions and the sediment transport is required to: (i) obtain detailed information on ongoing sedimentation processes, which can be used for the optimization of the operation of the reservoir, (ii) implement (additional) sediment management strategies, if necessary and (iii) monitor the success of already implemented management strategies.

Within this chapter the measurements are subdivided into three categories, namely bed level measurements, bed material and sediment characteristic analysis as well as sediment transport measurements.

6.1 *Bed level measurements*

Bed level measurements are not directly measurements related to sediment transport or sediment characteristics. However, with the information on bed level changes over time it is possible to quantify the amount and location of deposited sediments in the reservoir. This knowledge can be used to calculate the trapping efficiency of the reservoir, to evaluate the exact deposition pattern within the reservoir and to evaluate the consequences/success of reservoir management strategies. The results of several bed level measurements along a longitudinal section of the Solis reservoir in Switzerland are presented in figure 17. The figure shows the formation and the migration of the delta in direction of the dam. These measurements were used as a basis for an evaluation of the storage loss of the reservoir, but also for implementing sediment management strategies. Figures 58a-b show two bed level measurements of the Angostura reservoir in Costa Rica in 2010, where Figure 58a shows the

results of the bathymetric survey from September 22 (before a reservoir flushing operation) and figure 58b shows the survey after the flushing operation on November 17 (Haun and Olsen, 2012a). When comparing both measured bed levels, the bathymetric changes in the reservoir can be seen as a result of the reservoir flushing operation.

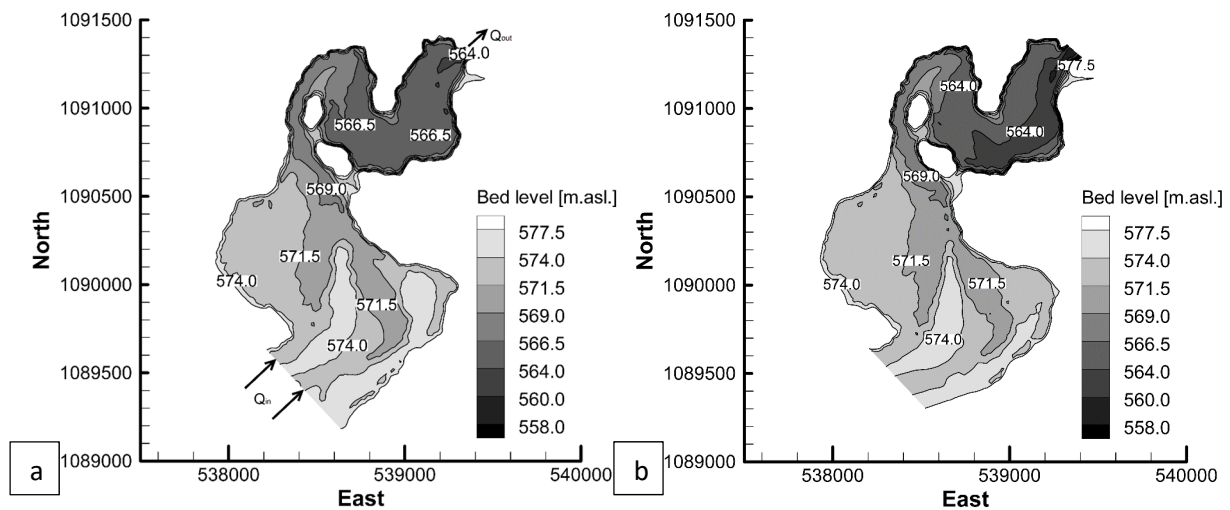


Fig. 58: Bathymetric survey of the Angostura reservoir (a) on September 22, 2010 before the flushing; (b) on November 17, 2010 after the flushing.

The state of the art technique for obtaining bathymetric data from reservoirs is sonar (sound navigation and ranging). Instruments based on sonar work in a way that the propagation of sound is measured and analyzed (e.g., Singal, 1997; Roux and Kuperman, 2004 among other), also called echo sounding. The principle is that the active sonar device emits a sound wave at a specific frequency and records returned echoes, which are reflected from objects or the surface of the bed. The distance between the emitting device and the reservoir bed is then calculated from the travel time of the returned echo. To evaluate the strength of the measured echo-return the active sonar equation (energy budget between transmitted, received and processed sonar signals) is used (Kerr, 1951; Urick, 1983; Lurton, 2010). However, during the measurement different losses of pulse energy occur, such as spreading and attenuation loss (Christ and Wernli, 2007). Hence, the sonar equation consists of different parameters, which are determined by the used equipment, the medium and the target to take losses into account (Eq. 5).

$$SL - 2 TL + TS - (NL - DI) = DT \quad (\text{Eq. 5})$$

where SL is the Source Level (equipment), TL is the Transmission Loss (medium), TS is the Target Strength (target), NL is the Noise Level (medium, equipment), DI is the Directivity Index (equipment) and DT is the Detection Threshold (equipment). All parameters are levels in units of decibels [dB].

An important factor for applying sonar is the effect of noise, which limits the applicable range of the instrument. The quality of the measurement can be analyzed regarding the signal-to-noise ratio (SNR-ratio), where the SNR needs to be above the detection threshold (DT) for reliable measurements. The sound frequencies of sonar devices are as a consequence different and range e.g., for side scan sonars between 20 and 500 kHz. For the correct choice of the instrument it is important to keep in mind that higher frequencies tend to have a better resolution, but have less profiling range. Due to completeness reasons it should be mentioned that ultrasonic devices can be distinguished between active and passive devices, where passive devices only detect sounds, which are emitted by other sources (Aberle et al., 2017), and are not that frequently used in rivers and reservoirs.

For the evaluation of reservoir beds three equipment types are used, namely: single beam, multibeam and side scan sonars. Single beam devices perform only a single point measurement of the local depth for each ping, whereas multibeam devices perform measurements of several points per ping and have as a consequence a higher spatial resolution. Figure 59a shows sonar measurements at the Wasserfallboden reservoir in 2010. Figure 59b presents measured transects along the Angostura reservoir in 2010, where a single beam device was used. The most sophisticated method for obtaining bed levels is by using a side scan sonar, which has as additional advantage the possibility of distinguishing between sound reflections and absorptions of materials with different characteristics. Side scan sonars measure and cover a larger area of the bed at each ping compared to single or multibeam devices, and have consequently also a far higher spatial resolution. A typical use in reservoir management is for monitoring dredging operations in sensitive regions of the reservoir, e.g., in front of intakes or the bottom outlets.

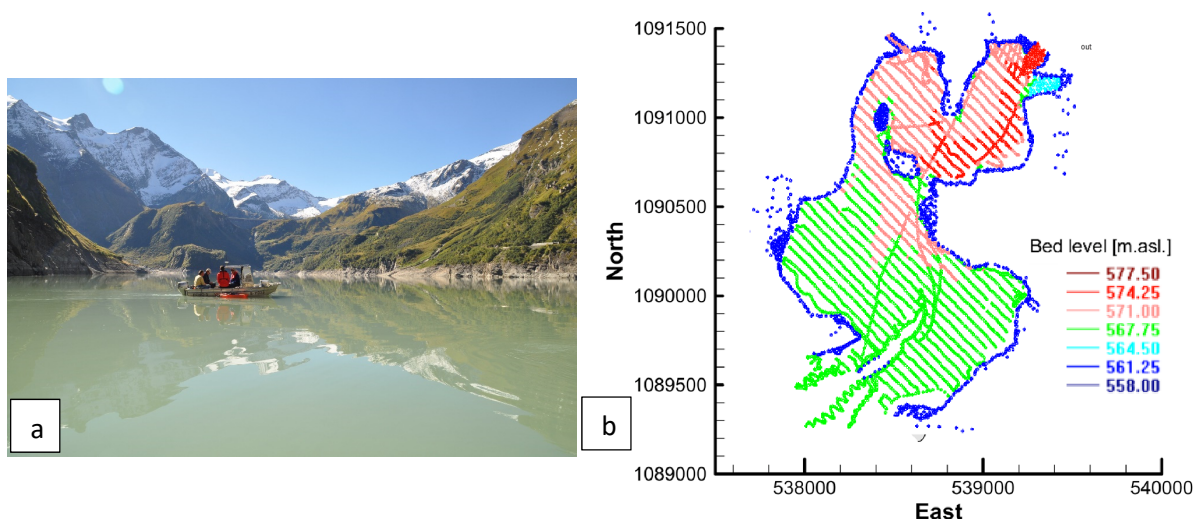


Fig. 59: (a) bathymetric survey of the Wasserfallboden reservoir in 2010; (b) measurement points of the bed levels of the Angostura reservoir, obtained by sonar measurements in 2010.

An important point when conducting sonar measurements is the correct allocation of the instrument, which is usually ensured by using a high precision Global Positioning System (GPS).

GPS systems will not be explained in detail in this thesis, as this is a research field by its own. However, a basic overview on the quality of available GPS systems is presented, which may help for a pre-selection of the GPS system depending on the necessary accuracy.

Usual GPS systems, as they are used in cars for navigation purposes, are meanwhile inexpensive devices, but have a resolution within a meter's range only. This is due to the fact that the accuracy is depending on the number of satellites, the on-site conditions, but also the available correction services.

A Differential Global Positioning System (DGPS) increases the accuracy of the position measurement, compared to an ordinary GPS system, by transmitting correction data from fixed antennas, the so-called ground based reference stations, where the exact position is known (Gusek, W. 2015; Moorefield Jr., 2020). When the deviation of the actual position of the ground based reference station is known it is feasible to determine the real propagation times of the signals for each satellite very precisely, means the shift between the real location and the one determined by the satellite can be calculated. This information is further used to correct the currently received GPS data of the rover, which is used to allocate the location of the measurement (Asbeck et al., 2012). For practical reasons the correction data of the reference station are transmitted to the receivers via Global System for Mobile Communications (GSM). The spatial resolution, which can be achieved by DGPS, is within the meter or sub-meter range, but it has to be taken into account, that the accuracy of DGPS decreases with the distance from the reference station.

Real Time Kinetic (RTK) measurements is the most precise method to obtain position coordinates. The principle is similar to the DGPS, but in this case several ground based reference stations are used. Due to an existing RTK network the rover obtains in a first step its approximate coordinates, which are then corrected by an optimum triangular meshing by using several ground based reference stations. The precise positions of the rover (often also called virtual ground station) are determined with a spatial resolution of 1 - 2 cm (Moorefield Jr., 2020). However, this high accuracy of the measurement is no only derived by using a network of ground based reference stations. This is also possible by the fact that for RTK the phases of the signal's carrier wave are correlated with each other to only processing the information content of the signal. Finally, the distances to the respective satellites are determined (carrier-phase enhancement) (Wanninger, 2018).

6.2 *Bed material measurements*

The grain size distribution of bed material is an important parameter for reservoir management. It provides information on the characteristics of sediments entering the reservoir, and enables additional insight into the ongoing processes within the reservoir, such as grading effects or information on the amount and location of cohesive sediments. The bed

material analysis itself is mostly conducted in the laboratory by sieving and/or an analysis of very fine sediments (e.g., by a hydrometer analysis), if necessary. An important point in obtaining the grain-size distribution of bed sediments is the sampling procedure of the bed material.

The choice of the method depends on the in-situ conditions (e.g., water depth), the sediment characteristics (e.g., grain size distribution) and whether disturbed or undisturbed sediment samples need to be obtained. Different surveying and sampling methods are available for surface sediments and depth-oriented sediment sampling.

In shallow reservoirs, such as check-dams, samples are collected usually by an excavator, manually by grab sampling (both disturbed samples) or by using the freeze-core technique (undisturbed sampling) (Bunte and Abt, 2001). Figure 60a shows a Van Veen sediment grabber used at the Geesthacht reservoir at the river Elbe, Germany, for obtaining disturbed surface samples. Beside the Van Veen grabber different kinds of grab samplers exist (e.g., the Ekman grab sampler or the Ponar type sampler), however, the measurement principle of all samplers is similar (WHOI, 2020). The cocked grabber will be released to the reservoir bed and triggered by an implemented mechanism. Either by its own weight or by a spring the sampler will be closed and can be lifted immediately. The kind of samplers are designed for relatively fine sediments, as consequence coarser particles may clog the opening of the sampler, resulting in a loss of the sample material during lifting the grabber. The advantage of sampling with by an excavator (figure 60b) or a grab sampler is that sediment samples can be obtained fast and with comparable less effort compared to e.g., freeze core sampling. In both cases the samples are disturbed and cannot be analyzed in a depth oriented manner. In addition, fine sediments may be washed out when the sample is lifted from the reservoir bed to the surface. Freeze-core sampling overcomes many of these disadvantages (e.g., Carling and Reader, 1981). By freeze-core sampling the sediment sample will be frozen by the use of liquid nitrogen (Pachuret al. 1984; Dück et al., 2019), which enables the extraction of sediments without losing fine particles (figure 60c). This method works best for coarser sediment depositions, such as gravel beds. However, the sediment sample will expand during this process as ice has an approximately 9 % higher volume compared to water (Kell, 1975), resulting in a change of the porosity of the sample (Seitz et al., 2018). Also the quantity plays a major role in obtaining a representative bed material sample and depends on the largest grain of the sample (DIN EN ISO 17892-4, 2017). Especially for coarser sediment depositions the required amount of sampled sediments may be larger than the sample volume which can be obtained from freeze-coring or grab samplers.

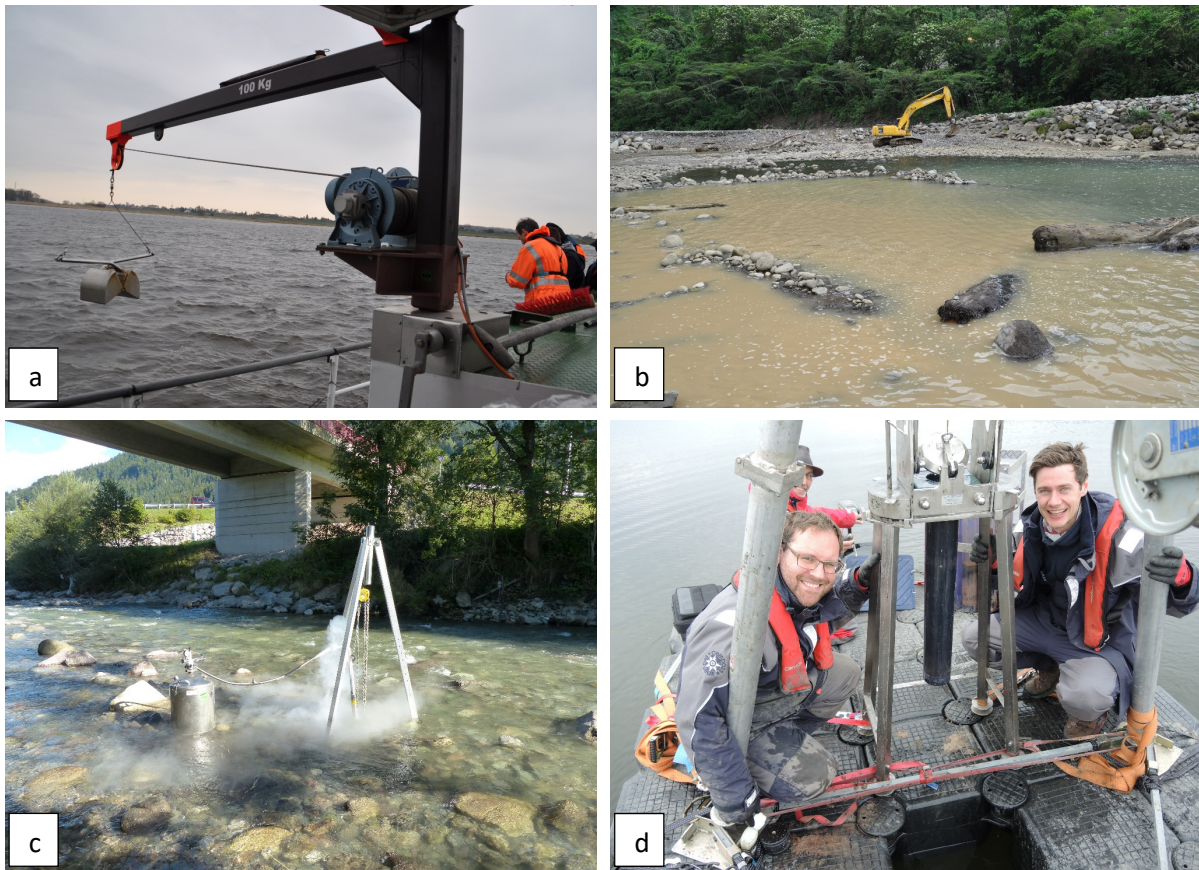


Fig. 60: (a) Van Veen grabber used at the Geesthacht reservoir at the river Elbe, Germany, in April 2013; (b) sampling with an excavator at the Peñas Blancas reservoir, Costa Rica, in 2014; (c) freeze-core sampling in the residual stretch of the Brixentaler Ache, Austria, in 2015; (d) core sampling with the Frahm-lot at lake Brombach in 2017.

In impounded reservoirs grab sampling (disturbed samples), but also coring techniques (disturbed or undisturbed) are used to obtain samples. Depth-oriented sediment sampling is usually performed by coring to overcome the disadvantages of surface samples or disturbed samples. Here cylindrical tubes, made of metal or plastic, penetrate the reservoir bed and are lifted containing the relatively undisturbed sediment sample. A variety of different coring techniques exist; in sediment research gravity coring is usually performed. Here the tubes penetrate the bed by their own weight or by an additional falling weight (compare e.g., Blomqvist, 1991; Chant and Cornett 1991; Jutzeler et al. 2014). Examples are the Piston Corer, the Box Corer, the Multicorer or the Frahm-Lot (Evers, 2020). Figure 60d shows the extraction of a sediment core from a depth of 17 m in the lake Brombach in Germany by the so called Frahm-Lot. In some cases, also a penetration with the help of vibrations is initiated (e.g., by the Vibrocorer; OSIL, 2020), however, this may result in larger disturbances of the layering of the core. For almost all methods small disturbances of the sample occur due to the extraction of the sample itself (e.g., boundary effects within the core), transport and storage (e.g., vibrations), temperature differences between the environment at the reservoir bed and the surface, but also due to the change in hydrostatic pressure, when releasing the sediment sample from large depths of the reservoir (Dueck et al., 2019). An attempt was made by Dueck

et al. (2019) to use the freeze-coring technique, which is often used in rivers and in shallow reservoirs, to extract undisturbed sediment cores to analyze the layering of the samples.

After releasing the sediment cores a variety of investigation possibilities exist (compare Rothwell and Rack, 2006). The most often obtained parameter is the grain size distribution of the sample. The grain size distribution is for coarser sediment fractions usually obtained by dry sieving. During sieving the sample will be separated into pre-specified grain-size groups by using square-hole sieves or meshed sieves (DIN EN ISO 17892-4, 2017). For dry sieving the sample will first be dried in an oven at a temperature of 105°C and afterwards sieved in a sieving tower. Beside dry sieving also the possibility of wet sieving exists. Here the sample will first be suspended in liquid and thus the binding forces between the particles below 100 µm can be reduced and the formation aggregates can be limited. Therefore, this method is to be favored especially for finer samples. Finest particles (0,01µm - 300µm) can further be evaluated either by hydrometer analysis or by the laser diffraction method.

6.2.1 *Critical shear stress measurements*

Especially for a sustainable sediment management of reservoirs the critical bed shear stress of the deposited sediments is an important parameter for planning and implementing management strategies. The erosion behavior of sediments containing a large amount of fine particles remains largely unpredictable, since it is a result of complex biological and physico-chemical interactions. Several attempts were made in the past to invent measurement devices to obtain values for the critical shear stress in-situ or in the laboratory. However, almost all of these methods try to examine only the critical shear stress, without gaining deeper insight and knowledge on sediment properties. An overview on different existing in-situ devices for investigating cohesive sediments was given by Black and Paterson (1997). The existing tools can be subdivided mainly into two groups, namely benthic flumes and miscellaneous devices. Miscellaneous devices are mainly based on alternative methods for assessing the potential for erosion of cohesive beds (Aberle, 2008). These devices are often based on methods, which do not obtain the bed shear stress directly, but deliver the potential for erosion as a proxy parameter, where the critical bed shear stress can be derived from. These methods are based on vertical jets (Paterson, 1989), vertically oscillating grids (Tsai and Lick 1986), rotating flows in small cylinders (Gust, 1991; Schünemann and Kühl, 1991), shear strength testing using a shear pad and shear vane testing (figure 61a; Bassoullet and Le Hir, 2007). Many of these tests are conducted at a rather limited area, which may be a disadvantage of these methods compared to others. The critical shear stress obtained from benthic flumes is a direct result of the erosion caused by the occurring hydraulic conditions. From a construction point of view benthic flumes can be subdivided into recirculating and flow-through types. Recirculating flumes are closed systems, with rectangular parallel-walled channels and with either an annular or a straight flume (Aberle, 2008). In both cases the channel floor is formed by natural sediments. In annular flumes the eroding flow is driven by different methods, such as a

rotating lid (e.g., Maa et al. 1993, Widdows et al. 1998), a rotating lid with paddles (e.g., Amos et al. 1992, Thompson and Amos 2002, Bale et al. 2006) or by paddles only (e.g., Peirce et al. 1970). The flow in a straight flume is initiated by a propeller (Black and Cramp 1995), paddles (Houwing and van Rijn 1998), but most often by a pump (Nowell et al. 1985). By initiation of motion the concentration within the water phase increases until the circulated water gets saturated. In case that deposition occurs the concentration reduces. Straight benthic flow through flumes are constructed as straight canals with moveable bed (open bottom). The flume consists in this case of an out- and an inlet, where the flow is driven by propellers (Scoffin 1968, Hawley 1991, Aberle et al. 2003, Debnath et al. 2007, Plew et al. 2007), pumps (figure 61b; Young 1977, Manzenrieder 1983, Gust and Morris 1989, Ravens and Gschwend 1999, Krishnappan and Droppo 2006; Noack et al., 2015) or by gravity (sub-aerial devices of Grissinger et al. 1981, Cowgill 1994). Depending on the construction of the flume either the whole bottom consists of a movable bed and erosion can occur on the whole area or only within an open frame. When the water flow is increased, erosion is initiated. In case of a straight benthic flow through flumes, the eroded sediments are washed out through the flume outlet.

Each developed system has pros and cons, which should be taken into account when selecting an appropriate method for the investigations. Examples for disadvantages are: (i) the possibility of saturation in recirculating flumes, (ii) occurring secondary currents in annular flumes or (iii) a not fully developed boundary layer in the test section in the case of too short straight flumes. A comparison of different instruments was conducted by Cornelisse et al. (1997), Tolhurst et al. (2000) and Widdows et al. (2007), where the experiments were conducted simultaneously and for the same sediment.

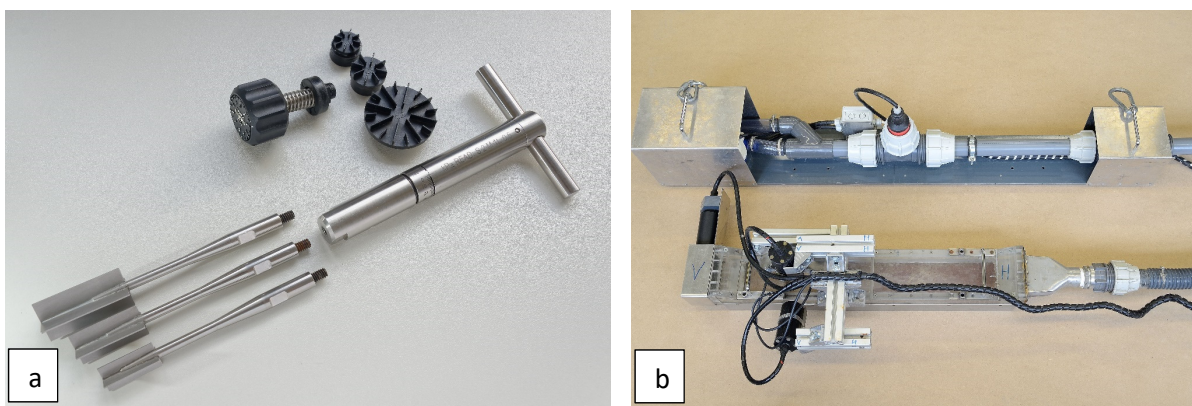


Fig. 61: (a) Vane shear (Geonor Inc., 2021) and Torvane Soiltest (Humboldt, 2021) instruments (photo courtesy: Bojan Skodic); (b) the straight benthic flow through flume “EROMOB”, developed at the University of Stuttgart (photo courtesy: Bojan Skodic).

However, in the future the goal is not only to derive a single number for the critical shear stress, but also to investigate the governing processes behind it. Especially for reservoir sediments further investigations and the identification of key parameters, which dominate

resuspension processes, are indispensable to increase the understanding of the erosion stability of fine sediment accumulations. Rodrigues Silva et al. (2018) made an attempt to investigate the influence of several parameters by using a fuzzy-logical approach, where the critical bed shear stresses of undisturbed sediment cores from run-of river reservoirs were correlated with physico-chemical and biological parameters of the sediments to unravel such key parameters. Gerbersdorf et al. (2007) and Beckers et al. (2021) introduced in addition more relevant biological parameters (such as total organic carbon content, Chlorophyll-a and the extracellular polymeric substances divided into proteins and sugars), but also the physico-chemical parameters (such as the cation exchange capacity) to further find statistical relationships.

A protocol was developed at the University of Stuttgart to standardize the process of investigating cohesive/non-cohesive sediment mixtures from reservoirs, to gain prominent parameters and to finally reduce the subjective assessment. The process can be subdivided into six steps:

- (i) Obtaining relatively undisturbed sediment cores from the reservoir,
- (ii) measuring the bulk density profile,
- (iii) selecting layers, which will be investigated, based on the vertical bulk density profile,
- (iv) investigating the critical bed shear stress for the selected layers,
- (v) investigating biological and physico-chemical parameters,
- (vi) performing a statistical analysis of the parameters.

The sediment cores are obtained from the reservoir by the so called Frahm-Lot, which was developed at the Leibniz Institute for Baltic Sea Research in Warnemünde for sampling deep sea sediments (MacArtney Germany GmbH, 2020). The device uses sampling tubes with a length of up to 100 cm and a diameter of 10 cm (Figure 60d). Although the Frahm-Lot was developed for the marine environment, it has been tested in several reservoirs (e.g., the Schwarzenbach reservoir or the lake Brombach in Germany) in depths up to 40 meters. By lowering the sampler, it penetrates the reservoir bed by its own weight (which can be modified to a certain extend), and closes the tube by a quick clamping unit and the lid as well as a locking arm.

The analysis of the extracted cores starts with obtaining a vertical bulk density profile by using a non-destructive gamma-ray attenuation method (Mayar et al., 2020; Figure 62a). A detailed overview on the method is given in Beckers et al. (2018; 2020). These high resolution data allow for deeper insights into the structure of the sediment depositions and are an indicator for changes in the sediment characteristics over depth. In addition, a first overview on consolidation effects of the sediment depositions can be given, which has subsequently an

influence on the critical shear stress (Mehta et al. 1989). Based on these investigations layers will be chosen for a more detailed investigation of critical shear stress and biological and physico-chemical parameters. Berlamont et al. (1993) proposed a list of 28 parameters, which have to be evaluated and taken into account to describe the behavior of natural cohesive sediments for establishing an analytical theory for cohesive sediment resuspension. As an evaluation of all these parameters is not feasible to manage (technically and economically) variables are selected, which can be used in further studies to encompass the critical shear stresses based on a limited number of measurements.

For the selected layers a set of parameters are investigated (Gerbersdorf and Wieprecht, 2015; Beckers et al., 2018; Beckers et al., 2020), these are:

- (i) Particle size distribution (PSD; clay, silt and sand),
- (ii) total organic carbon (TOC),
- (iii) cation exchange capacity (CEC),
- (iv) extracellular polymeric substances (EPS), divided into proteins and sugars and
- (v) chlorophyll-a (CHL-a).

In addition, an investigation of the mineralogical composition is possible, but also to determine the amount of gases (e.g., CH₄) in the pore water of different layers of the cores, to examine contaminants as well as to define the amount of micro plastic particles in the sample (e.g., Pohlert et al., 2011; Encinas Fernández et al., 2014; Encinas Fernández, 2020; Scherer et al., 2020).

Finally, high resolution data of depth-dependent critical bed shear stress measurements are performed by the so called SETEG flume (Stroemungskanal zur Ermittlung der tiefenabhaengigen Erosionsstabilitaet von Gewaessersedimenten; Witt and Westrich 2003). The SETEG flume is a straight benthic flow through flume, operated under pressurized flow, and is installed in the hydraulic laboratory of the Institute for Modeling Hydraulic and Environmental Systems at the University of Stuttgart. The flume has been in operation since 2004, but since then it has been continuously further developed. Especially during the last decade, a special focus has been set on the implemented measurement devices to enable erosion tests with a very high spatial and temporal resolution (Noack et al., 2019; Beckers et al., 2020). The system consists of a straight, rectangular and closed flume, with a total length of 8.32 m, a width of 0.145 m and a height of 0.10 m (Figure 62b).

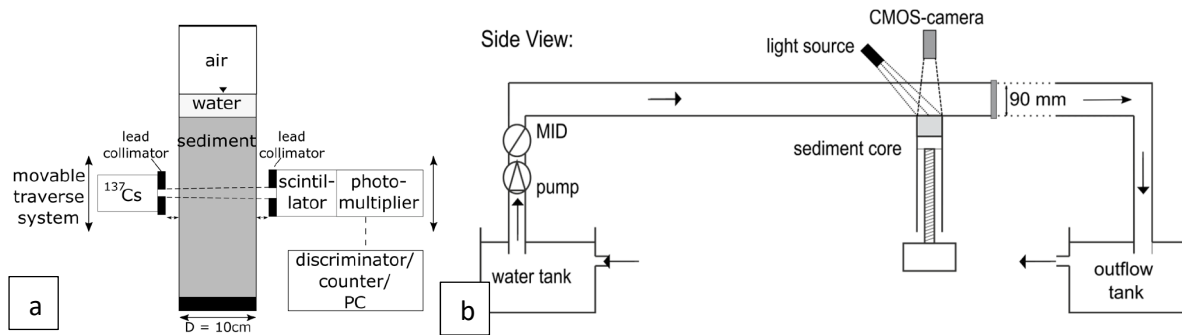


Fig. 62: Schematic view of (a) the gamma-ray densitometer; (b) the SETEG flume, constructed at the University of Stuttgart (Beckers et al., 2018).

During experiments the sediment cores are locked in position at the bottom of the flume and the sediment layer is exposed to stepwise increasing discharges of regular intervals and of constant time periods. The corresponding shear stresses, with respect to the discharges, are determined by a hydraulic calibration curve (Q - τ -relation), which was established from high-resolution Laser Doppler Anemometer (LDA) measurements (Noack et al., 2015). Due to the implemented method PHOTOSSED (PHOTOgrammetric Sediment Erosion Detection; Noack et al., 2019; Beckers et al., 2020) it is feasible to detect the erosion process with a high spatial (erosion rates with volumes smaller than 10 mm^3) as well as temporal resolution (CCD video camera with 10 Hz is used). After the experiment, the measured erosion rates are plotted over the corresponding shear stresses. The critical bed shear stress can then be calculated by extrapolating the shear stress for an erosion rate to 0 mm s^{-1} (Ravens and Gschwend, 1999; Sanford and Halka, 1993). Figure 63a shows different layers of a sediment core, obtained from the Schwarzenbach reservoir in Germany before and after the investigation of the critical bed shear stress in the SETEG flume. The critical bed shear stress was investigated for three layers in depths of 4 cm, 8 cm and 12 cm. Due to PHOTOSSED it is feasible to divide the core in regions which will be analyzed. The mean sediment deepening for the three sediment layers (depths: 4 cm, 8 cm, 12 cm) and four regions of interest (ROIs) of the core can be seen in figure 63b. Each shear stress was exposed to the sample for a period of 600 s.

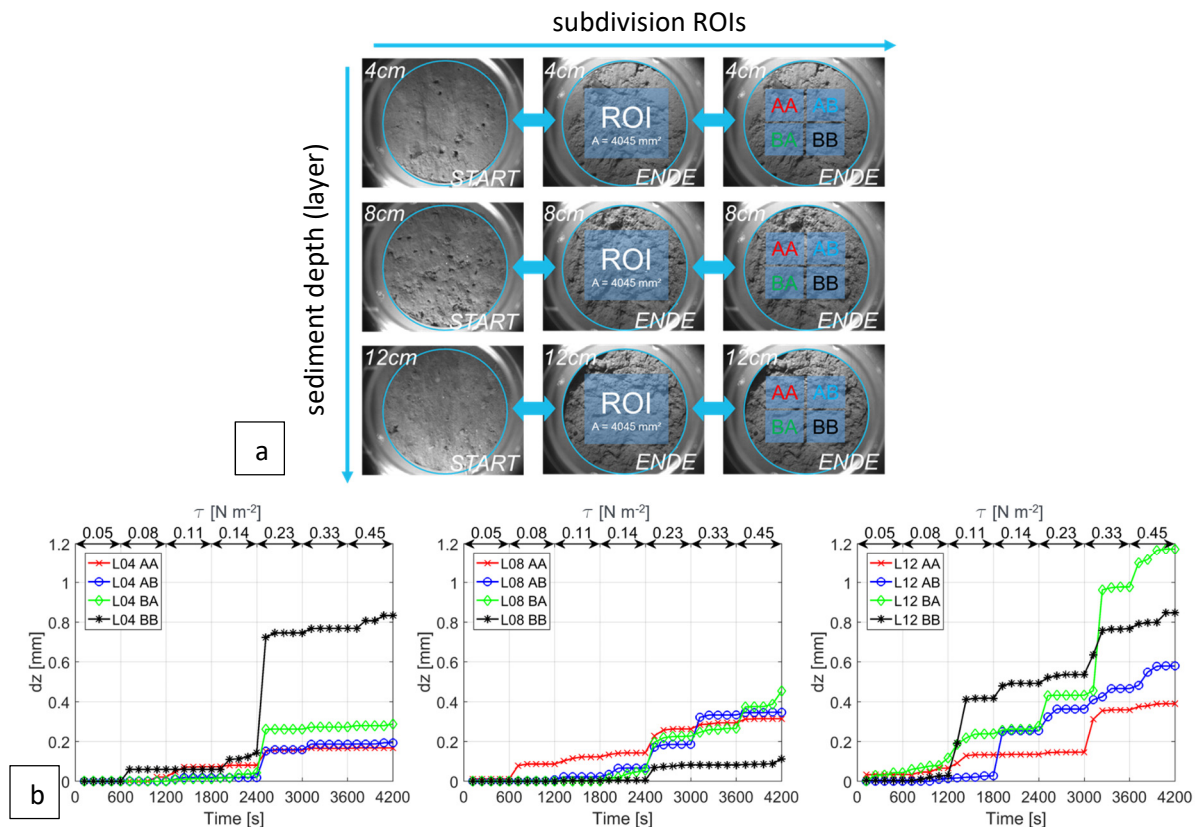


Fig. 63: (a) subdivision of the investigated area of a sediment core, obtained from the Schwarzenbach reservoir in Germany into regions of interest (ROIs) for 3 investigated layers; (b) mean sediment deepening for a subdivision of 4 ROIs for 3 investigated layers (4cm, 8cm, 12cm).

6.3 Sediment transport measurements

Sediment transport can be divided into bed load and suspended sediment load transport (see chapter 3.2 *Transport*). Although, the share of bed load or suspended load, as part of the total sediment load, cannot be quantified exactly, as it is very site specific and may temporary vary. An indicator may be that approximately 75 – 95 % of the total sediment load in rivers is transported in suspension (e.g., Pye, 1994; Morris and Fan, 1998; Wu, 2008; Ashley et al., 2020). Maddock and Borland (1950) reported values of transported bed load of 0 to 20 % for sand and gravel dominated water bodies and 2 to 8 % for waterbodies dominated by rock.

Within this chapter the main focus is set on suspended sediments as it represents the majority on sediment deposits in reservoirs. However, also a short overview on bed load measurement devices will be presented, as bed load represents an important parameter in high head reservoirs (e.g., in the Alps or in the Himalaya region). An important point for bed load as well as for suspended sediment measurements is, on the one hand, the spatial and temporal resolution of the measurements and, on the other hand, the collection of representative samples, which is especially for bed load measurements a challenging task.

6.3.1 *Suspended sediment transport measurements*

Suspended sediment concentration (SSC) measurements are in most cases the basis to calculate the transport through a pre-defined cross section. The suspended sediment concentrations in a water column are obtained either by direct or by indirect methods. By applying a direct method, the suspended sediment concentration is obtained from a sample through a subsequent laboratory analysis. For indirect methods a re-calculation and often a calibration of acoustical signals and/or the measured turbidity is necessary. Although a calibration of the measured values is necessary when using indirect methods, the big advantage is that a higher spatial and/or temporal resolution can be achieved.

Physical sampling and subsequent laboratory analysis (direct method)

Physical or gravimetric sampling, often called traditional sampling, is based on taking water samples directly from the reservoir. The simplest method is by taking a bucket sample from the shore (figure 64a) or by using a pumping device. However, such a surface sample is only a single spot measurement and may not be representative for a cross section, neither along the cross section nor over depth. Figure 64b shows for instance the acoustic backscatter signal (ABS) from Acoustic Doppler Current Profile (ADCP) measurements in a section of the Peñas Blancas reservoir, Costa Rica in 2014 (Haun and Lizano, 2016; 2018). The measurement was performed at the head of the reservoir, with the main inflow at the orographic left side (high backscatter signal strength; red). At the orographic right side, a lower backscatter signal strength was recorded (mainly green) showing smaller concentrations. In addition, also a change in concentration over depth can be seen, especially for the middle region. Although the backscatter signal shown in figure 64b is not calibrated with suspended sediment concentration measurements, it gives a quantitative impression regarding the suspended sediment concentrations within this cross section, with its heterogeneous distribution along the section. A more detailed overview on using the acoustic backscatter signal from acoustic devices is given in chapter 6.3.1. *Suspended sediment transport measurements*.

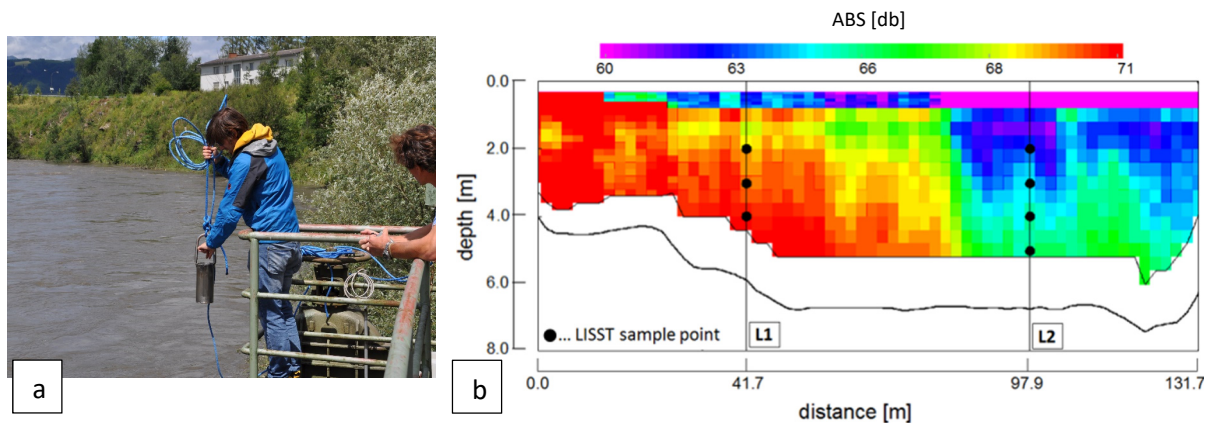


Fig. 64: (a) taking a gravimetric sample downstream of the Fischen reservoir, Austria, during a reservoir flushing operation in 2012 by using a bucket sampler; (b) acoustic backscatter signal distribution along a transect at the Peñas Blancas reservoir, Costa Rica.

As a consequence, multipoint sampling (measurements at several points along the transect and in several depths) is necessary for obtaining a correct image of the concentrations and to calculate accurate sediment transport rates. Figure 65a shows a recommendation by an Austrian Ministry for the acquisition of the suspended sediment matter in rivers (BMLFUW, 2008), where a representative distribution of single measurements over the cross section is presented. For larger rivers information on the number of verticals needed in a section, for obtaining reliable results, can also be found in Edwards and Glysson (1999). For such measurements samplers are used, which are lowered to a certain depth with a closed nozzle and as soon as the required depth is reached the nozzle will be opened remotely and the sample is taken. Figure 65b shows a P61 A1 suspended sediment sampler, which enables an isokinetic correct sampling, also due to the alignment with the flow due to its shape (Hauer et al., 2017).

Due to the labor and time intensive work of multipoint sampling, in many practical cases a multipoint sampling campaign is only performed once, with the goal to obtain relative differences between the measured points. This knowledge is then used in further measurement campaigns, where a smaller amount of samples will be taken (often only single point measurements are performed in subsequent campaigns). During the emptying of the Gepatsch reservoir in Austria in 2016 the downstream suspended sediment concentrations were monitored during a reservoir drawdown by this measurement strategy (Hauer et al., 2020a; 2020b).

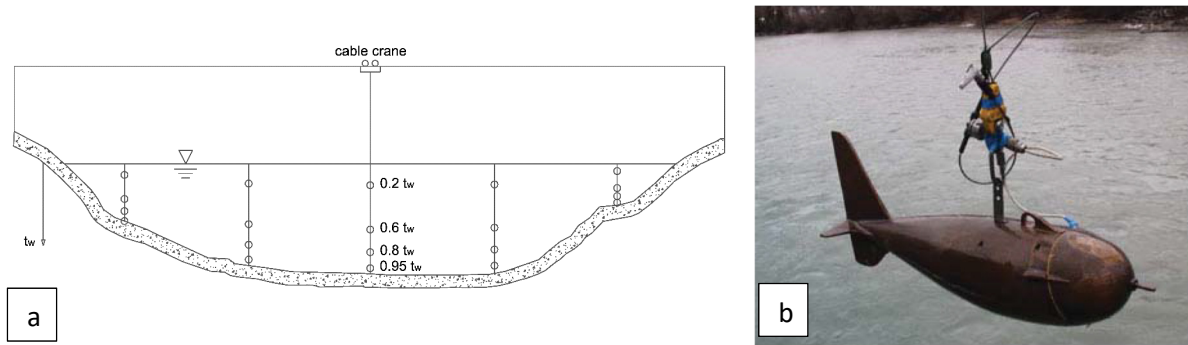


Fig. 65: (a) recommended distribution of single measurements over the cross section for an acquisition of the suspended sediment matter in rivers; (b) P61 A1 suspended sediment sampler, which enables an isokinetic correct sampling of single point samples, operated during the reservoir drawdown of the Gepatsch reservoir in Austria in 2016 (Hauer et al., 2017).

Beside single-point measurements, also depth-integrated samplers are used, especially when the total sediment load of a river/reservoir section will be investigated. During the lowering of the depth-integrated sampler the nozzle is opened and the mixture of water and sediment is collected. Figure 66a shows a USD-49 depth-integrated sampler at the Peñas Blancas river in Costa Rica downstream of the Peñas Blancas reservoir during reservoir flushing in 2013. Figure 66b shows the depth-integrated sampler “Cuxi”, used at the Geesthacht reservoir at the river Elbe, Germany in 2013. The lowering and raising of the device is performed at a constant rate, which should be associated to the depth of the location as well as to the inlet nozzle of the device. In case that the sampling itself (lowering and lifting of the sampler) happens too fast the amount of collected water may be too small for obtaining a representative sample. If the sampling time is too long a so called oversampling may occur, which means that the sampling bottle is already filled with water/sediment mixture, but due to the drag force additional sediments will enter the nozzle. As a consequence, the obtained suspended sediment concentration will be higher as the real concentration (Edwards and Glysson, 1999). Finally, also the nozzle dimension has to be selected with care, as it governs the amount of collected water, and should also be related to the suspended sediment size (Haun et al., 2015).

In case samplers with incorporated pumps are used, it is important to ensure an isokinetic correct sampling, otherwise the sediment concentration cannot be obtained correctly (Edwards and Glysson, 1999). This is especially for sampling in reservoirs from high importance, as in reservoirs the flow velocities are much smaller compared to rivers (Haun et al., 2015).

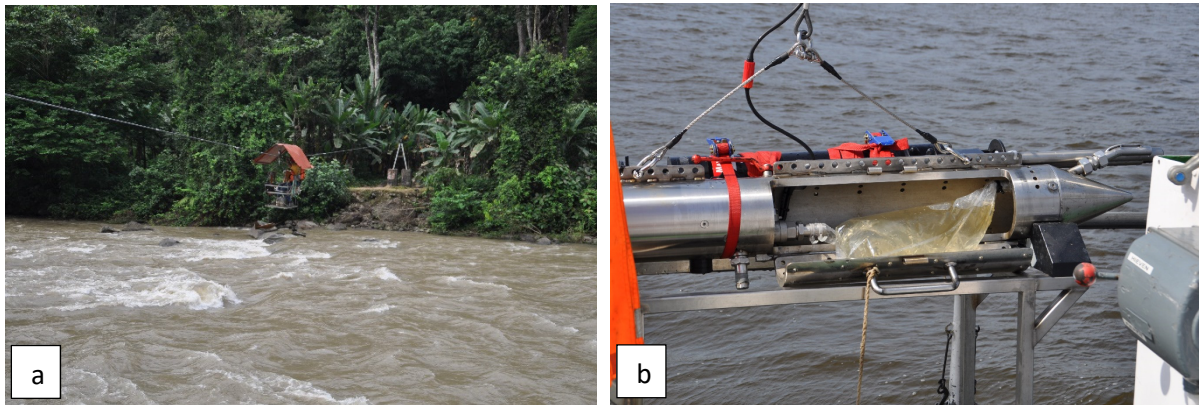


Fig. 66: (a) USD-49 depth integrated sampler downstream of the Peñas Blancas reservoir in Costa Rica during reservoir flushing in 2013; (b) depth integrated sampler “Cuxi” at the Geesthacht reservoir at the river Elbe, Germany in 2013.

In multiple year storage reservoirs with much larger water depths compared to e.g., run-of river reservoirs, mainly point samplers are used to obtain representative samples. The principle of such point samplers is similar to the presented point sampler in figure 65b, where the sampling device is lowered to a certain depth to obtain the sample. However, instead of opening a nozzle, often the sampler is lowered with open inflow and outflow, followed by a closing of the sampling chamber by an electric valve or by using a mechanic trigger. Depending on the architecture of the sampler the opening is either horizontally (figure 67a) or vertically located, where the water enters the sampler through the opening on the top and the bottom during lowering of the sampler (figure 67b). Due to the small flow velocities in large reservoirs, often an isokinetic correct sampling cannot be achieved with a horizontal sampler in reservoirs; therefore, vertical samplers are the most used device. It is important to ensure measurements in the correct depth of the reservoir. Even small flow velocities in reservoirs lead to drag forces, resulting in a lateral shift of the measurement device but also in height (compare also Topping et al., 2011).

A limitation of both, depth integrated as well as point sampling, is that due to the design of the devices and the nozzle (if available) measurements close to the bed are not feasible. The suspended sediment transport in this area has to be calculated with care when obtaining sediment transport rates, as the highest suspended sediment concentrations occur close to the bottom (see, figure 25; Haun and Lizano, 2018).

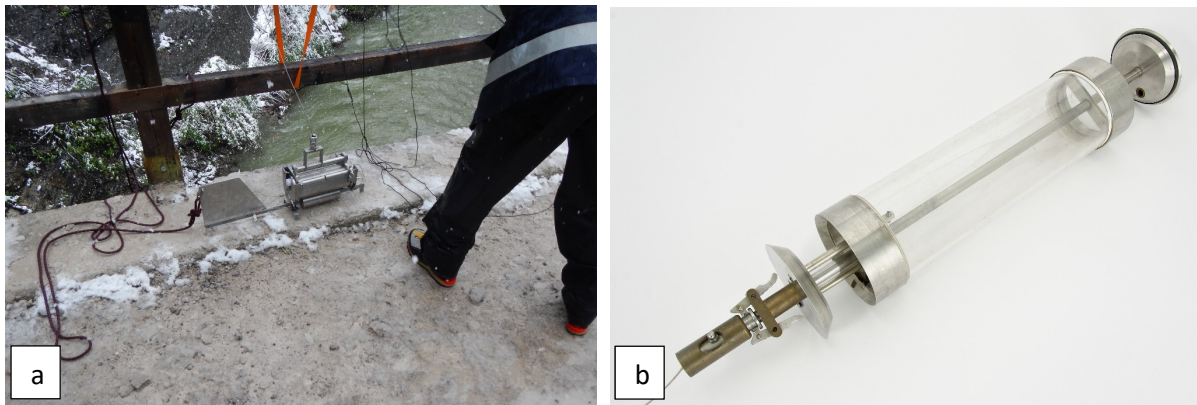


Fig. 67: (a) water sampler with horizontally located in- and outflow, used at the Bächental reservoir in Austria in 2016; (b) water sampler with vertically located in- and outflow (type Kemmerer, photo courtesy: Bojan Skodic).

To obtain the suspended sediment concentration (SSC) or the grain-size distribution (PSD) of a sample a subsequent analysis is necessary for all direct measurement methods. In the laboratory often vacuum filtration and an analysis of the samples by loss of ignition is used. The determination of particle size distribution of the samples with fine sediments is performed either by hydrometer analysis or by laser diffraction (figure 68a). For a more detailed overview on the laboratory analyses of suspended sediment samples it is referred to DIN 38409 (1987) or DVWK (1986).

Especially for reservoir management purposes, such as to monitoring suspended sediment concentrations, which develop downstream of the reservoir during a flushing operation, a method is required, which delivers information in almost real time, to adapt the flushing process, if necessary. An often used method are the so called “Imhoff-cones”, coming from urban water management (figure 68b). The obtained water/sediment samples are poured in the cones and after a pre-defined time slot (15 to 30 minutes) the amount of settled particles is read off. Based on a site specific calibration curve, the obtained values can be converted in mass concentrations. However, due to the necessity of a site specific calibration function, this method is only reliable if data already exist.

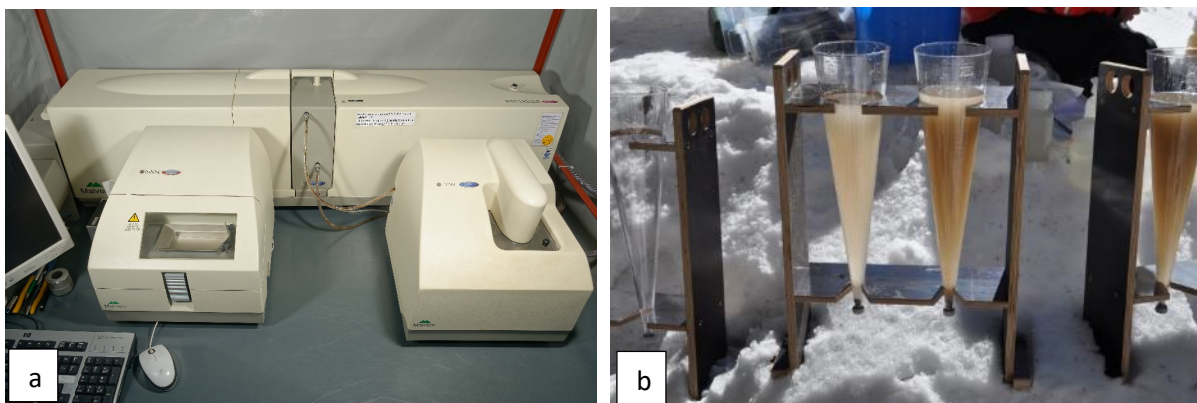


Fig. 68: (a) Malvern Mastersizer 2000 (Malvern Instruments Ltd, 2021) to obtain PSD for sediments in the range of 0.01 – 10,000 μm (photo courtesy: Bojan Skodic); (b) “Imhoff-cone” samples taken downstream of the Bächental reservoir in Austria in 2015.

Finally, it should be mentioned that suspended sediment sampling requires a lot of human intervention, skilled personal and is labor intense, especially due to the subsequent laboratory analysis. Measurements have to be taken during different hydrological conditions (low flow as well as high flow conditions), which is especially difficult for high flow conditions, and often even dangerous. However, direct sampling with a subsequent laboratory analysis is currently the only available method to obtain accurate and correct results. Hence, physical sampling is the only accepted reference technique (Aberle et al., 2017). In addition, the taken sample itself does not underlie any calibration process. To reduce the labor intense work load direct samples are more and more coupled with indirect methods to reduce the work load, and in addition to increase the spatial and temporal resolution of the measurements.

Indirect methods based on optics

(1) Optical backscattering

For measurements based on the principle of optical backscatter (OBS) incident light (infrared or visible light) is scattered by transported undissolved substances in suspension (e.g., suspended matter) and a series of photodiodes detect the backscattered light (figure 69a). The concentration of the suspended matter is determined by an empirical calibration, which converts the weakening of the light flow (as result of the turbidity) to a concentration (Black and Rosenberg, 1994). Turbidity sensors are currently the most used devices to obtain a series of suspended sediment concentrations in rivers and reservoirs. Figure 69b shows a turbidity sensor, located downstream of the Bächental reservoir in Austria to observe the occurring SSC during the water release from the reservoir. Compared to other devices turbidity sensors are (i) cheap, (ii) robust and (iii) can measure almost continuously. However, measurement instruments based on optical backscatter are only able to perform point measurements, as a consequence the spatial resolution is limited. Another disadvantage is that turbidity sensors need calibration to obtain results for suspended sediment concentrations.

The calibration has to cover all possible ranges of concentrations and grain size distributions as especially for turbidity sensors a large grain size dependency is recognized. The light attenuation is generally less for sand particles compared to equal mass concentration of smaller particles (Davis-Colley and Smith, 2001); therefore, the response of an OBS increases with a decreasing particle size (Conner and DeVisser, 1992; Downing, 1996; Sutherland et al., 2000). In addition, a large dependency on organic matter and the color of the transported particles is given. It can be concluded that the application range of OBS sensors strongly dependent on the particle size, shape, color, refractive index and the electronic configuration (Gray and Gartner, 2009). Anderson (2005) gives guidelines on the calibration process, also taking into account such influencing factors.

Beside instruments, which work on optical backscatter also instruments based on optical transmission are available. Here infrared or visible light is scattered/absorbed by undissolved

substances. However, in case of optical transmission instruments the receiving sensor is located opposite of the light source, where the attenuation of light is measured. It is often stated that instruments based on optical transmission are flow intrusive and are more sensitive for low concentrations (Downing, 1996). As a result, these devices are not being used that frequently to obtain suspended sediment concentrations.

For instruments, used for measurements for a longer period and based on optics biofouling of the sensor may occur. Many of them are therefore equipped with cleaning devices (figure 69b).

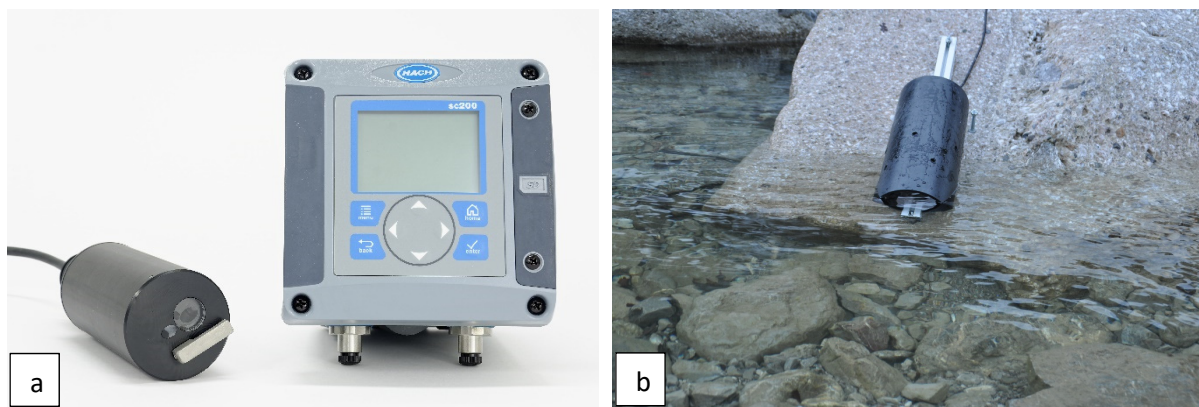


Fig. 69: (a) OBS-3 sensor with automatic wiper to prevent from biofouling (photo courtesy: Bojan Skodic); (b) OBS-3 sensor installed downstream of the Bächental reservoir in Austria in 2015.

(2) Laser diffraction

The measurement principle of laser diffraction is based on the Mie-theory. The characteristics of scattered laser light patterns by diffraction, refraction, reflection and absorption are used to obtain the particle size distribution of an ensemble of spherical particles within a defined sampling volume (e.g., Hirleman, 1987). A collimated laser beam is then sent through a sample with a pre-defined path length, where the light will be absorbed, reflected and scattered. Light which is scattered by the particles, is received by a lens and consequently printed on a detector or an array of detectors that allow the measurement of the scattering angle (Agrawal and Pottsmith, 2000). Subsequently, the particle-size distribution will be calculated based on the angle of the scattered light. Small particles are represented by large angles and coarse particles by small angles within this power distribution. The laser-diffraction method delivers the PSD equivalent to sphere sizes, where shape effects of natural sediment grains (rounded or angular grains) have to be included in processing the results (e.g., Agrawal et al., 2008). The huge benefit of this method is that beside particle size distribution also the suspended sediment concentration can be obtained by mathematical inversion of the data, to finally achieve a volume distribution. A detailed description of the inversion process was presented by Hirleman (1987).

For in-situ application the Laser In-Situ Scattering and Transmissometry instruments (LISST) by *Sequoia Scientific, Inc.* are available (e.g., figure 70a), which were built for measurements in the freshwater environment (Lynch et al., 1994; Agrawal and Hanes, 2015; Haun et al., 2013a; Haun and Lizano, 2016; 2018; Czuba et al., 2015 or Gitto et al., 2017). The LISST-SL (SL stands for stream lined, figure 70b) for instance covers a particle size range from 1.9 to 381 microns by a detector representing 32 small forward angles with logarithmically increasing radii (0.0017 – 0.34 radians). Due to the mathematical inversion of the data the volume distribution can be achieved (Eq. 6).

$$E = K N \quad (\text{Eq. 6})$$

where E is the 32-element data vector that contains the angular scattering energy, K is the scattering property kernel matrix and N is the volume distribution.

The range of the SSC depends in principle on the diameter of a particle (d) and on the path length (l) of the collimated laser beam and is approximately d/l (Agrawal et al., 2011). Additionally, the instrument has integrated depth and temperature sensors. Compared to other optical devices, which are e.g., based on turbidity, no calibration is necessary here. While converting of volume concentrations (measured by the LISST-SL) to mass concentrations, the LISST-SL software uses by default a density of 2.65 g/cm. This should be taken into account when processing the data (Czuba et al., 2015). The influence of mica (Felix et al., 2013; 2018) or due to flocculation is often neglected (Haun et al., 2015; Ehrbar et al., 2017, Haun and Lizano, 2018).

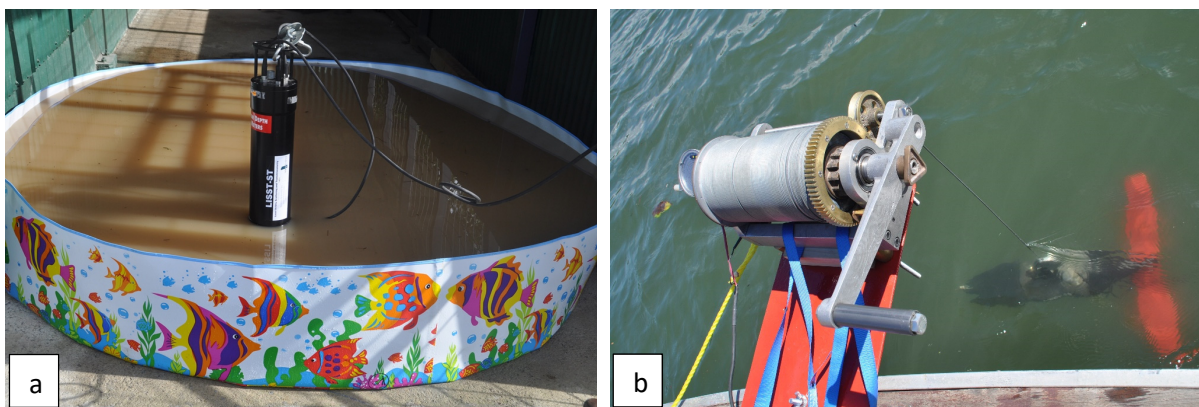


Fig. 70: (a) LISST-ST sensor, used for obtaining suspended sediment concentrations from a sample taken from the Angostura reservoir after a flood event in 2012; (b) LISST-SL applied at the Sandillal reservoir in Costa Rica in 2013.

Indirect methods based on acoustics

Suspended sediment concentration measurements based on acoustics are generally possible with every acoustic measurements device, starting from Acoustic Doppler Velocimetry (ADV), mainly used in the laboratory for measurements of the flow velocity, to Acoustic Doppler

Current Profiles (ADCPs), mainly used in open water environments for discharge and velocity measurements. ADCPs allow stationary as well as moving measurements, which enables a high spatial resolution of the measurements. As a consequence, ADCPs are nowadays the most important and most used devices for discharge and flow velocity measurements in river systems. Thus, the focus within this chapter is set on ADCP measurements.

The measurement principle of acoustic devices is based on the Doppler effect, where the acoustic properties of sound are used to determine flow velocities (Kinsler et al., 1980; Urlick, 1983). The device transmits a sound impulse at a fixed frequency. The sound impulse will be reflected by transported particles in the water body, such as plankton or sediment particles and the returned signal will be measured by the device. The distance can be obtained based on the travelling time of the sound impulse and due to the shift in frequency (Doppler effect) flow velocities of particles within the water column can be measured. By using the geometrical details of the river cross section in combination with the measured flow velocities the discharge can be obtained (Gordon, 1989; Adler, 1993). A more detailed overview on the topic of the Doppler effect, radial current velocities and broadband Doppler processing can be found in Gordon (1996).

Beside the flow velocities also the acoustic backscatter signal (ABS) is recorded by the ADCP, which represents losses in the signal strength as a result of beam spreading, the absorption by water and the absorption by sediments. Therefore, an analysis of the strength of the reverberated sound gives qualitative information regarding the occurring SSC (Eq. 7) and their distribution (e.g., Hay, 1983; Thevenot et al., 1992; Gartner, 2004; Deines, 1999; Guerrero et al., 2011). The relationship between the SSC and the relative ABS can be expressed as (Thevenot et al., 1992):

$$SSC = 10^{(A+B \cdot BS)} \quad (\text{Eq. 7})$$

where *SSC* is the suspended sediment concentration, intercept *A* and slope *B* are parameters from a regression function, evaluated by sediment samples and *BS* is the corrected acoustic backscatter signal.

As indicated in equation 7, a calibration with water samples is required due to the limited sensitivity of the applied device with only a single frequency. The use of a regression function is only possible if the occurring conditions show a similar grain-size distribution and an almost constant water temperature over the depth. In case of using an ADCP for determining sediment fluxes, no data is available within the blanking distances close to the water surface (due to the ringing effect) and close to the bottom (due to the side-lobes effect; Baumert et al., 2005; Muste et al., 2006; Duclos et al., 2013; Lee et al., 2016). An approach often used in literature is to extrapolate into these zones with a gradient development from the last three valid cells of the measured data. For deeper parts of the reservoir a gradient for the

extrapolation is used, which is developed from a number of cells with a similar height as the blanking-zone height itself (Latonski et al., 2014; Haun and Lizano, 2018).

Figure 71a and 71b show two measurements of the same transect in the Peñas Blancas reservoir in Costa Rica on November 28, 2013 (figure 71a) and December 19, 2013 (figure 71b) with a RDI RiverRay ADCP (RD Instruments, 1999). The figures present the distribution of the ABS as well as the dimensions of the blanking distances and the difference in the ABS strength during the two measurements, where the measurements on November 28, 2013 (figure 71a) showed up to 60 times higher concentrations SSC compared to the measurements on December 19, 2013.

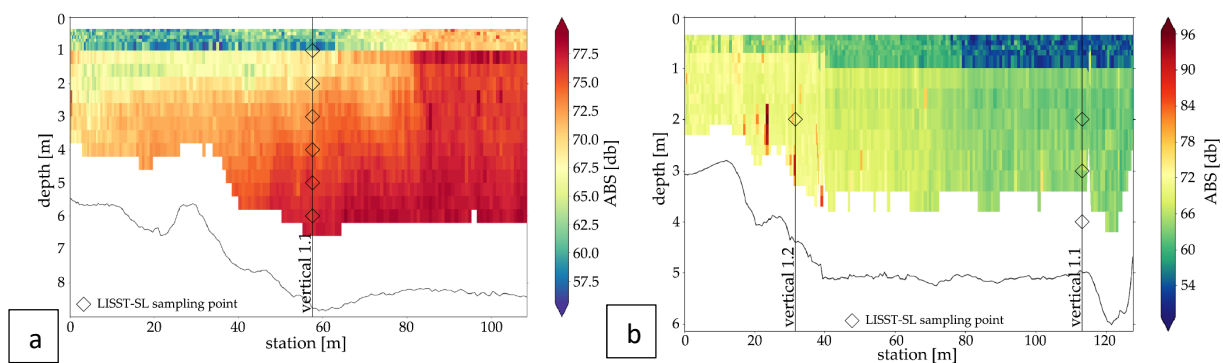


Fig. 71: Measured ABS by a RDI RiverRay for a transect in the Peñas Blancas reservoir in Costa Rica on (a) November 28, 2013; (b) December 19, 2013.

Although the use of ABS for obtaining SSC from single-frequency devices is meanwhile often used in rivers (Guerrero et al., 2011; 2016; among others), an application in reservoirs is seldom. In reservoirs ADCPs are most of the time installed in a stationary mode, e.g., for investigating density currents (e.g., Chikita et al., 1990; De Cesare et al., 2001), however, a use in moving operation mode is even more rarely performed due to the challenging small flow conditions within the reservoir (Umeda et al., 2006; Menczel and Kostaschuk, 2013; Haun and Lizano, 2018).

Ongoing research is performed by several research groups to develop a multi-frequency acoustic approach for suspended sediment as well as grain size distribution measurements. Here two devices, operating at different frequencies, are deployed at the same measuring profile. Guerrero et al. (2013) have reported good agreement between measurements in the Parana river compared to physical samples. An overview about recent research in the field of acoustics and sediment transport was presented by Sassi et al. (2012).

Indirect methods based on density differences

Especially for high suspended sediment concentrations an evaluation can be performed based on the density of the water-sediment mixture. The measurements are conducted with oscillating U-tubes, also called Vibrating Tube Density Meters or Coriolis Flow and Density Meters. Vibrating Tube Density Meters work on the principle of the Mass-Spring Model,

means that the density is measured based on the natural frequency of the measuring tubes (Kalotay, 1999). During the measurement the sample fluid flows continuously through a U-Shaped tube and the frequency of oscillation is measured (Lipták, 2003). It is important to measure accurately the frequency of oscillation of the sample because the density of the fluid is directly related to the frequency of oscillations. Figure 72a and 72b show the application of a Coriolis Flow and Density Meter at the Fieschertal hydropower plant in the Swiss Alps and the Kaunertal hydropower plant in the Austrian Alps, respectively.

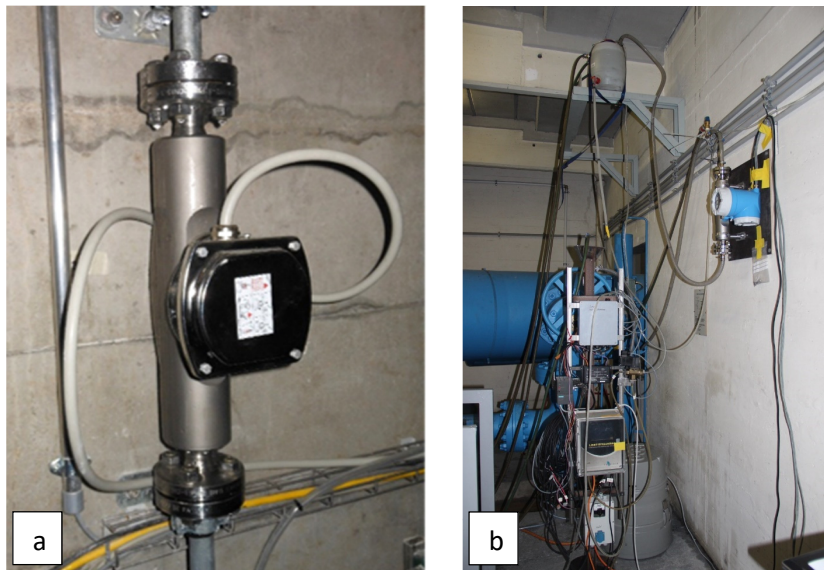


Fig. 72: Vibrating Tube Density Meter installed in the powerhouse of (a) the Fieschertal hydropower plant in 2015 (photo courtesy: David Felix); (b) the Kaunertal hydropower plant in 2016 (photo courtesy: Martin Schletterer).

6.3.2 *Bed load transport measurements*

As previously mentioned, bed load represents only approx. 5 – 30 % of the total sediment load transported in rivers (e.g., Ashley et al., 2020). However, for gaining deeper knowledge on ongoing sediment transport processes in open water bodies also a quantification of sediments, which are transported on the stable bed by sliding, rolling or saltation is necessary (Aberle et al., 2017). Techniques for bed load measurements can be subdivided into:

- (i) Direct methods, such as sampling bed load over a certain time period,
- (ii) indirect methods, such as using acoustics,
- (iii) tracer methods, where e.g., the transport path of single particles is tracked.

An important point in measuring and quantifying bed load transport is the spatial as well as the temporal resolution of the measurements, which influences the accuracy of the results. However, most bed load transport measurement devices are either limited in their spatial resolution, such as bed load samplers, or they only provide time-integrated results, as it is the

case for sediment traps. As bed load transport has a higher spatial and temporal variability compared to suspended sediment transport, it makes it even more difficult to obtain representative samples for bed load transport (Bunte and Abt, 2005). In addition, many of the available methods need calibration, which is often conducted in the laboratory and may introduce measurement errors by applying the method in the field. Gray et al. (2010) presented an overview on such possible measurement errors.

6.3.3 *Direct measurement methods*

Direct measurement methods collect bed load over a certain period of time with a sampler or a trap, which are withdrawn from the water body to determine its weight. Then, the bed load transport is calculated according to the sampling time. In addition, direct methods allow the analysis of the particle size distribution of the transported material in the laboratory. Direct measurement methods can be subdivided into (i) physical traps and (ii) bed load samplers.

Physical traps

(1) Pit traps

Pit traps are fixed installations in the river bed (figure 73a). Transported bed load is collected by containers located beneath the bed, which are frequently emptied and analyzed regarding the amount and characteristics of the transported particles (Tritton, 1988; Schneider et al., 2016). According to literature, the trapping efficiency of pit traps can be considered to be relatively high (Hubbell, 1987), if an appropriate design is chosen. Here e.g., the length of the pit trap needs to be sufficient to avoid that jumping particles are not collected. In addition, pit traps do often not cover the whole transect. This has to be taken into account when calculating the transport through a river or reservoir transect. To overcome this problem artificial cross sections may be constructed, where the bed load is mainly transported through the deepest point of the cross section. Figure 73b shows such an installation at the Schöttlbach in Austria. Last but not least, the selection of an appropriate interval for emptying the containers should be selected depending on the flow conditions. Especially flood events carry a higher amount of bed load, where the volume of the sampler needs to be designed in a way that no oversampling of the container occurs. However, even if the sampler is emptied frequently, an assignment of bed load transport rates to specific discharges is often not possible.

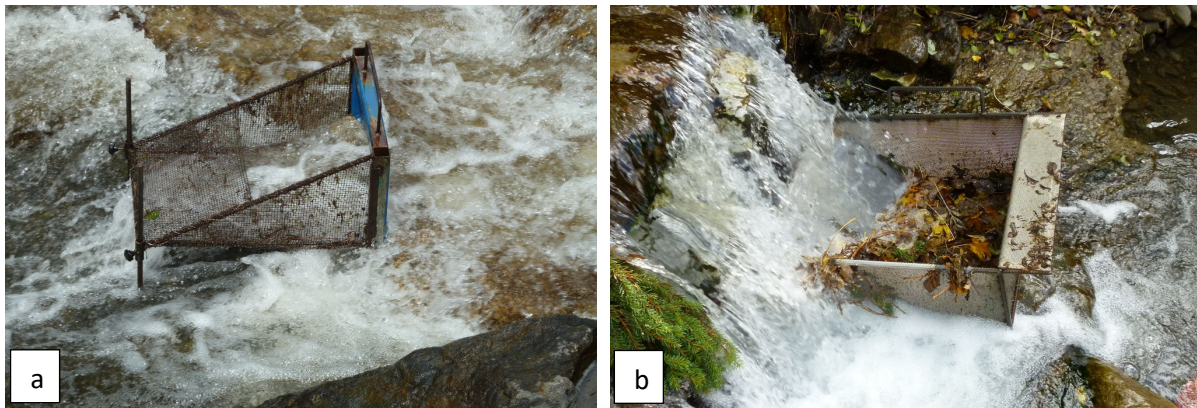


Fig. 73: (a) pit trap installed at the Schöttlbach, Austria to collect sediments and to determine bed load transport (photo courtesy: Gabriele Harb); (b) bed load trap at the Schöttlbach, Austria, placed downstream of an artificially built cross section (photo courtesy: Gabriele Harb).

(2) Check dams

Check dams are a possibility to decrease the sediment inflow into reservoirs (see chapter 5.2.2 *Pre- and check dams*). They are located at the head of the reservoir or even further upstream in tributaries to prevent sediments being carried into the main stream (figure 46a-b). Especially in mountainous regions these structures retain a high amount of coarse sediments, which would be transported as bed load into the reservoir (figure 47a-b). During emptying the check dam, the amount of trapped sediments can be estimated. As a consequence, check dams are a simple option to estimate bed load transport of the tributary or river (Rickenmann, 1997). In addition, it is feasible to analyze the characteristics of the trapped sediments.

Bed load samplers

Bed load samplers are mobile devices, which will be placed on the river bed. After a pre-defined time, which is depending on the amount of transported sediments and which is chosen in a way that no oversampling occurs, the sampler is raised to the surface, the sampler is emptied and the material is weighed to determine the bed load transport per unit time. Many different designs of bed load samplers have been developed over the years. The most predominant bed load sampler is the pressure-difference sampler, e.g., the Helley-Smith bed load sampler (figure 74a, Helley and Smith, 1971). Depending on the size of the sampler and the design (e.g., net openings) different fractions can be sampled, from sand to medium gravel. A limiting factor for bed load samplers is often the operation during high flow conditions.

For wadeable areas portable bed load samplers are widely used. These samplers are often also called mobile bed load traps due to their design, as they have a large opening and compared to e.g., Helley-Smith bed load sampler, a large sampling time (Bunte et al., 2001). To ensure a good contact with the ground, which is required for a reliable sampling, and to stabilize the sediment trap these samplers are often mounted on a ground plate (Bunte et al., 2004).

For sampling bed load with mobile samplers, important factors are the spatial as well as the temporal resolution of the measurements. Bed load samplers are, on the one hand, very flexible regarding their location, however, the spatial resolution is limited due to their comparably small opening of the mouth of the sampler in contrast to the width of the river. For reliable measurements, several spots along a predefined transect are necessary. Figure 74b shows a bed load trap array along the Riedbach in Switzerland to ensure a high spatial resolution when obtaining sediment transport rates (Schneider et al., 2016). An advantage compared to pit traps discharge rates during sampling are known, which results in the possibility to obtain a sediment transport - discharge function.

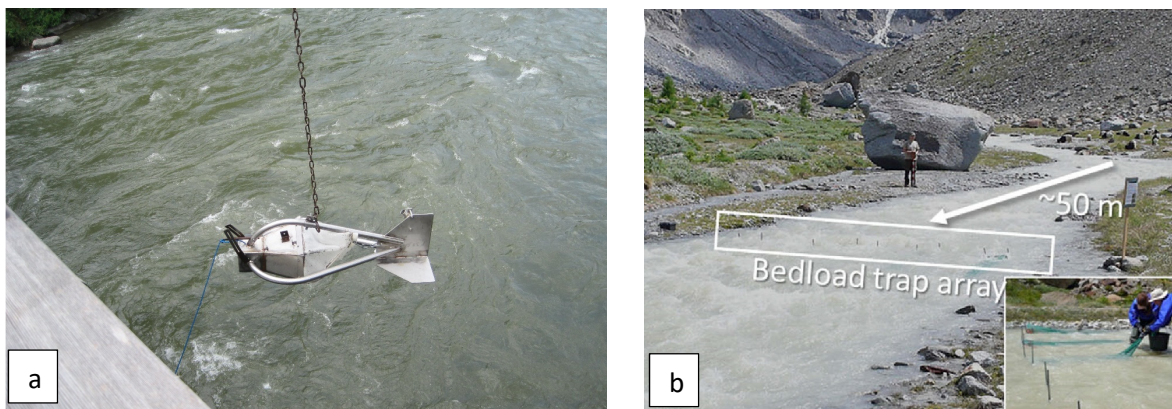


Fig. 74: (a) Helley-Smith sampler used to sample bed load transport at the head of the Bodendorf reservoir, Austria (photo courtesy: Gabriele Harb); (b) bed load trap array at the Riedbach in Switzerland (Schneider et al., 2016).

6.3.4 *Indirect measurement methods*

Indirect measurement methods for bed load are based on proxy parameters, such as the use of acoustic detectors. Similar to most indirect methods used for suspended sediment measurements no exact quantification of the characteristics of the transported sediments is possible as sediments are not directly collected. However, acoustics are meanwhile widely used as indirect measurement technique to obtain bed load transport in rivers and streams. Two different approaches are available, namely active and passive techniques.

Active acoustic measurements

Active acoustic measurements use stationary or moving ADCP measurements to determine bed load transport (Figure 75a). When employing an ADCP for discharge or flow velocity measurements, usually the so called bottom tracking (Doppler sonar) is used to measure the velocity of the instrument, relative to the river bed (Aberle et al., 2017). In case of a mobile bed, this value is biased by the transported sediments at the river bed. By taking into account a second measure of the boat velocity (e.g., by a Differential Global Positioning System; DGPS), this bias can be calculated, where the difference between the biased bottom track velocity and the DGPS velocity is similar to the occurring bed load velocity. Figure 75b shows a moving

ADCP measurement at the head of the Bodendorf reservoir, Austria, in 2010. The blue line represents the measured track of the ADCP obtained by bottom tracking, and the yellow line by DGPS measurements. For bed load measurements the ADCP can be used in a moving operation, means mounted on a vessel, or can be installed in a stationary mode. For both applications (moving and stationary measurements) several authors (e.g., Rennie et al., 2002a; 2002b; Rennie and Villard, 2004 and 2007; Gaeuman and Jacobsen, 2006; Conevski et al., 2019; 2020) recommend an averaging over a certain time period (for stationary measurement) and spatially (for moving measurements) to reduce the errors as result of the variance of bed load transport, but also as result of the instrument noise. With this information it is possible to obtain a linear calibration between the apparent bed load velocity and the transported bed load (Rennie et al., 2002a). However, in most cases such a calibration is only valid for individual river reaches. Beside the site-specific characteristics, also the applied instrument is of importance when obtaining such a calibration, as the calibration also depends on the frequency of the instrument, the bottom track algorithm, pulse length and the grain-size distribution of the bed material (Aberle et al., 2017). In addition to active acoustic measurements bed load samples can be taken to get information on the composition of transported sediments.

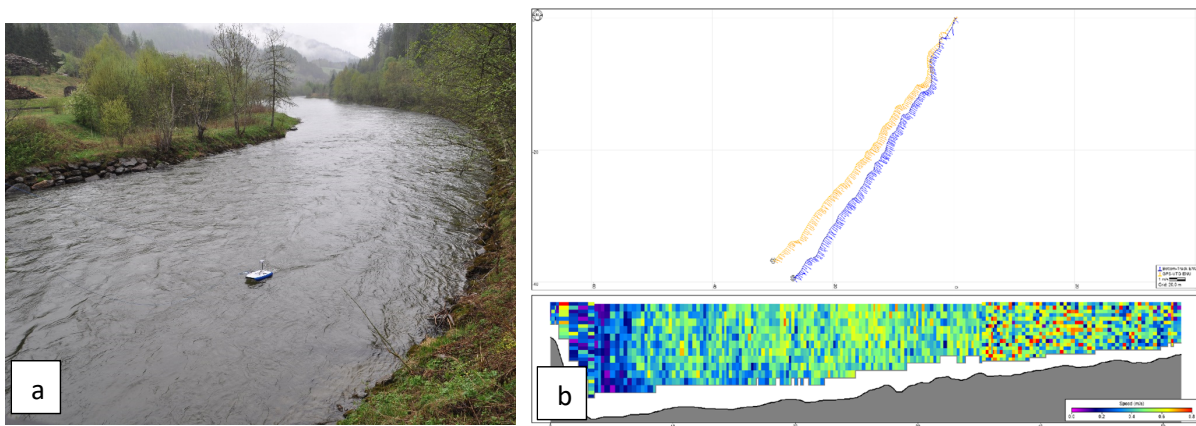


Fig. 75: (a) moving ADCP measurements at the Bodendorf reservoir in Austria in 2010 with a Sontek M9 ADCP; (b) with a clear indication of bed load transport.

Passive acoustic measurements

Passive acoustic measurement methods are based on measurements of sound or vibration signals generated by moving sediment particles. This happens either by measuring the impact of sediment particles on impact structures, such as pipes or plates, or by detecting the noise of inter particle collisions, as an indirect result of bed load transport. For measuring the noise of inter particle collisions or of the collisions between the bed load and the river bed, hydrophones are used, which receive the underwater sound generated during bed load movement (Barton et al., 2010; Geay et al., 2017). In case of hydrophone measurements, the signal response is strongly dependent on the location of the acoustic source (Geay et al., 2017), where an integrated recording of the surrounding is performed. As a result, underwater

microphones record also other noise in the stream, generated e.g., by turbulence (hydrodynamic noise) (Basset et al., 2013). For obtaining a higher resolution multiple hydrophones can be placed at different locations (Basset et al., 2013) to at least overcome the disadvantage of a limited spatial resolution.

Other systems are based on a direct impact of particles on pipes or plates. The sound generated by the collision of particles on an air-filled steel pipe (also called Japanese microphones / hydrophones; Mizuyama et al., 2010a) is measured. The steel pipe is usually embedded in the bed along a selected transect (Aberle et al., 2017). An alternative system is to measure the impact on steel plates, equipped with a geophone (also called Swiss plate geophones; figure 76a, b) system (Rickenmann et al., 2012). The bed load transport can be measured only on a local spot. However, in case a higher spatial resolution is required an array of impact plates is installed along a transect, which provides the possibility of obtaining information on bed load transport along the whole transect. Also resulting vibrations of the steel plate by accelerometers or piezoelectric sensors can be measured (Rickenmann, 2017).

An important issue in using passive acoustic measurement methods is a profound calibration, preferable in-situ, to obtain reliable values regarding the sediment fluxes. Flume experiments with hydrophones have shown that the energy of the resulting acoustic signal is related to the bed load flux by a power law function (e.g., Thorne, 1986), whereas field calibrations with impact sensors show that an approximately linear relationship exists between the number of impulses and the bed load mass (Mizuyama et al., 2010b; Rickenmann et al., 2012). Both systems (impact sensors and hydrophones) deliver continuous measurements over time, however, no information on sediment characteristics can be gained, even if ongoing research tries to quantify that issue by taking the intensity of the signal into account.

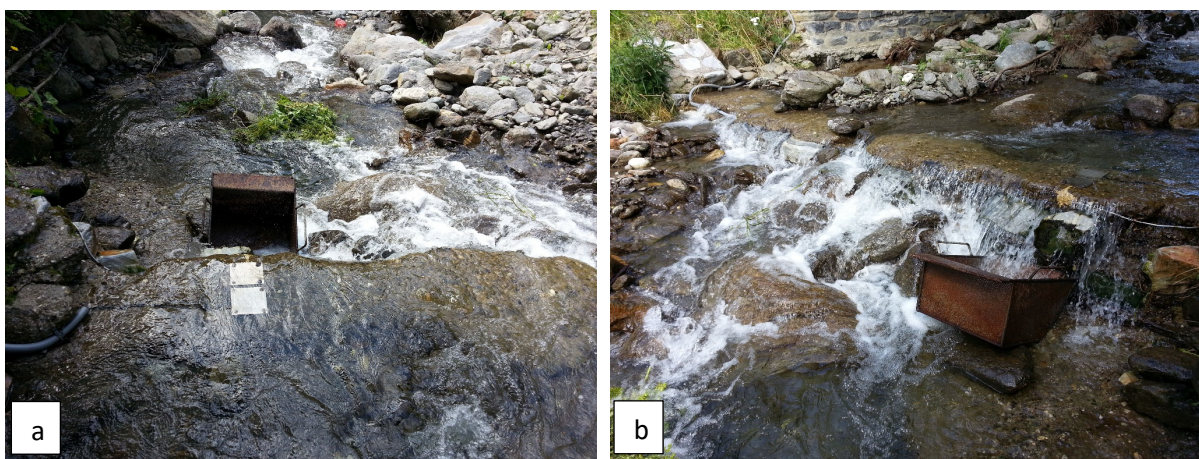


Fig. 76: steel plates, equipped with a geophone installed at the Schöttlbach, Austria, with an installed bed load trap (photo courtesy: Gabriele Harb) (a) view in downstream direction; (b) view in upstream direction.

6.3.5 Particle tracers

Tracer particles represent one of the oldest approaches for bed load measurements. This method allows for a determination not only of bed load rates, but provide also the capability to obtain information on pathways, directions and travel times of single particles of different grain sizes (Hassan and Ergenzinger, 2003). For the purpose of visualizing and recording bed load transport, tracers or markers in combination with detectable sensors are applied. The simplest form is using painted stones (figure 77a). Due to the ongoing development more sophisticated methods are used, such as luminescent, naturally colored minerals, radioactive, magnetic and passive radio tracers (Laronne and Carson, 1976; Hassan et al., 1984; Ergenzinger and Custer, 1983; Hubbel and Sayre, 1964). The movement of these passive tracers is usually recorded by observations in pre-defined time intervals or before and after events, which means that the particle displacement is a function of the flow history (Aberle et al., 2017). The observation of passive tracers is depending on the used method. The simplest form is the visible inspection (e.g., for painted stones). But also technical identification systems are available. For passive integrated responder tags a radio frequency identification is common (Nichols, 2004). In addition, it is possible to measure the passage of particles in pre-defined cross sections, which are instrumented (Ergenzinger and Custer, 1983; Schneider et al., 2010 and 2014). It has to be taken into account that particles buried in the river bed may not be found during the survey anymore, and passive tracers might get lost. To ensure a continuous monitoring active transponders are in use (figure 77b), where radio transmitter communicate the position of the particle continuously (Ergenzinger et al., 1989; Habersack, 2001). With this technology it is feasible to increase the spatial, but also temporal resolution. The latter represents the newest development, however also the most expensive one. Hence, only a limited number of tagged particles can be exploited.

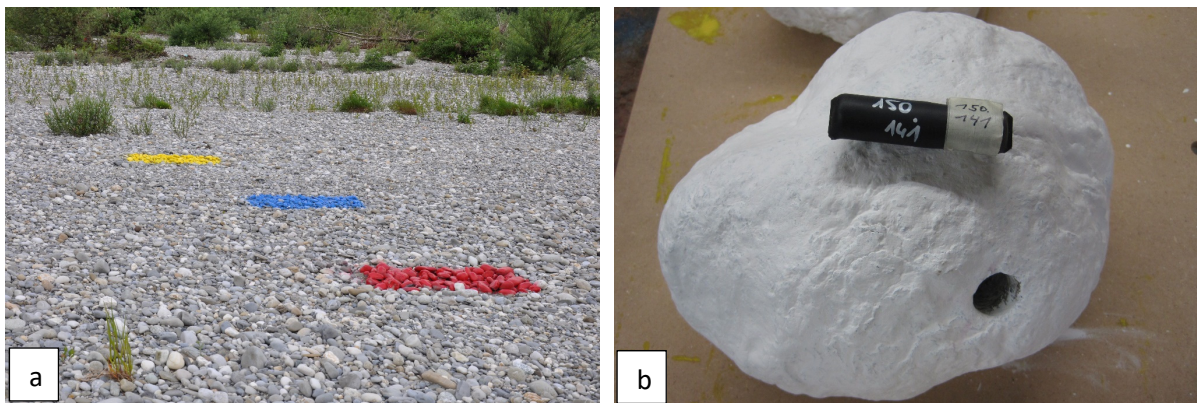


Fig. 77: (a) tracer stones used at the river Rhone to investigate the occurring bed shear stress and bed load transport during a eco-friendly flushing in 2017; (b) remote Frequency Identification (RFID) transponder inserted into a tracer stone, implemented at the Schöttlbach in Austria (photo courtesy: Gabriele Harb).

7 HYDRO-MORPHODYNAMIC NUMERICAL MODELS

Within this chapter an overview on existing approaches in hydro-morphodynamic modeling is given. Apart from an introduction to the basic equations in hydrodynamic modeling, a special focus is set on modeling hydro-morphodynamic processes. For gaining a deeper understanding on hydrodynamic modeling the book “An introduction to Computational Fluid Dynamics, The Finite Volume Method” by Versteeg and Malalasekera (1995) is recommended. For obtaining a deeper understanding on hydro-morphodynamic modeling the book “Computational River Dynamics” by Wu (2008) is suggested literature.

As a result of an increased computational power and due to further development of numerical solvers and computational techniques, computational fluid dynamics (CFD) has become a powerful tool in civil engineering (e.g., Shoarinezhad et al., 2020b). As a consequence, numerical models are meanwhile also in hydraulic engineering state of the art for simulating hydrodynamics in rivers and reservoirs. Within the last decade more and more often numerical models have been used to simulate sediment transport in complex environmental systems. This is a direct result of a better understanding of underlying processes and the implementation of sediment-related algorithms into the models.

In general, the models consist of two parts: the solver for the hydrodynamics and the solver for the simulation of the hydro-morphodynamic processes. Usually, for each time step the hydrodynamic calculations are performed first, followed by the morphodynamic routine, which simulates bed and suspended load transport as well as the subsequent morphodynamics, including bed changes. Depending on the model, hydrodynamics and morphodynamics are solved for each time step, or the morphodynamics are computed only after a certain amount of hydrodynamic time steps, which reduces the simulation time.

7.1 *Basics in hydrodynamic modeling*

The simulation of turbulent flow of fluids is based on the conservation equations for mass (continuity equation) and momentum (Newton’s second axiom), resulting in the so-called partial differential equations of flow. In the following the partial differential equations are given based on Versteeg and Malalasekera (1995).

The continuity equation in its general form, for non-stationary conditions in all three dimensions can be seen in Eq. 8. For steady state conditions (transient flow conditions) no accumulation of mass is given (Eq. 9). As a result, mass can be accumulated or depleted within the control volume only by a corresponding change in the fluid density. By neglecting the variation in density (for incompressible fluids) Eq. 10 develops.

$$\frac{\partial \rho}{\partial t} + \left(\frac{\partial \rho v_x}{\partial x} \right) + \left(\frac{\partial \rho v_y}{\partial y} \right) + \left(\frac{\partial \rho v_z}{\partial z} \right) = 0 \quad (\text{Eq. 8})$$

$$\left(\frac{\partial \rho v_x}{\partial x} \right) + \left(\frac{\partial \rho v_y}{\partial y} \right) + \left(\frac{\partial \rho v_z}{\partial z} \right) = 0 \quad (\text{Eq. 9})$$

$$\left(\frac{\partial v_x}{\partial x} \right) + \left(\frac{\partial v_y}{\partial y} \right) + \left(\frac{\partial v_z}{\partial z} \right) = 0 \quad (\text{Eq. 10})$$

where ρ is the fluid density, t represents the time and v_x , v_y , v_z are the flow velocities in x , y and z direction, respectively.

Based on the Newton's second axiom the rate of change of momentum of a fluid is directly proportional to the applied force. Or, in other words, a conservation of momentum is given for the case where the convective transport of momentum (by means of the kinetic energy of the fluid mass) as well as the diffusive transport of momentum (by means of the viscous shear stresses) are considered together with the acting sum of forces (gravity and pressure). The equations for the conservation of momentum in all three directions can be seen below (Eqs. 11-13).

$$\rho g_x - \frac{\partial p}{\partial x} + \frac{\partial \tau_{xx}}{\partial x} + \frac{\partial \tau_{yx}}{\partial y} + \frac{\partial \tau_{zx}}{\partial z} = \rho \left(\frac{\partial v_x}{\partial t} + \frac{\partial v_x}{\partial t} v_x + \frac{\partial v_x}{\partial t} v_y + \frac{\partial v_x}{\partial t} v_z \right) \quad (\text{Eq. 11})$$

$$\rho g_y - \frac{\partial p}{\partial x} + \frac{\partial \tau_{xy}}{\partial x} + \frac{\partial \tau_{yy}}{\partial y} + \frac{\partial \tau_{zy}}{\partial z} = \rho \left(\frac{\partial v_y}{\partial t} + \frac{\partial v_y}{\partial t} v_x + \frac{\partial v_y}{\partial t} v_y + \frac{\partial v_y}{\partial t} v_z \right) \quad (\text{Eq. 12})$$

$$\rho g_z - \frac{\partial p}{\partial x} + \frac{\partial \tau_{xz}}{\partial x} + \frac{\partial \tau_{yz}}{\partial y} + \frac{\partial \tau_{zz}}{\partial z} = \rho \left(\frac{\partial v_z}{\partial t} + \frac{\partial v_z}{\partial t} v_x + \frac{\partial v_z}{\partial t} v_y + \frac{\partial v_z}{\partial t} v_z \right) \quad (\text{Eq. 13})$$

where ρ is the fluid density, g is the acceleration of gravity, p is the instantaneous pressure, τ is the deviatoric stress tensor, which has an order of two, t represents the time and v_x , v_y , v_z are the instantaneous flow velocities in x , y and z direction, respectively.

By transformation of friction forces into velocity gradients, which is possible for Newtonian fluids due to the fact that friction forces are proportional to velocity gradients for this kind of liquids, the Navier-Stokes equations can be derived (Eqs. 14-16).

$$\rho g_x - \frac{\partial p}{\partial x} + \mu \left(\frac{\partial^2 v_x}{\partial x^2} + \frac{\partial^2 v_x}{\partial y^2} + \frac{\partial^2 v_x}{\partial z^2} \right) = \rho \left(\frac{\partial v_x}{\partial t} + \frac{\partial v_x}{\partial t} v_x + \frac{\partial v_x}{\partial t} v_y + \frac{\partial v_x}{\partial t} v_z \right) \quad (\text{Eq. 14})$$

$$\rho g_y - \frac{\partial p}{\partial x} + \mu \left(\frac{\partial^2 v_y}{\partial x^2} + \frac{\partial^2 v_y}{\partial y^2} + \frac{\partial^2 v_y}{\partial z^2} \right) = \rho \left(\frac{\partial v_y}{\partial t} + \frac{\partial v_y}{\partial t} v_x + \frac{\partial v_y}{\partial t} v_y + \frac{\partial v_y}{\partial t} v_z \right) \quad (\text{Eq. 15})$$

$$\rho g_z - \frac{\partial p}{\partial x} + \mu \left(\frac{\partial^2 v_z}{\partial x^2} + \frac{\partial^2 v_z}{\partial y^2} + \frac{\partial^2 v_z}{\partial z^2} \right) = \rho \left(\frac{\partial v_z}{\partial t} + \frac{\partial v_z}{\partial t} v_x + \frac{\partial v_z}{\partial t} v_y + \frac{\partial v_z}{\partial t} v_z \right) \quad (\text{Eq. 16})$$

where ρ is the fluid density, g is the acceleration of gravity, p is the instantaneous pressure, μ is the molecular dynamic viscosity, t represents the time and v_x , v_y , v_z are the instantaneous flow velocities in x , y and z direction, respectively.

With the developed Navier-Stokes equations the turbulent flow of liquid fluids can be simulated, e.g., by Direct Numerical Simulations (DNS), even for the most complex flows and without any simplifications of the equations (Orszag, 1970). However, due to the enormous required computational power a direct simulation with DNS is currently only possible for small Reynolds numbers, means cases where almost no turbulences occur, as DNS requires resolving a very wide range of time and length scales. Kuwata and Suga (2016) used DNS for simulating the transport mechanism of interface turbulence over porous and rough walls for a bulk Reynolds number of 3,000. Although, in the meantime a lot of research has been conducted in the development of DNS and the computational power has increased over the last decades, DNS is still limited to cases with a very reduced spatial and temporal scale (e.g., Shen et al., 2020). In addition, many simulated cases have been performed on simplified geometries so far (Stubbs et al., 2018).

An even more frequently used approach in research are Large Eddy Simulations (LES; Smagorinsky, 1963). For LES the smallest length scales are ignored within the simulations by using a low-pass filtering of the Navier-Stokes equations (e.g., Stoesser, 2010). This filtering is a time- and spatial-averaging, which removes small-scale information from the numerical solution. But this method can only be used in cases where small-scales are not playing an important role. Similar to DNS simulations, most LES simulations are still performed over exactly defined roughness elements and are not applicable for natural conditions (e.g., Leonardi et al. 2003; Stoesser and Nikora 2008). Yue et al. (2006) and Stoesser et al. (2008) performed simulations over typical bed form geometries, such as sand dunes. In addition, solute transport simulations on synthesized sediments were performed by using LES in a study published by Han et al. (2018), which is also an indicator that the number of LES simulations with natural boundary conditions, including transport phenomena, are increasing.

However, in river engineering, and especially for the simulation of hydro-morphodynamics, simpler approaches are necessary, as a result of the high temporal and spatial resolution of

the simulation domains. In addition, in rivers, but also in reservoirs during e.g., reservoir flushing, far higher Reynolds numbers can be expected, means fully turbulent flow conditions occur. As a consequence, models based on the Reynolds-averaged Navier-Stokes equations (RANS) are used for practical applications (Reynolds, 1895). Reynolds-averaging describes the process of subdividing the flow characteristic into an average value and a fluctuation term, resulting in a symmetrical viscous tensor. The decomposition approach by Reynolds (1895) is based on the assumption that the averaging time is much longer compared to the time scale of the turbulent motion (Dorfmann, 2017). Eq. 17 shows the decomposition of the flow velocity v .

$$v = \bar{v} + v' \quad (\text{Eq. 17})$$

where \bar{v} is the mean component of the flow velocity and v' is the velocity fluctuation component of the flow velocity.

The RANS equations are given below (Eq. 18; Einstein summation convention applies to repeated indices), where a turbulent Reynolds stress term ($-\rho\overline{u_i u_j}$) is introduced, which represents the momentum transport due to the turbulent motion.

$$\frac{\partial v_i}{\partial t} + v_j \frac{\partial v_i}{\partial x_j} = \frac{1}{\rho} \frac{\partial}{\partial x_j} (-P \delta_{ij} - \rho \overline{v_i v_j}) \quad (\text{Eq. 18})$$

where v_i is the averaged velocity, P is the dynamic pressure, δ_{ij} is the Kronecker delta and $-\rho\overline{u_i u_j}$ are the turbulent Reynolds stresses.

In the RANS equations the transient and the convection terms are placed on the left side, whereas the pressure term and the Reynolds stress term are located on the right side. However, due to the introduced unknown variables no closed solution can be found (also called *the closure problem*). To overcome this problem, turbulence modeling is introduced, where the turbulent Reynolds stress term is modelled by the Boussinesq's approximation (Boussinesq, 1897; *eddy viscosity concept*). In this eddy viscosity concept, it is assumed that the turbulent stresses are proportional to the mean velocity gradients (Eq. 19).

$$\overline{u_i u_j} = \vartheta_t \left(\frac{\partial v_i}{\partial x_j} + \frac{\partial v_j}{\partial x_i} \right) - \frac{2}{3} k \delta_{ij} \quad (\text{Eq. 19})$$

where ϑ_t is the turbulent viscosity (eddy viscosity), k is the turbulent kinetic energy and δ_{ij} is the Kronecker delta.

As the turbulent kinetic energy is a direct measure of the intensity of turbulent fluctuations in the three spatial directions it can be calculated by Eq. 20.

$$k = \frac{1}{2} \overline{u_i u_j} \quad (\text{Eq. 20})$$

where k is the turbulent kinetic energy and $\overline{u_i u_j}$ are the turbulent Reynolds stresses.

To calculate the unknown turbulent eddy viscosity, either a constant eddy viscosity (zero equation model) or more advanced turbulence models can be applied. Depending on the complexity of the corresponding correlations, a one-equation (Spalart-Allmaras model; Spalart and Allmaras, 1992), two-equation (k - ϵ or k - ω turbulence model; Launder and Spalding, 1972; Wilcox, 2008) or the more advanced Reynolds Stress model is applied. The Reynolds Stress model represents the most complete turbulence modeling approach available (Hanjalić and Launder, 2011).

In addition, other concepts, such as the Prandtl's mixing-length concept (Prandtl, 1925) or the Smagorinsky model, implemented for the sub-grid scale eddy viscosity (Smagorinsky, 1963) in LES, were developed. Prandtl's mixing-length concept for instance is based on the idea of an influence of the boundary layer, where for wall-bounded turbulent flows, the eddy viscosity varies with the distance from the wall, introducing a mixing-length (Prandtl, 1925).

The most often used approaches in river engineering are the k - ϵ turbulence model (Launder and Spalding, 1972) with its modifications by Rodi (1984) or Prandtl's mixing-length concept (Prandtl, 1925).

7.2 Dimensionality in hydrodynamic modeling

The Reynolds-averaged Navier-Stokes equations, developed in chapter 7.1 *Basics in hydrodynamic modeling*, are valid for all three spatial dimensions and for non-stationary flow conditions. However, for domains where the temporal and spatial dimension increases, such as studies for whole river systems, a simplification of the models needs to be performed to decrease the computational effort. As a consequence, the dimensionality of the models is reduced, and two dimensions or even only one dimension are simulated. Such a simplification has the benefit of a reduction in computational power, but needs to be done with care, as along with the reduction in simulation time, also the accuracy of the simulated results decreases.

7.2.1 2D Shallow water equations

The shallow water equations (SWE) are a set of partial differential equations, which are derived from the depth integrated Navier-Stokes equations (e.g., Vreugdenhil, 1994; Dawson and Mirabito, 2008). The basis for the shallow water assumption is that the wavelength (horizontal length scale) is much greater than the wave height (vertical length scale). The velocities in the vertical direction, as implied by the conservation of mass, can therefore be neglected (Eq. 21).

$$\frac{\partial h}{\partial t} + \frac{\partial q}{\partial x} + \frac{\partial r}{\partial y} = 0 \quad (\text{Eq. 21})$$

where h is the water depth, q is the x - component of specific flow and r is the y - component of specific flow.

The momentum equation shows that the vertical pressure gradients may be assumed to be hydrostatic as the streamline curvature is small. Thus the unknown pressure can be replaced by the water depth. In addition, the horizontal pressure gradients imply that the horizontal velocity field is constant throughout the depth of the fluid. As a result, also the vertical velocity component can be removed from this set of equations (Eqs. 22-23).

$$\frac{\partial q}{\partial t} + \frac{\partial}{\partial x} \left(\frac{q^2}{h} + \frac{gh^2}{2} - \frac{h}{\rho} \tau_{xx} \right) + \frac{\partial}{\partial y} \left(\frac{qr}{h} - \frac{h}{\rho} \tau_{xy} \right) = -gh \frac{\partial z_b}{\partial x} - \frac{\tau_{0x}}{\rho} \quad (\text{Eq. 22})$$

$$\frac{\partial r}{\partial t} + \frac{\partial}{\partial x} \left(\frac{qr}{h} - \frac{h}{\rho} \tau_{xy} \right) + \frac{\partial}{\partial y} \left(\frac{r^2}{h} + \frac{gh^2}{2} - \frac{h}{\rho} \tau_{yy} \right) = -gh \frac{\partial z_b}{\partial y} - \frac{\tau_{0y}}{\rho} \quad (\text{Eq. 23})$$

where ρ is the fluid density, h is the water depth, z_b is the bottom elevation, τ_0 is the bottom shear stress, τ_{ij} are the turbulent normal stresses and τ_{ij} are the turbulent shear stresses.

By using 2D shallow water equations, the model calculates flow velocities in a horizontal sectional plane (x - and y -direction) and neglects the velocities perpendicular to it (z -direction). As a consequence, averaged water velocities are assumed over the depth. However, the flow velocities in the vertical direction are not necessarily zero in reality. Using 2D shallow water equation models may result in large vertical velocity components, also resulting in curved streamlines. In such a case the hydrostatic pressure assumption is no longer applicable and the transport of sediments is not a function of the mean velocity anymore.

7.2.2 1D Saint-Venant equations

On the basis of the 2D shallow water equations, and the assumption that only velocities and momentum in the main flow direction (x -direction) have to be taken into account in the simulations, the 1D Saint-Venant equations can be derived (Saint-Venant, 1871). As closure of the hyperbolic system of equations, developed by Saint-Venant, the geometry of cross sections, by means of the hydraulic radius (or for shallow water assumptions the water depth) and the bed as well as the friction slopes, are taken into account (Ven Te Chow, 1959). The resulting equation for continuity (Eq. 24), expressing conservation of water volume for an incompressible and homogeneous fluid, as well as the momentum equation (Eq. 25), giving the balance between forces and momentum change rates.

$$\frac{\partial h}{\partial t} + v \frac{\partial h}{\partial x} + h \frac{\partial v}{\partial x} = 0 \quad (\text{Eq. 24})$$

$$\frac{\partial v}{\partial t} + v \frac{\partial v}{\partial x} + g \frac{\partial h}{\partial x} + g(S_f - S) = 0 \quad (\text{Eq. 25})$$

where h is the water depth, S_f is the slope of the bed (friction term) and S is the friction slope (gravity term).

When using the 1D Saint-Venant equations the flow velocity will be averaged over the entire cross-section, means only the flow velocity in x-direction is available from the simulations. This simplification is therefore only valid in cases where the velocities in transverse direction are small compared to those in the main flow direction, as it is the case for transient open-channel flow and surface runoff (e.g., Haestad, 2007). For these cases the velocity in y-direction can be neglected. However, 1D Saint-Venant equation models for hydro-morphodynamic simulations distribute the bed shear stresses uniformly along the cross sections. Especially in the case of compound channels this fact may lead to unrealistic morphological bed changes within the cross section.

7.3 *Discretization in numerical modeling*

In CFD complex environmental systems are transferred into numerical models by using a system of non-linear partial differential equations (chapter 7.1 *Basics in hydrodynamic modeling*). This set of equations is solved by partitioning the modelled area in numerous small (finite) parts and by dividing the simulation time in discrete time-steps. The discretization is therefore a key part in obtaining reliable results from hydro-morphodynamic numerical models and needs to be considered with care when selecting an appropriate model.

7.3.1 *Spatial discretization*

Spatial discretization describes a mathematical technique of distributing the model domain in subareas (finite parts), also called elements. During the process of distributing the model domain, the unknowns are considered node-wise, means a replacement of an infinite-dimensional operator equation into a finite-dimensional algebraic equation (e.g., DeCarlo, 1989; Heinzl, 2007). By deriving stable, consistent and accurate algebraic replacements, the distribution between the unknown variables can be assumed, where the nature of this distribution varies accordingly to the used discretization method. In this case the variable in a node is then a function of the neighboring node and can be solved by a solution algorithm. However, it needs to be considered that the algebraic expressions are only valid for limited and small subareas.

Several methods exist for a spatial discretization of the simulation domain. The approaches mainly used in river engineering are:

- (i) *Finite Volume Method* (FVM): The partial differential equations are transformed into a conservative form by using the conservation laws in an integral form (Barth and Ohlberger, 2004). This enables the equations to be solved over discrete control volumes by considering the fluxes, sources/sinks or the changes over time in each cell. A benefit of the FVM is that it is flux-conserving by nature, since it is based on the approximation of conservation laws directly in its formulation (Heinzl, 2007). The method has in addition an advantage in memory usage, solution speed, and is able to simulate turbulent flow conditions (high Reynolds number) as well as source term dominated flows (Patankar, 1980).
- (ii) *Finite Element Method* (FEM): The FEM has its main application in the structural analysis of solids (Johnson, 1987). However, this method can also be used for simulating fluid dynamics, but requires special care, so that the formulation is given in a conservative form to ensure a conservative solution (Surana et al., 2004). The FEM uses the so-called weak integral form by applying the weighted residual method to the initial equations. As a consequence, an error occurs resulting in the fact that the balance equation is only fulfilled over the whole domain, but not in each individual element, as it is the case for the FVM. However, the FEM can be much more arbitrary with fewer quality constraints (Heinzl, 2007). Even if the FEM is more stable, it may require a higher memory usage, resulting in a slower solution speed (Huebner et al., 1995).
- (iii) *Finite Difference Method* (FDM): The FDM uses a quite different approach compared to the two previous presented methods (Heinzl, 2007). Within the FDM the partial differential equations are approximated by a series of difference quotients, means the non-linear equations are transferred in a system of linear equations, which are solved by matrix algebra techniques (Strand, 1994). The FDM has an advantage of a high computational efficiency along with a simple implementation and is therefore one of the most used approaches (Grossmann et al., 2007).

In principle all three methods are suitable in computational fluid dynamics. In CFD further methods, such as the spectral element method or the Lattice Boltzmann method are available, but not frequently used for the simulation of hydrodynamics in water bodies.

7.3.2 Temporal discretization

Temporal discretization describes a mathematical technique, applied to transient problems, which is performed for discretizing the governing equations in time, by means of the integration of every term in the general discretized equations within a time step. For temporal discretization two approaches are available, namely an explicit and an implicit procedure

(Olsen, 2000), to obtain a value at a time step (t) as a function of the previous time step ($t-1$) and/or as function of the neighboring values at the same time step.

Within an *explicit time discretization* the value of the variable at time step t is depending on the value of the variable at the previous time step $t-1$, including the values of the neighboring nodes of the previous time step (figure 78a). For instance, in case of calculating the discharge, the initial discharge is known in the node itself and in the neighboring nodes at $t-1$. The computation starts with the current time step (t), where for each node the discharge can be calculated from the discharge at the previous time step. This procedure is repeated for all nodes to calculate the current discharge. The explicit time discretization is easy to implement in a model. However, the procedure will become unstable in case of too large time steps. To avoid such instabilities, the convergence condition by Courant–Friedrichs–Lewy (Courant et al., 1928) is used (Eq. 26).

$$C = \Delta t \left(\sum_{i=1}^n \frac{v_i}{\Delta_i} \right) \leq C_{max} \quad (\text{Eq. 26})$$

where C is the Courant number, Δt is the time step, n is the spatial dimension, v_i is the flow velocity with respect to the spatial dimension, Δ_i is the length interval with respect to the spatial dimension and C_{max} is the maximum Courant number to avoid instabilities.

Eq. 26 presents a maximum Courant number to obtain stable simulations, which has, in case of an explicit solver, a value equal to unity. In other words, when keeping the maximum Courant number constant, the time step size is a function of the maximum flow velocity and the minimum element size. As a result, in cases with high flow velocities, such as spillways, usually small time steps are required. In river engineering larger time steps are feasible, due to the usually occurring subcritical flow conditions. Additionally, the time step size can also be governed by the element size.

Within an *implicit time discretization* the value of a variable at a time step t is depending on the values from the previous time step ($t-1$), as it is the case for the explicit time discretization, as well as on the values of the neighboring variables at the time step t (figure 78b). When a semi-implicit time discretization is used, in addition to the values of the neighboring variables t , also the values from the previous time step $t-1$ are considered, which improves the accuracy of the method. For instance, in case of calculating the discharge, the computation starts with the current time step (t), where for each node the discharge can be iterated from the current discharge values of the neighboring variables (implicit time discretization). This iterative procedure is repeated for all cells to calculate the discharge. As a consequence, for an implicit, but also semi-implicit time discretization, a complex system of equations must be set up and solved by the model. However, larger time steps can be used in the model without creating instabilities, which represents an advantage of the method. However, this does not mean that

arbitrary time steps can be chosen, as then results can occur in a range, which is physically not correct.

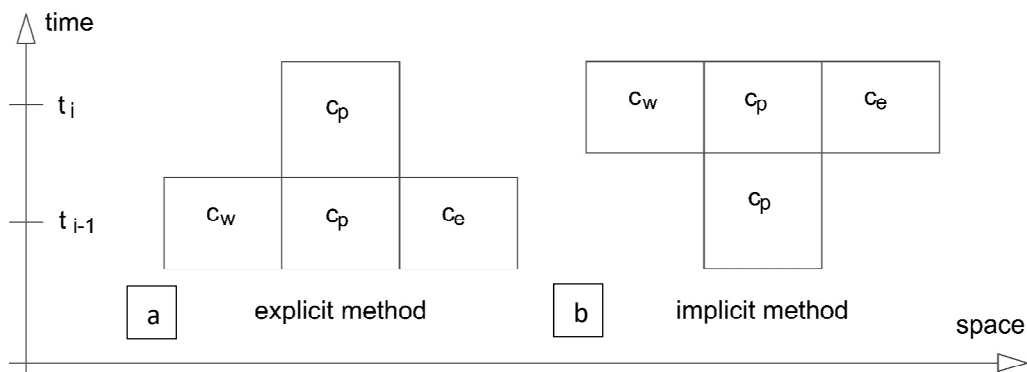


Fig. 78: Overview on the discretization procedure for time dependent calculations with an (a) explicit time discretization; (b) implicit time discretization.

7.4 Basics in hydro-morphodynamic modeling

This chapter is structured similarly to chapter 3 *Mechanism of sediment transport and river morphology*, including subchapters on erosion, transport and deposition. Especially in hydro-morphodynamic modeling many tailor made codes are available, which results in a relatively high number of different developed code structures. In addition, due to the stochastic nature of sediment transport and the use of many empirical approaches and formulae for simulating hydro-morphodynamics, the possibilities for implementing different algorithms are manifold. As basis for this chapter implemented approaches and algorithms within the three-dimensional numerical model *SSIM* (Sediment Simulation In Intakes with Multiblock option) are used to give an overview on the architecture and the possibilities of a code (Olsen and Kjellesvig, 1998; Olsen, 2020).

7.4.1 Erosion and re-suspension of particles

To quantify whether erosion takes place at the bed, usually the actual occurring bed shear stress is compared with the critical bed shear stress of the deposited sediments. The actual bed shear is calculated through the shear velocity (Eq. 27), which can be obtained by using a wall law (Eq. 28; Schlichting, 1979) Hence, the bed shear stress is calculated by using the velocity in the bed cell, the height of the bed cell, defined as the distance between the bed cell and the wall, and the wall roughness.

$$\tau_0 = \rho u_*^2 \quad (\text{Eq. 27})$$

$$\tau_0 = \frac{v_{bed} \kappa}{\ln\left(\frac{30y}{k_s}\right)} \quad (\text{Eq. 28})$$

where τ_0 is the bed shear stress, u_* is the shear velocity of the main flow, v_{bed} is the velocity in the bed cell, κ is the Von Kármán constant and equal to 0.4, k_s is the wall roughness and y is the distance between the bed cell and the wall.

Alternatively, the actual bed shear stress can be calculated by using the turbulent kinetic energy. When e.g., the k - ε turbulence model is used to solve the closure problem, it can be assumed that close to the wall the production and dissipation of turbulences are in equilibrium conditions. As a consequence, the bed shear stress can be calculated from the turbulent kinetic energy close to the bed (Eq. 29).

$$\tau_0 = c_1 \rho k = 300k \quad (\text{Eq. 29})$$

where τ_0 is the bed shear stress, c_1 is a proportionality constant equal to 0.19 (Soulsby, 1983), and k is the turbulent kinetic energy.

The critical bed shear stress is a function of the particle characteristic, and in *SSIM* calculated by using the Shields curve (see chapter 3.1. *Erosion*), where the dimensionless critical shear stress (Eq. 1) is related to the grain Reynolds number (Eq. 2). Depending on the model, the critical shear stress of sediment mixtures can be obtained for a characteristic grain diameter of the bulk mixture (e.g., the d_{50}) or for different grain-sizes separately.

However, if the bed material consists of a mixture of multiple sediment sizes, also additional phenomena, such as bed armoring effects, have to be taken into account. Smaller particles can interact with coarser particles, which results in a reduction of erosion of smaller sediment classes, even in cases where the actual bed shear stress exceeds their critical shear stress. Wu et al. (2000b) developed an approach to incorporate hiding and exposure effects in numerical models (Eq. 30-32).

$$p_{hi} = \sum_{j=1}^N f_j \frac{d_j}{d_i + d_j} \quad (\text{Eq. 30})$$

$$p_{ei} = \sum_{j=1}^N f_j \frac{d_j}{d_i + d_j} \quad (\text{Eq. 31})$$

$$\eta_i = \left(\frac{p_{ei}}{p_{hi}}\right)^m \quad (\text{Eq. 32})$$

where N is the number of particle size fractions of the non-uniform sediment mixture, f_i and d_i are the percentage and the diameter of the i^{th} fraction, respectively, η_i is the correction factor and m is a constant and equal to 0.6.

If sediment particles are moving on sloped beds, additional forces are acting on these particles, resulting in a change of their transport behavior. However, also the threshold for the initiation of sediment motion changes. Thus, a correction factor of the critical bed shear stress is introduced, which considers the required reduction. In *SSIM* the approach developed by Brooks (1963) is used, in cases, where the bed slope is orientated upwards or sideways compared to the velocity vector (Eq. 33).

$$K = -\frac{\sin\phi\sin\alpha}{\tan\theta} + \sqrt{\left(\frac{\sin\phi\sin\alpha}{\tan\theta}\right)^2 - \cos^2\phi \left[1 - \left(\frac{\tan\phi}{\tan\theta}\right)^2\right]} \quad (\text{Eq. 33})$$

where α is the angle between the flow direction and a line normal to the bed plane, ϕ is the slope angle and θ is an empirical factor found from flume studies and based on the angle of repose for the material.

Another, but very important factor in simulating reservoir sedimentation and especially reservoir management scenarios, like reservoir flushing, is the occurrence of cohesive sediments. The threshold for sediment movement is drastically higher if the bed material contains cohesive sediments (see chapter 3.1. *Erosion*). The simplest way of incorporating cohesive sediment properties is by artificially increasing the critical bed shear stresses with a single value or a ratio, based on in-situ measurements. More advanced approaches in numerical modeling were developed e.g., by Kranenburg and Winterwerp (1997), which focused on the flocculent surface layer, where the entrainment process is besides the hydraulic conditions mainly governed by the vertical density gradient induced by the mud suspension (Violeau et al. 2002). McAnally and Metha (2001) took two different erosion rates into account, distinguishing between an upper recently deposited and a deeper consolidated layer with uniform features.

Finally, and a very special form of erosion are sand slides (geotechnical failures), which may occur in e.g., meandering rivers by river bank erosion (lateral erosion), but are crucial in modeling reservoir flushing. When the water level in the reservoir is drawn down and a flushing channel develops, the lateral extension of this channel is mainly governed by sand slides into the flushing channel (Haun, 2012). In its simplest form the angle of repose of the bed material can be used in the numerical model, where at each time step the angle of the river or channel banks will be observed. In case that banks have a steeper angle as the defined angle of repose, erosion occurs until the banks have reached a steepness equal to the angle of repose (Olsen and Kjellesvig, 1998; Olsen, 2001). However, this approach has two disadvantages, first, it is only valid for non-cohesive sediments and second, the angle of repose for fully saturated sediment mixtures needs to be obtained for each study experimentally. Olsen and Haun (2018; 2020) developed an approach for taking into account geotechnical bank failures in hydro-morphodynamic models. The slide location is thereby determined on

the basis of an equilibrium limit approach and the actual movement is computed by the Reynolds-averaged Navier-Stokes equations, assuming that the soil in the slide is a viscous fluid. Beside the groundwater levels near to the banks of the reservoir also the cohesion as well as the coefficient of elasticity (*E-modulus*) and the shear modulus (*G-modulus*) of the soil are taken into account in this method. As a result, bed levels changes are governed by erosion and deposition, as a result of the sediment transport, and as a result of the slide movements and the subsequent depositions on the bed (Olsen and Haun, 2020).

7.4.2 Sediment transport modeling

Bed load and suspended sediment transport are based on completely different physical principles (see chapter 3.2. *Transport*), which needs to be reflected in numerical models accordingly.

For simulating suspended sediment transport either an empirically developed formula (Chandrasekhar, 1943) or the transient convection-diffusion equation is used, which describes the physical phenomena where particles are transferred inside a physical system. The convection-diffusion equation (Eq. 34) represents the two main transport processes in water bodies, namely convection and diffusion. The convection is governed by the stream power and the fall velocity of sediment particles, and is therefore the dominant transport process in rivers, whereas the turbulent diffusion is governed by random and chaotic time-dependent motions. In reservoirs the influence of diffusion is as a result of the low flow velocities increasing, means the dominating forces are in very large reservoirs often the turbulent mixing and the concentration gradients in the computation domain.

$$\frac{\partial c_S}{\partial t} + \frac{\partial(v_x c_S)}{\partial x} + \frac{\partial(v_y c_S)}{\partial y} + \frac{\partial(v_z c_S)}{\partial z} - \frac{\partial(w_s c_S)}{\partial z} = \varepsilon \left(\frac{\partial^2 c_S}{\partial^2 x} + \frac{\partial^2 c_S}{\partial^2 y} + \frac{\partial^2 c_S}{\partial^2 z} \right) \quad (\text{Eq. 34})$$

where c_S is the sediment concentration, t represents the time, w_s is the fall velocity of the particle, ε is the diffusion coefficient and v_x , v_y , v_z are the flow velocities in x , y and z direction, respectively.

In case of multiple sediment sizes, the convection-diffusion equation is solved for each grain-size separately (e.g., Olsen, 2000; Eq. 35).

$$\frac{\partial c_{S,j}}{\partial t} + \frac{\partial(v_x c_{S,j})}{\partial x} + \frac{\partial(v_y c_{S,j})}{\partial y} + \frac{\partial(v_z c_{S,j})}{\partial z} - \frac{\partial(w_{s,j} c_{S,j})}{\partial z} = \varepsilon \left(\frac{\partial^2 c_{S,j}}{\partial^2 x} + \frac{\partial^2 c_{S,j}}{\partial^2 y} + \frac{\partial^2 c_{S,j}}{\partial^2 z} \right) \quad (\text{Eq. 35})$$

where $c_{S,i}$ is the sediment concentration for the i^{th} sediment fraction, t represents the time, $w_{s,i}$ is the fall velocity of the specific particle size and ε is the diffusion coefficient.

As a boundary condition for the convection-diffusion equation an equilibrium sediment concentration needs to be specified in the model close to the bed. Eq. 36 shows the equation

developed by van Rijn (1984b), where the sediment concentration is within the model converted into an entrainment rate.

$$C_{bed,i} = 0.015 \frac{d_i}{a} \frac{\left(\frac{\tau_0 - \tau_{c,i}}{\tau_{c,i}}\right)^{1.5}}{\left(d_i \left(\frac{\rho_s / (\rho_w - 1)g}{\vartheta^2}\right)^{1/3}\right)^{0.3}} \quad (\text{Eq. 36})$$

where $C_{bed,i}$ is the concentration of the suspended load at the bed for the i^{th} fraction, d_i is the diameter of the i^{th} fraction, a is equal to the height of the center of the bed cell, τ_0 is the bed shear stress, $\tau_{c,i}$ is the critical shear stress for d_i , which is calculated by an analytical formula from the Shields curve, ρ_s is the density of sediments, ρ_w is the density of water, g is the acceleration of gravity and ϑ is the kinematic viscosity.

Alternatively, empirical suspended load transport equations can be used. However, most equations are developed for certain boundary conditions, such as for specific gradients of the bed and subsequent energy slopes or different grain size distributions of the sediment mixtures.

For an accurate simulation of settling and deposition processes of very fine particles (clay and silt), also flocculation processes need to be considered in the model, as flocs have very different particle properties, compared to the single grains (see chapter 3.3 *Deposition*). Within the last decade more and more development in the numerical implementation of flocculation (aggregation and disaggregation processes) has been done. Numerical models are often subdivided into macro-scale sediment processes, such as sediment transport and deposition and micro-scale processes, such as flocculation (Klassen, 2017). These micro-scale processes are mainly taken into account through mathematically and physically based flocculation algorithms or through empirical approaches. However, considering aggregation and disaggregation processes correctly is still challenging due to the high complexity of the ongoing processes and the still existing research gaps. As a consequence, approaches with a different degree of complexity are implemented in different models, e.g., by incorporating aggregation processes only. For only taking aggregation processes into account different flocculation models exist. However, they are all based on one fundamental coagulation equation, derived by Smoluchowski (1916). The disadvantages of the Smoluchowski formulation are the introduced simplifications, such as the assumption that flocs do not break up once they are formed. Klassen, 2017 implemented a size-class based flocculation model, derived by McAnally (2000) into the numerical model *SSIIM*, where a combination of a statistical and a deterministic physics-based representation of aggregation and disaggregation processes is considered.

Due to the stochastically behavior of bed load transport (see chapter 3.2. *Transport*) no analytical approach exists, which describes this transport process, resulting in the implementation of empirical bed load transport formulae in numerical models. A large

number of developed bed load transport formulae exists, however, every single formulation was developed for certain and very specific boundary conditions. In addition, many of these formulae were developed as a result of flume experiments in the laboratory. An overview of different bed load transport formulae is given for instance by Graf (1971). As examples the transport equations developed by Meyer-Peter-Müller (1948; Eq. 37) and van Rijn (1984b; Eq. 38) are presented.

$$q_{b,i} = \frac{8}{g} \frac{\rho_s}{\rho_s - \rho_w} \sqrt{\frac{1}{\rho_w}} [\tau_0 - \tau_c]^{3/2} \quad (\text{Eq. 37})$$

where $q_{b,i}$ is the transport rate of the total bed load per unit width, ρ_s is the density of sediments, ρ_w is the density of water, g is the acceleration of gravity, τ_0 is the bed shear stress and τ_c is the critical shear stress.

$$q_{b,i} = 0.053 d_i^{1.5} \sqrt{\frac{(\rho_s - \rho_w)g}{\rho_w}} \frac{\left(\frac{\tau_0 - \tau_{c,i}}{\tau_{c,i}}\right)^{2.1}}{d_i^{0.3} \left(\frac{(\rho_s - \rho_w)g}{\rho_w \vartheta^2}\right)^{0.1}} \quad (\text{Eq. 38})$$

where $q_{b,i}$ is the transport rate of the i^{th} fraction of bed load per unit width, d_i is the diameter of the i^{th} fraction, ρ_s is the density of sediments, ρ_w is the density of water, g is the acceleration of gravity, τ_0 is the shear stress at the bed, $\tau_{c,i}$ is the critical shear stress for d_i , which is calculated using an analytical formula from the Shields curve and ϑ is the kinematic viscosity.

Meyer-Peter-Müller's and van Rijn's equations were chosen to show the different boundary conditions, for which these two equations were developed. Table 2 gives an overview on the application range for the grain diameter and the hydraulic conditions.

Table 2: Boundary conditions for Meyer-Peter-Müller's and van Rijn's bed load transport equations (U.S. Army Corps of Engineers, 1998).

Sediment transport formula	Grain diameter [mm]	Average velocity [m/s]	Flow depth [m]	Energy gradient [%]
Meyer-Peter-Müller (1948)	0.4 - 29	0.37 - 2.87	0.009 - 1.19	0.04 - 2.0
van Rijn (1984)	0.32 - 1.44	0.36 - 1.29	0.2 - 0.73	-

Depending on the boundary conditions, such as hydraulics and sediment characteristics, bed forms may occur within a river or a reservoir. This needs to be considered in the model to ensure an accurate prediction of transport processes. On the one hand, these morphological structures have a major influence on the roughness of the bed (see chapter 3.2. *Transport*) and, on the other hand, Zanke (1982) and Wieprecht (2001) stated that for a wide range of discharges and grain-sizes bed forms are the governing type of bed load transport. Within

numerical models the bed roughness can be calculated by taking into account the grain roughness as well as the bed form height (Eq. 39).

$$k_s = 3.0d_{90} + 1.1\Delta \left(1.0 - e^{\left(\frac{-25\Delta}{7.3h}\right)} \right) \quad (\text{Eq. 39})$$

Where k_s is the total roughness in the model, taking grain roughness as well as the bed form height into account, d_{90} is the characteristic sediment size, Δ is the bed-form height and h is the water depth.

The bed form height and length need to be obtained from empirically developed equations, even if simplifications and limitations of these approaches have to be accepted. Eq. 40 shows an approach developed by van Rijn (1984c), which gives a ratio between bed form height and the water depth. However, this approach was developed for uniform and small sediment sizes and is recommended for small Froude numbers only. However, Haun et al. (2013a) have shown good simulation results by using this equation even for high Froude numbers during reservoir flushing.

$$\frac{\Delta}{h} = 0.11 \left(\frac{d_{50}}{h} \right)^{0.3} \left(1.0 - e^{-0.5 \left(\frac{\tau_0 - \tau_{c,i}}{\tau_{c,i}} \right)} \right) \left(25 - \left(\frac{\tau_0 - \tau_{c,i}}{\tau_{c,i}} \right) \right) \quad (\text{Eq. 40})$$

where Δ is the bed-form height, h is the water depth, d_{50} is the characteristic sediment size, τ_0 is the shear stress at the bed and $\tau_{c,i}$ is the critical shear stress for d_i , which was calculated using an analytical formula from the Shields curve.

For simulating sediment transport also additional physical processes, such as sediment transport on sloping beds, need to be taken into account by the numerical model. Sediment particles move generally parallel to the main flow velocity vector. However, in case of a bed, which is sloped perpendicular to the velocity vector, sediment particles move in addition slightly in the direction of bed slope. Kikkawa et al. (1976) developed an approach, which calculates the angle between the sediment transport vector and the velocity vector (Eq. 41).

$$\Phi = \frac{0.6}{\sqrt{\tau_*}} \tan A \quad (\text{Eq. 41})$$

where Φ is a function of the angle of the slope perpendicular to the water flow direction A and τ_* is the dimensionless shear stress.

7.4.3 Bed level changes within the hydro-morphodynamic model

In case of erosion of bed sediments (when the actual bed stress exceeds the critical bed shear stress) or deposition of transported sediments (when the critical bed shear exceeds the actual bed stress) a change in the bed levels takes place. This vertical movement is in its simplest form calculated from the continuity defect in the cell close to the bed. A widely used and

implemented approach in many models is the equation developed by Exner (Eq. 42; e.g., Paola and Voller, 2005; Parker, 2006).

$$(1 - n_p) \frac{\partial z_b}{\partial t} + \nabla \overline{q_b} = D_B - E_B \quad (\text{Eq. 42})$$

where n_p is the bed porosity, $\frac{\partial z_b}{\partial t}$ is the change in bed elevation of the bed over time, $\nabla \overline{q_b}$ is the sediment flux, and E_B and D_B are external sink/source terms, e.g., as a result of dredging or sediment supply.

In hydro-morphodynamic models often an exchange layer needs to be indicated, which specifies to which extent (depth) the bed is linked to the bed load transport within the system. The erosion process, formation of bed forms, bed armoring but also subsequent deposition occurs within this layer. Parker et al. (2000) subdivided the bed into an active layer and an inactive layer. As within the active layer all morphological processes may occur, the selection of the active layer height is crucial for obtaining reliable results. The active layer thickness is often scaled with the d_{90} (Parker, 1991). However, Blom (2008) showed for cases with sandy rivers that the active layer thickness should also be scaled with the bed form height. Meanwhile even more sophisticated layer models are used, e.g., the Hirano-Ribberink or the Continuous Vertical Sorting model (C-VSM model) (Bleyel and Kopmann, 2018), which enable the use of multiple layers with different boundaries.

8 MEASUREMENTS AS BASIS FOR SETTING UP HYDRO-MORPHODYNAMIC PREDICTION MODELS

As a result of the ongoing development of hydro-morphodynamic models within the last decades, they have been used to replicate events from the past, but also to predict future hydro-morphodynamic processes in reservoirs. However, the availability of good data is the basis for setting up, calibrating and validating numerical models and subsequently for performing reliable prediction simulations. In this chapter the related workflow is presented, with a special focus on the required input data and how to obtain it.

The availability of data with a high spatial and temporal resolution is an important factor for setting up hydro-morphodynamic models, their calibration and validation. However, the quantity of data is often limited and the quality is unknown. An example are bathymetric data for setting up the geometry of a reservoir, where huge differences in the available data sets exist for different reservoirs regarding the spatial and temporal resolution. For the Bodendorf reservoir (run-of river power plant), located in Austria cross sectional surveys with a single beam echo sounder and a distance of 150 – 200 m between the measured cross sectional profiles have been performed (Badura, 2007). Considering the temporal resolution, for the Bodendorf reservoir only eight surveys of the reservoir bed were conducted between the years 1980 and 2002 (Badura, 2007). For many reservoirs all over the world the database is comparable. However, exceptions can be seen for reservoirs, which need to be regularly maintained or where an active sediment management is implemented. Examples are the Iffezheim reservoir, located at the river Rhine in Germany, which is part of a federal waterway where a safe navigation on the river has to be ensured (Hillebrand et al., 2012) or the Angostura and the Cachí reservoirs in Costa Rica. In Angostura and Cachí an active sediment management in the form of an annual reservoir flushing is implemented and surveys are performed before and after each flushing operation. Subsequently, good databases are available for the Angostura, Cachí and the Iffezheim reservoir.

8.1 *Choice of a model*

Numerical modeling of sediment transport in reservoirs started in the 1980s (compare Harb, 2013), when mainly one-dimensional numerical models were used (e.g., White and Bettess, 1984, Peng and Niu, 1987 or Lai and Shen, 1996). The use of two-dimensional numerical models started at the end of the 1990s, when on the one hand the computational power increased and, on the other hand, more and better data were available for the simulations. Ziegler and Nisbet (1995) performed long-term simulations of fine-grained sediment transport in a large reservoir and Olsen (1999b) conducted simulations of the flushing process of the Kali Gandaki reservoir in Nepal. Almost simultaneously three-dimensional numerical models were developed and used, e.g., for the Three Gorges project, China, (Fang and Rodi, 2003) or

the Garita reservoir in Costa Rica (Olsen, 1999a). An overview on the development of numerical modeling of sediment transport with CFD can be found in Papanicolaou et al. (2008).

8.1.1 *Commercial models and models available for free*

In general, available hydrodynamic and hydro-morphodynamic models can be commercial models and models available for free.

Commercial models, such as *MIKE HYDRO River* including the module ST – sediment transport (1D) developed by *DHI* (DHI, 2017), *Hydro_AS* and *Hydro_FT* (2D) released by *Hydrotec* (Nujic, 2013) or *Flow-3D* (3D) programmed by *Flow Science* (Flow-3D, 2010) are models developed for large markets and have mostly a broad field of applications. *Flow-3D* can due to high sophisticated solvers and turbulence models be used to simulate complex hydraulic structures, such as spillways or weirs as well as for the simulation of fluids with other characteristics, in e.g., foundries. *MIKE HYDRO River* can also be incorporated into an integrated water modeling platform (*MIKE+*), which enables a direct coupling of collection systems, distribution networks and rivers within the modeling platform.

Freely available models (often tailor-made models) are mainly used for special applications, such as river engineering purposes. Examples for freely available models are *HEC-RAS* (1D) developed by the *United States Army Corps of Engineers* (*U.S. Army Corps of Engineers*, 2016), *Telemac-2D* coupled with the sediment module *Sisyphe* (2D) developed by the *Telemac-Mascaret Consortium* (Galland et al., 1991) or *SSIIM* (3D) developed by Nils Reidar B. Olsen at the Norwegian University of Science and Technology (Olsen, 2020). Tailor-made models, however, are often characterized by a missing user friendliness, a weak documentation, missing or no support from the developer team and by having a smaller community of users, means in many cases these models have not been well tested and may contain a high number of bugs.

Especially in hydro-morphodynamic modeling a large number of available models are freely available, e.g., *SSIIM* or *BASEMENT* developed at the ETH in Zurich, Switzerland (Vetsch et al., 2015). However, also these freely available codes may have a broad user community, e.g., *HEC-RAS* is worldwide one of the most used software packages for 1D hydrodynamic modeling. For *Telemac-2D* coupled with *Sisyphe*, the community is even involved in the further development of the code by making the code publicly available (open source). Such open access codes enable the user to implement new algorithms, such as flocculation models or additional bed load transport formulae.

8.1.2 *Based on the dimension of the model (1D – 3D)*

Based on the scope of the study and the demands on the modeling results the choice of the dimension of the model is an important step. However, the selection of a suitable dimension of a numerical model is not trivial and depends on several factors, which have to be taken into account. On the one hand, the level of detail of the processes, which shall be reproduced by the numerical model needs to be considered. For example, whether the required result of a reservoir flushing simulation is only the amount of flushed sediments or of the exact erosion pattern. On the other hand, the selection is based on the spatial extent of the modeling domain (e.g., local scour simulations vs. reservoir flushing of a prototype reservoir) and the timespan to be simulated (e.g., short-term flushing operations vs. long-term deposition simulations).

The most accurate results are obtained by full three-dimensional codes, such as *SSIIM* or *Telemac-3D*. In this case three-dimensional effects, such as secondary currents in bends, or complex flow situations, such as river confluences, are considered correctly. However, for a large spatial extent of the modeling domain, high grid resolution or a long-time span, full three-dimensional simulations have too high computational demands and instead lower model dimensions may be chosen.

Hence, in this chapter an overview on the advantages and disadvantages of models with different dimensions is given, with a special focus on practical applications in river engineering and reservoir management. However, due to the rapid development in computational power some of the given values and statements are estimates based on the current simulation possibilities and may in some years or decades not be valid anymore. A detailed overview of the governing equations for the full three-dimensional RANS equations, the 2D shallow water equations and the 1D Saint-Venant equations can be found in chapter 7.2 *Dimensionality in hydrodynamic modeling*.

One-dimensional numerical models are often characterized by short simulation times, but a low accuracy of the simulated results, as important hydrodynamic and hydro-morphodynamic processes are not reproduced in detail by the model. However, one-dimensional hydro-morphodynamic models are still in use, especially when large river networks, such as the rivers Rhine, Elbe or Danube in Germany are modelled (BfG, 2013). One-dimensional numerical models are able to simulate long periods, such as the complete lifetime of a reservoir. In both cases, models with a higher order of dimension would result in high computational efforts and are therefore not appropriate for this kind of simulations. Another inconvenience of one-dimensional numerical models is that only general trends of the hydro-morphodynamics can be modelled and no exact insight into ongoing processes is given. One-dimensional numerical model simulations give results only cross sectional wise and hydraulic as well as morphological results are given as average values over the entire transect. This results in only one value for

the flow velocity, equally distributed bed shear stresses or morphological bed changes along each transect. For simulating hydro-morphodynamics in reservoirs one-dimensional numerical models are used e.g., to estimate sediment fluxes downstream of the dam during reservoir flushing operation (Guertault et al., 2016) or general sedimentation trends in reservoirs (Ehrbar et al., 2018). Figure 79 shows simulated bed level changes of the Gebidem reservoir in Switzerland, as a result of a calibration simulation for the period between June and September 2015, where monthly-averaged water levels were used as input data (Ehrbar et al., 2018).

One-dimensional hydro-morphodynamic models need a certain amount and quality of input data. To assume that a reduction of the dimension of the model also leads to a reduction in input data is only partially correct and case dependent. Nevertheless, the spatial resolution of the data can be reduced. An example are bathymetric data, which for a one-dimensional numerical model do not need to be available as areal data, obtained e.g., by a side scan sonar, as only cross sectional data will be implemented in the model. However, the selection of the cross sections can be adapted, if morphological relevant structures are identified within the simulation domain. Also reliable grain-size distributions of the bed material are necessary at least for the location of the cross sections. Nevertheless, bathymetric surveys as well as grain-size distributions need to be available with a high temporal resolution also for 1D models. Also the upstream and downstream boundaries, such as inflow discharge and the quantity of inflowing sediments need to be available in a high resolution to obtain reliable simulation results, independently from the number of dimensions.

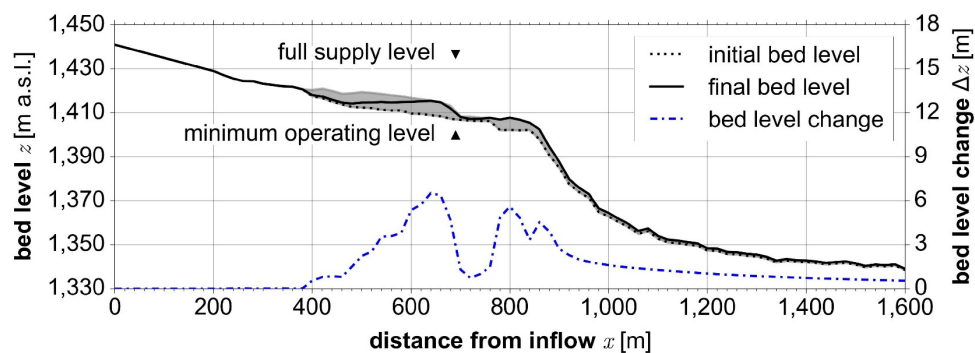


Fig. 79: Simulated bed level changes in the Gebidem reservoir, Switzerland, for the 2015 calibration season (June to September), by using monthly-averaged water levels. Bed level changes and maximum bed levels, which evolved in the simulations, are shaded in grey (Ehrbar et al., 2018).

Two-dimensional numerical models are chosen either when an influence of the hydraulics (e.g., secondary currents in bends or meanders) on the sediment transport is expected or when deeper insight into the ongoing hydraulic and morphological processes is necessary. The Bodendorf reservoir in Austria can be classified as a long and narrow reservoir. However, Badura (2007) showed a clear influence of secondary currents on the model results when simulating the 2004 and 2006 reservoir flushing operations. Figure 80 shows a comparison of simulated results of the 2004 flushing operation, including measured bed levels before and

after the flushing operation. From the figure the alteration of deposition and erosion along the transect can be seen. By means of a two-dimensional numerical model also a sediment-flushing concept for a run-of river hydropower plant located in the Saalach River in the southeastern part of Germany was applied (Reisenbüchler et al., 2020). Whereas 1D numerical models are able to simulate complete river reaches (>100 km) and to perform long term simulations (>100 years) with reasonable computational effort, 2D hydro-morphodynamic models are limited to river sections (<100 km) and short to mid-term simulations (<100 years).

Also for 2D hydro-morphodynamic models sufficient and high quality input data are necessary for performing reliable numerical simulations. However, for 2D models still cross-sectional data are used in many cases for the impounded reservoir (bathymetry), although the models are able to resolve areal bathymetric data by using a simulation mesh. In such cases between the transects an interpolation of the bed and in most cases also of the bed material is performed. Inaccuracies in this interpolation results finally also in inaccurate modeling outcomes. Two-dimensional numerical models are often classified as being sufficiently accurate for engineering practice. These models are for instance state of the art for flood inundation and flood risk mapping. The use of 2D models in hydro-morphodynamic modeling has been increasing, but they are not state of the art yet.

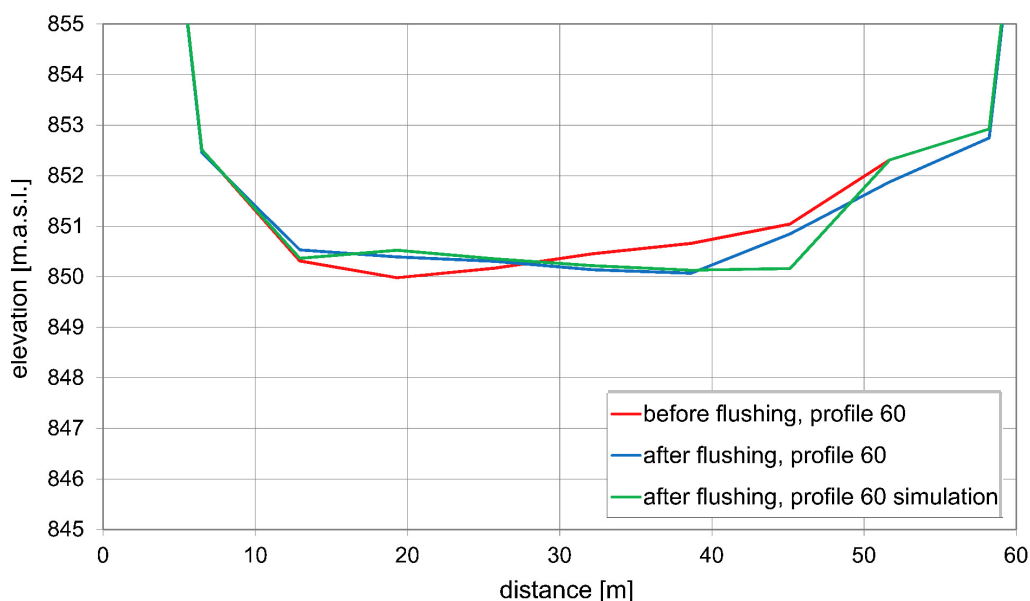


Fig. 80: Comparison of the simulation results of a reservoir flushing operation conducted in the Bodendorf reservoir in 2004, with the obtained digital terrain model.

The use of a *three-dimensional numerical model* represents the most accurate way of modeling hydro-morphodynamic processes in reservoirs. When simulating reservoir sedimentation, the vertical velocity component has a strong influence on the settling behavior of sediments. A fully three-dimensional code is able to tackle these required characteristics of the hydraulic processes within the reservoir. Subsequently, three-dimensional numerical models can gain detailed information regarding hydro-morphodynamic processes, such as

sediment transport, deposition and erosion. In practice, rivers and reservoirs of 30 to 50 km in length are possible simulation areas. Three-dimensional numerical models are used e.g., for the simulations of floodwater intrusion and sedimentation in the Shichikashuku reservoir in Japan (Umeda et al., 2006), reservoir sedimentation of the Angostura reservoir in Costa Rica (Haun et al., 2013a), the flushing process of the Bodendorf reservoir in Austria (Haun et al., 2012b), flow velocity distribution and sediment transport in the Iffezheim reservoir in Germany (Hillebrand et al., 2016) or the flushing process, including the investigation of possibilities to increase the flushing efficiency, of the Dashidaira reservoir in Japan (Esmaeili et al., 2015; 2017; 2021). Figure 81 shows the flushing simulation of the Angostura reservoir in Costa Rica, where figure 81a presents the initial grid in the neighborhood of the dam, figure 81b the adaptive grid during the full drawdown stage and figure 81c the simulated bed levels of the reservoir after the flushing simulation. Especially long-term simulations around the reservoir lifetime (usually 100 years) have an extremely high computational effort and may become problematic when conducted with an ordinary desktop PC (personal computer). Olsen and Hillebrand (2018) used for instance a full three-dimensional numerical model of the Iffezheim reservoir in Germany to predict bed changes in the reservoir as a result of sedimentation and dredging, but only for a period of eleven years. Fang and Rodi (2003) simulated flow and suspended sediment transport for the Three Gorges reservoir in the Yangtze River over a period of 76 years, but only in the neighborhood of the dam. An overview on further studies, also performing long-term sedimentation simulations in reservoirs is given by Abood et al. (2009).

The amount and the quantity of input data do not differ much between models with different dimensions. Also three-dimensional hydro-morphodynamic models require high-quality input data to perform reliable simulations. Although three-dimensional numerical models are meanwhile more frequently used for studying hydro-morphodynamic processes in reservoirs, these models are still almost only applied by universities and research institutions, or by institutions, which develop their own code.

A generalized recommendation for the choice of the dimension of a model is not reasonable, as many site-specific factors have to be considered for making an appropriate selection. For each study a decision needs to be taken in particular and with care by taking into account the spatial and temporal extent of the study site, as well as the processes, which shall be simulated by the model.

The larger the spatial and temporal extent, the smaller the dimension of the model needs to be. This requires a simplification of hydrodynamic and hydro-morphodynamic processes. Basically, it needs to be considered, that the introduced error due to empirically developed formulae for simulating hydro-morphodynamics may often be in the same range or even higher compared to the introduced inaccuracy through the reduction of a dimension, although this is often neglected.

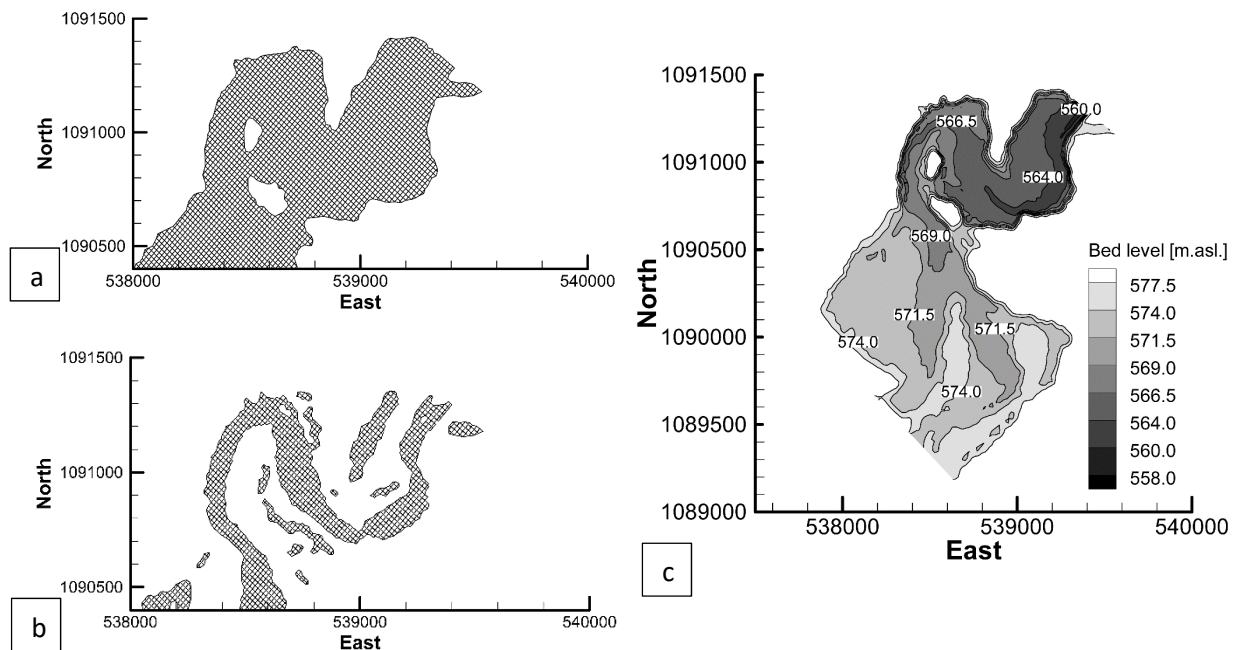


Fig. 81: Flushing simulation of the Angostura reservoir in Costa Rica (a) initial grid for the flushing simulations in close vicinity of the dam, spillways and the intake; (b) adaptive grid during the full drawdown stage of the flushing with a formed flushing channel; (c) simulated bed levels at the end of the flushing simulation (Haun et al., 2012a).

8.1.3 Based on the available algorithms for hydro-morphodynamic simulations

Commercial hydrodynamic models are usually developed for large markets and not many of them are able to consider hydro-morphodynamic processes as well. The reason is twofold: first, hydro-morphodynamic modeling is still a niche, and second, due to the high number of available empirical approaches it is difficult to implement all possible algorithms, which may be necessary for simulating different boundaries (e.g., steep vs. mild sloped rivers or coarse vs. fine sediment fractions). In addition, spatial and temporal scales may vary. Many important processes, such as deposition of fine sediments as a result of flocculation or sand slides during reservoir flushing, are not taken into consideration by these models. When selecting an appropriate code, a detailed overview on the expected boundaries and processes within the simulation domain (domain-specific parameters) is the basis for the decision.

Chapter 8.2 *Basic steps in setting up a hydro-morphodynamic prediction model* gives an overview of processes, which may be handled by the program. Important and basic factors, which need to be considered are:

- (i) The number of sediment sizes used by the model (single size or multiple sizes),
- (ii) how the initiation of motion is modelled and whether cohesive sediment properties are taken into account,
- (iii) how suspended sediment transport is simulated,
- (iv) which bed load transport equations are available in the code,
- (v) whether bed forms can be simulated,
- (vi) whether interactions between the grain-sizes are simulated (hiding/exposure, flocculation, etc.),
- (vii) the available number of sediment layers at the bed,
- (viii) whether additional processes can be calculated, such as sediment movement on tilted slopes or geotechnical bank failure.

8.2 *Basic steps in setting up a hydro-morphodynamic prediction model*

Set up and operation of a reliable prediction model consists of the following four basic steps (adapted from Cunge, 2003):

- (i) Model setup (including bathymetry, topography, in- and outflow boundaries as well as boundaries at the bed and the walls),
- (ii) calibration of the model with hydraulic and morphological data,
- (iii) validation of the model with hydraulic and morphological data,
- (iv) sensitivity analysis to quantify the uncertainty of model-specific parameters and the domain-specific parameters.

The accuracy of a prediction model strongly depends on two factors, namely: (i) the quality and quantity of input data as well as (ii) the accuracy of the model itself, or in other words the degree of simplification of the model. A profound calibration and validation of the hydro-morphodynamic numerical model is essential to ensure accurate and reliable results in predicting hydro-morphodynamic processes. Finally, a sensitivity analysis gives information on the uncertainty of the model itself (model-specific parameters, e.g., the bed load transport formula) and of the input data (domain-specific parameters, e.g., the sediment inflow). However, in many studies the steps calibration, validation and especially the sensitivity analyses are not performed in depth, due to a lack of data or due to the inexperience of the modeler. Further details are provided in chapter *8.4 Calibration and validation* and chapter *8.5 Sensitivity analysis*.

8.3 *Model setup*

A CFD model is the model-based reconstruction of the nature and follows in the case of a hydrodynamic model the following basic steps:

- (i) The reconstruction of the initial conditions, including bathymetry of the reservoir itself, the topography of the surrounding area and, if necessary, the up- and downstream river regions,
- (ii) the implementation of hydraulic structures, such as bridge piers and weirs, in a constructive way or as an inner boundary condition,
- (iii) the implementation of boundary conditions upstream (e.g., as hydrographs), downstream (e.g., as stage-discharge curve, or the amount of extracted water from the reservoir) and at the bed and walls through the implementation of roughness values.

After the reconstruction of the geometry, the implementation of hydraulic structures and the selection of roughness values, in a first step stationary simulations are performed with a constant inflow discharge and a constant water level, on the basis of a downstream located stage-discharge curve as boundary condition. When the simulation is started, the reservoir will be filled in the model within the first time steps of the simulation and the hydrodynamic flow field will develop. In most numerical programs it is also feasible to initially “pre-fill” the reservoir, often by specifying a horizontal water level within the entire reservoir or an initial slope, which reduces the simulation time, as the filling processes of the reservoir has not to be performed. An additional benefit of this procedure, is that instabilities during the filling may be avoided. Both procedures are known as *cold start* of the model, as the flow field within the reservoir needs first to develop during the simulation. If the simulation already starts with the correct hydrodynamic flow field, known as *hot start* procedure, a further reduction of the simulation time will be a direct result.

In case that hydro-morphodynamic simulations are performed, in addition to the already mentioned data, also the following morphological data sets are required input:

- (i) The grain-size distribution of the bed sediments (spatial resolved within the reservoir and in several layers over depth),
- (ii) the in- and outflowing sediments (amount and grain-size distribution) as well as the associated settling velocities as boundary conditions.

In hydro-morphodynamic modeling *hot start* simulations are usually performed to avoid unrealistic hydro-morphodynamic processes during the numerical filling process of the reservoir.

A detailed overview on the input data, required for setting up hydrodynamic and hydro-morphodynamic models is given in the following subchapters.

8.3.1 *Geometrical data (topographic and bathymetric data) and their implementation in numerical models with different dimensions*

Data for setting up the geometry of the reservoir itself, of the surrounding area and, if necessary, the up- and downstream river regions is usually obtained by using different measurement methods and is often available with a different spatial and temporal resolution. In general, it can be distinguished between bathymetric data, which represent the bed of the impounded part of the reservoir or the river (under water) and topographic data, which represent terrestrial data (above water, but which may be flooded during high flow conditions).

Topographic data, often available as Digital Elevation Model (DEM), can be obtained by a:

- (i) Terrestrial survey (land surveying),
- (ii) laser scan survey (light detection and ranging data),
- (iii) photogrammetric survey (structure from motion data).

Terrestrial survey (land surveying)

Most existing data sets from the past are only available as terrestrial survey data. New technologies, such as remote sensing, have been developed especially during the last decades. Land surveying describes the technique of determining the terrestrial or three-dimensional positions of points and the distances as well as the angles between them. However, it is labor intense and subsequently associated with high costs. Nowadays classical terrestrial surveys with total stations and theodolites are only used if a small amount of data points is necessary (small spatial extend) or in case that other methods are not target-aimed. Such surveys may include hydraulic structures (dam, weirs, bridge piers within the reservoir) with a limited accessibility for other techniques. For reservoirs, terrestrial surveys are often performed in case that within the reservoir cross sections are obtained, which will be extended and surveyed outside of the reservoir. Figure 82 shows a terrestrial survey campaign at the head of the Bodendorf reservoir in 2010, where the shore line was determined during low flow conditions. Modern systems are meanwhile based on high precision GPS solutions, such as Real Time Kinetic (RTK) measurements, which determine the positions of the rover with a spatial resolution within a range of 1 - 2 cm (see chapter 6.1 *Bed level measurements*).



Fig. 82: Terrestrial survey along the Bodendorf reservoir, Austria, in 2010 (a) total station located at a fixed point on a bridge; (b) rover for taking points along the shore of the reservoir.

Laser scan survey based on light detection and ranging data (LIDAR-data)

To obtain either a higher spatial resolution or to enable a survey of a larger extend of the domain laser scan surveys, either by UAS (uncrewed aircraft system, also known as drones) or by small airborne are used as alternative methods (Ring, 1963; NOAA, 2008). When using laser scanning technology the travel time of laser pulses from a transmitter to a receiver is measured and when using the speed of light, the distance is obtained for around 1,000 points per second (Shan and Toth, 2018; Taylor, 2019). The advantage of this method is the comparably high spatial resolution of about 0.1 m (without vegetation) and a labor reduction in obtaining the data. However, the post-processing of these sort of data is very labor intense and requires high computational power. Figure 83 shows a bathymetric scan of a lake, obtained with a RIEGL VQ-840-G Laser Measurement Systems (RIEGL, 2020). The point cloud contains 10 million points and is displayed by the software *Potree*, developed at the Vienna University of Technology (Schuetz, 2020).

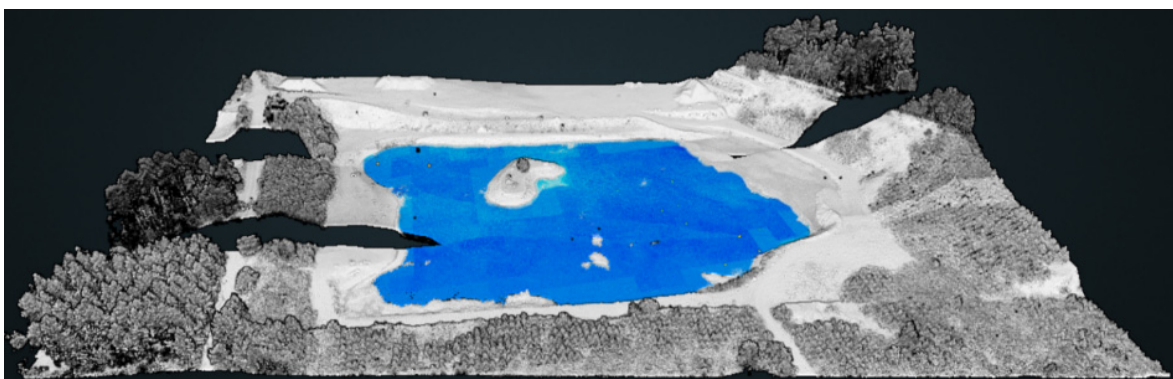


Fig. 83: Point cloud of a lake, obtained with a RIEGL VQ-840-G Laser Measurement Systems and displayed by *Potree*, a viewer for LIDAR data sets (RIEGL, 2020; Schuetz, 2020).

Photogrammetric survey (Structure from Motion - SfM)

An alternative to the use of laser technology is the use of two-dimensional image sequences, obtained with high density and Structure from Motion (SfM) for post-processing. SfM is a photogrammetric range imaging technique, which estimates three-dimensional structures from two-dimensional image sequences, coupled with local motion signals (Ullman, 1979). Figure 84 shows a survey of the Murgtalsperre Kirschbaumwasen, located in the Black Forest in Germany with SfM. On the right hand side of the picture a part of the reservoir can be seen and on the left hand side the Murg river.

The two-dimensional image sequences can either be obtained by hand (in case of small structures) or by UAS, always ensuring a certain overlap of the pictures (Seitz et al., 2018). An important aspect for large spatial extends is the accuracy of the used GPS of the UAS, or as an alternative pre-recorded fixed points in the surveyed domain with known coordinates. An advantage of using a photogrammetric method is also the availability of aerial images of the investigated domain, as they give an overview on land use and/or urbanized areas and can also be used to estimate roughness-values or provide the possibility of assuming the infiltration capacity of the area.



Fig. 84: Survey of the Murgtalsperre Kirschbaumwasen by an UAS in 2013 and a subsequent analysis with SfM (photo courtesy: I AM HYDRO).

Bathymetric data, also available as DEM, can be obtained by means of a:

- (i) Single beam echo sounder,
- (ii) multi beam echo sounder,
- (iii) side scan sonar.

Due to the large water depths, bathymetric data in reservoirs are usually obtained by single beam and multi beam echo sounders or side scan sonars with a high spatial resolution. A description of all three methods has already been given in chapter 6.1 *Bed level measurements*, as bathymetric surveys are also used to measure bed level changes as a result

of reservoir sedimentation. Figure 85 shows a survey of the Schwarzenbach reservoir, located in the Black Forest in Germany, with a single beam echo sounder conducted in 2016.

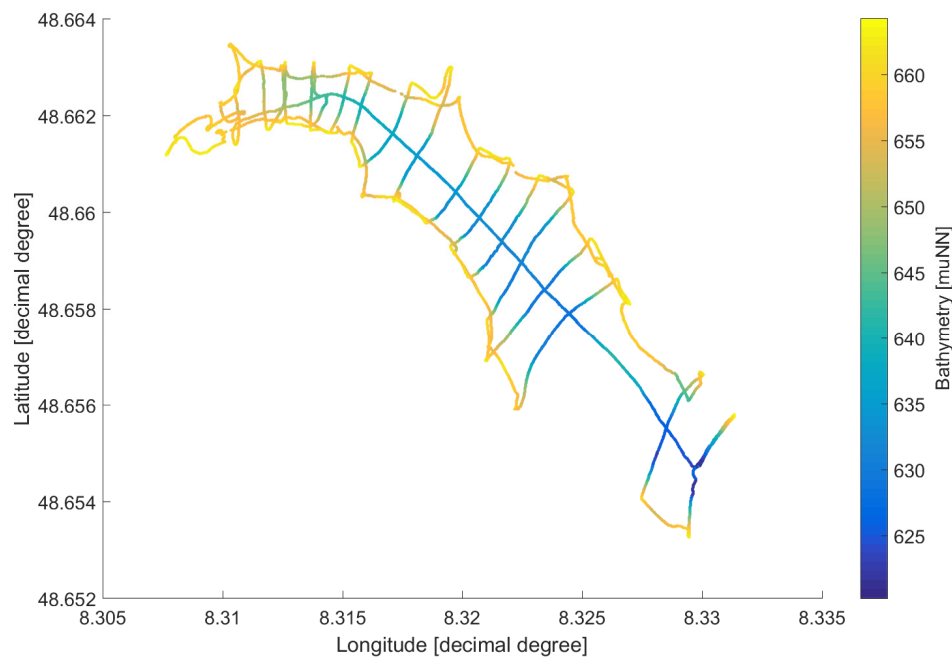


Fig. 85: Bathymetry of the Schwarzenbach reservoir, located in the Black Forest in Germany, obtained by single beam echo sounder in 2016.

In shallow areas of rivers and reservoirs (wadeable areas) also terrestrial surveying or laser scan surveys are possible. However, the use of laser scan technology to obtain bathymetric data strongly depends on the kind of laser used (e.g., green laser), the depth of the reservoir and the water turbidity (e.g., Mandlbürger et al., 2015; Zhao et al., 2017). Especially for reservoirs the use of LIDAR data for obtaining bathymetric data is still limited due to the large depths of reservoirs. Figure 86 shows the same bathymetric scan of a lake, as it is given in Figure 83. In the figure the layer representing the water surface is enabled and the bathymetry below the water surface is presented. When comparing both figures, it becomes obvious, that only the shallow area of the lake could be captured by the laser scan survey, deeper parts (indicated in black in the figure) cannot be resolved.

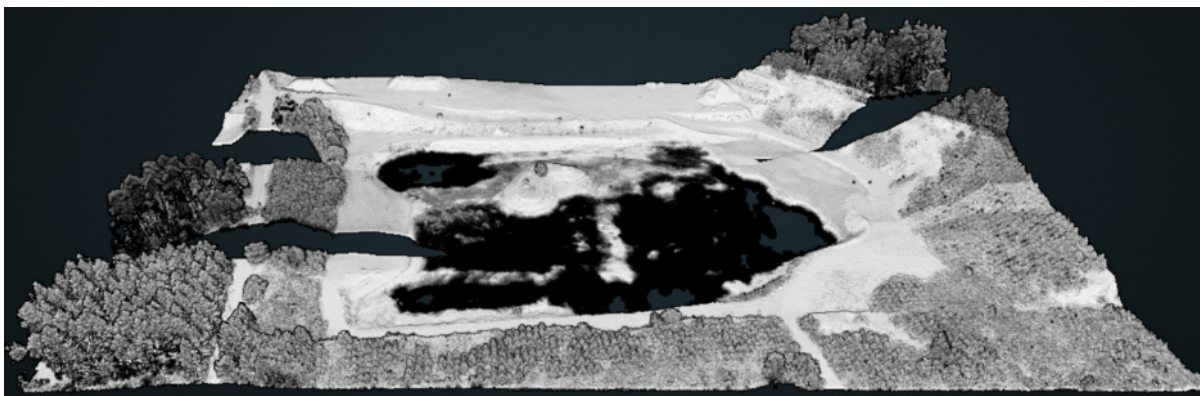


Fig. 86: Point cloud of a lake, obtained with a RIEGL VQ-840-G Laser Measurement System and displayed by Potree, a viewer for LIDAR data sets (RIEGL, 2020; Schuetz, 2020).

As already mentioned in chapter 8.2 *Basic steps in setting up a hydro-morphodynamic prediction model* the quantity and quality of input data is of high importance to obtain reliable modeling results. Depending on the model dimension, either cross sectional data are used for the reconstruction of the bathymetry and the topography (1D models; figure 87a), or a grid is implemented for subdividing the computational domain into discrete elements (2D and 3D models; figure 87b and figure 87c). In case of 1D models the selection of appropriate cross sections needs to be handled with care. A pure subdivision of the modeling domain into cross sections with equal distances may only work properly in straight river channels and without significant differences in the bed morphology. As soon as river bends occur, changes in the shape of the cross section emerge or when the bed morphology changes, the cross sections need to be selected in a way, that all these changes are reflected by the model. As a result, a higher spatial resolution of the bathymetric data is also beneficial for 1D models (see chapter 8.1.2 *Based on the dimension of the model (1D – 3D)*).

When setting up a hydro-morphodynamic model, usually the modeling domain is not restricted to the domain where simulation results should be obtained. The model is often expended to the up- and downstream region, which enables a sufficient inflow and outflow length in a way that the hydraulic and morphological conditions within the modeling domain are not affected by the boundaries and a numerical kinematic equilibrium (normal discharge conditions) is established in the study area.

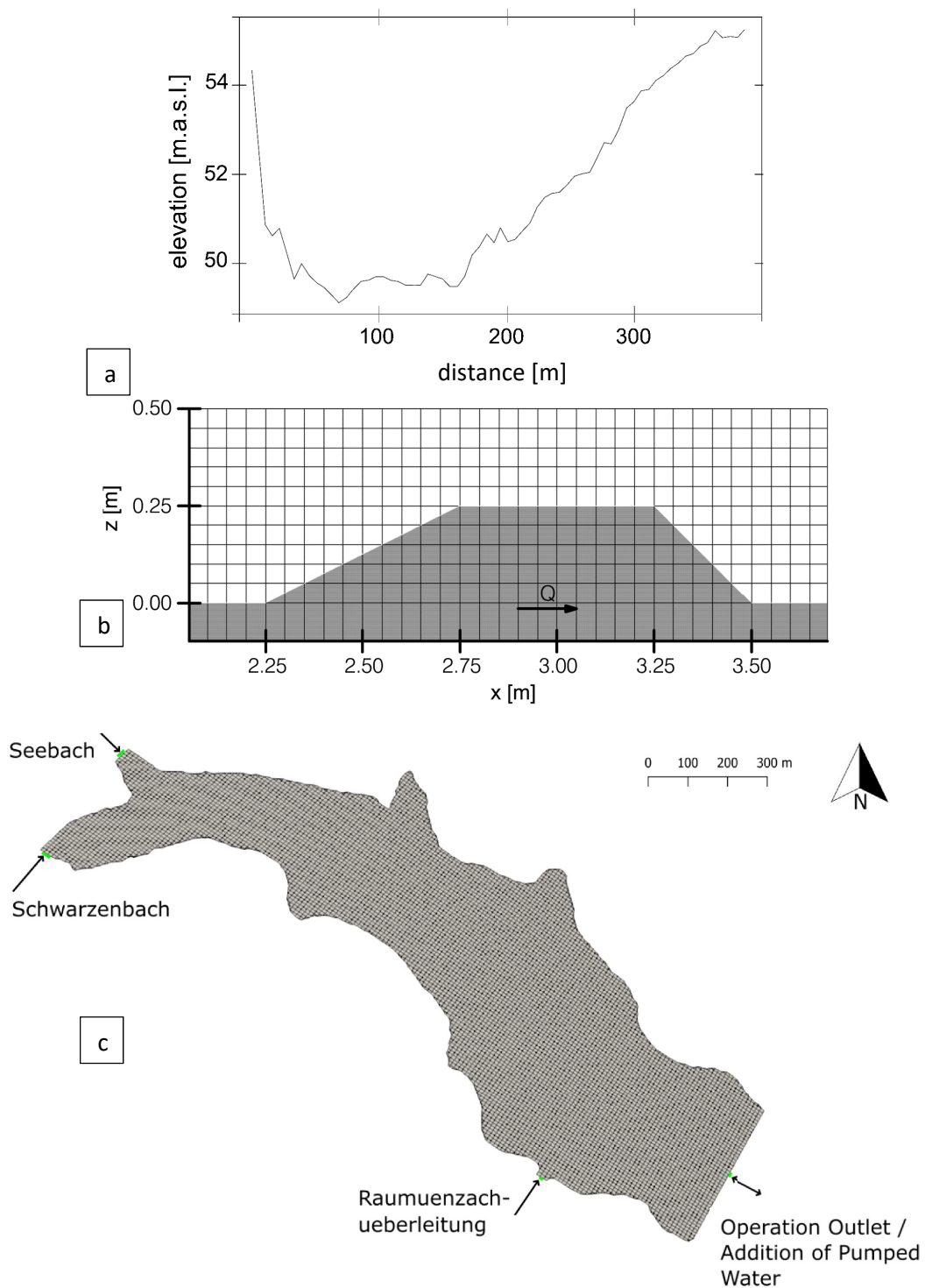


Fig. 87: (a) cross section of a Wadi in the United Arab Emirates, implemented in the model *Basement*; (b) sketch of the orthogonal, structured and non-adaptive grid, used in *Flow-3D*. (Haun et al., 2011); (c) sketch of the non-orthogonal, unstructured and adaptive grid of the Schwarzenbach reservoir, setup in *SSIIM* (Mouris et al., 2018).

Computational meshes, as they are used in numerical models, can in general be subdivided into structured (figure 87b) and non-structured (figure 87c) grids. Structured grids with their regular connectivity are one of the simplest ways for subdividing the simulation domain in

discrete elements (e.g., quadrilateral cells in 2D and hexahedral cells in 3D). Within a structured grid each node of the grid can be identified by three numbers (in case of three dimensions). In this case each node can also be identified through its neighbor cells (neighborhood relationships), as the nodes are continuously numbered, and the numbers do not change during the simulation (Castillo, 1991). Hence, with structured grids comparably fast simulations can be performed as the memory requirements are small, and the location of each node can be stored in a simple matrix (storage arrangement), which will be solved by the program (Mavriplis, 1996). However, structured grids are geometrically not flexible, and often a high number of cells is necessary to resolve natural geometries. Non-structured grids (irregular connectivity) on the contrary allow such an adaption on complex geometries, by using e.g., triangles in 2D and tetrahedral cells in 3D. However, the disadvantage of unstructured grids is the longer simulation time (Mavriplis, 1996). The reason therefore is that each node is allocated to a single number, and due to the missing structure of the grid, this numbering does not follow a logical system. As a result, the node cannot be allocated by the neighbor nodes. As a consequence, within the model an explicit matrix is used containing the position of the node with respect to the neighbor nodes (neighborhood relationship). This step results in higher computational efforts for non-structured grids and in some cases also in a worse convergence compared to structured grids.

However, the characterization of grids is also possible on the basis of other parameters, such as the orthogonality, shape, position of variables or if grid movement or nested grids are used. Most of these parameters are important for the quality of the simulations. An example is the orthogonality of the grid cells (for non-orthogonal meshes), as this parameter governs next to the accuracy of the simulation results also the stability and the convergence time of the simulation. As a result, the angle between crossing grid lines should be nearly 90 degrees. (Olsen, 2000).

8.3.2 *Hydraulic structures in numerical models*

An accurate implementation of hydraulic structures, such as bridge piers, weirs, but also gates, intakes and bottom outlets is of high importance for achieving reliable results from the hydro-morphodynamic model. Many numerical models offer two possibilities of implementing such types of structures, either by implementing them in a constructive way, means that for instance weirs are integrated in the grid geometrically correctly, or by implementing an inner boundary condition. Figure 88a shows the geometrical correct implementation of a weir in the 2D hydro-morphodynamic software *Hydro_FT*. Figure 88b shows a weir implemented in the model *Basement* as an inner boundary condition (Vetsch et al., 2011). The benefit of an inner boundary condition is that operation rules of gates and bottom outlets as well as capacity-water level curves for spillways can be implemented.

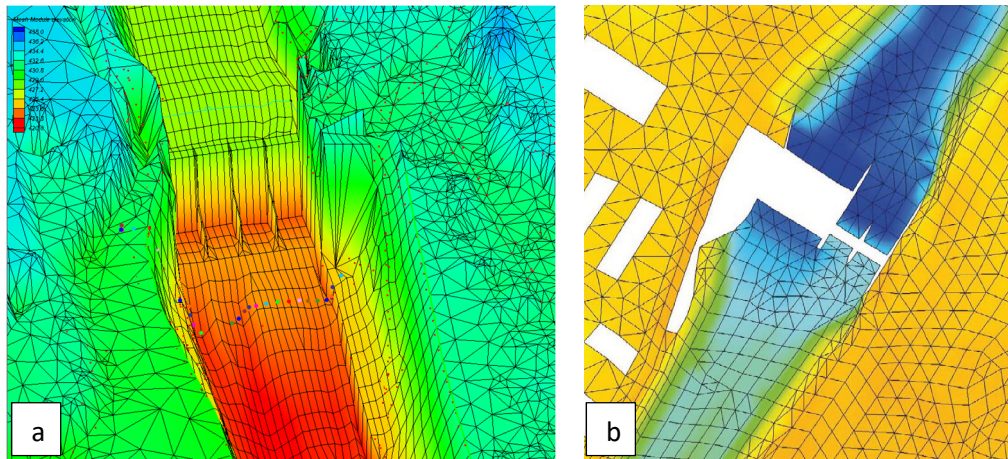


Fig. 88: (a) geometrically correctly implemented Zollhaus weir, located at the river Saalach, into the 2D hydro-morphological model *Hydro_FT*; (b) 2D computational grid in *Basement*, with an implemented inner boundary condition at the weir (Vetsch et al., 2011).

8.3.3 *Boundary conditions for hydrodynamic and hydro-morphodynamic modeling*

For the simulation of hydrodynamic as well as hydro-morphodynamic processes boundary conditions need to be specified within the reservoir itself, such as roughness and grain-size distribution at the bed, but also for the in- and outflow sections of the model, such as hydrological and sedimentary data. In cases of modeling hydraulic structures, and selecting an inner boundary condition, additional information needs to be specified in the model (see chapter 8.3 *Model setup*).

Figure 89 gives an overview on different required hydrological and sedimentological boundary conditions for the simulation of open water environments; in this case for modeling of a reservoir cascade. However, as each reservoir is unique, the boundaries may change from case to case. Hence, the figure gives an overview on the minimum required boundary conditions, for which accurate measurement data are required. Within the figure also dredging and sediment replenishment are shown, as these kind of measures may be implemented in reservoirs of run-of river power plants and within the downstream sections as a result of an emerging supply-limited-system.

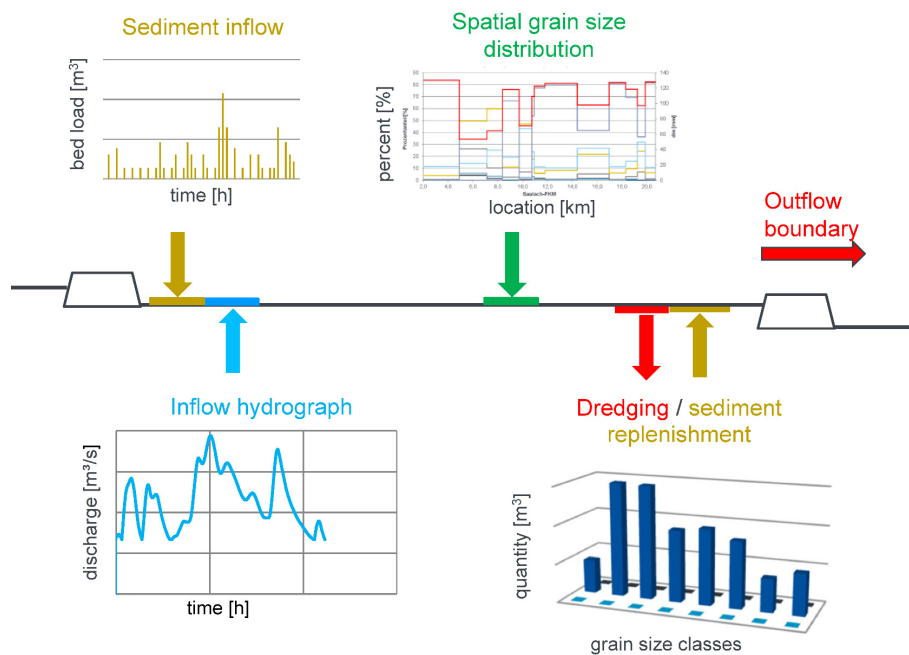


Fig. 89: Overview on different hydrological and sedimentological boundary conditions for numerical modeling of hydro-morphodynamics (Haun and Wieprecht, 2017).

Upstream boundary conditions

As upstream boundary conditions into the model inflow fluxes are specified, either as a constant value for stationary simulations, or as a time series for non-stationary simulations. In case of non-stationary simulations, a discharge hydrograph, e.g., from an upstream located gauging station or as a result of a rainfall-runoff-model, is usually implemented in the model. In case of stationary simulations only a single value for the discharge is required. Figure 90a shows a gauging station upstream of the Angostura reservoir in Costa Rica, located at the Reventazòn river. Based on these measurements an inflow time series was developed for the numerical simulation of reservoir sedimentation for 250 operation days (between November 2010 and September 2011; figure 90b). For the numerical simulations weekly averaged values were used. The measurements show a clear trend for the dry and wet season. To specify an inflow discharge is one of the simplest methods of implementing the upstream boundary conditions. However, in several codes it is also possible to specify the flow velocities at the inlet (Versteeg and Malalasekera, 1995). In case that even a velocity profile is known from measurements, a shorter distance between the inlet boundary of the model and the investigated domain can be chosen, as the flow field may develop faster and no long pre-section is required to achieve a numerical kinematic equilibrium.

For hydro-morphodynamic simulations also the quantity and grain size distribution of inflowing sediments need to be specified as upstream boundary condition. Usually for suspended sediments a concentration-discharge relationship is developed, which is subsequently coupled with the inflow hydrograph (figure 90c). However, a large number of

suspended sediment concentration measurements is required to obtain a reliable relationship function, which can be implemented in the numerical model and it is essential, that the measurements are performed during different flow conditions. Figure 90d shows the sampling of water probes for obtaining suspended sediment concentrations for the Reventazòn river in Costa Rica and for analyzing the grain-size distribution (see chapter 6.3.1. *Suspended sediment transport measurements*). However, the specification of the grain-size distribution has even a higher importance when specifying bed load at the upstream boundary condition. As measurements of the bed load transport are challenging especially during flood events (see chapter 6.3.2 *Bed load transport measurements*), exact numbers are rare. As a result, often the sediment transport capacity upstream of the reservoir (free flow zone) is calculated and implemented as upstream boundary condition in the model (e.g., Harb et al., 2012). When grain-size distributions are selected for the hydro-morphodynamic simulations, also the settling velocities of the single fractions need to be specified. An overview on techniques to attain reliable settling velocities is given in chapter 3.3. *Deposition*.

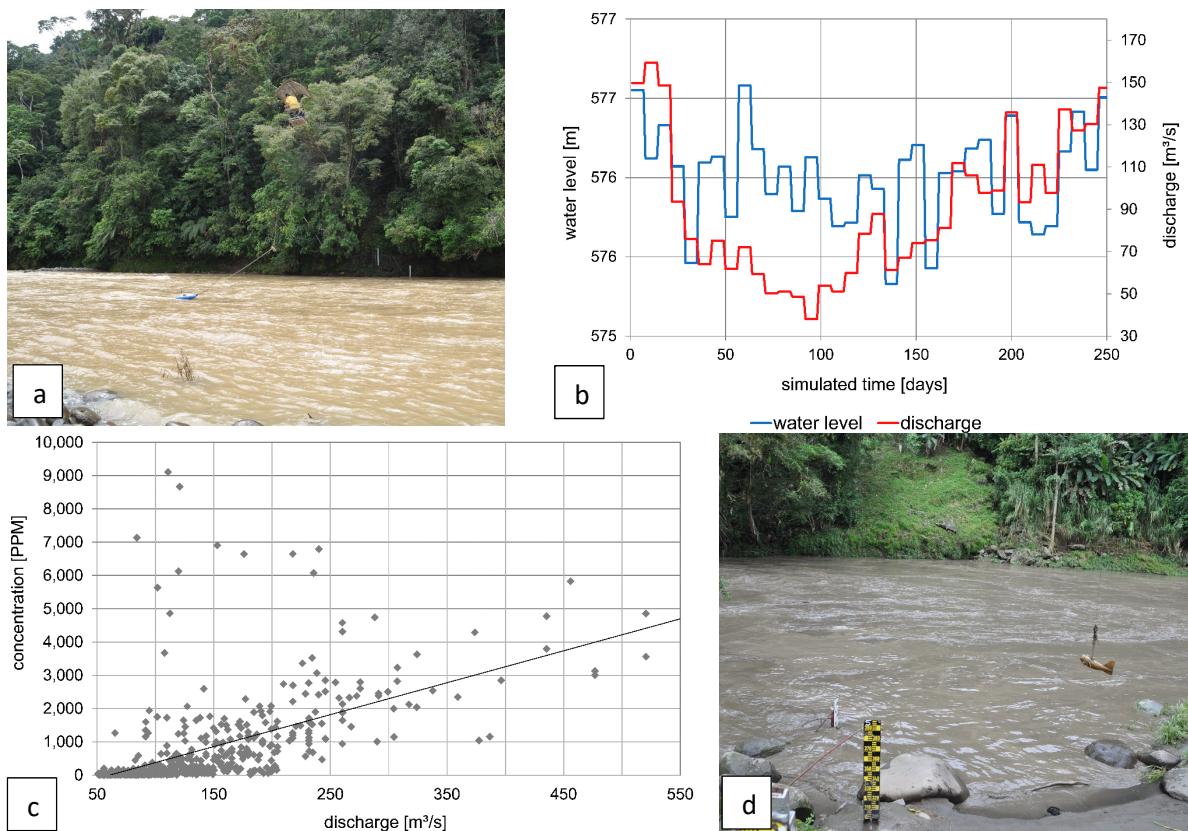


Fig. 90: (a) gauging station at the Reventazòn river in Costa Rica, upstream of the Angostura reservoir; (b) inflow time series for the numerical simulation of reservoir sedimentation (weekly averaged values for discharge and water levels); (c) concentration-discharge relationship developed for the Reventazòn river in Costa Rica, upstream of the Angostura reservoir; (d) suspended sediment sampling at the Reventazòn river in Costa Rica, downstream of the Angostura reservoir.

Boundary conditions within the reservoir

Within the reservoir the boundary conditions are specified on the one hand through the reconstruction of the bathymetry of the bed and the embankments, including the selection of associated roughness values, and on the other hand by the free water surface. The simulation of the free water surface represents a particular challenge in numerical modeling. For models with fixed grids (e.g., *Flow-3D*) often the Volume of Fluid method (VOF) is chosen, which represents a two-phase approach where both, the water- and the air phase, are modelled in the grid (Hirth and Nicols, 1981). Within the VOF method each cell contains a fraction of water. In case the fraction is 1, the cell is filled with water; if the fraction is 0, the cell is filled with air and in case the fraction is between 0 and 1 the cell contains the free water surface. On the contrary, in models with adaptive grids, all cells are filled with water and the upper boundary (the highest grid cell) represents subsequently the free water surface (Haun et al., 2011).

An important factor in modeling hydro-morphodynamics is the bed and wall roughness. The roughness is set in most models as a boundary condition and is also used as a parameter for calibration. Subsequently, it is important for a correct simulation of the flow field, including water level height, flow velocities and the bed shear stresses. A deeper overview on the selection of appropriate roughness values is given in chapter *8.4 Calibration and validation*.

For hydro-morphodynamic simulations the composition of bed material, including sediment thickness, grain-size distribution and, if possible, the specification of layers is required. Due to grain sorting processes in reservoirs, large deviations in the characteristics of deposited sediments may occur along its thalweg. As a result, grain-size distributions are often determined for different areas of the reservoir (see chapter *6.2 Bed material measurements*). Figure 91a shows a sample of the surface sediments of the Angostura reservoir in Costa Rica obtained in 2010 with a small Van Veen grabber (figure 91b). In addition, Vane shear measurements were performed to find out the critical bed shear stresses of the cohesive bed material (figure 91c). Figure 91d shows the sieve analysis of eight samples, taken along the thalweg of the Angostura reservoir, where fine sediment fractions dominate. Nevertheless, the typical fining along the thalweg is observed.

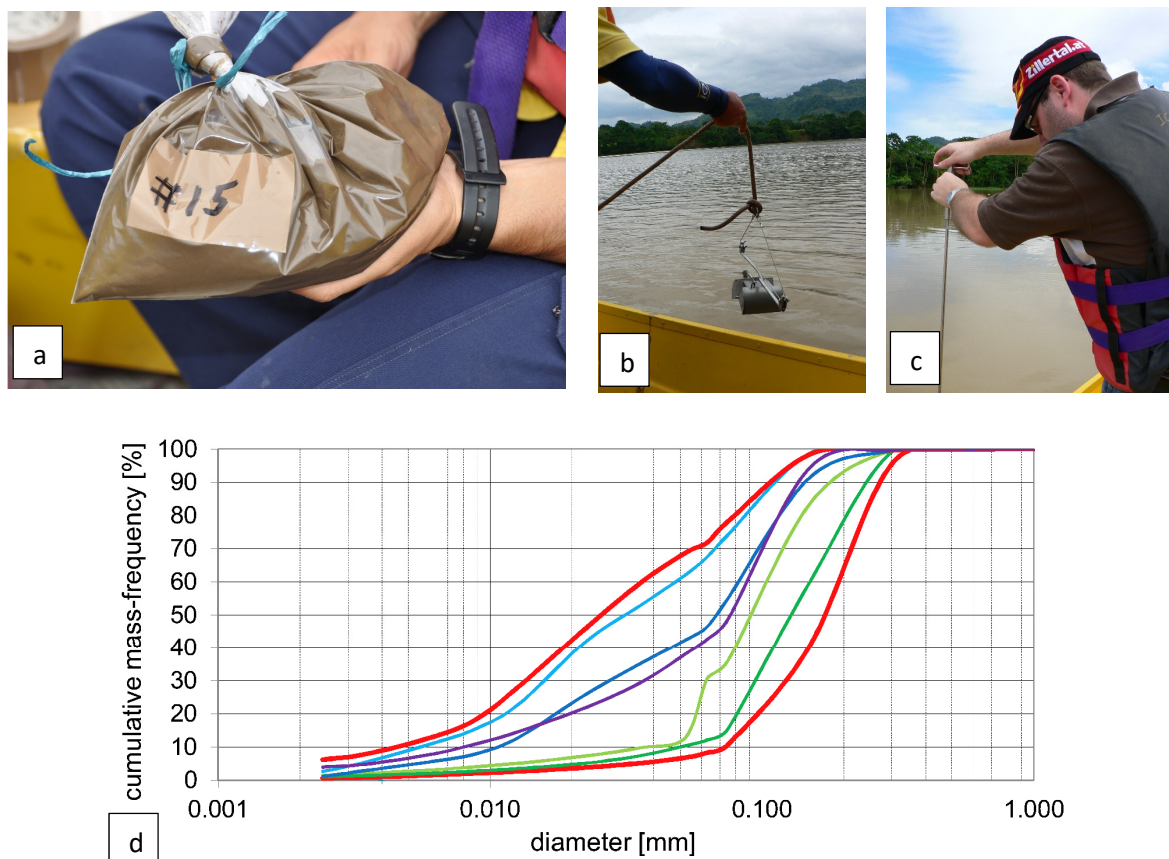


Fig. 91: (a) bed material sample obtained from the bed surface of the Angostura reservoir in Costa Rica in 2010; (b) Van Veen grabber for obtaining bed surface samples; (c) Vane shear measurements of critical bed shear stresses of the cohesive bed material; (d) results of the sieve analysis of eight samples, taken along the thalweg of the Angostura reservoir.

Downstream boundary conditions

When simulating reservoirs, exact values of the water extraction through the operational outlets and the bottom outlets are available. Otherwise, a stage-discharge curve can be used for the downstream boundary condition. In the case of spillway overflow, associated discharge values can be calculated. In addition, in reservoirs the water level is monitored during operation. Figure 92a and 92b show a pressure flushing operation at the Peñas Blancas in Costa Rica. During the whole flushing process, the water level in the reservoir is recorded at the intakes (figure 92a) and the water outflow through the bottom outlets is known (figure 92b). Figure 92c shows the outflow and the water levels in the Bodendorf reservoir in Austria during the flushing operation in 2004. The water level was drawn down until free flow conditions occurred. At the same time the discharge increased, as a result of an occurring flood wave. The figure also illustrates that the drawdown was to be stopped as soon as the downstream suspended sediment concentrations increased above a set threshold, as a result of geotechnical failures (sand slides) within the reservoir.

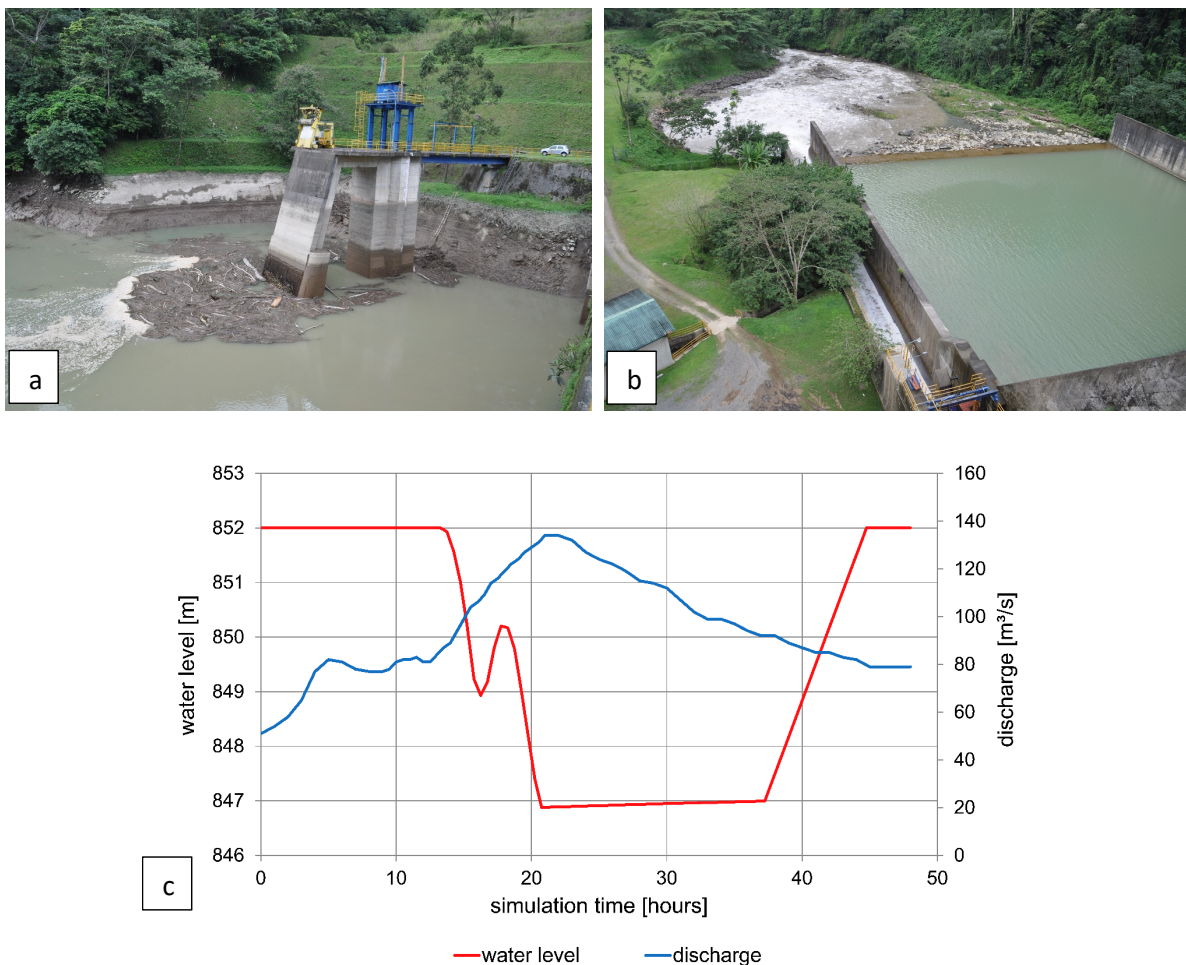


Fig. 92: (a) water level fixations at the intake of the Peñas Blancas reservoir in Costa Rica during pressure flushing; (b) outflow of the Peñas Blancas reservoir in Costa Rica through the bottom outlets; (c) water level and outflow of the Bodendorf reservoir in Austria during the flushing operation in 2004.

8.4 Calibration and validation

After having set up a CFD model and the boundary conditions up- and downstream as well as within the reservoir are specified (see chapter 8.3.3. *Boundary conditions for hydrodynamic and hydro-morphodynamic modeling*) first simulations can be conducted to assess the numerical model stability. Then, the performance of the model with respect to e.g., simulation time can be evaluated. However, as already mentioned in chapter 7.2 *Dimensionality in hydrodynamic modeling*, simplifications of the model influence the accuracy of the simulated results. In addition, governing processes may not be reflected by models with lower dimensionality in an accurate manner. To use a hydro-morphodynamic model for making accurate predictions of hydraulics, sediment transport and morphological processes an in-depth calibration and validation are necessary to ensure the reliability of the numerical model.

The aim of the calibration is the diminution of uncertainties by updating model parameters and the subsequent comparison of simulated results with observed data (e.g., water levels or bed level changes) (Oberkampf et al., 2004). During the calibration process, sensitive parameters that are subject to calibration are selected in a first step. They are adjusted in a way that the simulated results match in the best case the observed values from nature in a second step (Oreskes et al., 1994; Kleijnen, 1995), or at least achieve an agreement within a reasonable tolerance. Sensitive but also uncertain parameters are a result of the stochastically behavior of the environmental fluid system, the simplified structure of the hydro-morphodynamic model itself, the implemented empirical equations, the unknown boundary conditions, or imprecise input data (Shoarinezhad et al., 2020b). The simplest and most often used procedure to calibrate hydrodynamic and hydro-morphodynamic models is a manual adjustment of parameters until a satisfactory agreement between simulated and measured values is reached (trial-and-error method). However, this method may become time-consuming and cost-intensive and often depends on the user's knowledge of the model structure and the environmental system (Duan et al., 1993; Boyle et al., 2000). In addition, the calibration process itself may be biased by the modeler, as the selected sensitive parameters are often adjusted based on practical experience. Botterweg (1995) compared the outcomes of a calibration of the same hydrological model, performed by two independent modelers with an identical set of measured data. Although the calibration yielded in both cases in reasonable results, different model parameters were used by the modelers to achieve this goal.

To overcome these disadvantages in calibration automated and semi-automated calibration methods can be used in hydrodynamic but also in hydro-morphodynamic numerical modeling (Troy et al., 2008; Hogue et al., 2000; Doucet et al., 2018; Acuña et al., 2019; Shoarinezhad et al., 2020a; 2020b). Automated calibration consists in principle of three elements: an objective function to assess the differences between model outputs and observations, an optimization algorithm for sequential adjustment of pre-selected model parameters, with regard to the reduction of the objective function's value, and a convergence criterion (Vidal et al., 2005; 2007). The choice of the optimization algorithm is essential. It can either be based on a global method, means based on sampling the proposed values of parameters over the entire space, or on a local method (gradient-based approach). Local methods are computationally more efficient and need fewer model runs. However, these methods have the disadvantage that they may be trapped in local minima (Abbaspour et al., 2001; Deslauriers and Mahdi 2018; Shoarinezhad et al., 2020b).

Although the hydrodynamic or hydro-morphodynamic numerical model is calibrated, it may still contain uncertainties, as a result of simplifications and limited input data, which allow the model only to reproduce the conditions, selected for calibration (e.g., floods with certain return periods) (Muleta and Nicklow, 2005; Bahremand and De Smedt, 2008). Hence, after calibration, a validation is required, before the model can be applied for reliable predictions

and to ensure the versatility of the model (Rebba et al., 2006; Sargent, 2013). During validation the model is tested on the basis of a different data set compared to the one used during calibration. For the validation runs the calibrated model parameter shall not be changed. Additionally, it has to be ensured, that the data set used for validation is independent from the data set used for calibration. As a consequence, it is possible to conclude whether the achieved agreement between the observed values and the simulated results fit well enough and thus the calibrated parameter set is applicable for a broad range of conditions.

Within the next two subchapters an overview on hydrodynamic as well as hydro-morphodynamic calibration and validation of numerical models is given. As the possibilities are limited in reservoirs, within this chapter a broader overview is given, which can also be used for river sections up- and downstream of a reservoir.

8.4.1 *Hydrodynamic calibration and validation of numerical models*

For hydrodynamic calibration and validation different potential parameters can be used to compare model results with observed data.

- (i) Water level fixations (measured water levels and inundated areas) for known flow conditions (e.g., base flow or flood events),
- (ii) measured flow velocities for specific flow conditions (e.g., base flow or flood events),
- (iii) duration of flood inundation for selected extreme events.

A broad range of different flow conditions has to be captured during calibration and validation, such as high flow events (flood events), but also low flow events (base flow). Although major morphological changes occur during high flow conditions (e.g., morphological relevant bed load transport happens during bank full discharge), processes, such as colmation are governed by low flow conditions (see chapter 3.1 *Erosion*). Usually, hydrodynamic calibration and validation are carried out by performing stationary simulations, as water level fixations and measured flow velocities are available for certain flow conditions only. In addition, the simulation time for stationary conditions is by far smaller, compared to a non-stationary simulation of a flood event, which may last several days (Hauer et al., 2019).

In 2D and 3D models, areas with similar characteristics are usually specified by a similar roughness (e.g., river stretches with similar characteristics, river banks, forest, meadows, sealed surfaces). However, in most models it is possible to specify a certain roughness even for a single cell, which makes it possible to react also on local situations. However, in such cases, detailed measurement data and information on the local conditions are necessary. Finally, and of utmost importance, all chosen roughness values have to be within a physical plausible range.

Figure 93 (center) shows simulated water levels as result of the hydrodynamic calibration simulations of the Goldersbach stream in Tübingen, Germany, with the 2D numerical model *Hydro_AS*. A flood retention reservoir with a controllable weir and a maximum retention volume of 135,000 m³ was constructed, to safe the downstream located city of Tübingen from flooding. The numerical computations model the inundated areas up- and downstream of the reservoir during a flood event. In order to ensure the reliability of the model, the simulation results of the 1987 Goldersbach flood (without flood retention reservoir) were compared with discrete water level observations for calibration. By adjusting the roughness values within the stream and the flooded areas a good agreement was found between the water level fixations and the simulated water levels (Doucet et al., 2018). Afterwards the new flood retention reservoir was implemented to conduct prediction simulations of future flood events (see figure 93).

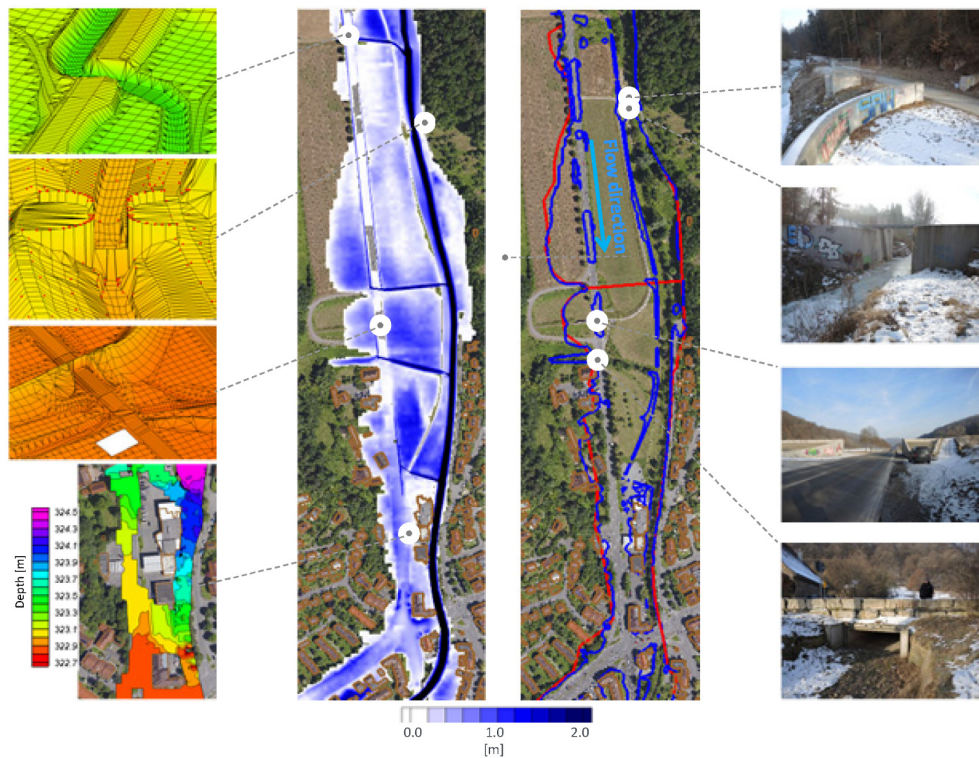


Fig. 93: Flood inundation map from calibration simulations of the 1987 Goldersbach flood (center), including important hydraulic structures of the implemented flood retention reservoir (Doucet et al., 2018; modified).

In hydro-morphodynamic models the roughness of the bathymetry can be calculated based on bed material composition, including bed forms where applicable (Haun et al., 2013a; compare also chapter 7.4.2 *Sediment transport modeling*). The advantage of this method is twofold. First, it ensures that in different regions of the reservoir, different roughness values are incorporated, e.g., a higher roughness can be considered at the head of the reservoir where coarse sediments settle compared to areas close to the dam where fine sediments are found. Second, changes in the roughness during the simulation, which have a major influence on the hydraulics, are taken into account in the simulations (see chapter 3.2.3 *Factors*

influencing the sediment transport). There exist many different recommendations how the roughness should be calculated in the numerical model. Often, it is scaled with the d_{50} or d_{90} and if needed taking bed forms into account (Parker, 1991; Blom, 2008). Bed forms play an important role as they might change the hydraulic conditions considerably (e.g., Haun and Olsen, 2012).

In most cases the calibration and validation of the model is based on water level fixations and less frequently also on measured flow velocities. Especially during high flow conditions, which are crucial for the calibration and validation, measurements of flow velocities are challenging and are often not conducted. However, in literature also studies can be found, where flow velocity measurements, mainly conducted with ADCPs, are applied for the calibration. Harb et al. (2012) modelled the reservoir of the Leoben run-of river power plant in Austria with *Telemac-2D* and used for hydrodynamic calibration ADCP measurements along the relatively narrow reservoir for a comparison with modelled results (figure 94). Flow velocities in large reservoirs are rather small compared to free flow sections of rivers or reservoirs of run-of river power plants, resulting in inaccurate measurements of the flow velocities. Thus, flow velocity measurements in reservoirs are undertaken very seldom. However, for calibration Dorfmann and Knoblauch (2009) used moving ADCP measurements also for the comparably large reservoir of the Feistritz-Ludmannsdorf hydropower plant, located at the river Drava in Austria (Dorfmann et al., 2010). Haun et al. (2013b) conducted moving ADCP measurements in the Angostura reservoir in Costa Rica, but due to the small flow velocities, measurements were only conducted close to the dam, where the reservoir has the smallest width and subsequently the highest flow velocities could be measured. Beside moving ADCP measurements, also horizontally or vertically mounted stationary mounted devices may be used for hydrodynamic calibration. Mouris et al. (2018) used data from a stationary mounted ADCP in the Schwarzenbach reservoir in Germany, for a hydraulic plausibility check of the numerical model results obtained by *SSIIM 2*.

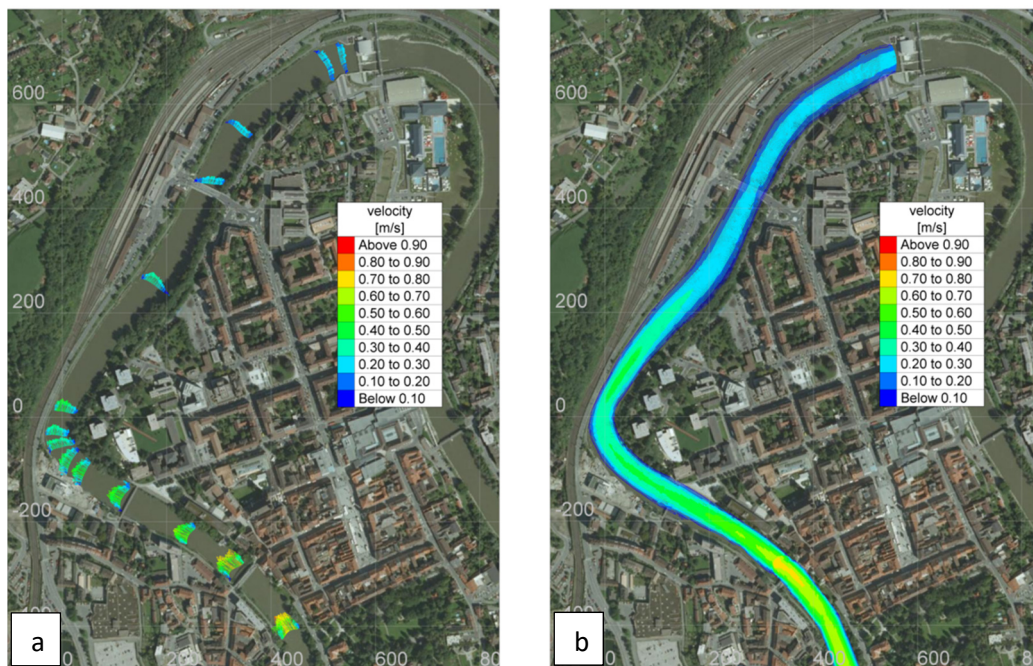


Fig. 94: Flow velocities within the reservoir of the Leoben run-of river power plant (Austria) based on (a) ADCP measurements; (b) the numerical simulation with *Telemac-2D* for the same discharge (Harb et al., 2012).

Calibration of hydrodynamics in reservoirs is seldom performed based on the duration of flood inundation. However, for the up- and downstream located river stretches, this may be a feasible approach. If such data sets are available, non-stationary simulations need to be executed. To ensure a reliable calibration, the duration and also the water depths are required.

If the validation differs significantly from the calibration, three further steps are recommended:

- (i) Improvement of the calibration,
- (ii) plausibility checks of data sets used for calibration and validation (measured data),
- (iii) clarification if any processes are present in the validation that were not considered for the conditions chosen for calibration.

For most cases it is sufficient to slightly adapt the model parameters during validation, which were selected for calibration. Mostly, the roughness values are modified and the calibration and validation simulations are repeated with the new boundary conditions until satisfying results are obtained for both cases.

If no good results can be achieved for the different scenarios, a deeper investigation of the input data is necessary, as differences in the modeling results may be the outcome of imprecise or missing input data. However, also the seasonality of vegetation in the

surrounding area or land use changes need to be considered, as they result in differences in the roughness values.

Another important issue for calibration and validation, are model-specific parameters to increase the performance of the numerical model. As a result of simplifications, governing processes, such as secondary currents, may not be well reflected by models with lower dimensionality. However, in many 2D models additional algorithms are available to take such simplifications at least partially into account. Furthermore, even 3D numerical models may not predict the flow field accurately. This maybe a result of false diffusion in case that a too coarse grid is used, an insufficient upwind scheme is chosen or the grid is not in alignment with the flow. Mouris et al. (2018) used during a hydraulic plausibility check of the simulations of the Schwarzenbach reservoir in Germany (3D) a power law scheme as well as a second order upwind scheme to investigate differences in the modeling results. Figure 95 shows the differences in the simulated depth averaged flow velocities for a steady state situation and for the two different upwind schemes. Especially in the upstream part of the reservoir, where a third large eddy occurs when using a higher upwind scheme, the simulation results differ.

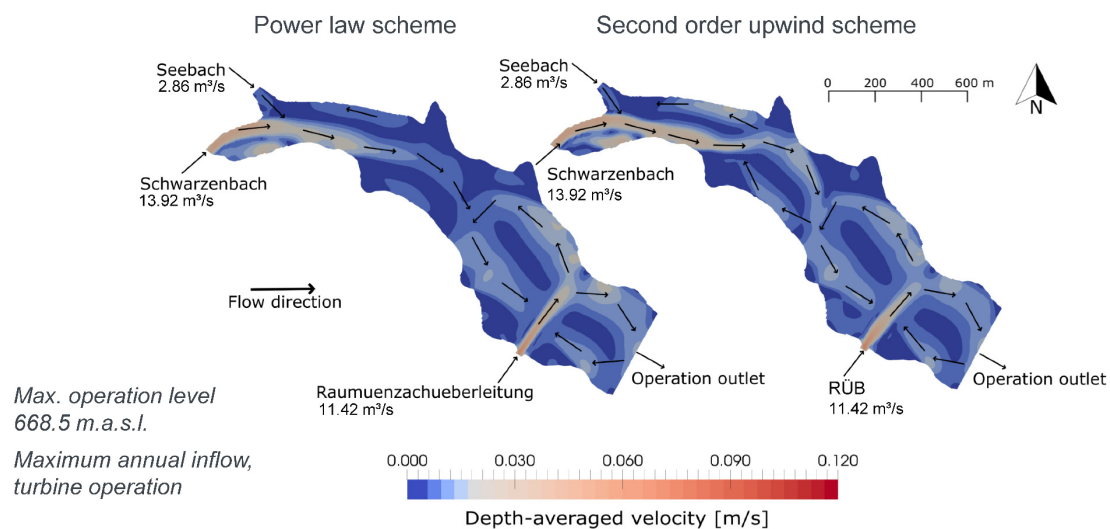


Fig. 95: Simulated depth averaged flow velocities in the Schwarzenbach reservoir in Germany, simulated with the numerical program *SSIIM 2* by (a) using a first order upwind scheme (power law scheme); (b) a second order upwind scheme (Mouris et al., 2018).

Boundary conditions, such as vegetation roughness, can differ in summer or winter and may result in different roughness values for the foreland. Especially for large reservoirs also external wind forces or seasonal stratification within the water body may be of importance when modeling hydraulics. An example of the influence of wind is given in figure 96, where for the same steady state simulation of the Schwarzenbach reservoir in Germany (figure 96a) wind is introduced into the system (figure 96b). A clear influence can be seen, as the eddies in the upstream and the middle part of the of the reservoir merge, resulting in one large eddy when wind is acting on the surface of the reservoir (Mouris et al., 2018).

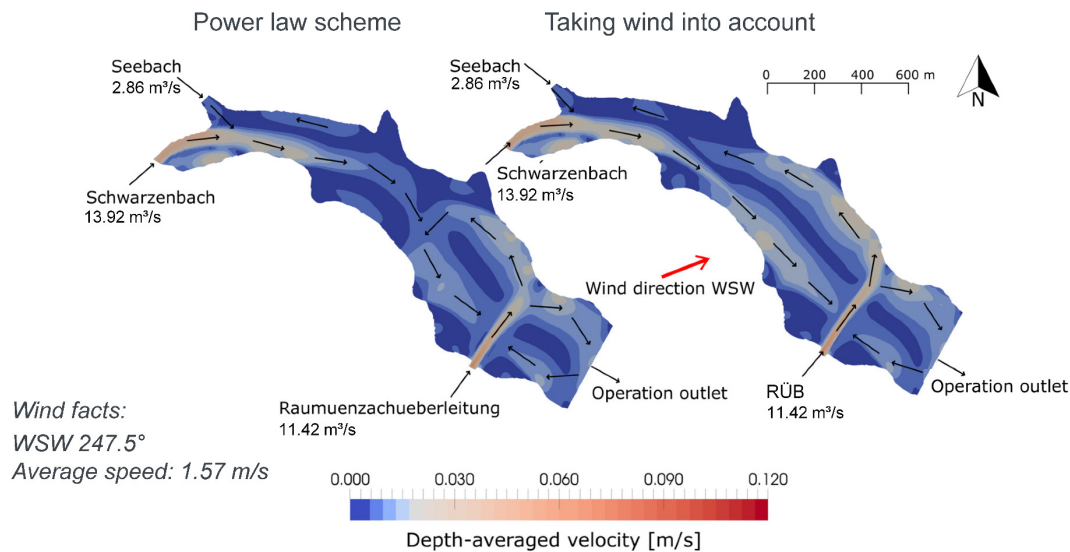


Fig. 96: Simulated depth averaged flow velocities in the Schwarzenbach reservoir in Germany with the numerical program *SSIIM 2* by (a) using a first order upwind scheme (power law scheme); (b) the same upwind scheme, but taking wind forces into account (Mouris et al., 2018).

8.4.2 Hydro-morphodynamic calibration and validation of the numerical models

Hydro-morphodynamic processes are a result of the sediment characteristics as well as of the hydraulic forces acting on the particles. Hence, inaccuracies in the hydrodynamic conditions will inevitably result in inaccurate predictions of sediment transport and morphological processes. Consequently, a hydrodynamic as well as a hydro-morphodynamic calibration and validation is required (see chapter 8.4.1 *Hydrodynamic calibration and validation of numerical models*).

In general, a large number of different possibilities exist to calibrate and validate a hydro-morphodynamic model, nevertheless available data sets are of major importance. Sediment transport and morphological data, especially with the required temporal and spatial resolution, is in many cases scarce. Hence, often only limited possibilities exist for a hydro-morphodynamic calibration and validation. Examples for data sets are:

- (i) Bed level changes within the model domain for a given period,
- (ii) sediment transport rates at specified transects (bed load, suspended load or total load) for known hydrological conditions,
- (iii) changes in grain-size distributions within the model domain within a given period.

The most common way for calibration of hydro-morphodynamic models is a comparison of the sediment balance (sediment in- and outflow). Such a comparison is possible for models in all dimensions. However, by just comparing the sediment balance inaccuracies are often introduced, as information, with respect to spatial bed development, is not given (e.g., from 1D hydro-morphodynamic models).

An example is the calibration of the numerical *SSIIM 2* with data from the reservoir flushing simulation of the Bodendorf reservoir in Austria, conducted in 2004 (Haun et al., 2012c). The boundary conditions of the flushing (water levels and outflow from the reservoir) are shown in figure 92c. During the flushing 47,300 m³ of sediments were flushed out, approximately 31,500 m³ as bed-load (Badura et al., 2007). The hydro-morphodynamic simulations resulted in 23,400 m³ (by using the bed load transport formula by van Rijn, 1984a) and 31,200 m³ (by using the bed load transport formula by Meyer-Peter Müller, 1948) of flushed out sediments. However, to gain deeper insight into the ongoing processes in the reservoir and to obtain knowledge on areas where erosion occurs, a look into bed level changes within the model domain is required. Figure 97 shows (a) the grid used for the simulations with only 15,358 cells at the beginning of the flushing simulation (maximum operation level), (b) the measured bed levels after the conducted flushing, (c) the simulated bed levels by *SSIIM 2* after flushing and (d) a cross section with measured and simulated bed levels. The comparison of Figure 97b and (c) reveals that the simulated bed levels globally agree with the measured bed levels. A higher degree of details and more insights are given in Figure 97d. Here, the differences between the two used bed load transport equations, namely Meyer-Peter-Müller (1948; Eq. 37) and van Rijn (1984a; Eq. 38), are visible. The equation developed by Meyer-Peter-Müller (1948) results in a higher accuracy, as the reservoir can be characterized by steep gradients and coarse sediments.

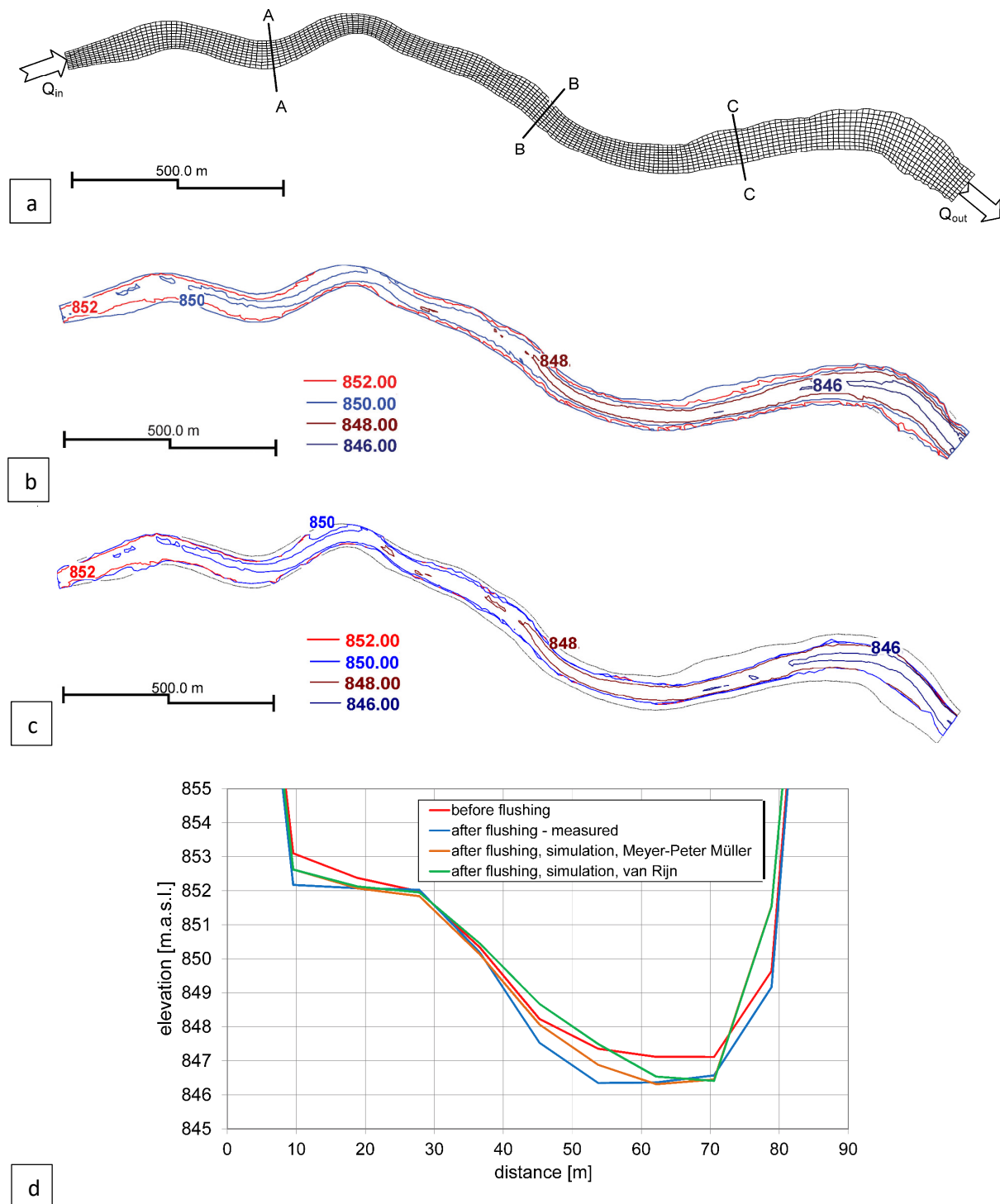


Fig. 97: (a) grid for the flushing simulation of the Bodendorf reservoir with 15,358 cells at the beginning of the flushing simulation; (b) bed geometry of the reservoir after the flushing (measured); (c) bed geometry of the reservoir after the flushing (simulated); (d) measured and simulated bed level changes with different bed-load transport formulae in a cross section of the reservoir.

For calibration and validation also information on the sediment transport rates at specified transects (Haun et al., 2013a) and changes in grain-size distributions (Beckers et al., 2015; Sadid et al., 2016) may be used. Although this type of data is not available for most case studies

yet, due to the ongoing development of measurement techniques (see chapter 6 *Hydro-morphodynamic measurements*) and a subsequent increase in spatial and also temporal resolution of measured data, such data sets will become more and more available in future. Haun et al. (2013a) used suspended sediment concentration measurements within the Angostura reservoir in Costa Rica to calibrate an existing numerical model. Figure 98a shows the simulated depth averaged suspended load concentrations, whereas figure 98b presents the measured concentrations for the points highlighted in figure 98a. Figure 98b indicates that the sophisticated measurement method, based on laser diffraction, is able to resolve the concentrations even for different grain-sizes. In combination with flow velocity measurements in different sections of the reservoir, also the suspended sediment transport rates can be calculated and compared with the results of the numerical model.

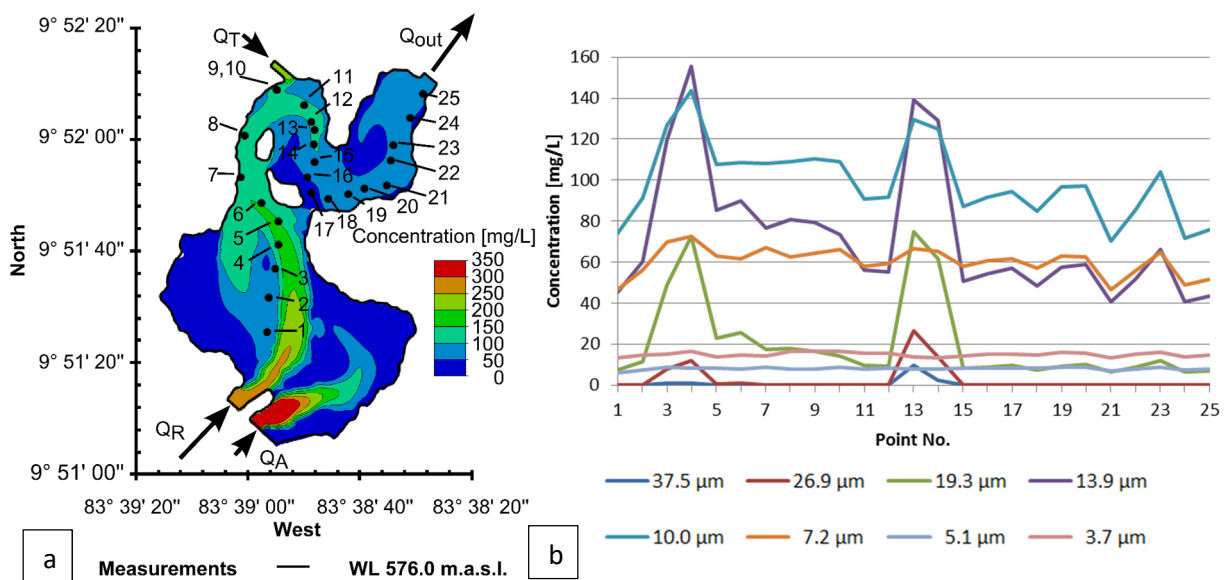


Fig. 98: Depth averaged suspended sediment concentrations at the Angostura reservoir in Costa Rica (a) simulated with the numerical model *SSIIM 2*; (b) measured with a LISST-SL device at discrete points (Haun et al., 2013a).

8.5 Sensitivity analysis

A large number of domain-specific (input parameters) as well as model-specific (algorithms) parameters characterize hydrodynamic, and especially hydro-morphodynamic models. By conducting a sensitivity analysis, it is possible to obtain sensitive parameters, which may be adjusted during calibration and validation, and at the same time to quantify also the influence of these parameters on the simulation results. Often the output from the model simulations is just a single value (e.g., water level at a certain location). However, the sensitivity analysis enables to provide a range of possible results, taking uncertainties into account. Beckers et al. (2018) used a first-order second moment method with numerical differentiation for their sensitivity analysis to determine such a range of possible model outcomes for the investigated

river stretch of the lower River Salzach, located at the Austrian-German border. The simulations were performed with the 2D numerical program *Hydro_FT*.

To investigate the sensitivity of a parameter, this parameter is varied within a certain range (+/- a certain value), while all other parameters remain unchanged during the simulation. This step is repeated for the model as well as for the domain-specific parameters to investigate the sensitivity of the parameters and their uncertainties introduced to the modeling results.

In the hydraulic calibration of the Goldersbach stream in Tübingen, Germany (see figure 93) the roughness values (Strickler coefficients; k_{St}) were varied to obtain reliable predictions of future flood scenarios. In absence of data for validation, a sensitivity analysis was conducted to gain information on the robustness of the model and on its sensitivity to alterations of the roughness values (Doucet et al., 2018). Hence, the Strickler coefficients (e.g., initial value for the stream bed $k_{St} = 33 \text{ m}^{1/3}/\text{s}$) were varied by +/- $1 \text{ m}^{1/3}/\text{s}$. Then the impact on the water levels at discrete points along the modeling domain was reviewed (compare table 3). The model results show that the changes in water levels were only within a millimeter range, which proved the robustness of the model and shows that the model has a minor sensitivity to changes of the roughness values.

Table 3: Overview on terrain parameters and their impact on modelled water levels when changing the Strickler coefficients by increments of $1 \text{ m}^{1/3}/\text{s}$.

Terrain	Strickler coefficients (k_{St}) [$\text{m}^{1/3}/\text{s}$]	Water level change [mm per $\text{m}^{1/3}/\text{s}$]
Grassland	27	2.5
Crops	13	0.7
Forrest	11	0.4
Bushes	9	0.2
Roads	37	0.4
Stream bed	33	2.1

Within a study conducted by Shoarinezhad et al. (2021) two symmetric shallow reservoirs (with a lozenge and a hexagon shape) were modelled with the three-dimensional numerical model *SSIIM 2*. Both reservoir shapes were initially investigated by Kantoush (2008) in physical model tests to explore the shape effects of shallow reservoirs on the flow field and the sediment transport. The physical models had a maximum inner length of 6.0 m and an inner width of 4.0 m. The inlet and outlet were constructed as rectangular channels with dimensions of 1.0 m length and 0.25 m width. During the experiments, the discharge and water depth were kept constant at 7 l/s and 0.20 m, respectively. As sediment substitutes crushed walnut shells with a median diameter of $d_{50} = 50 \text{ }\mu\text{m}$ and a density of $1.5 \text{ g}/\text{cm}^3$ were used and an

inflow concentration of 3.0 g/l was selected. Each of the experiments was subdivided into five phases: the first phase was a one-hour clear water test, followed by four sediment feeding phases (in total 7.5 hours for the lozenge-shaped and 9 hours for the hexagon-shaped reservoir). The geometry of the shallow reservoirs can be seen in figure 99, in which the final bed levels of the experiments and the results of the numerical simulations are presented. The shape of the reservoirs causes a highly unstable flow field in the lozenge-shaped reservoir, which tends to deviate towards the walls. During the laboratory investigations as well as in the hydro-morphodynamic simulation, the deposited sediments alter the flow field, resulting in a change of the flow path from one side of the reservoir to the other. The flow field within the hexagonal-shaped reservoir was stable during the entire experiment in the physical model as well as in the numerical simulation, resulting in a direct flow path from the inlet to the outlet (Shoarinezhad et al., 2021).

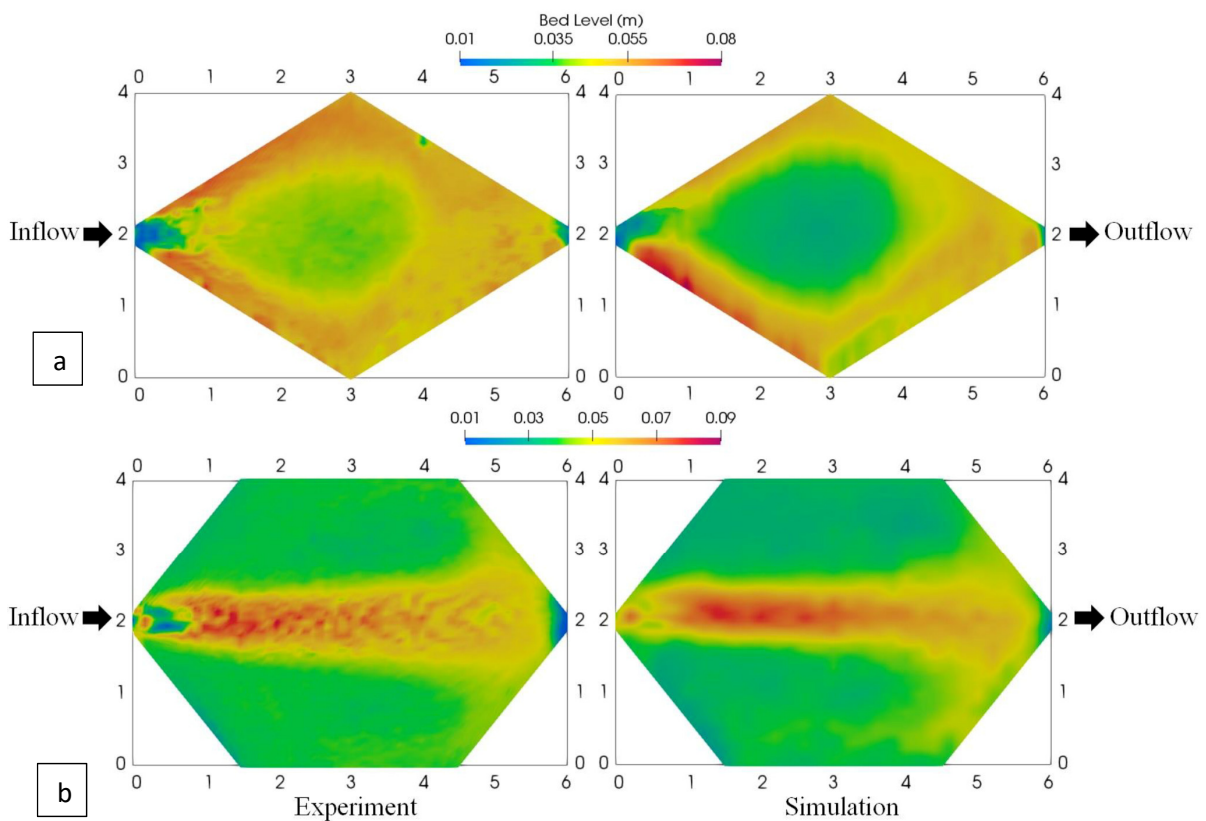


Fig. 99: Final bed levels of the experiments (left) compared to the simulation results (right) for (a) the lozenge-shaped reservoir; (b) the hexagonal-shaped reservoir; all dimensions are given in meters (Shoarinezhad et al., 2021).

For the calibration of the lozenge- and hexagonal-shaped reservoirs the automated calibration tool PEST (Parameter ESTimation Tool; Doherty, 2016) was implemented. PEST uses the Gauss-Marquardt-Levenberg (GML) algorithm, which is a gradient-based optimization method (local method; see chapter 8.4 *Calibration and validation*). Purnomo (2018) investigated the sensitivity of several parameters on the final sedimentation pattern within the lozenge-shaped reservoir, to finally chose the most sensitive parameters that are subject to adjustment during

the calibration process. Because the input parameters (domain-specific parameters) in the physical model are available in a very high quality (e.g., water inflow, sediment in- and outflow), mainly model-specific parameters (algorithms) were tested. Four out of ten varied parameters show a high influence on the simulation results. Subsequently, during calibration only parameters with high influence on the simulation results were taken into account. Table 4 provides an overview on selected parameters and their sensitivity on the model results.

Table 4: List of selected parameters and their sensitivity on the model results, investigated during a sensitivity analysis.

Parameter	Sensitivity	Parameter	Sensitivity
Roughness	Low	Sediment transport formula	Low
Upwind scheme	High	Hiding / exposure	Low
Turbulence model	High	Correction for sloping bed	Low
Type of wall law	Low	Compacted sediment fraction	High
Fall velocity of particles	High	Active layer thickness	Low

The sensitivity analysis of the fall velocity of the particles was assumed approximately 1 mm/s (Kantoush, 2008). It was varied and set to 2.45 mm/s, 1.1 mm/s, 0.9 mm/s, 1.3 mm/s, and 0.5 mm/s. In the sensitivity analysis also two extreme variations are included. In Figure 100 four cross sections along the reservoir are presented, including the depositions for the variation of the fall velocities in the model. As a result of the fall velocities of the particles, especially at the entrance area of the reservoir the large influence on the deposition pattern is obvious. Hence, the sensitivity of the fall velocity and its influence on the resulting deposition pattern in the reservoir can be stated to be high.

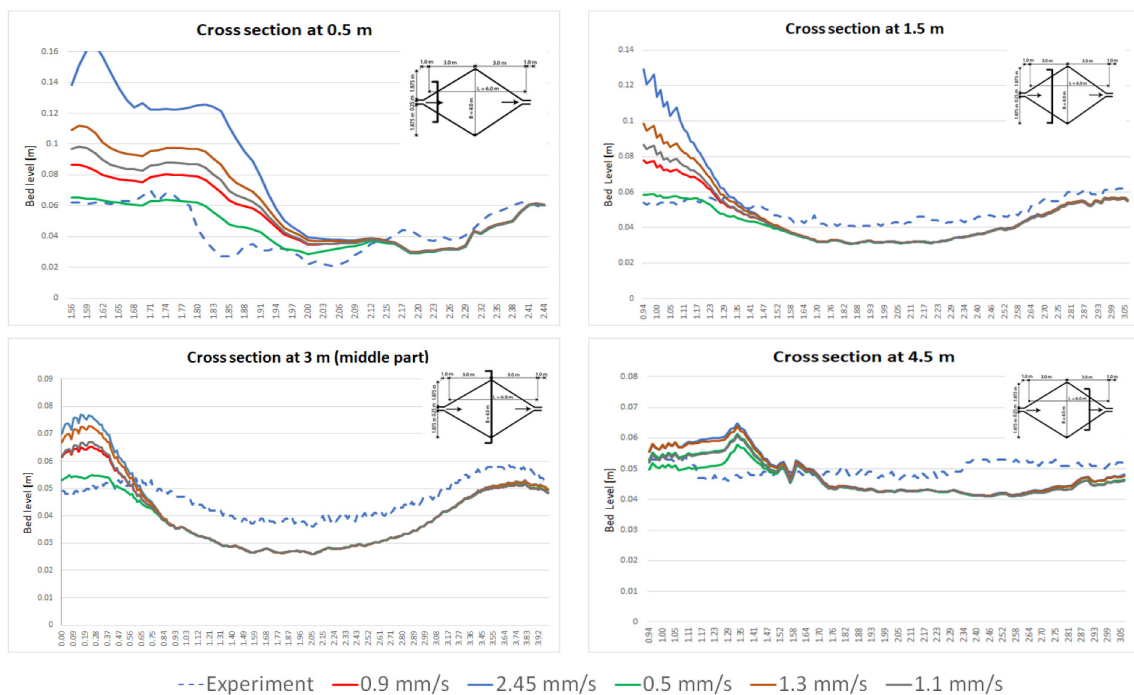


Fig. 100: Final bed levels of experiments and the numerical simulations at four cross sections along the shallow reservoir for different fall velocities (Purnomo, 2018).

For the calibration, validation and also for the sensitivity assessment of numerical model parameters, meanwhile more sophisticated approaches are available. Beckers et al. (2020a) suggest a stochastic Bayesian approach for calibrating and validating hydro-morphodynamic models. This approach was tested on a 2D hydro-morphodynamic model (*Hydro_FT*) of the lower River Salzach (section of 11.0 km for the period 2002–2013) for the three most sensitive input parameters, namely: critical Shields parameter, grain roughness, and grain-size distribution (see chapter 9.1 *Selection of measurement and monitoring parameters based on sensitive domain-specific parameters*). However, to avoid the high number of model runs required for the Monte Carlo-based technique for a Bayesian calibration (global method), a surrogate model was used to reduce the number of required numerical simulations.

Another approach, implemented by Kopmann and Schmid (2008; 2010) is the First-Order Reliability Analysis Method (FORM), which they used in combination with the 2D hydro-morphodynamic model *Telemac-2D*. In this scatter analysis the probability distributions of the output variables, as a result of a sensitivity analysis, are available without conducting a high number of simulations, compared to the Monte Carlo method (global method). Kopmann and Schmid (2008) performed the sensitivity analysis for two laboratory experiments and three parameters, namely: the roughness coefficient, mean grain-size and the critical Shields parameter. A comparison with the results provided by Monte Carlo simulations (global method) show that the FORM is able to reliably predict hydro-morphodynamic processes. However, for all local methods the variations of the input parameters need to be specified within a physically plausible range. It is important to consider, that the application of most of

the local methods is only adequate for linear or slightly non-linear problems. Kopmann and Schmid (2010) investigated in a second study a 10 km long stretch of the river Danube, for which the development of the bed levels was predicted by *Telemac-2D*, coupled with the morphodynamic program *Sisyphé* (Villaret, 2005). 13 model parameters were examined and for each model parameter, a probability distribution was assumed. The simulation time of the Monte Carlo simulations was 37 times longer compared to the scatter analysis (local method), although the results are comparable in their quality.

9 HYDRO-MORPHODYNAMIC MODELS AS BASIS FOR IMPLEMENTING RELIABLE MEASUREMENTS

Hydrodynamic and hydro-morphodynamic models give insight into ongoing processes, sensitive domain-specific parameters as well as into the spatial extent and the temporal scales of hydraulics, sediment transport and morphological changes. Within this chapter an approach is presented, where numerical models are used to design optimized measurement concepts, to perform reliable measurements and to set up a sustainable monitoring strategy.

For conducting field measurements as well as for the implementation of a monitoring an accurate planning and a sufficient overview on the actual hydrodynamic and hydro-morphodynamic situation within the water body is required. Ongoing hydraulic and hydro-morphodynamic processes need to be covered by such a monitoring campaign. However, the number of possible measured parameters, and also the amount of the measurements itself, are often limited, because measurements are labor-intensive and thus associated with high costs. Hence, the spatial and temporal resolution of measurements is in many cases lower as desirable for a complete understanding of the system. As a consequence, the selection of vital parameters, which will be measured and/or monitored as well as a sustainable choice of the spatial and temporal resolution is necessary ahead of a measurement campaign. However, measurement and monitoring campaigns are often set up based on a subjective selection. In addition, the temporal and spatial resolution of measurements are often chosen based on personal experience.

When planning a measurement or a monitoring campaign, in a first step a measurement concept has to be elaborated. It contains the basic conditions of the campaign and includes information on:

- (i) Which processes and subsequently which parameters need to be covered by the measurements,
- (ii) which measuring devices are required for the campaign to gain reliable measurement data for the selected parameters,
- (iii) what is the significance of the measurement results, also depending on the spatial and temporal resolution of the measurements,
- (iv) how the measurement results can be interpreted.

Within this chapter an approach is presented, in which the results of hydro-morphodynamic models are used as a decision basis for the implementation of a reliable measurement and/or monitoring concept. Based on the knowledge from numerical models an objective assessment on (i) the sensitive domain-specific parameters and (ii) the necessary spatial and temporal resolution is feasible.

In three subchapters examples are given, where knowledge on sensitive domain-specific parameters and the required spatial and temporal resolution can be gained from conducted hydro-morphodynamic simulations. Often this knowledge can be collected at the same time, as it can also be seen in the case studies presented here. Based on numerical simulations an objective decision support for implementing measurements is provided to ensure a reliable and optimized measurement campaign.

9.1 *Selection of measurement and monitoring parameters based on sensitive domain-specific parameters*

When setting up a reliable hydro-morphodynamic prediction model several parameters are varied during calibration and validation to find an optimum agreement between the simulation results and in-situ measurements (chapter 8.4 *Calibration and validation*). As shown in chapter 8.5 *Sensitivity analysis* numerical models are sensitive to model-specific parameters (algorithms) and to domain-specific parameters (input parameters). However, as the sensitivity of the parameters strongly depends on the modeling domain and the given boundary conditions, they may vary for each study site. Hence, a statement, which are sensitive parameters in general, cannot be made.

Sensitivity analysis of the hydro-morphodynamic long-term simulations of the river Saalach, located at the German - Austrian border

The first example refers to the uncertainty (sensitivity) analysis of a 2D hydro-morphodynamic model of the heavily modified river Saalach, located at the German - Austrian border (Beckers et al., 2016). The model was used for conducting long-term predictions (84 years) of the morphodynamic bed changes of a 18.3 km long river stretch, located between the Kibling dam and the hydropower plant Rott. Within the simulation domain additional 5 weirs and 7 other hydraulic structures (mainly ramps) are located. The Kibling dam interrupts the sediment continuity of the river Saalach almost completely and was specified as upstream boundary of the model. As a compensating measure, ongoing sediment replenishment (mainly coarse sediments), with a constant feeding rate of 50,000 m³ per year, is performed downstream of the Kibling dam. In addition, a reservoir flushing operation is performed every year, which results in an additional 10,000 m³ of mainly fine sediments as input into the simulation domain. For calibration, several model and domain-specific parameters were selected and adapted to find an optimum agreement between the simulated and measured bed level changes for the period between 1999 and 2009. The subsequent validation was performed for the period between 2009 and 2013. Beside the bed level changes, also the sediment balance was used for calibration and validation. In a second step, an in-depth sensitivity analysis for several parameter alterations were performed during calibration and validation. In total, eight parameters were chosen (table 5), of which four are related to domain-specific parameters

and the additional four parameters are model-specific parameters. The model-specific parameters are the critical Shields parameter, the empirically developed pre-factor of the Meyer-Peter and Müller bed load equation, the active layer thickness and the acceleration factor used for hydro-morphodynamic simulations. As domain-specific parameters (shaded in light grey in table 5) the total roughness and the grain roughness, the amount of replenished sediments as well as the discharge are counting. Table 5 gives an overview of the values obtained from the calibration and validation and used in the reference simulation as well as the range of variation of the single parameters during the sensitivity analysis (Beckers et al., 2016).

Table 5: Overview of parameters investigated during the sensitivity analysis as well as reference values of the parameters and varied ranges during the sensitivity analysis.

Parameter	Reference value	Range of variation	
Critical Shields parameter (θ_{crit}) [-]	0.040	0.033	0.047
Scaling factor of Meyer-Peter and Müller bed load equation (MPM) [-]	1	0.625	1.375
Active layer thickness (PAL) [m]	0.14	0.07	0.21
Acceleration factor (SCFG) [-]	4	1	6
Total roughness (GR) [$m^{1/3}/s$]	$k_{St, G0}$	$k_{St, G-3}$	$k_{St, G+3}$
Grain roughness (KR) [$m^{1/3}/s$]	$k_{St, K0}$	$k_{St, K-2}$	$k_{St, K+2}$
Amount of replenished sediments [m^3/a]	50,000	30,000	70,000
Discharge (Q) [m^3/s]	Q	Q _{-15%}	Q _{+15%}

To evaluate the sensitivity of the varied parameters, the difference of the simulated erosion and deposition volumes was compared with the volumes of the reference simulation, for each parameter separately. Figure 101 gives an overview of the differences of eroded and deposited volumes. The model-specific parameters are located on the left side (yellow) and domain-specific parameters on the right side (blue). For the model-specific parameters, a variation of the critical Shields parameter and the pre-factor of the Meyer-Peter and Müller bed load equation results in the highest differences of erosion and deposition volumes and can be classified as parameters with high sensitivity. The results of the sensitivity analysis of the domain-specific parameters show a comparably large influence on the simulated volume of erosion and deposition. In other words, the accuracy of the input parameters of the model is of high importance, as all parameters proved to be sensitive and may introduce uncertainties into the model results.

Based on these findings sensitive domain-specific parameters can be identified, which need to be covered during future measurement campaigns, to increase the reliability of future

studies and to gain additional insight into the ongoing processes of this river section. Beside continuous measurements of the discharge, additional investigations of the bed material (surface and sub-surface samples) are required for obtaining knowledge on the grain roughness. In addition, an exact evaluation of the amount of replenished sediments, including an analysis of the grain-size distribution, is recommended (Haun and Wieprecht, 2017).

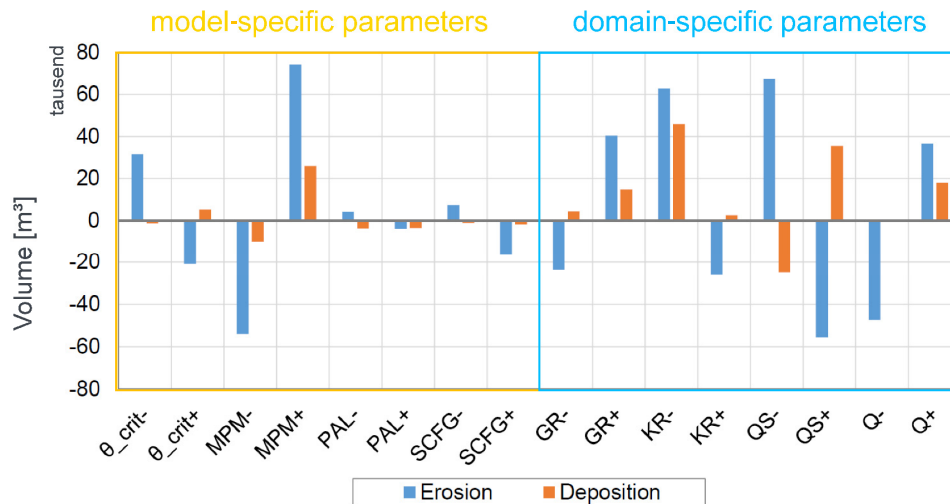


Fig. 101: Evolution volume difference of the reference simulation subtracted by the outcomes of the respective parameter variations for model-specific parameters (left) and domain-specific parameters (right) (Beckers et al., 2020b; modified).

Sensitivity analysis of the hydro-morphodynamic flushing simulations of the Schwarzenbach reservoir in Germany

Within the research project CHARM – CHALLENGES of Reservoir Management – (Beckers et al., 2018; Wieprecht and the CHARM Team, 2020) the Schwarzenbach reservoir, located in the Black Forest in Germany, was investigated by means of hydrodynamic and hydro-morphodynamic simulations as well as by field surveys. The Schwarzenbach reservoir has been in operation since 1926 and is part of the first large scale pump storage power plant in Europe. The reservoir itself has a length of 2,200 m, a maximum width of 600 m, a maximum depth of 47 m and a total storage volume of 14.4 mio m³ (Urban et al., 2006; Beckers, 2021). The Schwarzenbach reservoir in Germany has no acute sedimentation problem, nevertheless sedimentation as well as reservoir management by means of reservoir flushing were investigated within the collaborative research project (Mouris et al., 2018; Saam et al., 2019). Figure 102 shows the dependency of the modelled suspended sediment distribution in the reservoir as a function of the water level and the inflowing water volume (Mouris et al., 2018). The simulations were performed with the numerical model *SSIIM 2* for the finest grain fraction $d = 5.09 \mu\text{m}$ and with a settling velocity of only 0.002 m/s.

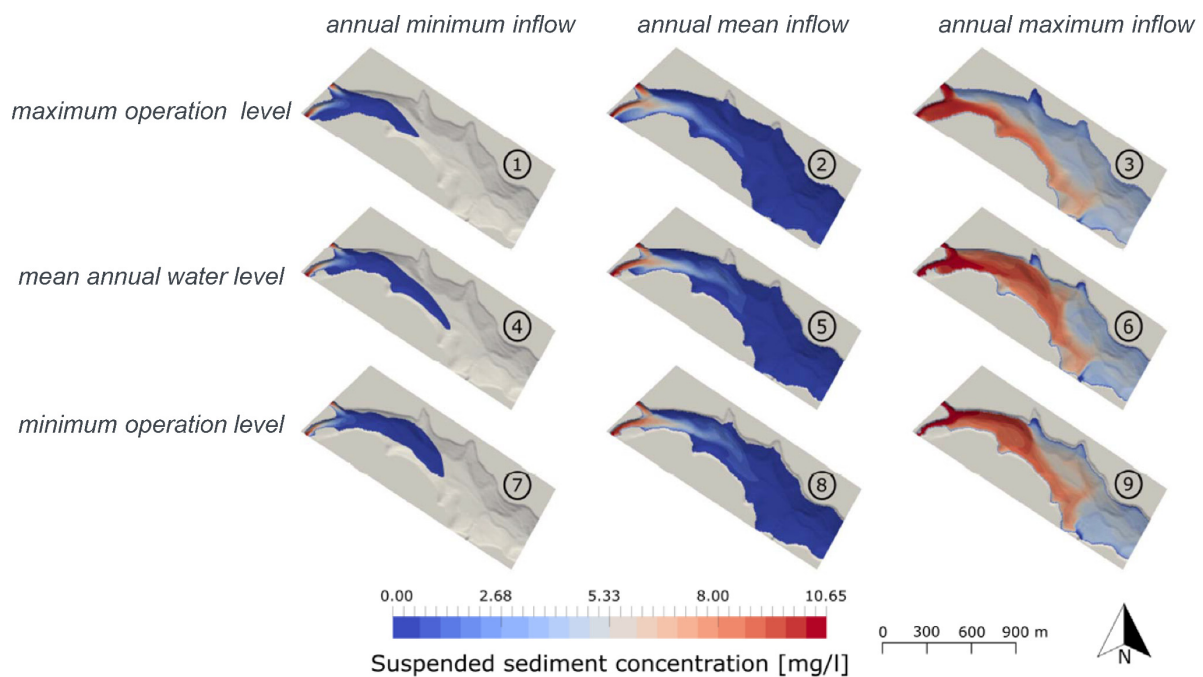


Fig. 102: Suspended sediment distribution of the finest grain fraction $d = 5.09 \mu\text{m}$ as function of the water level and the inflowing water volume (Mouris et al., 2018).

Saam et al. (2019) used the same 3D hydro-morphodynamic numerical model to investigate the efficiency of a reservoir flushing operation for different boundary conditions, which is presented as second case study. In total, three flushing scenarios were investigated, where the duration of the flushing (350 hours) as well as the inflow into the reservoir were kept constant. In three simulation scenarios the water level was kept at the maximum operational level (S1), lowered to minimum operation level (S2) and lowered until free flow conditions occurred (S3). The simulated sediment thickness after the flushing simulations can be seen in figure 103. For the three cases, the numerical model calculated for the different scenarios with different boundary conditions an amount of flushed-out sediments of 39 tons (S1), 10,344 tons (S2) and 34,638 tons (S3), respectively.

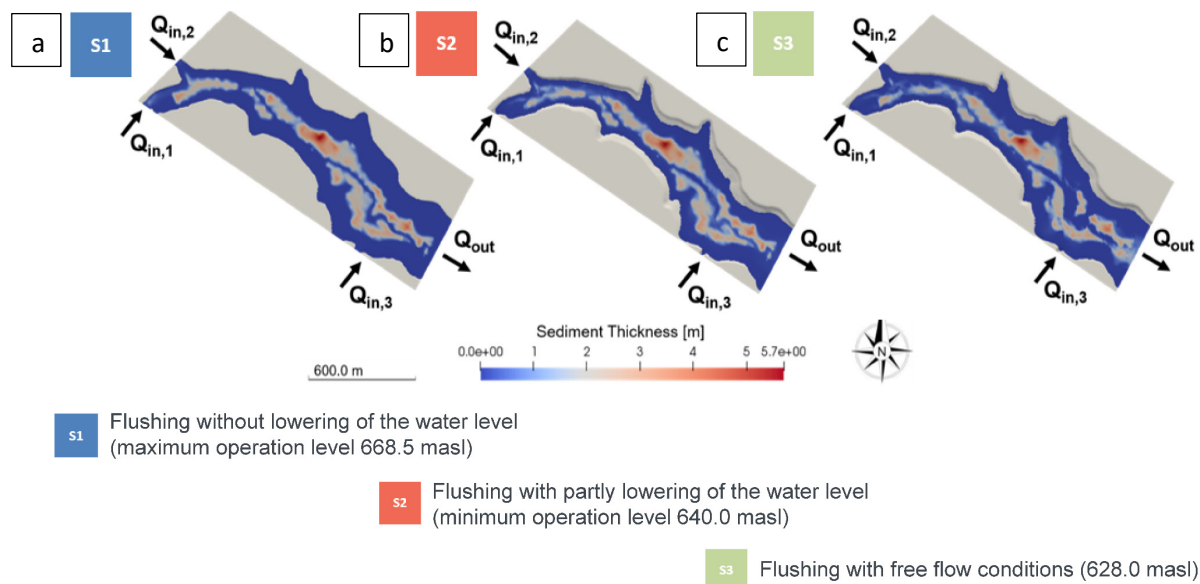


Fig. 103: Sediment thicknesses after the simulated flushing operations with different drawdown targets of the water level (a) maximum operational level; (b) minimum operation level; (c) free flow conditions (Saam et al. 2019).

As for this reservoir no flushing operation was performed yet, no data for calibration and validation of the hydro-morphodynamic model is available. To increase the performance of the prediction simulations, a sensitivity analysis was performed for domain-specific parameters. Thus, the inflowing discharge, the grain-size distribution of the deposited sediments, the bed porosity (water content within the reservoir bed) and cohesiveness were selected. Table 6 gives an overview of the selected parameters, their variations as well as the amount of flushed-out sediments for the different simulations, which can be compared with the reference simulation, which resulted in 34,638 tons of flushed-out sediments for a full drawdown. The grain size distribution was modified in a way that out of the eight grain size classes during the first simulation the coarser four fractions were increased by 3 % each and the finer four fractions were decreased by 3 % (each fraction). In a second simulation the opposite adaption was applied, with an increase of the finer four fractions by 3 % and a decrease of the coarser four fractions by 3 %. Additionally, cohesiveness was added to the deposited sediments. In *SSIIM 2* the cohesiveness of the bed can be simply modified by increasing the critical shear stress. Based on investigations of Beckers et al. (2021) a value of 1.61 Pa was additionally added.

Table 6: Sensitivity analysis of parameters related to the properties of bed sediments and the inflow discharge during the flushing simulation (domain-specific parameters).

Parameter	Range of variation		Amount of flushed out sediments [tons]	
Discharge (Q) [m ³ /s]	Q _{-10%}	Q _{+10%}	32,466	41,746
Particle size distribution (PSD) [%]	PSD _{+3% coarse}	PSD _{+3% fine}	27,548	41,803
Water content (WC) [%]	40	60	30,294	39,731
Cohesiveness [Pa]	0	0.99	34,638	29,799

The results of the sensitivity analysis clearly indicate that changes in the inflow discharge (up to 20.5 % uncertainty) as well as modifications of the sediment-related parameters influence the performance of the model and subsequently alter the model results. The discharges into the Schwarzenbach reservoir are monitored well, hence no sensitivity analysis would be required, however, in many cases the discharge measurements are especially biased during flood events, e.g., by floating debris or sediment transport. This needs to be considered when using measured discharge values. The deviations in the amount of flushed-out sediments are a result of variations in the grain-size distribution of the deposited sediments (up to 20.7 %) and the water content (up to 14.7 %). By adding artificial cohesiveness in the range found during the field investigations of Beckers et al. (2021), an additional influence on the simulation results can be seen. The amount of flushed-out sediments decreased by 13,9 % when taking these cohesive forces into account. A deeper investigation of deposited sediments, by means of obtaining grain-size distributions along the reservoir, determining porosities of the depositions and evaluating critical erosion thresholds, e.g., by sophisticated methods, such as the SETEG flume in combination with the PHOTOSSED method (see chapter 6.2.1 *Critical shear stress measurements*), can increase the reliability of the predictions of the flushing operation and is recommended for further field investigations.

Sensitivity analysis of the hydro-morphodynamic simulations of geotechnical bank failures during the reservoir flushing of the Bodendorf reservoir in Austria

A third example is a study performed by Olsen and Haun (2020), in which a sensitivity analysis for soil mechanic parameters was conducted when simulating geotechnical bank failures during the flushing of the Bodendorf reservoir in Austria. First flushing simulations show differences in the numerical model results, compared to field measurements, which originate from the lack of considering geotechnical bank failures accurately in the numerical model (Haun et al., 2012; Haun, 2012). A newly developed algorithm, which has been implemented in the numerical model *SSIIM 2*, is able to overcome this deficiency (Olsen and Haun, 2018; 2020). As input parameters the cohesion, soil viscosity as well as the coefficient of elasticity and the shear modulus are necessary.

Figure 104 shows a part of a cross section of the Bodendorf reservoir, where a slide occurred during the simulation (Olsen and Haun, 2018). In the figure the water body is shaded blue and the moving soil is shaded light red. In addition, the original river bank and the sliding plane (red lines) are shown.

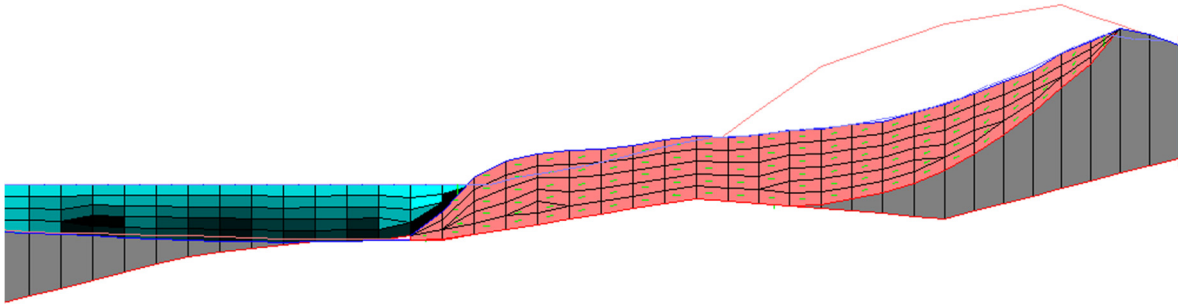


Fig. 104: Occurring geotechnical bank failure during the drawdown of the Bodendorf reservoir, simulated by the 3D hydro-morphodynamic model *SSIM 2* (Olsen and Haun, 2018).

During the reservoir flushing operation in 2004 no soil mechanic parameters were investigated (Badura et al., 2007; Badura, 2007). Olsen and Haun (2020) conducted an in-depth sensitivity analysis of parameters, implemented in the developed algorithm including geotechnical bank failures. Table 7 gives an overview on selected parameters, which were investigated during the sensitivity analysis, including their varied range and the deviations in the modeling results, compared to the default setup of the model. The selection of an appropriate variation range for each parameter should be in a physically plausible range. However, also values outside a physically plausible range are often selected by modelers aiming to gain additional information on the behavior of the numerical model.

The computed mean morphological reduction, as a result of sand slides, was equal to 0.4 m after the calibration of the model. The deviations in the computed lowering of the embankment (Table 7) show that cohesion has the highest influence on the model (up to 97 %). A variation of the viscosity or the E- and G- modules result only in minor deviations, which are in the range of 3-5 % and have a lower sensitivity.

As recommendation for future studies, measurements of the cohesion at the reservoir banks shall be carried out, to reduce the uncertainties of the hydro-morphodynamic numerical model and to obtain reliable and accurate predictions regarding possible geotechnical bank failures during the flushing operation.

Table 7: Sensitivity analysis of soil mechanic parameters used in the model to calculate the lowering of the embankment, as a result of geotechnical bank failures (selected parameters).

Parameter	Parameter change		Computed average lowering [m]	Deviation compared to default setup [%]
	from	to		
Cohesion [Pa]	1,000	500	0.56	40
Cohesion [Pa]	1,000	10,000	0.013	97
Viscosity [Pa]	1.5e7	2.5e7	0.39	3
E and G modules [Pa]	6.5e7	4.0e7	0.42	5

9.2 *Selection of a spatial resolution of measurements based on results from hydro-morphodynamic numerical models*

In a first step a measurement concept has to be elaborated, including the identification of important processes and subsequently parameters, which need to be covered. In a second step, a more detailed design of the campaign is performed. During this phase an organizational planning is conducted, in which sampling spots and the spatial resolution of the measurements are defined. In practice, this selection is often based on a subjective assessment instead of a selection on an objective basis.

The modeling results of 2D and 3D hydrodynamic and hydro-morphodynamic models provide insights on the hydraulic conditions, sediment transport, but also morphological changes with a high spatial resolution. Hence, knowledge on governing processes is available from these models as well as knowledge on areas within the river/reservoir, where these processes occur (e.g., areas of sediment depositions within the reservoir). This information can be used as basis for the selection of the spatial resolution of measurements or for the selection of measurement spots for future campaigns.

Analysis of the spatial extent of bed level changes as a result of long-term hydro-morphodynamic simulations of the river Saalach, located at the German - Austrian border

Due to changing hydraulics and differences in the hydro-morphodynamic conditions along the studied area, the sensitivity of certain parameters (e.g., grain-size distribution), and thus the introduced uncertainties, may vary along the modeling domain. Hence, during the sensitivity analysis of model and domain-specific parameters of the river Saalach (compare table 5) also an analysis of their influence on the spatial extent was performed in the 2D hydro-morphodynamic model. This enabled an identification of sensitive regions within the modeling domain (Beckers et al., 2016). Each parameter was separately varied and analyzed with respect to the spatial distribution of hydro-morphodynamic bed changes, annually transported bed load, grain-size distribution of the bed sediments and the total sediment

balance along the 18.3 km long modeling domain. The range of possible morphodynamic bed changes, as a result of a combination of all sensitive parameters, is presented in figure 105. Figure 105 shows the longitudinal section of the river Saalach with minimum (orange) and maximum (green) deviations of the simulated bed level changes, compared to the reference simulation (Beckers et al., 2016). In average, the minimum and maximum deviations in morphodynamic bed changes are in the range from -0.28 m to 0.26 m. However, the figure also reveals the spatial sensitivity and the subsequent variation of the influence on the modeling results along the river stretch. Larger deviations occur mainly in close vicinity of hydraulic structures (12 in total). However, from the modeling results a subdivision between structures with a higher (4 structures) and a lower (8 structures) impact can be made. In addition, the area around the downstream boundary (hydropower plant Rott) is the most sensitive region and requires highest attention during future studies. As a consequence, future field investigations should focus especially on this location, where a higher resolution of measurements will increase the reliability of the hydro-morphodynamic numerical model.

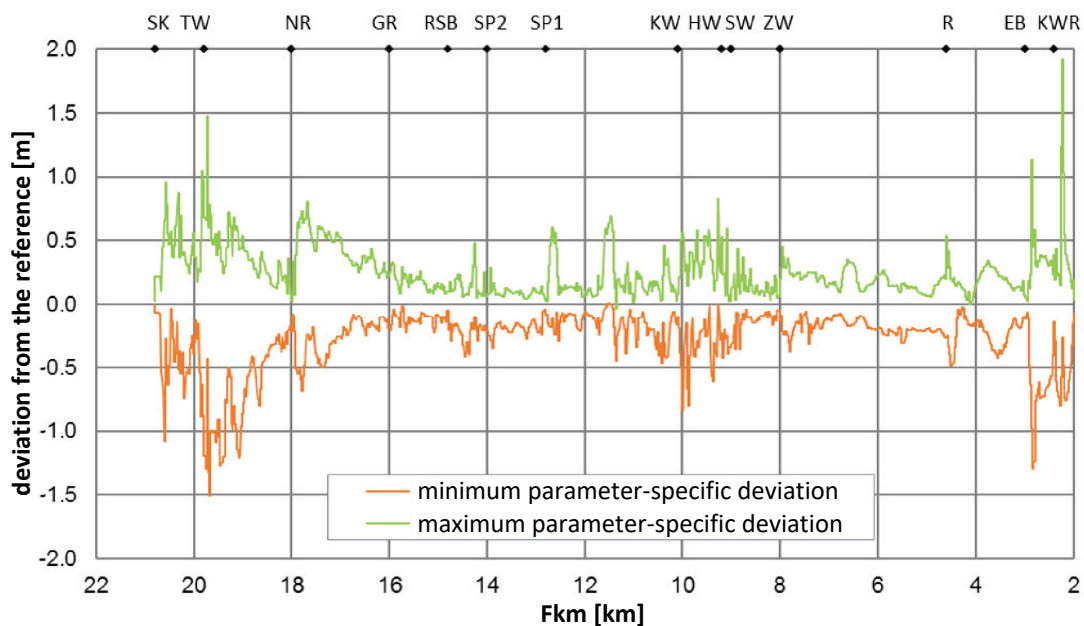


Fig. 105: Range of possible morphodynamic bed level changes along a longitudinal section of the river Saalach, as a result of a combination of sensitive parameters (Beckers et al., 2016).

Analysis of the spatial extent of erosion and deposition as a result of hydro-morphodynamic flushing simulations of the Schwarzenbach reservoir, Germany

Cohesiveness, but also the particle-size distribution of deposited sediments and the bed porosity proved to have a high impact on the predicted results and need to be investigated during future field campaigns in more detail. However, to withdraw undisturbed sediment samples with a high spatial resolution and to obtain depth dependent information on particle-size distribution, porosity and cohesiveness (critical shear stress) is from a labor and economical point of view not feasible for large reservoirs. Hence, recommendations on

specific locations where sampling should be conducted is required. Based on the results of hydro-morphodynamic simulations, information on the efficiency of a flushing, with respect to different boundary conditions, can be gained (figure 103). Furthermore, also an indication on the spatial distribution of erosion processes is given. This knowledge can be used to select spots where a deeper investigation of the deposited bed sediments will lead to an increase in the accuracy of the hydro-morphodynamic simulations. Figure 106 shows numerically simulated bed level changes (bed movements), as a result of the flushing operation with full water level drawdown (S3; figure 103). Green areas indicate depositions and red areas indicate those governed by erosion. Samples from surface sediments, as well as locations of undisturbed sediment core sampling, are marked (Beckers et al., 2018). Based on the erosion tendency indicated by the model results, four additional areas (red circles) can be specified where future field investigations should be performed. With these additional data, sufficient spatial resolution of particle size distributions is provided to obtain reliable hydro-morphodynamic simulations of the flushing event.

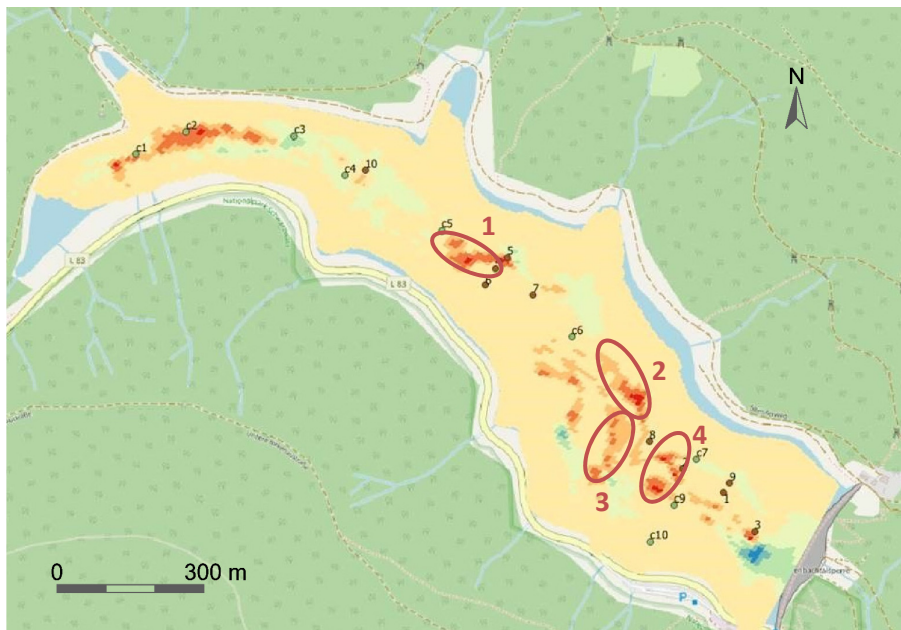


Fig. 106: Simulated bed level changes (bed movements) as a result of the flushing operation with full drawdown (erosion in red and depositions in green) as well as four recommended spots for further field investigations (red circles).

Analysis of the spatial extent of simulated geotechnical bank failures as a result of hydro-morphodynamic flushing simulations of the Bodendorf reservoir, Austria

During reservoir flushing operations often geotechnical bank failures are observed. These processes may happen either within the flushing channel, resulting in a lateral expansion of the channel, or along the shore of the reservoir. The expansion of the flushing channel goes together with an increase of flushed-out sediments from the reservoir. For a better prediction of the occurrence of possible geotechnical bank failures two aspects need to be taken into

account: the representation of soil parameters, which in this case govern the occurrence of geotechnical failure, and information on the location of the lowering of the embankment. For applying a full 3D hydro-morphodynamic model for the reservoir flushing operation of the Bodendorf reservoir (Haun et al., 2012; Olsen and Haun, 2018; 2020), information on sensitive parameters and on the location of slides could be gained. Figure 107 shows the results of the simulations with (a) the default values, obtained by the calibration, (b) a decrease of the cohesion from 1,000 Pa to 500 Pa and (c) an increase of the cohesion from 1,000 Pa to 10,000 Pa. The blue areas represent a lowering of the terrain in case geotechnical failure happens, and the red areas describe depositions at the foot of the slide. The results of the hydro-morphodynamic numerical model show that the slides occur more frequent close to the weir. Hence, the investigations can be limited to this part of the reservoir. The comparison of the slide patterns in figure 107a to c indicate that geotechnical failures occur in similar areas, but with a different magnitude. Consequently, the field measurements regarding cohesion of the soil can be limited to those areas, which lead to a reduction of measurement spots, time and costs.

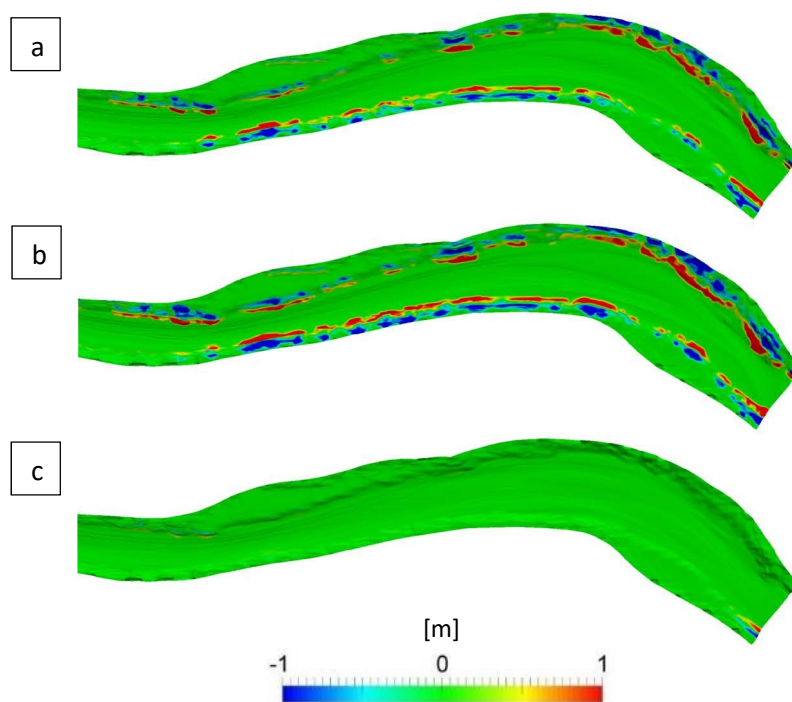


Fig. 107: Geotechnical bank failure (blue) and subsequent depositions (red) during the flushing of the Bodendorf reservoir in Austria for a simulation with (a) default values; (b) a decrease of the cohesion from 1,000 Pa to 500 Pa; (c) an increase of the cohesion from 1,000 Pa to 10,000 Pa (Olsen and Haun, 2020; modified).

9.3 Selection of a temporal resolution of measurements based on results from hydro-morphodynamic numerical models

During the detailed design of a measurement campaign, the spatial and temporal resolution of measurement hot-spots need to be defined. Selecting an optimum temporal resolution of

measurements is not a trivial task, as it depends on the one hand on the method and on the other hand on the boundary conditions. Basically, as many measurements as necessary should be conducted (high temporal resolution), to cover all important processes, at the same time as few as possible, to reduce labor and costs. Very often practical reasons need to be considered, such as the maximum possible measurement duration of an instrument or the availability of personnel.

Hydrodynamic and hydro-morphodynamic models are able to provide continuous time series of hydraulics, sediment transport and morphological changes. Hence, the results of the model provide accurate knowledge on the occurring hydro-morphodynamic conditions of the surveyed domain, with a high temporal resolution. With this knowledge the required intervals of measurement campaigns (e.g., for evaluating bed levels as a result of reservoir sedimentation), but also the interval of single measurements during a monitoring campaign can be selected and optimized (e.g., the time interval for suspended sediment concentrations during reservoir flushing).

Selection of a temporal resolution of bed load transport measurements at the river Saalach, located at the German - Austrian border, based on hydro-morphodynamic numerical modeling

Hydro-morphodynamic models are predestined for long-term simulations of hydro-morphodynamic processes in rivers and reservoirs. However, depending on the architecture of the code, the dimensionality, the spatial extension of the modeling domain, the grid resolution, the number of involved processes and many other parameters, the simulations may result in long computational times. To reduce the simulation time of hydro-morphodynamic models, often only the part of the flow hydrograph is modelled that is relevant for morphological bed changes. Beckers et al. (2015) and Sadid et al. (2016) investigated two characteristic flow hydrographs of the river Saalach to specify a discharge threshold, at which bed load transport initiates. Hence, only discharge rates above this threshold value were used for further simulations. One of the two hydrographs (2005) is presented in figure 108a. A sensitivity analysis with a linearly increasing flow hydrograph as boundary condition was performed. Additionally, at six cross sections the bed load transport rates were investigated to analyze the initiation of motion as a function of discharge (figure 108b). It shows that bed load transport starts around $150 \text{ m}^3/\text{s}$. Consequently, the hydrograph can be reduced to discharge values above $150 \text{ m}^3/\text{s}$, without affecting the accuracy of the model results. However, a more detailed analysis of regions shows that bed load transport is already initiated at discharge rates between 100 and $130 \text{ m}^3/\text{s}$ for fine bed material, and between 150 and $180 \text{ m}^3/\text{s}$ for coarse material (Sadid et al., 2016). This characterizes the spatial variation of hydraulics, but also of the sediment characteristics along the simulation domain.

Bed load transport measurements are often conducted mainly during lower discharge rates as existing measurement methods are difficult to apply during higher discharge rates (see chapter 6.3.2 *Bed load transport measurements*). Direct methods, e.g., bed load samplers from bridges, or indirect methods, such as moving ADCP measurements, are influenced by floating debris and waves and are, due to safety reasons, not performed during flood events. Also most tracer methods are not able to deliver reliable information on the transport path of single particles during such events. The results of the hydro-morphodynamic numerical model give an indication on the threshold discharge, above which measurements are required. Related to the high variability of e.g., the grain-size distribution or the geometry in a river section, the high spatial resolution of the numerical model simulations can provide details on the initiation of bed load transport for the different areas. Additionally, the numerical model generates results of the amount of transported bed load through selected sections, as a function of the discharge. Based on this information the selection of appropriate measurement equipment is feasible (e.g., sampler type and size), and an indicator is given on the required measurement intervals. With respect to the spatial resolution of the modeling results, it is even possible to recommend where to place the sampler along the river section to obtain reliable results. As for sampling suspended sediments an isokinetic correct sampling is required, the simulated flow velocities from the numerical model enable the selection and the use of an appropriate sampling device to ensure accurate measurements.

As a consequence, future measurements of bed load transport in the river Saalach should be conducted dependent on the region above the obtained threshold values. Additional measurements below the threshold discharge values ensure the reliability of the data. Nevertheless, the majority of samples should be taken above this threshold value.

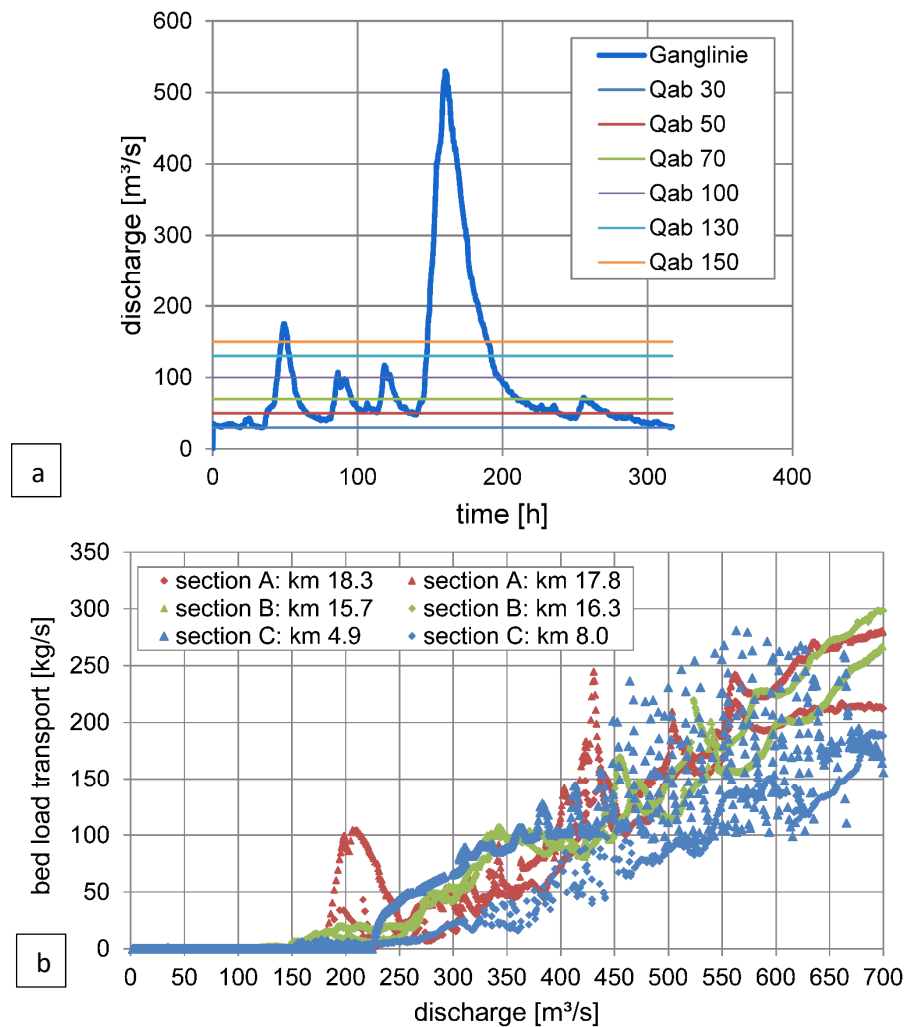


Fig. 108: (a) selected hydrograph from 2005 considering different threshold discharges to investigate the initiation of bed load transport (Beckers et al., 2016); (b) bed load transport rates for a linearly increasing flow hydrograph at six different river sections along the river Saalach (Beckers et al., 2016).

Selection of a temporal resolution for downstream suspended sediment measurements during the flushing of the Schwarzenbach reservoir in Germany, based on hydro-morphodynamic numerical modeling

During reservoir flushing usually a monitoring of the downstream occurring suspended sediment concentrations is performed (see chapter 5.4.3 *Reservoir flushing*). This facilitates the calculation of the total amount of flushed-out sediments, based on these measurements. However, when performing a flushing operation, which is sustainable as well as ecologically friendly, the downstream concentrations shall be below given thresholds. Therefore, the flushing operation is controlled based on downstream measured suspended sediment concentrations. As soon as critical values are reached (often warning limits are given) measures need to be initiated, such as closing the flushing gates and increasing the water level in the reservoir again. Hence, an almost continuous measurement series is required. Indirect

measurement methods, which are able to measure continuously, such as turbidity sensors, require an in-depth calibration, based on the local conditions from the flushing itself. In such cases often physical sampling is performed in combination with direct measurements e.g., by “Imhoff-cones”. Thereby no subsequent laboratory analysis is necessary and suspended sediment concentrations are available within minutes. However, the temporal resolution of such measurements is smaller compared to indirect methods, as a result of the high work load. Subsequently, from a practical point of view it is not feasible to perform such measurements during the whole flushing operation (often days) with a high temporal resolution. As a consequence, during periods with high sediment concentrations the temporal resolution of measurements is higher compared to periods in which low concentrations are expected.

A result of the simulations of the flushing operation of the Schwarzenbach reservoir is the detailed information on the amount of flushed-out sediments. Figure 109 shows the cumulated sediment outflow from the reservoir during a flushing with full drawdown. A sensitivity analysis investigated several domain-specific parameters to obtain differences in the amount of eroded sediments. Figure 109 shows that periods can be identified, in which a higher amount of sediments is eroded in a comparably smaller period, independently from the varied domain-specific parameters.

Based on the simulation results five different periods can be identified. Around simulation hour 120 (still above minimum operation level) bed erosion is initiated and a first increase in the flushed-out sediments is detected (P1). In period P2 the water level is lowered until free flow conditions occur after 170 hours. Here the strongest increase in the amount of flushed-out sediments occurs (P2). Subsequently, still an increase of flushed-out sediments is observed (P3). However, the gradient is not that steep compared to period P2. During period P4 the water level increases again (starting from hour 243) and the amount of eroded sediments decreases until the water level has reached the minimum operation level again (hour 264). Afterwards no erosion is observed anymore (P5). With this information from the numerical model different resolutions of the conducted measurements can be specified, which indicates that the highest resolution is necessary in period P2, followed by period P3. Period P1 and P4 show a comparably lower increase in the amount of flushed-out sediments, resulting in a much lower required measurement frequency. During the drawdown period (P2), the steepest gradient for the increase of flushed-out sediments is observed. The reason is that the wetted perimeter is much larger compared to the period of free flow conditions (P3) and where erosion happens only within the wetted flushing channel.

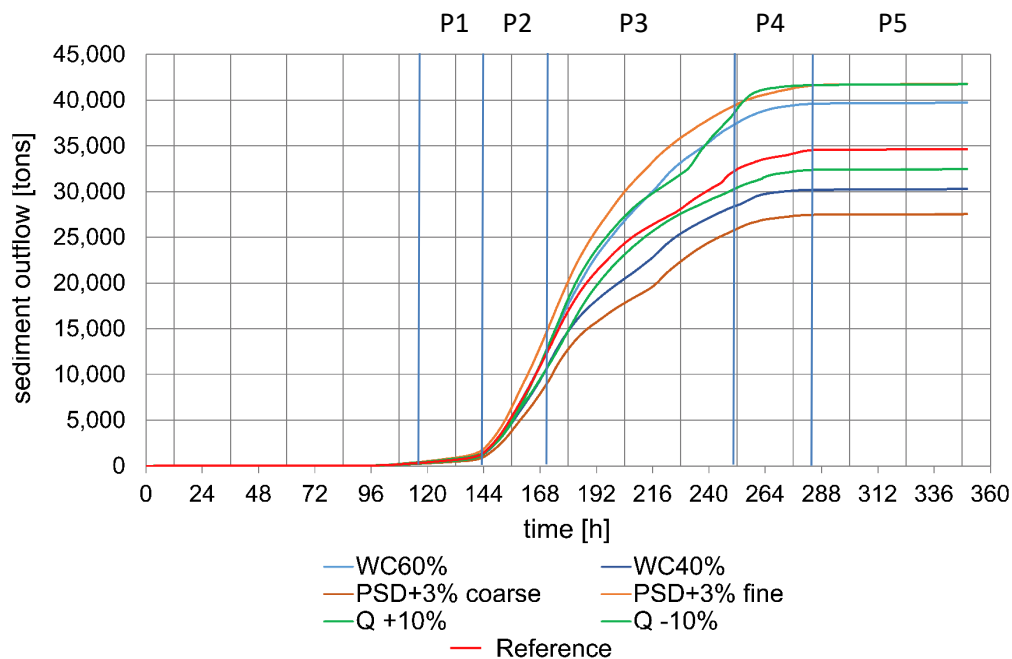


Fig. 109: Simulated cumulated sediment outflow from the Schwarzenbach reservoir during a reservoir flushing with full drawdown for different varied parameters.

Selection of a temporal resolution for bed level measurements of the Bodendorf reservoir in Austria, based on hydro-morphodynamic numerical modeling

The Bodendorf reservoir in Austria was built between 1979 and 1982 and had an initial storage capacity of 900,000 m³. A survey in 1994 showed that approximately 640,000 m³ of the storage capacity was lost due to sedimentation (Badura, 2007). Badura (2007) calculated that the complete storage volume would be lost by the year 2000, means only 18 years after impoundment. As a direct consequence, an active sediment management, by means of regular flushing operations, was initiated in 1996 (Badura, 2007). During the first five flushing operations in 1996, 1999, 2002, 2004 and 2006 in total approximately 460,000 m³ of deposited sediments were re-mobilized and flushed to the downstream river stretch (Hartmann et al., 2009). Since 2002, equilibrium conditions of the reservoir bed can be observed as a result of the implemented sediment management strategy. The bed levels measured by echo sounders in 2006 are shown in figure 110a. Figure 110b represents the thalweg of the reservoir for the years 1980, 1994, 1996, 1999 and 2002. A clear increase of the bed levels along the thalweg can be seen between 1980 and 1994. However, also the success of the flushing operations in 1996, 1999 and 2002 becomes visible: close to the dam and at the head of the reservoir almost equilibrium conditions could be reached as a result of the three flushing operations.

Meanwhile for many reservoirs hydro-morphodynamic models are setup ahead of their construction to simulate reservoir sedimentation and to predict the success of sediment management strategies. Therewith, knowledge on the progressive reservoir sedimentation

can be gained with a high spatial and temporal resolution. Hence, regular field surveys and their corresponding interval can be chosen based on the results from the numerical model. For the Bodendorf reservoir the first survey of bed levels was conducted 12 years after the impoundment and showed large depositions. Presumably, hydro-morphodynamic models could have helped to optimize the time period between the impoundment of the reservoir and the first measurements. In general, a first field survey short after the impoundment of the reservoir contributes to prove the reliability of the numerical model and if necessary the model can be re-calibrated. Specifically, in the case of the Bodendorf reservoir an earlier performed survey, based on the predictions of a hydro-morphodynamic numerical model, would have enabled an implementation of countermeasures already at an early stage.

From the echo sounder surveys of the Bodendorf reservoir, a clear difference between the loss of storage capacity during dry years and wet years can be seen. Compared to the mean yearly sediment input of about 53,000 m³, in 2003 (dry year) the sedimentation in the reservoir was only in the range of 64 % of the average rate. On the opposite, the year 2005 (wet year) contributed with 147 % of sedimentation compared to the mean yearly sediment input of the reservoir (Hartmann et al., 2009). Considering these variations, the temporal resolution of surveys can be adapted based on the hydrological conditions. As for the Bodendorf reservoir a 2D as well as a 3D hydro-morphodynamic model exists (Badura, 2007; Haun et al., 2012), it is feasible to optimize the temporal resolution of future bed level measurements.

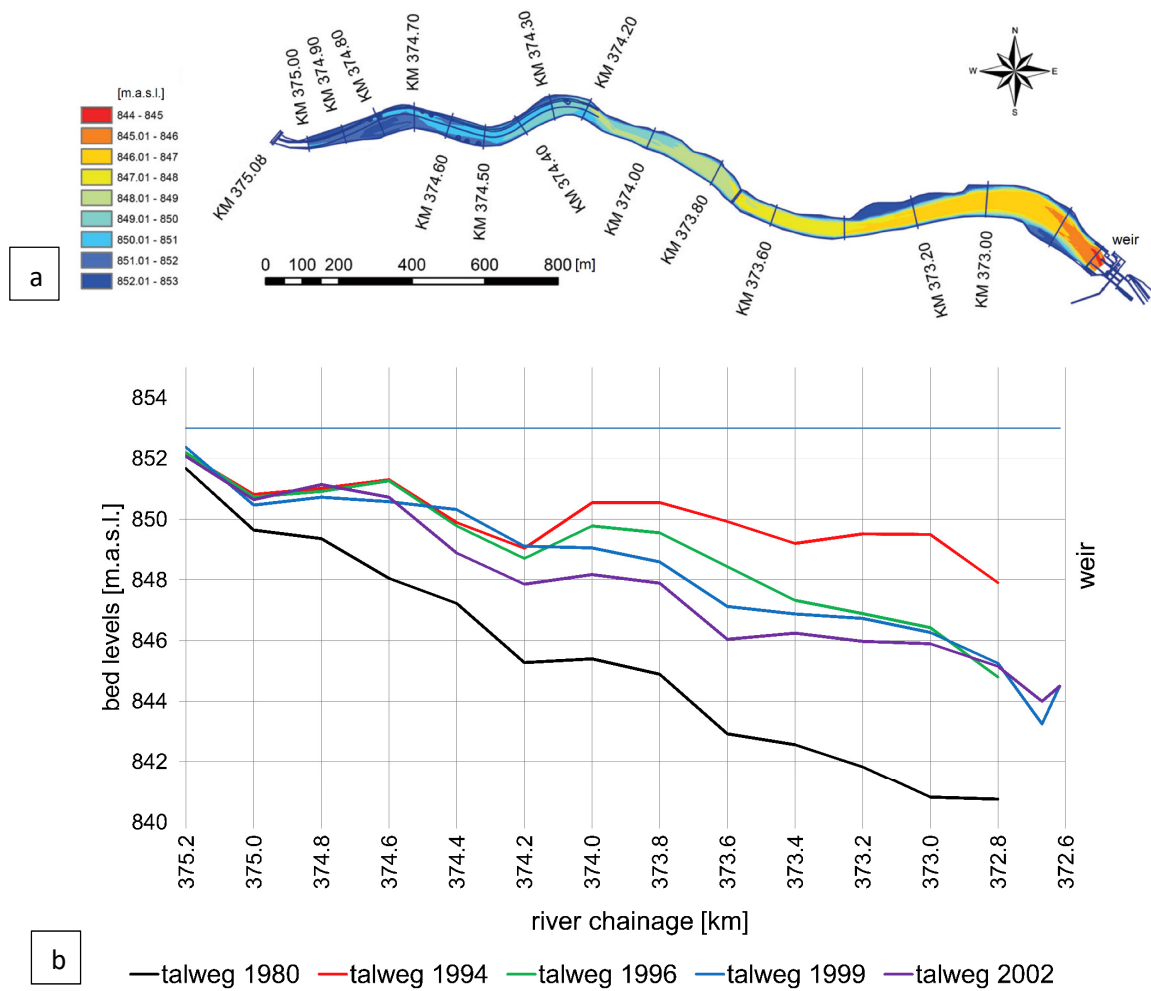


Fig. 110: (a) measured bed levels of the Bodendorf reservoir in Austria in 2006 after the flushing operation (Badura, 2007); (b) measured thalweg of the Bodendorf reservoir for the years 1980, 1994, 1996, 1999 and 2002.

10 SUMMARY AND CONCLUSIONS

The storage of water in reservoirs is vital for humans and for our society, as in many areas in the world water is not available on demand. Therefore, reservoirs have been constructed by mankind since ancient times (known from 5,000 BC) to store water for a multitude of different purposes. The main focus in storing water has been set on ensuring drinking and irrigation water, but due to the rising efforts in the renewable energy sector, the share of electricity produced by hydropower will increase in the future. In addition, reservoirs have become a momentum for the construction of navigable waterways, flood protection as well as for recreational activities and tourism, making them to multipurpose structures. In particular, those reservoirs providing access to clean water and green energy will become even more important in the near future due to demographic changes (the world population is expected to reach 9.8 billion in 2050) and climate changes (e.g., weather and precipitation extremes) as well as the ongoing globalization (e.g., intensified and unsustainable use of water).

However, the construction of dams and reservoirs is a severe anthropogenic intervention in the natural river course and leads inevitably to a disturbance of the continuity of water, sediments, ships, but also living organism (e.g., fish migration). As a consequence of the construction of dams and weirs, progressive reservoir sedimentation occurs, which reduces the available storage volume of reservoirs and reduces the ability to store water in case of flood events or to provide water in periods of low water availability. The average annual loss of storage volume due to sedimentation is about 1 % on a global scale. Regional differences indicate an estimated half lifetime of reservoirs between 50 years in Central Asia and 167 years in South-East Asia (White, 2001). However, the expected lifetime of some reservoirs in China is even only about 22 years (Fan and Morris, 1992).

Reservoir sedimentation as a serious problem in dam engineering, but also for a sustainable development of our society, was identified in the 20th century. The result has been an intensification of investigations on reservoir sedimentation and possible countermeasures starting from the 1960's. Studies on reservoir sedimentation start generally with the exploration of the catchment area, the origin of sediments. As a result of denudation processes in the catchment, such as weathering, erosion and mass wasting, sediments are produced in the so-called production zone. Depending on the given boundary conditions, eroded sediments re-settle either within the catchment or reach the transfer zone (rivers in the catchment), where they are transported as fluvial sediments. Often the sediment yield, as the amount of sediments measured at the intersection to the transfer zone and divided by the catchment area given on a yearly basis, is used to classify a catchment with respect to the production of sediments. It is assumed that worldwide around 20×10^9 tons/a of sediments are transported by rivers to the oceans (Milliman and Syvitski, 1992; Walling and Webb, 1996; Milliman and Farnsworth, 2011). However, anthropogenic structures in rivers lead to changes in flow velocities, turbulences and bed shear stresses and alter the transport process of

sediments. As a consequence, the dynamic equilibrium conditions of the natural rivers are interrupted, resulting in a change of morphodynamics. In reservoirs a transport-limited-system develops, as a direct result of the changes of flow characteristics. This developed system results in progressive reservoir sedimentation at this newly occurring depositional zone. Beside the loss of storage volume in the reservoir, also other effects, mainly on the environment, need to be considered when investigating reservoir sedimentation. Examples are the accumulation of organics and a subsequent production of greenhouse gases or the accumulation of pollutants and micro plastic particles, which are closely linked to reservoir sedimentation. However, not only upstream, but also downstream of a dam changes of the originally existing dynamic equilibrium conditions occur. At the downstream reach a supply-limited-system develops, as sediment is trapped within the reservoir. Hence, it is important to gain a holistic overview of the whole river system when investigating reservoir sedimentation (from large to small scales), additionally an understanding of the mechanism of sediment transport and river morphology is required to plan and implement sustainable sediment management strategies.

Sediment management strategies for reservoirs need to be developed if a negative influence on the lifetime of the reservoir, on its safe operation, but also on the downstream river reach is expected. Reservoir management strategies should be developed already in an early design phase, as at this time, adaptations in the design are still possible. For example, at an early planning stage the hydraulic structures of a dam can be adapted (e.g., the construction of bottom outlets with sufficient capacity for reservoir flushing), but also that the operation plan can be customized in accordance to the findings from conducted studies regarding expected sedimentation scenarios. Therefore, the aim of a holistic reservoir management concept is to reduce reservoir sedimentation, to minimize the associated loss of storage volume and to limit the unfavorable downstream effects, such as a negative impact on the environment. In addition, also legal aspects and economic considerations need to be taken into account when implementing sustainable reservoir management strategies.

The selection of a suitable sediment management strategy for a reservoir is not trivial as each reservoir is unique (e.g., shape, volume), but also due to the hydrological conditions as well as the characteristics of the catchment and subsequently the eroded sediments. Several approaches exist to overcome the problems of reservoir sedimentation. They include methods, which try to reduce the amount of sediment inflow into the reservoir from upstream (e.g., by soil conservation or check dams), or to divert the sediment laden flow through or around the reservoir (e.g., sediment bypass tunnels or turbidity current venting). Probably the most challenging sediment management approach is the handling of already deposited sediments and to recover lost storage volume (e.g., by dredging or reservoir flushing). Beside the technical feasibility, which is e.g., depending on the erosion threshold of deposited sediments, also economical, legal and environmental aspects need to be considered, which may limit the success of the management strategy. In case of reservoir flushing occurring

downstream suspended sediment concentrations will be limited to avoid a negative impact on the ecology. A reliable prediction of reservoir sedimentation and the success of different reservoir management strategies is based on two important pillars. These are accurate and sufficient measurement data as well as reliable hydro-morphodynamic prediction models.

Sediment transport measurements are the basis to understand ongoing processes in sediment transport and morphological changes and subsequently reservoir sedimentation. Hence, it is important to hold or obtain sufficient measured data, being able to answer the question whether reservoir sedimentation plays a vital role in influencing the lifetime and a safe operation of the reservoir. Investigations on reservoir sedimentation start with reliable measurements of sediment transport, well before the reservoir is constructed. Further, an important aspect is the assessment of the characteristics of the particles (e.g., grain-size distribution). Then, the estimation of reservoir sedimentation and an adequate implementation of reservoir management strategies are possible before the dam construction. After reservoir impoundment, additional measurements help to understand the hydraulic and morphological processes within the reservoir. Moreover, the evidence whether the occurring reservoir sedimentation corresponds to the predictions during the design phase can be proven. In case sediment management are already realized, a judgement on the success of the implemented measures is possible.

Due to the development of advanced measurement methods, an increase in temporal and spatial data resolution is possible, providing new insights into sediment transport and morphological development. An example are bed load measurements based on acoustics, which enable a high temporal resolution as well as a much higher spatial resolution, compared to common samplers or pit traps. Recent developments in the investigation of bed material characteristics enable the quantification of particle size distribution and the erosion threshold of cohesive sediments. This supports the optimization of predictions of reservoir sedimentation, but also the implementation of sustainable sediment management strategies for reservoirs, e.g., based on hydro-morphodynamic prediction models.

Hydro-morphodynamic models are meanwhile frequently applied for simulating hydro-morphodynamics of complex environmental systems. Models in all three dimensions (1D, 2D and 3D) are applied for predicting the impact of sediments on the life time of reservoirs and to develop sustainable reservoir management strategies. The choice of the model dimension depends, on the one hand, on the spatial and temporal extension of the modeling domain (e.g., for studies of the whole river systems a lower dimensionality is used). On the other hand, the type of information, which shall be obtained (e.g., whether only the trapping efficiency of the reservoir is required or detailed knowledge on the deposition pattern) is of importance. The temporal resolution of hydro-morphodynamic models allows simulating long-term depositions, but also effects for single events, such as floods or occurring density currents. The benefit of models with a high dimensionality (2D and 3D) and a subsequent high spatial

resolution is a detailed insight into changes of the hydromorphology as a result of the construction of the dam and the reservoir. Sensitive areas of the reservoir can be allocated, which is an important information for implementing future management strategies. The success can be assessed and recommendations on optimization can be made. Even if further development in the codes is still necessary, results can be optimized by an in depth calibration and validation of the hydro-morphodynamic numerical models. Nevertheless, the availability of accurate data is the basis for setting up, calibrating and validating numerical models in general, and for performing reliable prediction simulations in particular.

Measurements as basis for setting up reliable hydro-morphodynamic prediction models

The required measurement data for a prediction model can be grouped in geometrical data (bathymetric and topographic data), information on hydraulic structures as well as up- and downstream boundary conditions. Due to recent developments in measurement techniques high resolution geometrical data, based on LIDAR, Structure from Motion or Side Scan Sonars, can be obtained. However, the temporal resolution may often be a limiting factor, due to the high costs. In addition, hydro-morphodynamic models need data on sediment transport and the characteristics of sediments, to set up simulations of reservoir sedimentation and sediment management. Data on grain-size distribution of bed sediments and on the amount of in- and outflowing sediments is for most cases not available, or only with a low temporal and spatial resolution.

As a result, models with a lower dimensionality are often used, to reduce the computational effort and the required quantity of input data. However, a reduction of the model dimension does not lead to a reduction of the quantity or even the quality of input data. An example is the spatial resolution of the bathymetry, where the resolution can be reduced while using a 1D numerical model (cross sectional data is used), but not for a 2D numerical model (areal data is used). Hence, even for a 1D model, detailed information on sediment characteristics is required for each cross section, which is in most cases not available, or only with a low temporal resolution. To overcome the challenges associated with a reduction of dimensionality and with limited available data, a subsequent calibration, validation and sensitivity analysis is necessary.

Sensitive parameters (domain-specific as well as model-specific parameters) can be adjusted in a way that the simulated results match the observed values in nature. Beside the limitations given by the simplified structure of the model itself, the sensitive parameters are also a result of the stochastic behavior of fluvial systems. An in-depth calibration and validation of hydrodynamic models relies on data of water level fixations, measured flow velocities and the duration of flood inundation. Hydro-morphodynamic models use in addition the sediment balance for specific modeling sections, bed level changes, sediment transport rates or changes in grain-size distribution. While calibration and the validation are used to compare the model

performance with measured data, an additionally performed sensitivity analysis gives detailed information on the sensitivity of model and domain-specific parameters. As well a potential spatial variety of the parameters can be obtained and an insight into the temporal behavior of parameters is possible.

Hydro-morphodynamic prediction models used as decision basis for implementing measurements

Accurate field measurements are required to gain a deep understanding of the system, when investigating hydro-morphodynamic processes in open water environments. Hydro-morphodynamic models are on the one hand able to specify sensitive domain-specific parameters. On the other hand, they provide information on the spatial extent and the temporal scales of hydro-morphodynamic processes. As a direct consequence, calibrated and validated hydro-morphodynamic prediction models can be used as a decision basis for implementing future measurements and monitoring.

Based on several sediment related studies, a novel approach is presented in this thesis, on how future measurement campaigns can be planned. As a result of an in-depth sensitivity analysis of hydro-morphodynamic numerical models, domain-specific parameters, with a high uncertainty on the simulation results, can be selected. Therefore, it is possible to recommend on which parameters shall be the focus for future measurements. Also a ranking based on the introduced uncertainties is feasible. The spatial resolution of the measurements and of hot-spots may vary within larger domains. Finally, it is possible to select the temporal resolution for measurements on the basis of the simulation results and to decide whether parameters can be obtained during single measurement campaigns or whether a long-term monitoring is required. The availability of such detailed information enables the design of even complex measurement campaigns.

By applying this hybrid modeling approach, it is feasible to combine the advantages of both, hydro-morphodynamic numerical modeling and advanced field measurements. Where usually the selection of in-situ investigated parameters as well as their temporal and spatial resolution, are based on empirical knowledge, hydro-morphodynamic models provide the possibility of an objective selection. Thus, future measurements and monitoring can be implemented and adapted in a way to obtain better and deeper knowledge of the system, to optimize sediment management strategies and to develop customized operation plans for reservoirs.

Conclusions

As a result of an increasing demand on storing water, sustainable reservoir management will become more and more important in the future. Minimizing, or in the best case avoiding, the loss of storage due to sedimentation is a challenging task because each reservoir has unique

boundary conditions. Hence, not every management strategy is suitable for a given reservoir. Due to the combination of state of the art measurement methods and hydro-morphodynamic models, reservoir sedimentation can be better predicted in the future and the success of sediment management strategies can be assessed. The development of advanced measurement methods makes it possible to obtain data with a high accuracy, but also with a high spatial and temporal resolution. The combination of recent measurement approaches with reliable hydro-morphodynamic numerical prediction models, enhances a highly accurate prediction and understanding of governing processes. This opens new possibilities for an objective selection of important parameters, essential spatial domains as well as for the temporal resolution of measurements. This will finally lead to more reliable predictions about the future of reservoirs that provide water for human life, health and wealth.

Deutschsprachige Zusammenfassung

**Methoden für ein nachhaltiges Sedimentmanagement von
Stauräumen**

**In-situ Messungen und hydro-morphodynamische numerische Modelle als
Hilfsmittel für die Implementierung nachhaltiger
Sedimentmanagementstrategien**

Stefan Haun, PhD

Einleitung und Motivation

In vielen Regionen der Erde ist Wasser aufgrund des vorherrschenden Klimas nicht durchgängig verfügbar. Die Speicherung von Wasser in Stauräumen ist daher für viele Menschen, und die damit verbundene Entwicklung unserer Gesellschaft, essentiell. Bereits seit der Antike (bekannt ab ca. 5.000 v. Chr.) werden Staudämme und daraus resultierende Stauräume gebaut, um Wasser für eine Vielzahl verschiedener Zwecke zu speichern. Die Sicherstellung von Trink- und Brauchwasser ist dabei von höchster Bedeutung, vor allem in Ländern, die unter Wasserknappheit leiden oder deren Wasserressourcen aufgrund von anthropogenen Eingriffen negativ beeinflusst sind. Auch das momentane Ziel den Anteil an erneuerbare Energien zu erhöhen, bedeutet, dass der Anteil an Energie aus Wasserkraft in Zukunft weiter zunehmen muss, um dieses Ziel zu erreichen. Daher werden sich auch die notwendigen Kapazitäten zur Speicherung von Wasser in Zukunft erhöhen. Darüber hinaus wurden Talsperren und Stauräume zu einem Impulsgeber für den Bau von schiffbaren Wasserstraßen, sind essentiell für den Hochwasserschutz, aber finden auch immer mehr Anklang in der Naherholung und dem Tourismus. Die meisten der weltweit bestehenden Stauräume werden jedoch multifunktional genutzt. Stauräume, insbesondere solche die einen Zugang zu sauberem Wasser bieten, werden in naher Zukunft aufgrund des demografischen Wandels (die Weltbevölkerung wird bis zum Jahr 2050 voraussichtlich auf 9,8 Milliarden Menschen anwachsen), durch Klimaveränderungen (z. B. Wetter- und Niederschlags extreme) sowie der fortschreitenden Globalisierung (z. B. verstärkte und nicht nachhaltige Nutzung von Wasser) an Bedeutung gewinnen.

Der Bau von Talsperren und Stauräumen ist jedoch ein schwerwiegender und nachhaltiger Eingriff in den natürlichen Flusslauf und führt damit zu einer Störung der Durchgängigkeit von Fließgewässern für Sedimente, Schiffe sowie Lebewesen (z. B. im Zuge der Fischwanderung). Die im Fluss transportierten Sedimente landen sich aufgrund der reduzierten

Transportkapazität in den Stauräumen ab und führen zwangsläufig zu einer fortschreitenden Stauraumverlandung. Dadurch verringert sich die verfügbare Speicherkapazität des Stauraums und die damit verbundene Möglichkeit zur Speicherung von Wasser wird reduziert. Der durchschnittliche jährliche Verlust an Stauraumvolumen durch Stauraumverlandung beträgt weltweit etwa 1 % (Mahmood, 1987; Yoon, 1992; Bruk, 1996). Regionale Unterschiede, am Beispiel Asiens, zeigen eine deutliche Variation dieses Wertes auf lokaler Ebene. So liegt die geschätzte Nutzungsdauer von Stauräumen zwischen 50 Jahren in Zentralasien und 167 Jahren in Südostasien (White, 2001). Es wird aber auch von Stauräumen in China berichtet, bei denen die erwartete Nutzungsdauer bei nur etwa 22 Jahren liegt (Fan und Morris, 1992).

Stauraumverlandung (vom groß- zum kleinskaligen Prozess)

Der weltweit fortschreitende Stauraumverlust wurde erst im 20. Jahrhundert als ein ernstes Problem für die Speicherung und Verfügbarkeit von Wasser erkannt. Die Folge war eine Intensivierung von Untersuchungen zum Thema Stauraumverlandung sowie ab den 1960er Jahren auch zu möglichen Managementstrategien, um geeignete und nachhaltige Gegenmaßnahmen zu implementieren.

Analysen zur Stauraumverlandung beginnen in der Regel mit der Charakterisierung des Einzugsgebietes, das den Ursprung der Sedimente darstellt. Sedimente entstehen im Einzugsgebiet (Produktionszone) durch Verwitterung, Erosion und Massenbewegung. Abhängig von den gegebenen Randbedingungen setzen sich diese Sedimente entweder innerhalb des Einzugsgebietes wieder ab oder sie erreichen Bäche und Flüsse (Transferzone). Von hier aus werden sie als fluviale Sedimente weiter in Richtung der Ozeane (Ablagerungszone) transportiert. Die am Übergang von Produktions- zur Transferzone gemessene Menge an Sedimenten, geteilt durch die Einzugsgebietsfläche und auf einer jährlichen Basis berechnet, wird oft zur Klassifizierung eines Einzugsgebiets hinsichtlich der Produktion von Sedimenten verwendet. Studien zeigen, dass pro Jahr weltweit etwa 20×10^9 Tonnen an Sedimenten in Form von Schwebstoffen, aber auch als Geschiebe, in die Ozeane transportiert werden (Milliman und Syvitski, 1992; Walling und Webb, 1996; Milliman und Farnsworth, 2011). Dies ist dann möglich, wenn in natürlichen Fließgewässern dynamische Gleichgewichtsbedingungen herrschen. Anthropogene Bauwerke führen zu Veränderungen der Fließgeschwindigkeiten, Turbulenzen und Sohlschubspannungen und verändern dadurch den Transportprozess der Sedimente. Innerhalb eines Stauraums entwickelt sich ein transportlimitiertes System, in dem das Sedimentangebot die Transportkapazität des Fließgewässers übersteigt. Diese neuen Randbedingungen führen zu einem Erliegen des Sedimenttransports und zu fortschreitender Stauraumverlandung innerhalb dieser neu entstandenen Ablagerungszone. Erosion, Transport, Deposition und Konsolidierung sind hierbei die Hauptprozesse, die aufgrund ihrer Komplexität und der Interaktionen zwischen

den physiko-chemischen und biologischen Prozessen bislang nur teilweise analytisch beschrieben und daher oft anhand von empirischen Ansätzen abgeschätzt werden können.

Schließlich ist zu berücksichtigen, dass nicht nur oberstrom, sondern auch unterstrom eines Staubauwerkes Veränderungen der ursprünglich vorhandenen dynamischen Gleichgewichtsbedingungen auftreten. Im Unterlauf entsteht durch den Rückhalt von Sedimenten im Stauraum zwangsläufig ein angebotsbegrenztes System, da der Sedimentnachschub geringer ausfällt als vor dem Bau des Absperrbauwerks. Es ist daher wesentlich bei Studien zur Stauraumverlandung nicht nur die Mechanismen des Sedimenttransports und der Hydromorphologie zu verstehen und in die Untersuchungen mit einzubeziehen, sondern einen ganzheitlichen Ansatz zu verfolgen, der das gesamte Flussgebiet betrachtet (von der großen bis zur kleinen Skala). Nur durch diesen holistischen Ansatz können nachhaltige Sedimentmanagementstrategien erfolgsversprechend geplant und umgesetzt werden.

Sedimentmanagement von Stauräumen

Bei einem zu erwartenden fortschreitenden Stauraumverlust, ist es notwendig Sedimentmanagementstrategien zu planen und zu initiieren. Neben dem negativen Einfluss auf die Lebensdauer des Stauraums selbst, können auch Faktoren, wie ein sicherer Betrieb (z. B. Eindringen von Sedimenten in die Betriebsauslässe) oder Effekte auf ober- und unterstrom gelegene Abschnitte (z. B. reduzierte Hochwassersicherheit an der Stauwurzel oder Eintiefungstendenzen unterstrom der Staumauer) ein gezieltes Sedimentmanagement notwendig machen.

Sedimentmanagementstrategien sollten bereits in einer frühen Planungsphase entwickelt werden, da dann die Anzahl der möglichen Maßnahmen nicht durch die bestehenden Randbedingungen begrenzt ist. So kann z. B. in einem frühen Stadium die Konzeption der Talsperre angepasst werden, z. B. durch die Errichtung von Grundablässen mit ausreichender Kapazität für eine Stauraumpülung. Aber auch der Betriebsplan kann entsprechend den Erkenntnissen aus den durchgeführten Untersuchungen zur Stauraumverlandung, erstellt werden. Ziel eines ganzheitlichen Stauraumbewirtschaftungskonzeptes ist es daher, die Stauraumverlandung und den damit verbundenen Verlust an Speicherkapazität zu minimieren und negative Auswirkungen auf die ober- und unterstrom angrenzenden Fließgewässerabschnitte und die Umwelt zu vermeiden.

Die Auswahl einer geeigneten Sedimentmanagementstrategie ist jedoch nicht trivial, da jeder Stauraum in Bezug auf die gegebenen Randbedingungen, z. B. Form und Volumen des Stauraums, einzigartig ist. Zusätzlich unterscheiden sich aufgrund der unterschiedlichen Eigenschaften der Einzugsgebiete und der vorherrschenden hydrologischen Bedingungen sowohl die Qualität als auch die Quantität der in den Stauraum eingetragenen Sedimente. Im Allgemeinen gibt es verschiedene Ansätze, um die Stauraumverlandung und die damit

verbundenen Auswirkungen auf den Betrieb sowie die ober- und unterstrom gelegenen Flussabschnitte zu minimieren oder zu vermeiden. Zu diesen Ansätzen gehören Methoden, die den Sedimenteintrag aus dem Einzugsgebiet reduzieren (z. B. durch aktiven Bodenschutz im Einzugsgebiet oder den Bau von Geschiebe- oder Vorsperren) oder die ankommenden Sedimente durch- oder um den Stauraum herumleiten (z. B. durch Sedimentbypass-Tunnel oder das Durchschleusen von Trübeströmungen). Ein weiterer und wahrscheinlich der anspruchsvollste Ansatz für ein aktives Sedimentmanagement stellt die Remobilisierung angelandeter Sedimente und die damit verbundene Reaktivierung von bereits verlorener Speicherkapazität dar (z. B. durch Nass- und Trockenbaggerungen oder eine Stauraumpülung).

Wesentliche Aspekte einer nachhaltigen und holistischen Sedimentmanagementstrategie sind neben der technischen Machbarkeit auch wirtschaftliche, rechtliche und ökologische Überlegungen. Diese Aspekte können sogar den Erfolg der technisch vielversprechendsten Managementstrategie begrenzen. Bei einer Stauraumpülung müssen beispielsweise während der Maßnahme unterstrom auftretende Schwebstoffkonzentrationen begrenzt und ein minimaler Sauerstoffgehalt eingehalten werden, um negative Auswirkungen auf die Ökologie zu vermeiden.

Eine zuverlässige Prognose, nicht nur bezüglich des Verlustes der Speicherkapazität des Stauraums, sondern auch der technischen Machbarkeit verschiedener Sedimentbewirtschaftungsstrategien basiert auf zwei wichtigen Säulen; einerseits auf genauen und zeitlich sowie räumlich hoch aufgelösten Messdaten der transportierten Sedimente und der sich ändernden Sohlenlage im Stauraum und andererseits auf zuverlässigen hydro-morphodynamischen Prognosemodellen.

Hydro-morphodynamische Messungen

Messungen des Sedimenttransports sowie lang-, mittel- und kurzfristiger morphologischer Prozesse im Fließgewässer und im Stauraum, bilden die Grundlage, um den zukünftigen Verlust von verfügbarer Speicherkapazität des Stauraums abschätzen und beurteilen zu können.

Für ein proaktives Stauraummanagement ist es unumgänglich schon vor dem Bau des Absperrbauwerkes ausreichende Messdaten des vom Staubauwerk noch unbeeinflussten Fließgewässers zu erheben. Ein wesentlicher Aspekt ist dabei neben der Erfassung des Sedimenttransports (unterteilt in Schwebstoffe und Geschiebe) auch eine Beurteilung der Qualität.

Sobald der Stauraum eingestaut ist, helfen regelmäßig durchgeführte Messungen zu einem zusätzlichen Verständnis der vorherrschenden hydraulischen und morphologischen Prozesse im Stauraum. Anhand von z. B. Sohlvermessungen zeigt sich ob die tatsächliche Menge an angelandeten Sedimenten den Abschätzungen aus der Planungsphase entspricht. Zusätzlich

können aber auch Aussagen bezüglich der räumlichen Verteilung der Anlandungen getroffen werden, was speziell für das aktive Sedimentmanagement von großer Bedeutung ist. Wurde bereits vor dem Einstau ein solches Sedimentmanagement initiiert, ist auch eine Beurteilung des Erfolges der implementierten Maßnahmen durch wiederkehrende Sohlagenvermessungen möglich. Falls eingesetzte Maßnahmen zu keinem nachhaltigen Erfolg führen, werden diese auf Basis der Messdaten adaptiert oder zusätzliche Maßnahmen ergriffen. Aber auch für verschiedene Betriebszustände ist die Erhebung von Daten, teilweise auch als kontinuierliche Messreihen, notwendig oder vorgeschrieben. So haben während der Stauraumpülung unterstrom des Stauraums durchgeführte Schwebstoffmessungen nicht nur das Ziel die Menge an ausgespülten Sedimenten zu erfassen, sondern auch den Prozess selbst zu überwachen und wenn notwendig diesen zu adaptieren.

Durch die stetige Weiterentwicklung der Messmethoden, z. B. basierend auf Akustik oder Optik, ist neben einer Charakterisierung der Sedimente auch eine Erhöhung der zeitlichen und räumlichen Auflösung der Messungen möglich. Ein Beispiel hierfür ist die Messung des Geschiebetransports mit Hilfe akustischer Messmethoden, die im Vergleich mit den in der Vergangenheit eingesetzten mobilen Fangkörben oder stationären Geschiebefallen neben einer hohen zeitlichen auch eine wesentlich höhere räumliche Auflösung der Messungen bewerkstelligen. Dies ermöglicht einen detaillierteren Überblick bezüglich der morphologischen Prozesse. Neueste Methoden zur Untersuchung von im Stauraum angelandeten Sedimenten erlauben mittlerweile eine exakte Quantifizierung der Erosionsstabilität angelandeter kohäsiver Sedimente und damit auch Erkenntnisse zu den verschiedenen Erosionsprozessen. Mit Messdaten in einer solch hohen räumlichen und zeitlichen Auflösung, in Kombination mit hydro-morphodynamischen numerischen Prognosemodellen, ist es möglich Vorhersagen zur Stauraumverlandung zu verbessern, ein bestehendes Sedimentmanagement zu optimieren und zukünftig nachhaltige Stauraummanagementstrategien zu initiieren.

Hydro-morphodynamische numerische Modellierung

Aufgrund ihrer stetigen Weiterentwicklung und der gestiegenen Rechenleistung finden numerische Modelle immer öfter Anwendung in der Simulation von verschiedensten Prozessen in Wasser- und Umweltsystemen.

Durch die Implementierung von Algorithmen zur Modellierung von hydro-morphodynamischen Prozessen ist es möglich numerische Modelle zur zukünftigen Simulation der Stauraumverlandung einzusetzen. Modelle, in allen drei Dimensionen (1D, 2D und 3D), dienen nicht nur der Vorhersage des Einflusses der Stauraumverlandung auf die Lebensdauer von Stauräumen, sondern finden auch Verwendung in der Planung und Optimierung von Stauraummanagementstrategien. Die Wahl der Modelldimension hängt dabei wesentlich von der räumlichen Ausdehnung des Untersuchungsabschnittes ab, z. B. wird für die Modellierung eines gesamten Flusssystemes eine geringere Dimensionalität verwendet

als für kleinräumige Detailausschnitte. Die Wahl der Modelldimension hängt aber auch von der Art der Ergebnisse ab, die durch das numerische Modell erzeugt werden sollen, z. B. ob nur das Sedimentationsvermögen des Stauraums als Ergebnis der Studie benötigt wird oder detaillierte Kenntnisse über das Anlandungsmuster innerhalb des Stauraums. Durch die hohe zeitliche Auflösung hydro-morphodynamischer numerischer Modelle können nicht nur Langzeitsimulationen (gewöhnlich mit einer niedrigeren Modelldimension), sondern auch Einzelereignisse und die daraus resultierenden Prozesse, wie z. B. Hochwasserereignisse und mögliche auftretende Dichteströme, modelliert werden (dies erfordert eine hohe Modelldimension). Simulationsergebnisse aus Modellen mit hoher Dimensionalität (2D und 3D) und entsprechend hoher räumlicher Auflösung ermöglichen einen detaillierten Einblick in die Veränderungen der Hydromorphologie als Folge des Baus einer Talsperre und des dazugehörigen Stauraums. Dadurch können sensible Bereiche des Stauraums identifiziert und in der Planung und Umsetzung zukünftiger Managementstrategien berücksichtigt werden. Darüber hinaus sind auch Informationen über die Sedimentqualität, wie etwa die Korngrößenverteilung der Anlandungen, verfügbar.

Wesentlich dafür ist jedoch die Verfügbarkeit von Messdaten mit einer hohen zeitlichen und räumlichen Auflösung, die die Grundlage für die Erstellung, Kalibrierung und Validierung hydro-morphodynamischer numerischer Modelle darstellen.

Messdaten als Grundlage für den Aufbau hydro-morphodynamischer Prognosemodelle

Zuverlässige Prognosemodelle basieren auf qualitativ hochwertigen Messdaten, die einerseits zur Rekonstruktion der Randbedingungen verwendet werden und andererseits der Durchführung der Kalibrierung und Validierung hydro-morphodynamischer numerischer Modelle dienen.

Die erforderlichen Messdaten betreffen geometrische Daten (bathymetrische und topographische Vermessungen), Informationen zu konstruktiven Einbauten (Brückenpfeiler und Betriebsauslässe) sowie ober- und unterstrom auftretende Randbedingungen. Durch die jüngsten Entwicklungen in der Messtechnik können räumlich hochauflösende geometrische Daten, basierend auf LIDAR, Structure from Motion oder mittels Fächerecholotvermessungen erhoben werden. Allerdings ist die zeitliche Auflösung oft ein limitierender Faktor, da solche Untersuchungen aufgrund der hohen Kosten nur selten durchgeführt werden.

Daher werden häufig Modelle mit einer geringeren Dimensionalität verwendet, um einerseits den Rechenaufwand, und andererseits die benötigte Menge an Eingangsdaten zu reduzieren. Unabhängig von der Dimensionalität benötigt jedes Modell eine bestimmte Menge an Messdaten zum Aufbau, aber auch zur Kalibrierung und Validierung. Eine Reduzierung der Modelldimension führt daher nicht unmittelbar zu einer Reduktion der erforderlichen Messdaten und auf keinen Fall zu einer Reduzierung der Qualität der Eingangsdaten. Zum Beispiel kann die räumliche Auflösung der Bathymetrie bei Verwendung eines 1D numerischen

Modells (unter Verwendung von Querschnittsdaten) zwar reduziert werden kann, jedoch nicht bei der Verwendung eines 2D numerischen Modells (unter Verwendung von Flächendaten). Aber auch bei der Verwendung eines 1D Modells sind für jeden Querschnitt detaillierte Informationen bezüglich der Sedimenteigenschaften erforderlich, die in den meisten Fällen nicht oder nur mit einer geringen zeitlichen Auflösung verfügbar sind. Um die Herausforderungen, die mit einer Reduktion der Dimensionalität und mit begrenzt verfügbaren Daten verbunden sind, zu überwinden, ist eine Kalibrierung, Validierung und Sensitivitätsanalyse notwendig.

Neben den Einschränkungen, die sich aus der vereinfachten Struktur des numerischen Modells selbst ergeben, resultieren Unsicherheiten in den Modellergebnissen auch aus den in der Natur vorkommenden stochastischen Prozessen. Während der Kalibrierung und Validierung werden daher in einem ersten Schritt sowohl gebietsspezifische als auch modellspezifische Parameter, die mit großen Unsicherheiten belegt sein können, ausgewählt. Diese Parameter werden in einem zweiten Schritt so angepasst, dass für ausgewählte Zeiträume und Ereignisse die simulierten Ergebnisse mit den beobachteten Werten in der Natur übereinstimmen. Eine eingehende Kalibrierung und Validierung von hydrodynamischen numerischen Modellen wird üblicherweise mittels Hochwasseranschlagslinien (z. B. Geschwemmsellinien), gemessenen Fließgeschwindigkeiten und der Dauer der Überflutung durchgeführt. Hydro-morphodynamische numerische Modelle verwenden als Zielgröße für die Kalibrierung und Validierung zusätzlich die Sedimentbilanz für bestimmte Modellierungsabschnitte, die Sohllagenänderungen, die Sedimenttransportraten oder die Änderungen der Korngrößenverteilung.

Zur Validierung des numerischen Modells wird dieses mit denselben gebietsspezifischen und modellspezifischen Parametern, die bei der Kalibrierung festgelegt werden, für die Simulation eines zweiten und unabhängigen Datensatzes verwendet. Durch die Validierung wird sichergestellt, dass das numerische Modell nicht nur für spezifische Randbedingungen als Prognosemodell verwendet werden kann. Eine zusätzlich durchgeführte Sensitivitätsanalyse gibt außerdem einen detaillierten Einblick zu den Unsicherheiten verschiedener modell- und gebietsspezifischer Parameter. Darüber hinaus kann auf Basis der Modellierungsergebnisse eine mögliche räumliche Variation der gebiets- und modellspezifischen Parameter erkannt werden. Zusätzlich ist es möglich einen Einblick in das zeitliche Verhalten von Prozessen zu gewinnen. Daher ist die Verfügbarkeit von Messdaten mit einer hohen räumlichen und zeitlichen Auflösung ein wesentlicher Faktor bei der Erstellung eines zuverlässigen hydro-morphodynamischen Prognosemodells.

Hydro-morphodynamische numerische Modelle als Entscheidungsgrundlage für die Umsetzung zuverlässiger und nachhaltiger Messkonzepte

Hydro-morphodynamische numerische Modelle sind in der Lage sensible gebietsspezifische, aber auch modellspezifische Parameter zu identifizieren, die den Sedimenttransport und die

morphologischen Prozesse wesentlich beeinflussen. Zusätzlich sind aus den Modellierungsergebnissen Informationen zur räumlichen Ausdehnung und den zeitlichen Skalen dieser Prozesse verfügbar. Daher können kalibrierte und validierte numerische Modelle als Entscheidungsgrundlage für die räumliche und zeitliche Auflösung von zukünftigen Messungen verwendet werden. Basierend auf verschiedenen Studien, in denen hydro-morphodynamische numerische Modelle zum Einsatz kamen, wird in dieser Arbeit ein neuartiger Ansatz vorgestellt, wie zukünftige Messkampagnen basierend auf Modellierungsergebnissen objektiv geplant und durchgeführt werden können.

Als Resultat einer eingehenden Sensitivitätsanalyse von hydro-morphodynamischen numerischen Modellen ist es möglich eine Empfehlung auszusprechen, welche Parameter und in welcher Reihenfolge, im Zuge einer Messkampagne erhoben werden müssen, um Unsicherheiten in der Modellierung und zukünftigen Prognosen zu minimieren. Darüber hinaus ist es möglich die Wahl der räumlichen Auflösung der Messungen zu optimieren und Hot-Spots auf Basis der Modellergebnisse zu lokalisieren, da die Sensitivität bestimmter gebietsspezifischer Parameter innerhalb des Untersuchungsgebietes variieren kann. Zusätzlich ist es möglich die zeitliche Auflösung der Messungen auf der Basis der Simulationsergebnisse anzupassen und zu entscheiden, ob Daten während einzelner Messkampagnen erhoben werden können, oder ob eine Langzeituntersuchung (Monitoring) erforderlich ist. Die Verfügbarkeit solch detaillierter Informationen ermöglicht die Planung auch äußerst komplexer Messkampagnen und Langzeituntersuchungen.

Durch die Verwendung dieses hybriden Ansatzes ist es möglich, die Vorteile sowohl der hydro-morphodynamischen numerischen Modellierung als auch der modernen Messmethoden zu kombinieren. Während bislang die Auswahl der Messparameter sowie deren zeitliche und räumliche Auflösung überwiegend auf Basis von Erfahrungswerten erfolgte, bieten hydro-morphodynamische Modelle die Möglichkeit einer objektiven Auswahl. Darauf basierend können zukünftige Messungen so implementiert und angepasst werden, dass bessere und tiefere Kenntnisse des Systems gewonnen werden können. Damit können sowohl Sedimentmanagementstrategien optimiert als auch maßgeschneiderte Betriebspläne für Stauräume erstellt werden. Dies ermöglicht langfristig einen nachhaltigen Betrieb von Stauräumen, bei dem die Verlandung keine negativen Auswirkungen auf die zu erwartende Lebensdauer des Stauraums hat.

Schlussfolgerungen und Ausblick

Durch den steigenden Bedarf an Speicherung von Wasser und dem zeitgleichen Verlust von Stauraumvolumen durch eine fortschreitende Stauraumverlandung wird ein nachhaltiges Sedimentmanagement von Stauräumen in Zukunft ein immer wichtigerer Aspekt der Nachhaltigkeit. Den Verlust an Speicherkapazität zu minimieren, oder im besten Fall zu vermeiden, ist jedoch eine anspruchsvolle Aufgabe, da jeder Stauraum in Bezug auf die gegebenen Randbedingungen einzigartig ist. Auch die Charakteristik des Einzugsgebietes und

die zugehörige Hydrologie führen zu einer spezifischen Quantität des Sedimenteintrags in den Stauraum.

Modernste Messmethoden ermöglichen es hydro-morphodynamische Daten mit einer hohen Genauigkeit, aber auch mit einer hohen räumlichen und zeitlichen Auflösung, zu generieren. Die erhobenen Messdaten sind die Basis sowohl für Prognosen bezüglich des Sedimenttransportes und der morphologischen Prozesse als auch für den Aufbau zuverlässiger hydro-morphodynamischer Prognosemodelle. Die Kombination von Messdaten und Prognosemodellen ermöglicht es in Zukunft die Mengen an angelandeten Sedimenten in Stauräumen genauer zu prognostizieren, aber auch das Anlandungsmuster besser vorherzusagen.

Die Verwendung von hydro-morphodynamischen Modellen ermöglicht in Zukunft eine objektive Auswahl von Parametern und der relevanten räumlichen Bereiche, die im Zuge von Messkampagnen erfasst werden sollten sowie die Festlegung einer zeitlichen Auflösung der Messungen. Hydro-morphodynamische numerische Modelle können daher als Entscheidungsgrundlage für die Umsetzung zuverlässiger Messkonzepte dienen. Dies führt letztendlich zu verlässlicheren Prognosemodellen und einer besseren und nachhaltigeren Bewirtschaftung von Stauräumen.

Bibliography

- Abbaspour, K.C., Schulin, R., and van Genuchten, M.T. (2001). Estimating unsaturated soil hydraulic parameters using ant colony optimization. *Adv. Water Resour.* 24:827–841.
- Abdelhadi, M.L. (1995). *Environmental and Socio-economic impacts of erosion and sedimentation in North African Countries*. Proceedings: 6th International Symposium on River Sedimentation, New Delhi, India. Published by A.A. Balkema, Rotterdam, The Netherlands.
- Aberle, J. (2008). Measurement techniques for the estimation of cohesive sediment erosion. *Hydraulic Methods for Catastrophes: Floods, Droughts, Environmental Disasters*. Publications of the Institute of Geophysics, Polish Academy of Sciences, Wasaw.
- Aberle, J., Nikora, V., McLean, S., Doscher, C., McEwan, I., Green, M., Goring, D., and Walsh, J. (2003). Straight benthic flow-through flume for in situ measurement of cohesive sediment dynamics. *Journal of Hydraulic Engineering* 129(1): 63-67
- Abood, M.M., Mohammed, T.A., Ghazali, A.H., Mahmud, A.R., and Sidek, L.M. (2009). Review Study and Assessment for Sedimentation Models Applied to Impounding Reservoirs. *Journal of Engineering and Applied Sciences* 4(2):152-160.
- Acuña, G.J., Ávila, H., and Canales, F.A. (2019). River model calibration based on design of experiments theory. A case study: Meta River, Colombia. *Water* 11, 1382.
- Adler, M. (1993). Messungen von durchflüssen und strömungsprofilen mit einem ultraschall-Doppler gerät (ADCP). *Wasserwirtschaft* 83:192-196.
- Agrawal, Y.C., and Hanes, D.M. (2015). The implications of laser-diffraction measurements of sediment size distributions in a river to the potential use of acoustic backscatter for sediment measurements. *Water Resour. Res.*, 51:8854–8867.
- Agrawal, Y.C., and Pottsmith, H.C. (2000). Instruments for Particle Size and Settling Velocity Observations in Sediment Transport. *Marine Geology* 168:89-114.
- Agrawal, Y.C., Mikkelsen, O.A. and Pottsmith, H.C. (2011). *Sediment monitoring technology for turbine erosion and reservoir siltation applications*. Proceedings: HYDRO 2011 Conference, Prague, Czech Republic.
- Agrawal, Y.C., Whitmire, A., Mikkelsen, O.A. and Pottsmith, H.C. (2008). Light scattering by random shaped particles and consequences on measuring suspended sediments by laser diffraction. *Journal Geophysic Research* 113.
- Amos, C.L., Grant, J., Daborn, G.R., and Black, K. (1992). Sea Carousel – a benthic, annular flume, Estuarine. *Coastal Shelf Science* 34:557-577.
- Anderson, C.A. (2005). *Turbidity, in National Field Manual for the Collection of Water-Quality Data*. U.S. Geol. Surv. Tech. of Water Resour. Invest., Book 9, U.S. Geol. Surv., Reston, United States of America.
- Andrews, E.D. (1983). Entrainment of gravel from naturally sorted riverbed material: *Geological Society of America* 94:1225-1231.
- Annandale, G. (2013). *Quenching the thirst-sustainable water supply and climate change*. Charleston, SC: CreateSpace.

- Annandale, G.W. (1987). Reservoir Sedimentation. *Developments in Water Science* 29:1-221.
- Army Corps of Engineers Northwestern Division (2006). *Missouri River Mainstem Reservoir System, Master Water Control Manual: Missouri River Basin*. United States Army Corps of Engineers, U.S.
- Asbeck, M., Drüppel, S., Skindelines, K., and Stein, M. (2012). *Vermessung und Geoinformation*. Fachbuch für Vermessungstechniker und Geomatiker. Hrsg.: Michael Gärtner. Gärtner, Solingen, Germany. (in German)
- Ashley, T.C., McElroy, B., Buscombe, D., Grams, P.E., and Kaplinski, M. (2020). Estimating bedload from suspended load and water discharge in sand bed rivers. *Water Resources Research* 56: e2019WR025883.
- Ashraf, M., Kahlowan, M.A., and Ashfaq, A. (2007). Impact of small dams on agriculture and groundwater development: A case study from Pakistan. *Agricultural Water management* 9(2): 90-98.
- Atkinson, E. (1996). *The Feasibility of Flushing Sediment from Reservoirs*. TDR Project R5839, Report OD 137, H.R. Wallingford.
- Auel, C. and Boes, R. (2011). *Sediment bypass tunnel design – review and outlook*. In: Dams and Reservoirs under Changing Challenges, Eds.: Schleiss, A., and Boes, R.M., Taylor & Francis Group, London, United Kingdom.
- Auel, C., Boes, R.M. and Sumi, T. (2018). Abrasion prediction at Asahi sediment bypass tunnel based on Ishibashi's formula. *Journal of Applied Water Engineering and Research* 6(2):125-138.
- Auel, C., Kobayashi, S., Sumi, T., and Takemon, Y. (2017). *Effects of sediment bypass tunnels on sediment grain size distribution and benthic habitats*. Proceedings: 13th International Symposium on River Sedimentation, Stuttgart, Germany. Published by CRC Press, London, United Kingdom.
- Badura, H. (2007). Feststofftransportprozesse während Spülungen von Flusstauräumen am Beispiel der oberen Mur. Dissertation, Schriftenreihe zur Wasserwirtschaft der Technischen Universität Graz, 51. (in German)
- Bagnold, R.A. (1966). *An approach to the sediment transport problem from general physics*. Professional Paper 422-1, U.S. Geological Survey, United States of America.
- Bagnold, R.A. (1973). The Nature of Saltation and of Bed-Load Transport in Water. *Proceedings of the Royal Society of London A* 332(1591):473–504.
- Bahreman, A., and De Smedt, F. (2008). Distributed hydrological modeling and sensitivity analysis in Torysa Watershed, Slovakia. *Water Resources Management* 22:393–408.
- Bale, A.J., Widdows, J., Harris, C.B., and Stephens, J.A. (2006). Measurements of the critical erosion threshold of surface sediments along the Tamar Estuary using a mini-annular flume. *Continental Shelf Research* 26:1206–1216.
- Barth, T. and Ohlberger, M. (2004). *Finite Volume Methods: Foundation and Analysis*. [online] Available at: citeseer.ist.psu.edu/barth04finite.html [accessed: 2020-10-04].
- Barton, J.S., Slingerland, R.L., Pittman, S. and Gabrielson, T.B. (2010). *Monitoring coarse bedload transport with passive acoustic instrumentation: A field study*. In: Bedload-Surrogate Monitoring Technologies, U.S. Geol. Surv. Sci. Invest. Rep. 2010-5091, Eds.: Gray, J.R., Laronne, J.B., and Marr, J.D., U.S. Geol. Surv., Reston, United States of America.

- Bartosova, A., Ruther, N., Schwarzwälder, K., Förster, K., Van den Broek, M., Achleitner, S., Haun, S. and Wieprecht, S. (2021). *Evaluating sediment Delivery Impacts on Reservoirs in changing climaTe and society aCROSS scales and sectors (DIRT-X)*. Proceedings: 6th IAHR Europe Congress, Warsaw, Poland.
- Bassett, C., Thomson, J., and Polagye, B. (2013). Sediment-generated noise and bed stress in a tidal channel. *Journal of Geophysical Research: Oceans* 118:2249–2265.
- Bassoullet, P., and Le Hir, O. (2007). In situ measurements of surficial mud strength: A new vane tester suitable for soft intertidal muds. *Continent Shelf Research* 27:1200-1205.
- Bastviken, D., Tranvik, L.J., Downing, J.A., Crill, P.M., and Enrich-Prast, A. (2011). Freshwater methane emissions offset the continental carbon sink. *Science* 331(6013), 50.
- Batuca, D., and Jordaan, J. (2000). *Silting and Desilting of Reservoirs*. A.A. Balkema, Rotterdam, The Netherlands.
- Baumert, H.Z., Simpson, J., and Sündermann, J. (2005). *Marine Turbulence: Theories, Observations, and Models*. Cambridge University Press, United Kingdom.
- Baxter, R.M. (1977). Environmental effects of dams and impoundments. *Annual Review of Ecology and Systematics*:255-283.
- Bayerisches Landesamt für Umwelt (LfU) (2016). *Verzeichnis der Bach- und Flussgebiete in Bayern – Flussgebiet Isar*. [online] Available at: <https://www.lfu.bayern.de/wasser/gewaesserverzeichnisse/doc/tab16.pdf#page=1> [Accessed 2019-01-04] (in German).
- Bayrisches Landesamt für Statistik (2017). *Statistik kommunal 2017. Gemeinde Lenggries 09 173 135 - Eine Auswahl wichtiger statistischer Daten*. [online] Available at: <http://www.statistik.bayern.de/veroeffentlichungen> [Accessed 2019-01-04]. (in German)
- Bechteler, W. (2006). *The purposes of impounding facilities*. In ALPRESERV – Sediment Management Methods - Technical and legal aspects. Universität der Bundeswehr München, Volume 4/2006, Germany.
- Beckers, F., Haun, S., and Noack, M. (2018). *Experimental investigation of reservoir sediments*. Proceedings: Proceedings: 9th International Conference on Fluvial Hydraulics, River Flow 2018, Lyon, France.
- Beckers, F., Haun, S., Gerbersdorf, S.U., Noack, M., Dietrich, D.R., Martin-Creuzburg, D., Peeters, F., Hofmann, H., Glaser, R., and Wieprecht, S. (2018). CHARM – CHALLENGES of Reservoir Management – Meeting environmental and social requirements. *HydroLink* 3:80-82.
- Beckers, F., Heredia, A., Noack, M., Nowak, W., Wieprecht, S., and Oladyshkin, S. (2020a). Bayesian calibration and validation of a large-scale and time-demanding sediment transport model. *Water Resources Research* 56 e2019WR026966.
- Beckers, F., Inskeep, C., Haun, S., Schmid, G., Wieprecht, S., and Noack, M. (2020). High spatio-temporal resolution measurements of cohesive sediment erosion. *Earth Surface Processes and Landforms*; 45(11):2432-2449.

- Beckers, F., Koca, K., Haun, S., Noack, M., Gerbersdorf, S.U., and Wieprecht, S. (2021). Functional relationships between critical erosion thresholds of fine reservoir sediments and their sedimentological characteristics. *Journal Journal of Hydraulic Engineering* 2021 (submitted).
- Beckers, F., Noack, M., and Wieprecht, S. (2016). *Geschiebetransportmodellierung (GTM) Salzach und Saalach [Bed load transport modeling of the rivers Salzach and Saalach]* (08a/2015 and 08b/2015). Stuttgart: Institute for Modelling Hydraulic and Environmental Systems (IWS) Department of Hydraulic Engineering and Water Resources Management. (in German)
- Beckers, F., Noack, M., and Wieprecht, S. (2018). Uncertainty analysis of a 2D sediment transport model: An example of the lower river Salzach. *Journal of Soils and Sediments* 18:3133–3144.
- Beckers, F., Sadid, N., Haun, S., Noack, M., and Wieprecht, S. (2015). *Contribution of numerical modelling of sediment transport processes in river engineering: An example of the river Saalach*. Proceedings: 36th IAHR World Congress, The Hague, The Netherlands.
- Benner, J., Helbling, D.E., Kohler, H.-P.E., Wittebol, J., Kaiser, E., Prasse, C., Ternes, T.A., Albers, C.N., Aamand, J., Horemans, B., Springael, D., Walravens, E. and Boon, N. (2013). Is biological treatment a viable alternative for micropollutant removal in drinking water treatment processes? *Water Research* 47(16), 5955-5976.
- Berlamont, J., Ockenden, M., Toorman, E., and Winterwerp, J. (1993). The characterization of cohesive sediment properties. *Coastal Engineering* 21(1-3): 105-128.
- BfG (2013). *Der aktuelle Bestand der Bundeswasserstraßen im Fachdienst FLYS*. [online] Available at: https://www.bafg.de/DE/08_Ref/M2/03_Fliessgewmod/01_FLYS/flys_daten.pdf?__blob=publicationFile [Accessed 2021-04-19]. (in German)
- Black K.S., Tolhurst T.J., Paterson D.M., and Hagerthey S.E. (2002). Working with Natural Cohesive Sediments. *Journal of Hydraulic Engineering* 128(2): 1–8.
- Black, K., and Rosenberg, M. (1994). Suspended sand measurements in a turbulent environment: field comparison of optical and pump sampling techniques. *Coastal Engineering* 24:137–150.
- Black, K.S., and Cramp, A. (1995). A device to examine the in situ response of intertidal cohesive sediment deposits to fluid shear. *Continent Shelf Research* 15(15): 1945-1954.
- Black, K.S., and Paterson, D.M. (1997). Measurement of the erosion potential of cohesive marine sediments: A review of current in situ technology. *Journal of Marine Environmental Engineering* 26:43-83.
- Bleyel, B., and Kopmann, R. (2018). *Influence of the layer model on a 2D sediment transport model: Hirano-Ribberink versus C-VSM*. Proceedings: XXVth TELEMAC-MASCARET User Conference, Norwich, United Kingdom.
- Blom, A. (2008). Different approaches to handling vertical and streamwise sorting in modeling river morphodynamics. *Water Resources Research* 44:1-16.
- Blomqvist, S. (1991). Quantitative sampling of soft-bottom sediments: Problems and solutions. *Marine Ecology Progress Series* 72:295–304.
- Blöschl, G., et al. (2019). Twenty-three unsolved problems in hydrology (UPH) – a community perspective. *Hydrological Sciences Journal* 64(10):1141-1158.

Blum, M.D., and Törnqvist, T.E. (2000). Fluvial responses to climate and sea-level change: a review and look forward. *Sedimentology* 47:2–48.

BMLFUW (2008). *Schwebstoffe im Fließgewässer – Leitfaden zur Erfassung des Schwebstofftransportes*. Bundesministerium für Land- und Forstwirtschaft, Umwelt und Wasserwirtschaft, Vienna, Austria. (in German)

Boes, R., and Reindl, R. (2006). *Nachhaltige Maßnahmen gegen Stauraumverlandungen alpiner Speicher* ('Sustainable measures to counter sedimentation of Alpine reservoirs'). Proceedings: Symposium „Stauhaltungen und Speicher - Von der Tradition zur Moderne“, Graz, Austria. (in German)

Boes, R.M., Auel, C., Hagmann, M., and Albayrak, I. (2014). *Sediment bypass tunnels to mitigate reservoir sedimentation and restore sediment continuity*. Proceedings: River Flow 2014: Reservoir Sedimentation, Lausanne, Switzerland. Published by Taylor & Francis Group, London, United Kingdom.

Bogen, J. (1980). The hysteresis effect of sediment transport systems. *Norwegian Journal of Geography* 34(1):45-54.

Booth, D. (2006). ESS 426: *Fluvial Geomorphology* – 3 Full lecture 2006. Lecture Notes. Earth and Space Sciences, Colleague of the Environment, University of Washington, United States of America. Available at: http://gis.ess.washington.edu/grg/oldcourses/courses05_06/ess426%20not/pdfs-2006/3%20Full%20lecture%202006.pdf [Accessed 2019-01-17].

Botterweg, P. (1995). The user's influence on model calibration results: An example of the model SOIL, independently calibrated by two users. *Ecological Modelling* 81:71–81.

Boussinesq, J. (1897). *Théorie de l'écoulement tourbillonnant et tumultueux des liquides dans les lits rectilignes a grande section*. Gauthier-Villars. (in French)

Boyle, D.P., Gupta, H.V., and Sorooshian, S. (2000). Toward improved calibration of hydrologic models: combining the strengths of manual and automatic methods. *Water Resources Research* 36:3663–3674.

Branche, E. (2017). The multipurpose water uses of hydropower reservoir: TheSHARE concept, *Comptes Rendus Physique* 18:469-478.

Braun, U., Jekel, M., Gerdt, G., Ivleva, N.P., and Reiber, J. (2018). *Mikroplastik-Analytik Probenahme, Probenaufbereitung und Detektionsverfahren*. Diskussionspapier im Rahmen des Forschungsschwerpunktes Plastik in der Umwelt Quellen•Senken•Lösungsansätze. [online]<https://bmbf-plastik.de/sites/default/files/2018-10/Diskussionspapier%20Mikroplastik-Analytik.pdf> [accessed: 12.03.2019] (in German)

Breitung, V. (2009). *Statement on dredging at the barrage Iffezheim (spillway channel) (Rhine-km332,800-333,900)*. Technical report, Bundesanstalt für Gewässerkunde (BfG).

Brigham Young University (2003). *SMS (Surface Water Modelling System)*. Tutorials, Version 8.1. - Brigham Young University, Environmental Modelling Research Laboratory.

Bronstert, A., de Araújo, J.C., Batalla, R.J., Costa, A.C., Delgado, J.M., Francke, T., Förster, S., Güntner, A., Lopez-Tarazon, J.A., Mamede, G.L., Medeiros, P.H., Müller, E.N., and Vericat, D. (2014). Process-based modelling of erosion, sediment transport and reservoir siltation in mesoscale semi-arid catchments. *Journal of Soils and Sediments* 14:2001-2018.

- Brooks, N.H. (1963). Discussion of "Boundary Shear Stresses in Curved Trapezoidal Channels" by A.T Ippen and P.A. Drinker. *Journal of Hydraulics Division* 89(3):327–333.
- Browne, M.A., Dissanayake, A., Galloway, T.S., Lowe, D.M., and Thompson, R.C. (2008). Ingested microscopic plastic translocates to the circulatory system of the mussel, *Mytilus edulis* (L.). *Environmental Science & Technology* 42 (13): 5026–5031.
- Bruk, S. (1996). *Reservoir sedimentation and sustainable management of water resources – the international perspective*. Proceedings: International conference on reservoir sedimentation, Fort Collins, United States of America.
- Bunte, K., Abt, S.R., and Potyondy, J.P. (2001). *Portable bedload traps with high sampling intensity for representative sampling of gravel transport in wadable mountain streams*. Proceedings: 7th Interagency Sedimentation Conference, Reno, United States of America.
- Bunte, K., Abt, S.R., Potyondy, J.P., and Ryan, S.E. (2005). Measurement of Coarse Gravel and Cobble Transport Using Portable Bedload Traps. *Journal of Hydraulic Engineering* 130(9).
- Bunte, K., and Abt, S.R. (2005). Effect of sampling time on measured gravel bed load transport rates in a coarse-bedded Stream. *Water Resources Research* 41:W11405
- Bureau of Economic Geology (2020). *Impact of Soil Conservation Practices on Water Resources in the Loess Plateau, China*. [online] Available at: <http://www.beg.utexas.edu/research/programs/sustainable-water-resources/research-examples/china>. [Accessed 2020-05-29].
- Carling, P.A., and Reader, N.A. (1981). A Freeze-Sampling Technique suitable for coarser river bed-material. *Sedimentary Geology* 29:233–239.
- Carter, J. (1991). Niobrara, Nebraska: the Town Too Tough to Stay Put. *Nebraska History* 72:144-149.
- Castillo, J.E. (1991). *Mathematical aspects of grid Generation*. Proceedings: Mathematical aspects of numerical grid generation, Society for Industrial and applied Mathematics, Philadelphia, United States of America.
- Çelik, R. (2018). Impact of Dams on Groundwater Static Water Level Changes: a Case Study Kralkızı and Dicle Dam Watershed. *Uluslararası Mühendislik Araştırma ve Geliştirme Dergisi* 10(2):119 – 126.
- Chamoun, S., De Cesare, G., and Schleiss, A.J. (2016). Managing reservoir sedimentation by venting turbidity currents: A review. *International Journal of Sediment Research* 31(3): 195-204.
- Chandrasekhar, S. (1943). Stochastic Problems in Physics and Astronomy. *Reviews of Modern Physics* 15(1).
- Chant, L.A., and Cornett, R.J. (1991). Smearing of gravity core profiles in soft sediments. *Limnology and Oceanography* 67:1492–1498.
- Chikita, K., and Okumura, Y. (1990). Dynamics of turbidity currents measured in Katsurazawa reservoir, Hokkaido, Japan. *Journal of Hydrology* 117: 323–338.
- Chitata, T., Mugabe, F.T., and Kashaigili, J.J. (2014). Estimation of small reservoir sedimentation in semi-arid southern Zimbabwe. *Journal of Water Resources and Protection* 6:1017-1028

- Christ, R.D., and Wernli, R.L. (2007). *The ROV Manual: A User Guide for Observation-Class Remotely Operated Vehicles*. 2nd ed. Butterworth-Heinemann Ltd., Oxford, United Kingdom.
- Cole, J., Prairie, Y., Caraco, N., McDowell, W., Tranvik, L., Striegl, R., Duarte, C., Kortelainen, P., Downing, J., and Middelburg, J. (2007). Plumbing the global carbon cycle: integrating inland waters into the terrestrial carbon budget. *Ecosystems* 10(1):172–185.
- Conevski, S., Guerrero, M., Ruther, N., and Rennie, C.D. (2019). Laboratory investigation of apparent bedload velocity measured by ADCPs under different transport conditions. *Journal of Hydraulic Engineering* 145(11).
- Conevski, S., Guerrero, M., Winterscheid, A., Rennie, C.D., and Ruther, N. (2020). Acoustic sampling effects on bedload quantification using acoustic Doppler current profilers. *Journal of Hydraulic Research* 58(6): 1–19.
- Conner, C., and De Visser, A. (1992). A laboratory investigation of particle size effects on an optical backscatterance sensor. *Marine Geology* 108:151–159.
- Corcoran, P.L., Moore, C.J., and Jazvac, K. (2014). An anthropogenic marker horizon in the future rock record. *GSA Today* 24(6): 4–8.
- Cornelisse, J.M., Mulder, H.P.J., Houwing, E.J., Williamson, H.J., and Witte, G. (1997). *On the development of instruments for in situ erosion measurements*. In: Cohesive Sediments, Eds.: N. Burt, R. Parker, and J. Watts, John Wiley & Sons Ltd., New Jersey, United States of America.
- Courant, R., Friedrichs, K., and Lewy, H. (1928). Über die partiellen Differenzgleichungen der mathematischen Physik. *Mathematische Annalen, Band 100*:32–74.
- Cowgill, C.M. (1994). *In situ determination of fine grained sediment erodibility*. unpublished Doctoral thesis, University of Southampton, Southampton, United Kingdom.
- Crowder, B.M. (1987). Economic Costs of Reservoir Sedimentation: A Regional Approach to Estimating Cropland Erosion Damages. *Journal of Soil and Water Conservation* 42(3):194–197.
- Cunge, J.A. (2003). Of data and models. *Journal of Hydroinformatics* 5:75–98.
- Cyberski, J. (1973). *Accumulation of debris in water storage reservoirs of central Europe*. In: Man-made Lakes: Their Problems and Environmental Effects, Eds.: Ackermann, W.C., White, G.F., Worthington, E.B., and Ivens, J.L., Geophysical Monographs 17. American Geophysical Union, Washington D.C., United States of America.
- Czuba, J.A., Straub, T.D., Curran, C.A., Landers, M.N., and Domanski, M.M. (2015). Comparison of fluvial suspended-sediment concentrations and particle-size distributions measured with in-stream laser diffraction and in physical samples. *Water Resources Research* 51(1):320-340.
- Dahir, A.L. (2018). *A major geopolitical crisis is set to erupt over who controls the world's longest river* [online] Available at: <https://qz.com/1181318/ethiopia-egypt-sudan-and-eritrea-tensions-over-grand-ethiopian-renaissance-dam-on-nile-river/> [Accessed 2018-03-21].
- Dargahi, B. (2012). *Reservoir Sedimentation*. In: Bengtsson L., Herschy R.W., Fairbridge R.W. (eds) Encyclopedia of Lakes and Reservoirs. Encyclopedia of Earth Sciences Series. Springer, Dordrecht.
- Daus, M., Koberger, K., Koca, K., Beckers, F., Encinas Fernández, J., Weisbrod, B., Dietrich, D., Gerbersdorf, S.U., Glaser, R., Haun, S., Hofmann, H., Martin-Creuzburg, D., Peeters, F., and Wieprecht, S. (2021). Interdisciplinary Reservoir Management—A Tool for Sustainable Water Resources Management. *Sustainability* 13, 4498.

- Dawson, C., and Mirabito, Ch.M. (2008). *The Shallow Water Equations*. Lecture Notes, Institute for Computational Engineering and Sciences, University of Texas at Austin. [online] Available at: https://users.oden.utexas.edu/~arbogast/cam397/dawson_v2.pdf [Accessed 2020-04-30].
- De Cesare, G. (2006). In: *ALPRESERV - Sediment Management Methods - Technical and legal aspects, chapter Density currents*. Universität der Bundeswehr München, Volume 4/2006, ISSN 1862-9636.
- De Cesare, G., Schleiss, A., and Hermann, F. (2001). Impact of turbidity currents on reservoir sedimentation. *Journal of Hydraulic Engineering* 1271: 6–16.
- Debnath, K., Nikora, V., Aberle, J., Westrich, B., and Muste, M. (2007). Erosion of cohesive sediments: Resuspension, bed load, and erosion patterns from field experiments. *Journal of Hydraulic Engineering* 133(5): 508-520.
- DeCarlo, R. (1989). *Linear Systems: A State Variable Approach with Numerical Implementation*. Prentice Hall, NJ, United States of America.
- Deines, K.L. (1999). *Backscatter estimation using broadband acoustic Doppler current profilers*. Proceedings: 6th Working Conference on Current Measurement Technology, Current Measurement Technology Committee of the Oceanic Engineering Society Institute of Electrical and Electronics Engineers, Piscataway, United States of America.
- Der Spiegel GmbH & Co. KG (2011). *Aufforsten bremst Erderwärmung kaum*. [online] Available at: <https://www.spiegel.de/wissenschaft/natur/klimawandel-studie-aufforsten-bremst-erderwaermung-kaum-a-769315.html#> [Accessed 2019-05-30]. (in German)
- Deslauriers, S., and Mahdi, T.-F. (2018). Flood modelling improvement using automatic calibration of two dimensional river software SRH-2D. *Natural Hazards* 91:697–715.
- Detering M. (2014). *Betrieb und Instandhaltung eines Wasserkraftwerks*. In: Böttcher J. (eds) *Wasserkraftprojekte*. Springer Gabler, Berlin, Heidelberg. (in German)
- DHI (2017). *DHI Simulation Engine for 1D river and urban modelling*. Reference Manual, DHI, Hørsholm, Denmark.
- DIN 38409 (1987). *DIN 38409, Teil 2: Summarische Wirkungs- und Stoffkenngrößen (Gruppe H) - Bestimmung der abfiltrierbaren Stoffe und des Glührückstandes (H2)*, 03/1987. (in German)
- DIN EN ISO 17892-4 | 2017-04 (2017). *Geotechnische Erkundung und Untersuchung - Laborversuche an Bodenproben - Teil 4: Bestimmung der Korngrößenverteilung*; Deutsche Fassung EN ISO 17892-4:2016. (in German)
- Doherty, J. (2016). *PEST Model-Independent Parameter Estimation*. User Manual Part I, 6th Edition.
- Dorfmann, C. (2017). *Flow Phenomena in a Reservoir investigated by Field Measurements and Numerical Modelling*. Doctoral thesis, Technical University of Graz, Graz, Austria.
- Dorfmann, C., and Knoblauch, H. (2009). *Calibration of 2-D and 3-D Numerical Models of a Large Reservoir Using ADCP Measurements*. Proceedings: 33rd IAHR Congress, Vancouver, Canada.
- Dorfmann, C., Knoblauch, H., and Moser, A. (2010). Physikalische und numerische Modellierung des Strömungsverhaltens im Stauraum des KW Feistritz-Ludmannsdorf an der Drau. *Österreichische Wasser- und Abfallwirtschaft*, 62(3-4), 62-66. (in German)
- Doucet, M.P., Noack, M., Wieprecht, S., and Haun, S. (2018). *Performance evaluation of flood protection measures along the Goldersbach stream using 2D hydraulic modelling*. Proceedings: 5th IAHR European Congress, Trento, Italy.

- Downing, J. (2006). Twenty-five years with OBS sensors: The good, the bad, and the ugly. *Continental Shelf Research* 26:2299–2318.
- Duan C.G., and Karelin V.Y. (2002). *Abrasive Erosion & Corrosion of Hydraulic machinery*. Imperial College Press, London, United Kingdom.
- Duan, Q.Y., Gupta, V.K., and Sorooshian, S. (1993). Shuffled complex evolution approach for effective and efficient global minimization. *Journal of Optimization Theory and Applications* volume 76:501–521.
- Dück, Y., Lorke, A., Jokieli, Ch., and Gierse, J. (2019). Laboratory and field investigations on freeze and gravity core sampling and assessment of coring disturbances with implications on gas bubble characterization. *Limnology and Oceanography: Methods* 17(11): 585-606.
- Duclos, P.A., Lafite, R., le Bot, S., Rivoalen, E., and Cu villiez, A. (2013). Dynamics of turbid plumes generated by marine aggregate dredging: An example of a macrotidal environment (the Bay of Seine, France). *Journal of Coastal Research* 29(6A):25–37.
- Durán Zuazo, V.H., et al. (2020) *Terraced Subtropical Farming: Sustainable Strategies for Soil Conservation*. In: Meena R. (eds) *Soil Health Restoration and Management*. Springer, Singapore.
- DVWK (1986). *Schwebstoffmessungen DK 556.535.6 Schwebstoff*. DVWK Regeln 125/1986. Hamburg,1-42. (in German)
- DWA (2019). *DWA-M 513-1 „Umgang mit Sedimenten und Baggergut bei Gewässerunterhaltung und -ausbau - Teil 1: Handlungsempfehlungen und Untersuchungsprogramm“*. Deutsche Vereinigung für Wasserwirtschaft, Abwasser und Abfall e.V., Hennef, Germany. (in German)
- Edwards, T.K., and Glysson, G.D. (1999). *Field Methods for Measurement of Fluvial Sediment.: U.S. Geological Survey Techniques of Water-Resources Investigations*. Book 3, Chapter C2.
- Ehrbar, D., Schmocker, L., Doering, M., Cortesi, M., Bourban, G, Boes, R.M., and Vetsch, D.F. (2018). Continuous Seasonal and Large-Scale Periglacial Reservoir Sedimentation. *Sustainability* 10, 3265.
- Ehrbar, D., Schmocker, L., Vetsch, D.F., Boes, R.M. and Doering, M. (2017). Measuring suspended sediments in periglacial reservoirs using water samples, laser in-situ scattering and transmissometry and acoustic Doppler current profiler. *International Journal of River Basin Management* 15(4): 413-431.
- Einstein, H.A. (1950). *The Bed-Load Function for Sediment Transportation in Open Channel Flows*. Technical Bulletins 156389, United States Department of Agriculture, Economic Research Service.
- Einstein, H.A. (1968). Deposition of suspended particles in a gravel bed. *Journal of Hydraulic Engineering* 94: 1197–1205.
- Einstein, H.A., and Barbarossa, N.L. (1952). River channel roughness: *American Society of Civil Engineers Transactions* 117:1121-1132.
- Einstein, H.A., Anderson, A.G., and Johnson J.W. (1940). A distinction between bed-load and suspended load in natural streams. *Transactions of the American Geophysical Union's annual meeting* 22:628–633.
- EnBW Energie Baden-Württemberg AG (2017). *EnBW reprioritises its storage projects: The Atdorf pump storage project will not be pursued further* [online] Available at: https://www.enbw.com/company/press/press-releases/press-release-details_170304.html [Accessed 2020-01-20].

- Encinas Fernandez, J., Hofmann, H., and Peeters, F. (2020). Diurnal pumped-storage operation minimizes methane ebullition fluxes from hydropower reservoirs. *Water Resources Research* 56(12): 1-15.
- Encinas Fernández, J., Peeters, F., and Hofmann, H. (2014). Importance of the Autumn Over-turn and Anoxic Conditions in the Hypolimnion for the Annual Methane Emissions from a Temperate Lake. *Environmental Science & Technology* 48(13): 7297–7304.
- Engelund, F. (1965). *A criterion for the occurrence of suspended load*. La Houille Blanche 8: 7.
- Engelund, F., and Hansen, E. (1967). *A Monograph on Sediment Transport in Alluvial Streams*. Teknisk Forlag, Copenhagen, Denmark, 1967.
- Ergenzinger, P., Schmidt, K.-H., and Bußkamp, R. (1989). The Pebble Transmitter System (PETS): first results of a technique for studying coarse material erosion, transport and deposition. *Zeitschrift für Geomorphologie NF* 33:503–508
- Ergenzinger, P.J., and Custer, S.G. (1983). Determination of bedload transport using naturally magnetic tracers: First experiences at Squaw Creek, Gallatin County, Montana. *Water Resources Research* 19(1):187-193.
- Esmaeili, T., Sumi, T., Kantoush, S.A., Kubota, Y., Haun, S., and Rütther, N. (2017). Three-Dimensional Numerical Study of Free-Flow Sediment Flushing to Increase the Flushing Efficiency: A Case-Study Reservoir in Japan. *Water* 9:1-22
- Esmaeili, T., Sumi, T., Kantoush, S.A., Kubota, Y., and Haun, S. (2015). Numerical study on flushing channel evolution, case study of Dashidaira reservoir, Kurobe river. *Annual Journal of Hydraulic Engineering JSCE* 59.
- Esmaeili, T., Sumi, T., Kantoush, S.A., Kubota, Y., Haun, S., and Rütther, N. (2021). Numerical Study of Discharge Adjustment Effects on Reservoir Morphodynamics and Flushing Efficiency: An Outlook for the Unazuki Reservoir, Japan. *Water* 13(1624).
- European Environment Agency (2018). *Reservoirs and Dams*. [online] Available at: <https://www.eea.europa.eu/themes/water/european-waters/reservoirs-and-dams>, updated 18 Feb 2018 [Accessed 2018-02-18].
- European Working Group on Dams and Floods (2010). *Dams and Floods in Europe. Role of dams in Flood Mitigation*. Report. December 2010.
- Evers, F. (2020). *Sediment Sampling*. [online] Available at: <https://www.geomar.de/en/research/fb1/fb1-p-oz/infrastructure/sediment-sampling-1> [accessed: 2020-10-04].
- Fan, J., and Morris, G.L. (1992). Reservoir Sedimentation. II: Reservoir Desiltation and Long-Term Storage Capacity. *Journal of Hydraulic Engineering* 118(3).
- Fang, H., and Rodi, W. (2003). Three-dimensional calculations of flow and suspended sediment transport in the neighbourhood of the dam for the Three Gorges Project (TGP) reservoir in the Yangtze River. *Journal of Hydraulic Research* 41(4):379-394.
- Fang, H.-W., and Rodi, W. (2003). Three-dimensional calculations of flow and suspended sediment transport in the neighborhood of the dam for the Three Gorges Project (TGP) reservoir in the Yangtze River. *Journal of Hydraulic Research* 41:379–394.

- Felix D., Abgottspon A., Albayrak I., and Boes R.M. (2016). *Hydro-abrasive erosion on coated Pelton runners: Partial calibration of the IEC model based on measurements in HPP Fieschertal*. Proceedings: 28th IAHR Symposium on Hydraulic Machinery and Systems, Grenoble, France.
- Felix, D., Albayrak, I., and Boes, R.M. (2018). In-situ investigation on real-time suspended sediment measurement techniques: Turbidimetry, acoustic attenuation, laser diffraction (LISST) and vibrating tube densimetry. *International Journal of Sediment Research* 33(1): 3-17.
- Felix, D., Albayrak, I., and Boes, R.M. (2013). Laboratory investigation on measuring suspended sediment by portable laser diffractometer (LISST) focusing on particle shape. *Geo-Marine Letters* 33(6): 485-498.
- Ferguson, R.I. (2005). Estimating critical stream power for bedload transport calculations in gravel-bed rivers. *Geomorphology* 70(1–2):33-41.
- Fernandes, J., Boes, R., Titzschkau, M., Hammer, A., Haun, S., and Schletterer, M. (2016). *Suspended sediment concentrations and turbine wear during the drawdown of two Alpine reservoirs*. Proceedings: Hydro 2016 Conference & Achievements, Opportunities and Challenges, Montreux, Schweiz.
- Flow-3D (2010). *User Manual Version 9.4*. Flow Science Ink., Santa Fe, U.S.
- Folk, R.L. (1966). A review of grain-size parameters. *Sedimentology* 6 (2): 73–93.
- Folk, R.L. (1980). *Petrology of sedimentary rocks*. Austin, Tex., Hemphill Publishing, 184p.
- Foster, G.R. (2005). *Terraces and Terracing*. In Encyclopedia of Soils in the Environment, Elsevier.
- Fox, G.A., Sheshukov, A., Cruse, R., Kolar, R.L., Guertault, L., Gesch, K.R., and Dutnell, R.C. (2016). Reservoir Sedimentation and Upstream Sediment Sources: Perspectives and Future Research Needs on Streambank and Gully Erosion. *Environmental Management* 57: 945–955.
- Frings, R.M., Gehres, N., Promny, M., Middelkoop, H., Schüttrumpf, H. and Vollmer, S. (2014a). Today's sediment budget of the Rhine River channel, focusing on the Upper Rhine Graben and Rhenish Massif. *Geomorphology* 204:573-587.
- Frings, R.M., Döring, R., Beckhausen, Ch., Schüttrumpf, H. and Vollmer, S. (2014b). Fluvial sediment budget of a modern, restrained river: The lower reach of the Rhine in Germany. *CATENA* 122:91-102.
- Gaeuman, D., and Jacobson, R.B. (2006). Acoustic bed velocity and bed load dynamics in a large sand bed river. *Journal of Geophysical Research* 111(2):F02005.
- Galland, J.C., Goutal, N., and Hervouet, J.M. (1991). TELEMAC: A New Numerical Model for Solving Shallow Water Equations. *Advances in Water Resources AWREDI*, 14(3):138–148,
- García, H.M. (2008). *Sedimentation Engineering. Processes, measurements, modeling, and practice*. ASCE Manuals and Reports on Engineering Practice n. 110.
- Gartner, J.W. (2004). Estimating suspended solids concentrations from backscatter intensity measured by acoustic Doppler current profiler in San Francisco Bay, California. *Marine Geology* 211(3–4):169–187.
- Gayraud, S., and Philippe, M. (2003). Influence of Bed-Sediment Features on the Interstitial Habitat Available for Macroinvertebrates in 15 French Streams. *International Review of Hydrobiology* 88:77–93.

- Geay, T., Belleudy, P., Gervaise, C., Habersack, H., Aigner, J., Kreisler, A., Seitz, H., and Laronne, J.B. (2017). Passive acoustic monitoring of bed load discharge in a large gravel bed river. *Journal of Geophysical Research* 122:528–545.
- Gebler, T., Stolz, D., Fenrich, E., and Terheiden, K. (2014). Lecture Notes: Hydraulic Structures. Department of Hydraulic Engineering and Water Resources Management, Institute for Modelling Hydraulic and Environmental Systems, University of Stuttgart, Stuttgart, Germany.
- Geonor Inc. (2021). *H-10 Field Vane Shear Apparatus*. [online] Available at: <https://geonor.com/live/products/geotechnical-test-equipment/h-10-field-vane-shear-apparatus/> [accessed: 2020-05-18].
- George, M.W. (2016). *Reservoir Sedimentation: The Economics of Sustainability*. Master of Science thesis, Brigham Young University, United States of America.
- Gerbersdorf, S.U., and Wieprecht, S. (2015). Biostabilization of cohesive sediments: revisiting the role of abiotic conditions, physiology and diversity of microbes, polymeric secretion, and biofilm architecture. *Geobiology* 13: 68-97.
- Gerbersdorf, S.U., Hollert, H., Brinkmann, M., Wieprecht, S., Schüttrumpf, H., and Manz, W. (2011). Anthropogenic pollutants affect ecosystem services of freshwater sediments: The need for a "triad plus x" approach. *Journal of Soils and Sediments* 11(6):1099-1114.
- Gerbersdorf, S.U., Jancke, T., and Westrich, B. (2007). Sediment Properties for Assessing the Erosion Risk of Contaminated Riverine Sites. *Journal of Soils and Sediments* 7(1).
- Gerbersdorf, S.U., Jancke, T., and Westrich, B. (2007). Sediment Properties for Assessing the Erosion Risk of Contaminated Riverine Sites. An approach to evaluate sediment properties and their covariance patterns over depth in relation to erosion resistance. First investigations in natural sediments. *Journal of Soils and Sediments* 7:25–35.
- Gerbersdorf, S.U., Jancke, T., Westrich, B., and Paterson, D. (2008). Microbial stabilization of riverine sediments by extracellular polymeric substances. *Geobiology* 6:57-69.
- Gitto, A.B., Venditti, J.G., Kostaschuk, R., and Church, M. (2017). Representative point-integrated suspended sediment sampling in rivers. *Water Resources Research* 53:2956–2971.
- Gleick, P.H. (2003). Global Freshwater Resources: Soft-Path Solutions for the 21st Century. *Science* 302(5650): 1524-1528.
- Gordon, R.L. (1989). Acoustic measurement of river discharge. *Journal of Hydraulic Engineering* 115:925-936.
- Gordon, R.L. (1996). *Acoustic Doppler current profilers: Principles of operation, a practical primer, second edition for broadband ADCPs*. User manual. Teledyne-RDI, San Diego, CA, United States of America.
- Graf, W. (1971). *Hydraulics of Sediment Transport*. McGraw-Hill Book Co., New York, United States of America.
- Graf, W.H. and Acaroglu, E.R. (1968). *Sediment transport in conveyance systems (part 1) / A physical model for sediment transport in conveyance systems*. International Association of Scientific Hydrology. Bulletin 13(2): 20-39.

- Gray, J.R., and Gartner, J.W. (2009). Technological advances in suspended-sediment surrogate monitoring. *Water Resources Research* 45(4):1-20.
- Gray, J.R., Laronne, J.B., and Marr, J.D.G. (2010). *Bedload-surrogate monitoring technologies*. U.S. Geological Survey Scientific Investigations Report 2010–5091, 37 p.
- Grissinger, E.H., Little, W.C., and Murphey, J.B. (1981). Erodibility of streambank materials of low cohesion. *Transactions ASAE* 24(3):624-630.
- Grossmann, Ch., Roos, H.-G., and Stynes, M. (2007). *Numerical Treatment of Partial Differential Equations*. Springer Science & Business Media. p. 23.
- Guerin, F. (2006). *Emissions de Gaz a Effet de Serre (CO2 CH4) par une Retenue de Barrage Hydroelectrique en Zone Tropicale (Petit-Saut, Guyane Francaise): Experimentation et Modelization*. Thèse de doctorat de l'Université Paul Sabatier (Toulouse III). (in French)
- Guerrero, M., Nones, M., Saurral, R., Montroull, N., and Szupiany, R.N. (2013). Parana River morphodynamics in the context of climate change. *International Journal of River Basin Management* 11(4):423-437.
- Guerrero, M., Rütther, N., Szupiany, R., Haun, S., Baranya, S., and Latosinski, F. (2016). The Acoustic Properties of Suspended Sediment in Large Rivers: Consequences on ADCP Methods Applicability. *Water* 8(1):1-22.
- Guerrero, M., Szupiany, R.N., and Amsler, M. (2011). Comparison of acoustic backscattering techniques for suspended sediments investigation. *Flow Measurements and Instrumentation* 22(5): 392–401.
- Guertault, L., Camenen, B., Peteuil, C., Paquier, A., and Faure, J.B. (2016). One-Dimensional Modeling of Suspended Sediment Dynamics in Dam Reservoirs. *Journal of Hydraulic Engineering* 142.
- Gusek, W. (2015). *Globale Navigations-Satellitensysteme - GNSS - Fehlerquellen, Erweiterungen und Verbesserungen*. [online] Available at: <https://kompodium.infotip.de/id-4-fehlerquellen-erweiterungen-und-verbesserungen.html>. [Accessed 2020-10-01] (in German)
- Gust, G. (1991). *Fluid Velocity Measurement Instrument*. U.S. Patent No. 4, 986, 122.
- Gust, G., and Morris, M.J. (1989). Erosion thresholds and entrainment rates of undisturbed in situ sediments. *Journal of Coastal Research* 5:87-99.
- Habersack, H.M. (2001). Radio-tracking gravel particles in a largebraided river in New Zealand: A field test of the stochastic theory of bed load transport proposed by Einstein. *Hydrological Processes* 15(3):377–391.
- Haestad Methods Inc. (2007). *Computer applications in hydraulic engineering: connecting theory to practice*. Bentley Institute Press.
- Han, X., Fang, H., He, G., and Reib Le, D. (2018). Effects of roughness and permeability on solutetransfer at the sediment water interface. *Water Research* 129:39–50.
- Hanjalić, H., and Launder, B. (2011). *Modelling Turbulence in Engineering and the Environment: Second-Moment Routes to Closure*. Cambridge University Press, United Kingdom.
- Harb, G. (2013). *Numerical Modeling of Sediment Transport Processes in Alpine Reservoirs*. Doctoral thesis, Technical University of Graz, Graz, Austria.

- Harb, G., Dorfmann, C., Schneider, J., Haun, S., and Badura, H. (2012). *Numerical analysis of sediment transport processes in a reservoir*. Proceedings: 6th International Conference on Fluvial Hydraulics, River Flow 2012, San José, Costa Rica.
- Harb, G., Haun, S., Schneider, J., and Olsen N.R.B. (2014). Numerical analysis of synthetic granulate deposition in a physical model study. *International Journal of Sediment Research* 29: 110-117.
- Hartmann, S., Knoblauch, H., De Cesare, G., and Steinich, C. (2009). *ALPRESERV - Sustainable Sediment Management in Alpine Reservoirs considering ecological and economical aspects*. Universität der Bundeswehr München, Munich, Germany.
- Hassan, M., Schick, A., and Laronne, J. (1984). The recovery of flood-dispersed coarse sediment particles. *Catena Supplement* 5:153–162.
- Hassan, M.A., and Ergenzinger, P. (2003). *Use of tracers in fluvial geomorphology*. In: Tools in Fluvial Geomorphology, Eds.: Kondolf, G.M., and Pie'gay, H., John Wiley & Sons Ltd., New Jersey, United States of America.
- Hauer et al. (2019). *Floods and Flood Protection - Past events and future strategies*. Rivers of the Alps: Diversity in Nature and Culture Publisher: Haupt Verlag, Bern. (in German)
- Hauer, C., Haimann, M., Holzapfel, P., Holzer, G., Boschi, M., Wagner, B., Prenner, D., Fuhrmann, M., Brock, B., Schmalzer, B., Schachner, A., Holzer, G., Leitner, P., Graf, W., and Habersack, H. (2017). *Seeentleerung Gepatsch – Endbericht*. Studie im Auftrag der TIWAG. (in German)
- Hauer, Ch., Haimann, M., Holzapfel, O., Floedl, P., Wagner, B. Hubmann, M., Hofer, B., Habersack, H., and Schletterer, M. (2020a). Controlled reservoir drawdown – Challenges for sediment management and integrative monitoring: An Austrian case study – Part A: Reach Scale. *Water*, 12(4), 1058.
- Hauer, Ch., Holzapfel, P., Floedl, P., Wagner, B., Graf, W., Leitner, P., Holzer, G., Haun, S., Habersack, H. and Schletterer, M. (2020b). Controlled reservoir drawdown – Challenges for sediment management and integrative monitoring: An Austrian case study – Part B: Local Scale. *Water* 12(4),
- Haun S., Lizano L., and Olsen, N.R.B. (2013). *Measuring suspended sediment concentrations in a reservoir based on laser diffraction*. Proceedings: 35th IAHR World Congress, Chengdu, China.
- Haun, S. (2012). *Three-dimensional numerical modelling of sediment transport during the flushing of hydropower reservoirs*. Doctoral thesis, Norwegian University of Science and Technology, Trondheim, Norway.
- Haun, S., and Lizano, L. (2014). Measurements of spatial distribution of suspended sediment concentrations in a hydropower reservoir. Proceedings: 9th International Conference on Fluvial Hydraulics, River Flow 2014: Reservoir Sedimentation, Lausanne, Switzerland. Published by Taylor & Francis Group, London, United Kingdom.
- Haun, S., and Lizano, L. (2015). *Sensitivity analysis of sediment fluxes derived by using acoustic backscatter*. Proceedings: 36th IAHR World Congress, The Hague, The Netherlands.
- Haun, S., and Lizano, L. (2016). *Evaluation of a density current from ADCP backscatter data and LISST measurements*. Proceedings: 10th International Conference on Fluvial Hydraulics, River Flow 2016, St. Louis, United States of America.
- Haun, S., and Lizano, L. (2018). Sensitivity analysis of sediment flux derived by laser diffraction and acoustic backscatter within a reservoir. *International Journal of Sediment Research* 33: 18-26.

- Haun, S., and Olsen, N.R.B. (2012a). Three-dimensional numerical modelling of reservoir flushing in a prototype scale. *International Journal of River Basin Management* 10(4): 341-349.
- Haun, S., and Dietrich, S. (2021). Advanced methods to investigate hydro-morphological processes in open-water environments. *Earth Surface Processes and Landforms* 2021:1–11.
- Haun, S., and Wieprecht, S. (2017). *Geschiebetransport messen oder modellieren? – Von Synergieeffekten profitieren*. 19. Gewässermorphologisches Kolloquium. Messungen des Geschiebetriebes –Theorie und Praxis. 8./9. November 2017 in Koblenz. (in German)
- Haun, S., Dorfmann, C., Harb, G., and Olsen, N.R.B. (2012b). *3D Numerical Modelling of the Reservoir Flushing of the Bodendorf Reservoir, Austria*. Proceedings: 2nd IAHR European Congress, Munich, Germany.
- Haun, S., Kjærås, H., Løvfall, S., and Olsen, N.R.B. (2013a). Three-dimensional measurements and numerical modelling of suspended sediments in a hydropower reservoir. *Journal of Hydrology* 479: 180-188.
- Haun, S., Olsen, N.R.B., and Feurich, R. (2011). Numerical modelling of flow over trapezoidal broad-crested weir. *Journal of Engineering Applications of Computational Fluid Mechanics* 5(3):397-405.
- Haun, S., Rütger, N., Baranya, S., and Guerrero, M. (2015). Comparison of real time suspended sediment transport measurements in river environment by LISST instruments in stationary and moving operation mode. *Flow Measurement and Instrumentation* 41:10-17.
- Hawley, N. (1991). Preliminary observations of sediment erosion from a bottom resting flume. *Journal of Great Lakes Research* 17(3): 361-367
- Hay, A.E. (1983). On the remote acoustic detection of suspended sediment at long wavelengths. *Journal of Geophysical Research* 88:(C12):7525-7542.
- Heibaum, M. (2002). *Scour and Erosion*. ISSMGE Technical Committee 213, Karlsruhe, Germany. [online] Available at: <https://scour-and-erosion.baw.de/references/photos>. [accessed: 2021-04-10]
- Heinzl, R. (2007). *Concepts for Scientific Computing*. Doctoral thesis, Technical University of Vienna, Vienna, Austria.
- Helley, E. J., and Smith, W. (1971). *Development and calibration of a pressure difference bedload sampler*. U.S. Geol. Surv. Open File Rep., 18 pp.
- Heywood, M.J.T., and Walling, D.E. (2007). The sedimentation of salmonid spawning gravels in the Hampshire Avon catchment, UK: implications for the dissolved oxygen content of intragravel water and embryo survival. *Hydrological Processes* 21(6), 770-788.
- Hidalgo-Ruz, V., Gutow, L., Thompson, R.C., and Thiel, M. (2012). Microplastics in the Marine Environment: A Review of the Methods Used for Identification and Quantification. *Environmental Science & Technology* 46: 3060-3075.
- Hillebrand, G. (2008). *Transport behavior of cohesive sediments in turbulent flows – Investigations in the open annular flume*. Doctoral thesis, Universität Fridericiana zu Karlsruhe, Karlsruhe, Germany. (in German)
- Hillebrand, G., Klassen, I., and Olsen, N.R.B. (2016). 3D CFD modelling of velocities and sediment transport in the Iffezheim hydropower reservoir. *Journal of Hydrology Research* 48(1):147–159.

- Hillebrand, G., Klassen, I., Olsen, N.R.B., and Vollmer, S. (2012). *Modelling fractionated sediment transport and deposition in the Iffezheim reservoir*. Proceedings: 10th International Conference on Hydroinformatics, Hamburg, Germany.
- Hirleman, E.D. (1987). *Optimal scaling of the inverse Fraunhofer diffraction particle sizing problem: The linear system produced by quadrature*. In: Gouesbet G., Gréhan G. (eds) *Optical Particle Sizing*. Springer, Boston, MA, United States of America.
- Hirt, C.W., and Nichols, B.D. (1981). Volume of fluid (vof) method for the dynamics of free boundaries. *Journal of Computational Physics* 39:201–225.
- Hjulström, F. (1935). *The morphological activity of rivers as illustrated by river Fyris*. Bull. Geolog. Institution, Univ. Uppsala, Vol. 25.
- Hogue, T.S., Sorooshian, S., Gupta, H., Holz, A., and Braatz, D.A. (2000). Multistep automatic calibration scheme for river forecasting models. *Journal of Hydrometeorology* 1:524–542.
- Holzappel, P., Habersack, H., and Hauer, Ch. (2020). Das Gravel Bar Consolidation Meter: Ein Messgerät zur Bestimmung des Verfestigungsgrades von Kiesbänken. *Wasserwirtschaft* 4/2020:27-33. (in German)
- Houwing, E.-J., and van Rijn, L.C. (1998). In situ erosion flume (ISEF): determination of bed-shear stress and erosion of a kaolinite bed. *Journal of Sea Research* 39:243-253.
- Hubbell, D.W. (1987). *Bed load sampling and analysis*. In: *Sediment Transport in Gravel-bed Rivers*, Eds.: Thorne, C.R., Bathurst, J.C., and Hey, R.D., John Wiley & Sons Ltd., New Jersey, United States of America.
- Hubbell, D.W., and Sayre, W.W. (1964). Sand transport studies with radio-active tracers. *Journal of the Hydraulics Division* 90(HY3):39–68.
- Huebner, K.H., Thornton, E.A., and Byron, T.D. (1995). *The Finite Element Method for Engineers*. 3rd edition, Wiley Interscience.
- Humboldt (2021). *Pocket Shear Vane, Plastic*. [online] Available at: <https://www.humboldtmfg.com/torvane-shear-tester-set-plastic.html> [accessed: 2020-05-18].
- Hunziker, R.P. (1995). *Fraktionsweiser Geschiebetransport*. Mitteilung Nr. 138, VAW, ETH Zürich. (in German)
- IEA (2007). *Renewables in Global Energy Supply: An IEA Fact Sheet*. International Energy Agency, January 2007.
- International Association of Hydrological Sciences, IAHS (1998). *Sustainable Reservoir Development and Management*. IAHS International Commission on Water Resources Systems.
- International Commission for the Protection of the River Rhine (ICPR) (2009). *Sediment Management Plan Rhine*. Technical Report 175, Koblenz. (in German)
- International Commission on Large Dams – ICOLD (1998). *World register of large dams*. CD ROM.
- International Commission on Large Dams – ICOLD (2009). *Sedimentation and Sustainable Use of Reservoirs and River Systems*. Draft Bulletin 147, Paris, France.

International Commission on Large Dams – ICOLD (2020). World register of large dams. [online] Available at: www.icold-cigb.org [accessed: 18.05.2020].

IPCC (2007). *Climate Change 2007: The Physical Science Basis. Contribution of Working Group I to the Fourth Assessment Report of the Intergovernmental Panel on Climate Change*. Eds.: Solomon, S., Qin, D., Manning, M., Chen, Z., Marquis, M., Averyt, K.B., Tignor, M., and Miller, H.L., Cambridge University Press, Cambridge, United Kingdom and New York, United States of America.

IPCC (Intergovernmental Panel on Climate Change) (2013). *Climate change 2013: The physical science basis*. Working Group I contribution to the IPCC Fifth Assessment Report. Cambridge, United Kingdom: Cambridge University Press. www.ipcc.ch/report/ar5/wg1.

Jacobsen, T. (1997). *Sediment problems in reservoirs: Control of sediment deposits*. Doctoral thesis, Norwegian University of Science and Technology, Trondheim, Norway.

Jain, S.C. (1990). Armor or Pavement. *Journal of Hydraulic Engineering* 116(3): 436-440.

Jansson, M. (1988). A global survey of sediment yield. *Geografiska Annaler Series A Physical Geography* 70: 81-98

Jansson, M.B., and Rodriguez, A. (1992). *Sedimentological studies in the Cachì Reservoir, Costa Rica*. UNGI Rapport 81; Uppsala University, Department of Physical Geology.

Jenzer Althaus, J., and De Cesare, G. (2006). *Reservoir sedimentation*. Interreg III Alpreserv Project Sustainable Sediment Development in Alpine Reservoirs considering ecological and economical aspects, Volume 3/2006: 1862–9636.

Jimenez, A. (2012). Sediment problems at La Garita run-of-river plant, Costa Rica. *The International Journal on Hydropower & Dams* 19(1).

Johnson, C. (1987). *Numerical Solutions of Partial Differential Equations by the Finite Element Method*. Cambridge, Cambridge University Press, United Kingdom.

Jutzeler, M., White, J.D.L. Talling, P.J., McCanta, M., Morgan, S., Le Friant, A., and Ishizuka, O. (2014). Coring disturbances in IODP piston cores with implications for offshore record of volcanic events and the Missoula megafloods. *Geochemistry, Geophysics, Geosystems* 15: 3572–3590.

Kalotay, P. (1999). Density and viscosity monitoring systems using Coriolis flow meters. *ISA Transactions* 38:303-310

Kamphuis, J., and Hall, K. (1983). Cohesive material erosion by unidirectional current. *Journal of Hydraulic Engineering* 109(1).

Kantoush, S.A. (2008). *Experimental Study on the Influence of the Geometry of Shallow Reservoirs on Flow Patterns and Sedimentation by Suspended Sediments*. Doctoral thesis, Ecole Polytechnique Fédérale de Lausanne (EPFL), Lausanne, Switzerland.

Kell, G.S. (1975). Density, thermal expansivity, and compressibility of liquid water from 0.deg. to 150.deg.. Correlations and tables for atmospheric pressure and saturation reviewed and expressed on 1968 temperature scale. *Journal of Chemical & Engineering Data*, American Chemical Society 20(1): 97–105.

- Keller, M. (2008). *Contaminated Sediments in the Rhine Basin – Relevant Pollutants and Resuspension Risk*. Proceedings: CHR/ISI Sediment Workshop, Bern, Switzerland.
- Kennedy, R.H., and Walker, W.W. (1990). *Reservoir nutrient dynamics*. Reservoir limnology: Ecological perspective. Wiley.
- Kerr, D.E. (ed.) (1951). *Propagation of Short Radio Waves. M.I.T. Radiation Laboratory Series*. McGraw-Hill Book Company, New York, United States of America.
- Kikkawa, H., Ikeda, J., and Kitagawa, A. (1976). Flow and bed topography in curved open channels. *Journal of Hydraulic Engineering* 102(9):1327–1342.
- Kinnell, P.I.A. (2010). Event soil loss, runoff and the Universal Soil Loss Equation family of models: A review. *Journal of Hydrology* 385(1):384-397.
- Kinnell, P.I.A. (2010). The effect of slope length on sediment concentrations associated with side-slope erosion. *Soil Science Society of America Journal* 64(3):1004-1008.
- Kinsler, L.E., Frey, A.R., Coppins A.B., and Sanders, J.V (1980). *Fundamentals of Acoustics*. 3rd Edition, John Wiley and Sons, New York, United States of America.
- Kirchner, J.W., Dietrich, W.E., Iseya, F., and Ikeda, H. (1990). The variability of critical shear stress, friction angle, and grain protrusion in water worked sediments. *Sedimentology* 37:647-672.
- Klassen, I. (2017). *Three-dimensional Numerical Modeling of Cohesive Sediment Flocculation Processes in Turbulent Flows*. Doctoral thesis, Karlsruhe Institute of Technology, Karlsruhe, Germany.
- Kleijnen, J.P.C. (1995). Verification and validation of simulation models. *European Journal of Operational Research* 82:145–162.
- Klein, S., Worch, E., and Knepper, T.P. (2015). Occurrence and Spatial Distribution of Microplastics in River Shore Sediments of the Rhine-Main Area in Germany. *Environmental Science Technologie* 49: 6070–6076.
- Komar, P.D., and Carling, P.A. (1991). Grain sorting in gravel-bed streams and the choice of particle sizes for flow-competence evaluations. *Sedimentology* 38:489-502.
- Kondolf, G. M., Gao, Y., Annandale, G.W., Morris, G.L., Jiang, E., Zhang, J., Cao, Y., Carling, P., Fu, K., Guo, Q., Hotchkiss, R., Peteuil, Ch., Sumi; T., Wang, H-W, Wang, Z., Wei, Z., Wu, B., Wu, C., and Yang, T. (2014). Sustainable sediment management in reservoirs and regulated rivers: Experiences from five continents. *Earth's Future* 2:256–280.
- Kopmann, R., and Schmidt, A. (2008). *Reliability analysis of two-dimensional morphodynamic model results*. Proceedings of the 4th International Conference on Fluvial Hydraulics, River flow 2008, Çeşme, Izmir, Turkey.
- Kopmann, R., and Schmidt, A. (2010). *Comparison of different reliability analysis methods for a 2D morphodynamic numerical model of River Danube*. Proceedings: 5th International Conference on Fluvial Hydraulics, River flow 2010, Braunschweig, Germany.
- Kothyari, U., and Jain, R. (2010). *Erosion characteristics of cohesive sediment mixtures*. Proceedings: 5th International Conference on Fluvial Hydraulics, River flow 2010, Braunschweig, Germany

- Kothyari, U.C., and Jain, R. K. (2008). Influence of cohesion on the incipient motion conditions of sediment mixtures. *Water Resources Research* 44:W04410.
- Kranenburg, C., and Winterwerp, J. C. (1997). Entrainment of fluid mud layers, I: Entrainment model. *Journal of Hydraulic Engineering* 123(6):504–511.
- Krishnappan, B.G., and Droppo, I.G. (2006). Use of an in situ erosion flume for measuring stability of sediment deposits in Hamilton Harbour, Canada. *Water, Air, & Soil Pollution: Focus volume 6*:557-567.
- Kumar, A., Schei, T., Ahenkorah, A., Caceres Rodriguez, R., Devernay, J.-M., Freitas, M., Hall, D., Killingtveit, Å., and Liu, Z. (2011). *Hydropower. In IPCC Special Report on Renewable Energy Sources and Climate Change Mitigation*. Eds.: Edenhofer, O., Pichs-Madruga, R., Sokona, Y., Seyboth, K., Matschoss, P., Kadner, S., Zwickel, T., Eickemeier, P., Hansen, G., Schlömer, S., von Stechow, C., Cambridge University Press, Cambridge, United Kingdom and New York, United States of America.
- Kuwata, Y., and Suga, K. (2016). Transport mechanism of interface turbulence over porous and rough walls. *Flow, Turbulence and Combustion* 97:1071–109.
- Lai, J., and Shen, H. (1996). Flushing sediments through reservoirs. *Journal of Hydraulic Research* 34(2):237-255.
- Lamb, M. P., Dietrich, W. E., and Venditti, J.G. (2008). Is the critical Shields stress for incipient sediment motion dependent on channel-bed slope?. *Journal of Geophysical Research* 113:F02008.
- Lane, E.W. (1955). *The importance of fluvial morphology in hydraulic engineering*. Proceedings of the American Society Civil Engineers 81, Paper 745.
- Lang, T., and Overhoff, G. (2018). Der Sylvensteinspeicher – Nachrüstungen. *Wasserwirtschaft* 6:30-34. (in German)
- Laronne, J., and Carson, M. (1976). Interrelationships between bed morphology and bed material transport for a small, gravel-bed channel. *Sedimentology* 23:67–85.
- Latosinski, F., Szupiany, R., García, C., Guerrero, M., and Amsler, M. (2014). Estimation of Concentration and Load of Suspended Bed Sediment in a Large River by Means of Acoustic Doppler Technology. *Journal Hydraulic Engineering* 140(7):04014023.
- Launder, B.E., and Spalding, D.B. (1972). *Lectures in mathematical models of turbulence*. Academic Press, London, United Kingdom.
- Lebreton, et al. (2018). Evidence that the Great Pacific Garbage Patch is rapidly accumulating plastic. *Nature - Scientific Reports* 8.
- Lee, H., Shim, W.J., and Kwon, J.H. (2014). Sorption capacity of plastic debris for hydrophobic organic chemicals. *Science of the Total Environment* 470: 1545-1552.
- Lee, J., Liu, J.T., Hung, C.C., Lin, S., and Du, X. (2016). River plume induced variability of suspended sediment particle characteristics. *Marine Geology* 380:219–230.
- Lehner, B., Liermann, C.R., Revenga, C., Vörösmarty, Ch., Fekete, B., Crouzet, Ph., Döll, P., Endejan, M., Frenken, K., Magome, J., Nilsson, Ch., Robertson, J.C., Rödel, R., Sindorf, N., and Wisser, D. (2011). *Global Reservoir and Dam (GRanD) database*. Technical documentation, Version 1.1, March 2011.
- Lehner, B., Liermann, C.R., Revenga, C., Vörösmarty, Ch., Fekete, B., Crouzet, Ph., Döll, P., Endejan, M., Frenken, K., Magome, J., Nilsson, Ch., Robertson, J.C., Rödel, R., Sindorf, N. and Wisser, D. (2011b).

High-resolution mapping of the world's reservoirs and dams for sustainable river-flow management. *Frontiers in Ecology and the Environment* 9:494–502.

Lenzi, M.A., Mao, L., and Comiti, F. (2006). When does bedload transport begin in steep boulder-bed streams? *Hydrological Processes* 20:3517-3533.

Leonardi, S., Orlandi, P., Smalley, R.J., Djenidi, L., and Antonia, R.A. (2003). Direct numerical simulations of turbulent channel flow with transverse square bars on one wall. *Journal of Fluid Mechanics* 491:229–238.

Liedermann, M., Gmeiner, Ph., Pessenlehner, S., Haimann, M., Hohenblum, Ph., and Habersack, H. (2018). A Methodology for Measuring Microplastic Transport in Large or Medium Rivers. *Water* 10(4):414.

Lima, I.B.T., Ramos, F.M., Bambace, L.A.W., and Rosa, R.R. (2008). Methane Emissions from Large Dams as Renewable Energy Resources: A Developing Nation Perspective. *Mitigation and Adaptation Strategies for Global Change* 13:193–206.

Liptak, B.G. (2003). *Instrument Engineers' Handbook, Volume One: Process Measurement and Analysis*. Fourth Edition, CRC press, Boca Raton, United States of America.

Lu, H., Moran, C.J., and Sivapalan, M. (2005). A theoretical exploration of catchment-scale sediment delivery. *Water Resources Research* 41(9).

Lu, X.X., Ran, L.S., Liu, S., Jiang, T., Zhang, S.R., and Wang, J.J. (2013). Sediment loads response to climate change: A preliminary study of eight large Chinese rivers. *International Journal of Sediment Research* 28(1):1-14.

Luo, Y., Guo, W., Ngo, H.H., Long Duc, N., Hai, F.I., Zhang, J., Liang, S., and Wang, X.C. (2014). A review on the occurrence of micropollutants in the aquatic environment and their fate and removal during wastewater treatment. *Science of the Total Environment* 473:619-641.

Lurton, X. (2010). *An Introduction to Underwater Acoustics - Principles and Applications*. Second Edition, Springer-Verlag Berlin, Heidelberg, Germany.

Lynch, J.F., Irish, J.D., Sherwood, C.R., and Agrawal, Y.C. (1994). Determining suspended sediment particle size information from acoustical and optical backscatter measurements. *Continental Shelf Research* 14(10-11):1139-1165.

Lysne, D., Glover, B. Stole, H., and Tesakar, E. (2003). *Hydraulic Design. Publication No. 8*. Norwegian Institute of Technology, Trondheim, Norway.

Maa, J.P.-Y., Wright, L.D., Lee, C.-H., and Shannon, T.W. (1993). VIMS Sea Carousel: A field instrument for studying sediment transport. *Marine Geology* 115:271-287.

MacArtney Germany GmbH (2020). *Das Frahm-Lot – leichtes Gerät für unsichere Tiefen*. [Online]. Accessed: 04.10.2020. <https://www.macartney.de/nachrichten/das-frahm-lot-leichtes-geraet-fuer-unsichere-tiefen/49e47598814ac2f62f91c69767b08a8d/>. (in German)

Maddock, T., and Borland, W.M. (1950). *Sedimentation Studies for the Planning of Reservoirs by the Bureau of Reclamation*. Bureau of Reclamation, Hydrology Division, 1950, United States of America.

- Maeck, A., DelSontro, T., McGinnis, D.F., Fischer, H., Flury, S., Schmidt, M., Fietzek, P., and Lorke, A. (2013). Sediment Trapping by Dams Creates Methane Emission Hot Spots. *Environmental Science & Technology* 47:8130–8137.
- Maggi, F. (2005). *Flocculation Dynamics of cohesive sediment*. Doctoral thesis, Delft University of Technology, Delft, The Netherlands.
- Mahmood, K. (1987). *Reservoir sedimentation: impact, extent and mitigation*. World Bank Technical Paper. 71, Washington D.C., United States of America.
- Malvern Instruments Ltd. (2021). *Geologists use Mastersizer 2000*. [online] Available at: <https://www.malvernpanalytical.com/en/about-us/press-releases/news/PR1669GeologyMastersizer2000.html> [accessed: 2020-05-18].
- Mandlburger, G., Hauer, C., Wieser, M., and Pfeifer, N. (2015). Topo-Bathymetric LiDAR for Monitoring River Morphodynamics and Instream Habitats—A Case Study at the Pielach River. *Remote Sensing* 7(5):6160-6195.
- Mankin, J.S., Viviroli, D., Singh, D., Hoekstra, A.Y. and Diffenbaugh, N.S. (2015). The potential for snow to supply human water demand in the present and future. *Environmental Research Letters* 10: 114016.
- Manzenrieder, H. (1983). *Biological stabilization effects on wadden areas from engineering point of view*. Doctoral thesis, Technical University of Braunschweig, Braunschweig, Germany.
- Marshak, S. (2018). *Earth: Portrait of a Planet*. Sixth International Student Edition, WW Norton & Co., New York, United States of America.
- Martin, J.M., and Meybeck, M. (1979). Elemental mass-balance of material carried by major world rivers. *Marine Chemistry* 7:173– 206.
- Mavriplis, D.J. (1996). *Mesh Generation and adaptivity for complex geometries and flows*. Handbook of Computational Fluid Mechanics, Academic Press, Cambridge, United States of America.
- Mayar, M.A.; Schmid, G., Wieprecht, S., and Noack, M. (2020). Proof-of-Concept for Nonintrusive and Undisturbed Measurement of Sediment Infiltration Masses Using Gamma-Ray Attenuation. *Journal of Hydraulic Engineering* 146(5):04020032
- McAnally, W.H. (2000). *Aggregation and Deposition of Estuarial Fine Sediment*. Technical report, U.S Army Engineer Research and Development Center, United States of America.
- McAnally, W.H., and Metha, A. J. (2001). Coastal and Estuarine Fine Sediment Processes. *Proceedings in Marine Science* 507:3.
- Mead, A.A., Demas, C.R., Ebersole, B.A., Kleiss, B.A., Little, C.D., Meselhe, E.A., Powell, N.J., Pratt, T.C., and Vosburg, B.M. (2012). A water and sediment budget for the lower Mississippi-Atchafalaya River in flood years 2008–2010: Implications for sediment discharge to the oceans and coastal restoration in Louisiana. *Journal of Hydrology* 432: 84–97.
- Mehta, A., Hayter, E., Parker, W., Krone, R., and Teeter, A. (1989). Cohesive Sediment Transport. I: Process Description. *Journal of Hydraulic Engineering* 115(8):1076-1093.
- Menczel, A., and Kostaschuk, R. (2013). *Interfacial Waves as Coherent Flow Structures associated with Continuous Turbidity Currents: Lillooet Lake, Canada*. In: Venditti, J.G., Best, J.L., Church, M., Hardy R.J., John Wiley & Sons, Ltd., Burnaby, Canada.

- Meyer-Peter, E. and Müller, R. (1948). *Formulas for bed-load transport*. Proceedings: 2nd Meeting of the International Association for Hydraulic Structures Research, Delft, Netherlands.
- Milliman, J.D. and Farnsworth, K.L. (2011). *River Discharge to the Coastal Ocean - A Global Synthesis*. Cambridge University Press, United Kingdom.
- Milliman, J.D., and Syvitski, J.P.M. (1992). Geomorphic/tectonic control of sediment discharge to the ocean: the importance of small mountainous rivers. *Journal of Geology* 100:325–344.
- Mizuyama, T., et al. (2010a). *Calibration of a passive acoustic bedload monitoring system in Japanese mountain rivers*. In: *Bedload-Surrogate Monitoring Technologies*, U.S. Geol. Surv. Sci. Invest. Rep. 2010-5091, Eds.: Gray, J.R., Laronne, J.B., and Marr, J.D., U.S. Geol. Surv., Reston, United States of America.
- Mizuyama, T., Oda, A., Laronne, J.B., Nonaka, M., and Matsuoka, M. (2010b). *Laboratory tests of a Japanese pipe geophone for continuous acoustic monitoring of coarse bedload*. In: *Bedload-Surrogate Monitoring Technologies*, U.S. Geol. Surv. Sci. Invest. Rep. 2010-5091, Eds.: Gray, J.R., Laronne, J.B., and Marr, J.D., U.S. Geol. Surv., Reston, United States of America.
- Moore, C.J. (2008). Synthetic polymers in the marine environment: A rapidly increasing, long-term threat. *Environmental Research* 108(2):131–139.
- Moorefield Jr., F.D. (2020). *GPS Standard Positioning Service Performance Standard*. Monograph, 5th Edition Pentagon, Washington DC, United States of America.
- Morgan, R.P.C. (2005). *Soil Erosion and Conservation*. Third Edition, Blackwell Publishing, Oxford, United States of America.
- Morris, G.L. (1995). *Reservoir Sedimentation and Sustainable Development in India: Problem Scope and Remedial Strategies*. Proceedings: 6th International Symposium on River Sedimentation, New Delhi, India.
- Morris, G.L. and Fan, J. (1998). *Reservoir Sediment Handbook*. McGraw-Hill Book Co., New York, United States of America.
- Mossa, J. (1996). Sediment dynamics in the lowermost Mississippi River. *Engineering Geology* 45:457–479.
- Mouris, K., Beckers, F., and Haun, S. (2018). *Three-dimensional numerical modeling of hydraulics and morphodynamics of the Schwarzenbach reservoir*. Proceedings: Proceedings: 9th International Conference on Fluvial Hydraulics, River Flow 2018, Lyon, France.
- Muleta, M.K., and Nicklow, J.W. (2005). Sensitivity and uncertainty analysis coupled with automatic calibration for a distributed watershed model. *Journal of Hydrology* 306:127–145.
- Muste, M., Aberle, J., Admiraal, D., Ettema, R., Garcia, M.H., Lyn, D., Nikora, V., and Rennie, C. (2017). *Experimental Hydraulics: Methods, Instrumentation, Data Processing and Management*. Two Volume 1st Edition, CRC Press, Boca Raton, United States of America.
- Muste, M., Kim, D., Gonzalez-Castro, J., Burkhardt, A., and Brownson, Z. (2006). *Near-Transducer Errors in Acoustic Doppler Current Profiler Measurements*. Proceedings: World Environmental and Water Resource Congress 2006, Iowa City, Iowa.

Nakicenovic, N., and Swart, R. (eds.) (2000). *Emissions Scenarios: A Special Report of Working Group III of the Intergovernmental Panel on Climate Change IPCC*. Special Report on Emissions Scenarios. Cambridge University Press, Cambridge and New York, United States of America.

Nichols, M. (2004). A radio frequency identification system for monitoring coarse sediment particle displacement. *Applied Engineering in Agriculture* 20:783–787.

Nizzetto, L., Bussi, G., Futter, M.N., Butterfield, D., and Whitehead, P.G. (2016). A theoretical assessment of microplastic transport in river catchments and their retention by soils and river sediments. *Environmental Science: Processes Impacts* 18:1050.

NOAA (2008). *What is lidar?* [online] Available at: <https://oceanservice.noaa.gov/facts/eutrophication.html>. [Accessed 2020-12-21]

Noack, M., Gerbersdorf, S.U., Hillebrand, G., and Wieprecht, S. (2015). Combining Field and Laboratory Measurements to Determine the Erosion Risk of Cohesive Sediments Best. *Water* 7:5061-5077.

Noack, M., Ortlepp, J., and Wieprecht, S. (2017). An Approach to Simulate Interstitial Habitat Conditions during the Incubation Phase of Gravel-Spawning Fish. *River Research and Application* 33: 192–201.

Noack, M., Schmid, G., Beckers, F., Haun, S., and Wieprecht, S. (2018). PHOTOSSED—PHOTOgrammetric Sediment Erosion Detection. *Geosciences* 8:243.

Nowell, A.R.M., McCave, I.N., and Hollister, C.D. (1985). Contributions of Hebble to understanding marine sedimentation. *Marine Geologie* 66:397-409.

Nujic, M. (2003). *HYDRO_AS-2D – Ein zweidimensionales Strömungsmodell für die wasserwirtschaftliche Praxis*. Benutzerhandbuch Version 1.3x. (in German)

Oberkampf, W.L., Trucano, T.G., and Hirsch, C. (2004). Verification, validation, and predictive capability in computational engineering and physics. *Applied Mechanics Reviews* 57:345–384.

Olsen, N.R.B. (1999a). 3D CFD modelling of water and sediment flow in a hydropower reservoir. *International Journal of Sediment Research* 14(1):16–24.

Olsen, N.R.B. (1999b). Two-dimensional numerical modelling of flushing processes in water reservoirs. *Journal of Hydraulic Research* 37(1):3–16.

Olsen, N.R.B. (2000). *CFD Algorithms for Hydraulic Engineering*. Department of Hydraulic and Environmental Engineering, The Norwegian University of Science and Technology, Trondheim, Norway.

Olsen, N.R.B. (2001). *CFD modelling for hydraulic structures*. Department of Hydraulic and Environmental Engineering, The Norwegian University of Science and technology, Trondheim, Norway.

Olsen, N.R.B. (2020). *A Three-Dimensional Numerical Model For Simulate Of Sediment Movements In Water Intakes With Multiblock Option*, User's Manual by Nils Reidar B. Olsen, Department of Hydraulic and Environmental Engineering, The Norwegian University of Science and Technology, Trondheim, Norway.

Olsen, N.R.B., and Hillebrand, G. (2018). Long-time 3D CFD modeling of sedimentation with dredging in a hydropower reservoir. *Journal of Soils and Sediments* 18:3031–3040.

- Olsen, N.R.B., and Haun, S. (2018). *Numerical modelling of bank failures during reservoir draw-down*. Proceedings: Proceedings: 9th International Conference on Fluvial Hydraulics, River Flow 2018, Lyon, France.
- Olsen, N.R.B., and Haun, S. (2020). A numerical geotechnical model for computing soil slides at banks of water reservoirs. *International Journal of Geo-Engineering* 11(22).
- Olsen, N.R.B., and Kjellesvig, H.M. (1998). Three-dimensional numerical flow modelling for estimation of maximum local scour depth. *Journal of Hydraulic Research* 36(4):579–590.
- Oreskes, N., Shrader-Frechette, K., and Belitz, K. (1994). Verification, validation, and confirmation of numerical models in the earth sciences. *Science* 263:641–646.
- Orszag, S.A. (1970). Analytical Theories of Turbulence. *Journal of Fluid Mechanics* 41:363–386.
- OSIL (2020). *Vibrocorer (3m-12m)*. [online] Available at: <https://osil.com/product/vibrocorer-3m-12m/> [accessed: 2020-10-04].
- Owens, P., and Slaymaker, O. (1994). Post-glacial temporal variability of sediment accumulation in a small alpine lake. *International Association of Hydrological Science Publication* 224:187-195.
- Pachur, H.J., Denner, H.D., and Walter, H. (1984). A freezing device for sampling the sediment-water interface of lakes. *Catena* 11:65–70.
- Palmieri, A., Shah, F., Annandale, G., and Dinar, A. (2003). *Reservoir Conservation Volume I: The RESCON Approach Economic and engineering evaluation of alternative strategies for managing sedimentation in storage reservoirs*. The International Bank for Reconstruction and Development, The World Bank, Washington, United States of America.
- Paola, C., and Voller, V.R. (2005). A generalized Exner equation for sediment mass balance. *Journal of Geophysical Research* 110.
- Papanicolaou, A., Elhakeem, M., Krallis, G., and Edinger, J. (2008). Sediment Transport Modelling Review - Current and Future Developments. *Journal of Hydraulic Engineering* 134(1):1-14.
- Parker, G. (1990). Surface-based bedload transport relation for gravel rivers, *Journal of Hydraulic Research* 28:417–436.
- Parker, G. (1991). Selective sorting and abrasion of river gravel. I: Theory. *Journal of Hydraulic Engineering* 117(2):131-147.
- Parker, G. (2006). *1D Sediment Transport Morphodynamics with applications to Rivers and Turbidity Currents, Chapter 1*. [online] Available at: http://vtchl.uiuc.edu/people/parkerg/_private/e-bookPowerPoint/RTe-bookCh1IntroMorphodynamics.ppt Archived 2011-10-08 at the Wayback Machine [accessed: 2020-10-04].
- Parker, G., Fukushima, Y., and Pantin, H. M. (1986). Self-accelerating turbidity currents. *Journal of Fluid Mechanics* 171:145-181.
- Parker, G., Klingeman, P.C., and McLean D.G. (1982). Bedload and Size Distribution in Paved Gravel-Bed Streams. *Journal Hydraulics Division ASCE* 108:544-571.
- Parker, G., Paola, C., and Leclair, S. (2000). Probabilistic Exner Sediment Continuity Equation for Mixtures with no Active Layer. *Journal of Hydraulic Engineering* 126(11).

- Patankar, S.V. (1980). *Numerical Heat Transfer and Fluid Flow*. Hemisphere Publishing Corporation, United States of America.
- Paterson, D.M. (1989). Short-term changes in the erodibility of intertidal cohesive sediments related to the migratory behaviour of epipelagic diatoms. *Limnology and Oceanography* 34(1):223-234.
- Peirce, T.J., Jarman, R.T., and de Turville, C.N. (1970). An experimental study of silt scouring. *Proceedings of the Institute of Civil Engineering* 45:231-243.
- Peng, R., and Niu, J. (1987). Numerical model of headwater erosion on bed load. *Journal of Sediment Research* 3. (in Chinese)
- Peteuil, Ch. (2018). Sustainable Management of Sediment Fluxes in the Rhône River Cascade. *Hydrolink* 4:80-82.
- Plate, E.J. (1993). Sustainable Development of Water Resources: A Challenge to Science and Engineering. *Water International* 18(2):84-94.
- Plew, D., Debnath, K., Aberle, J., Nikora, V., and Cooper, G. (2007). *In situ flume for studying cohesive and non-cohesive sediment erosion*. Proceedings: XXXII IAHR Congress, Venice, Italy.
- Pohlert, T., Hillebrand, G., and Breitung, V. (2011). Trends of persistent organic pollutants in the suspended matter of the river rhine. *Hydrological Processes* 25:3803–3817.
- Pomázi, F., and Baranya, S. (2020). Comparative Assessment of Fluvial Suspended Sediment Concentration Analysis Methods. *Water* 12:873.
- Prandtl, L. (1925). *Bericht über Untersuchungen zur ausgebildeten Turbulenz*. Zs. Angew. Math. Mech. 2, Germany.
- Purnomo, S.E. (2018). *3D numerical modelling of shallow reservoirs*. Master's thesis. University of Stuttgart, Stuttgart, Germany.
- Pye, K. (1994). *Sediment transport and depositional processes*. Blackwell Scientific Publications, Oxford, Boston, United States of America.
- Rashid, F. (2020). *Numerical Modeling of Long-Term Sedimentation in Reservoirs*. Master's thesis. Amirkabir University of Technology, Iran.
- Ravens, T.M., and Gschwend, P.M. (1999). Flume measurements of sediment erodibility in Boston Harbor. *Journal of Hydraulic engineering* 125(10):998-1005.
- Ravens, T.M., and Gschwend, P.M. (1999). Flume measurements of sediment erodibility in Boston Harbor. *Journal of Hydraulic Engineering* 125:998–1005.
- RD Instruments (1999). *Acoustic Doppler Current Profiler, Principles of Operation A Practical Primer*. San Diego, CA, USA. Deployment In: www.rdinstruments.com/rdi_library.aspx.
- Rebba, R., Mahadevan, S., and Huang, S. (2006). Validation and error estimation of computational models. *Reliability Engineering and System Safety* 91:1390–1397.
- Reisenbühler, M., Bui, M.D., Skublics, D., and Rutschmann, P. (2020). Sediment Management at Run-of-River Reservoirs Using Numerical Modelling. *Water* 12:249.
- Renard, K.G., Foster, G.R., Weesies, G.A., and Porter, J.P. (1991). Revised universal soil loss equation. *Journal of Soil and Water Conservation* 46(1).

- Renard, K.G., Yoder, D.C., Lightle, D.T., and Dabney, S.M. (2011). *Universal soil loss equation and Revised universal loss equation – Handbook of soil erosion modelling*. First Edition, Blackwell Publishing Ltd., New Jersey, United States of America.
- Rennie, C., and Villard, P.V. (2004). Site specificity of bed load measurement using an acoustic Doppler current profiler. *Journal of Geophysical Research* 109(F03003).
- Rennie, C.D., Millar, R.G., and Church, M.A. (2002b). Measurement of bed load velocity using an acoustic doppler current profiler. *Journal of Hydraulic Engineering* 5(128):473-483.
- Reynolds, O. (1895). On the Dynamical Theory of Incompressible Viscous Fluids and the Determination of the Criterion. *Philosophical Transactions of the Royal Society of London A*. 186:123–164.
- Rheinheimer, D.E., and Yarnell, S.M. (2017). *Chapter 12 - Tools for Sediment Management in Rivers*. In: Avril C. Horne, J. Angus Webb, Michael J. Stewardson, Brian Richter, Mike Acreman (eds.): *Water for the Environment*, Academic Press: 237-263.
- Rickenmann, D. (1997). Sediment transport in Swiss torrents. *Earth Surface Processes and Landforms* 22:937–951.
- Rickenmann, D. (2017). Bed-Load Transport Measurements with Geophones and Other Passive Acoustic Methods. *Journal of Hydraulic Engineering* 143(6).
- Rickenmann, D., Turowski, J.M., Fritschi, B., Klaiber, A., and Ludwig, A. (2012). Bedload transport measurements at the Erlenbach stream with geophones and automated basket samplers. *Earth Surface Processes and Landforms* 37(9):1000–1011.
- RIEGL (2020). *Bathymetric scan data captured with RIEGL VQ-840-G. Point cloud by RIEGL Laser Measurement Systems*. RIEGL - RIEGL Laser Measurement Systems. [online] Available at: <http://www.riegl.com/nc/products/airborne-scanning/produktdetail/product/scanner/63/>. [Accessed 2021-04-19].
- Righetti, M., and Lucarelli, C. (2010). Resuspension phenomena of benthic sediments: The role of cohesion and biological adhesion. *River Research and Applications* 26(4): 404–413.
- Ring, J. (1963). The Laser in Astronomy. *New Scientist*, June 1963: 672–73, United States of America.
- Rodi, W. (1984). *Turbulence Models and their Application in Hydraulics*. IAHR State-of-the-art paper.
- Rothwell, R.G., and Rack, F.R. (2006). New techniques in sediment core analysis: an introduction. *Geological Society London, Special Publications* 267:1-29.
- Rouse, H. (1937). Modern conceptions of the mechanics of fluid turbulence. *Transactions of the American Society of Civil Engineers* 102: 463–554.
- Roux, P., and Kuperman, W.A. (2004). NPAL Group: Extracting coherent wave fronts from acoustic ambient noise in the ocean. *The Journal of the Acoustical Society of America* 116: 1995–2003.
- Rubey, W. (1933). Settling velocities of gravel, sand and silt particles. *American Journal of Science* s5–25(148):325–338.
- Rüther, N. (2006). *Computational fluid dynamics in fluvial sedimentation engineering*. Doctoral thesis, Norwegian University of Science and technology, Trondheim, Norway.
- Ryan, S.E., Dwire, K.A., and Dixon, M.K. (2011). Impacts of wildfire on runoff and sediment loads at Little Granite Creek, western Wyoming. *Geomorphology* 129(1–2):113-130.

- Saam, L., Mouris, K., Wieprecht, S., and Haun, S. (2019). *Three-dimensional numerical modelling of reservoir flushing to obtain long-term sediment equilibrium*. Proceedings: 38th IAHR World Congress, Panama City, Panama.
- Sadid, N., Beckers, F., Noack, M., Haun, S., and Wieprecht, S. (2016). *An Evolution Volume Balance Approach to Determine Relevant Discharge Threshold for Bed Load Transport*. In: M. Rowiński, Paweł; Marion, Andrea (eds.): *Hydrodynamic and Mass Transport at Freshwater Aquatic Interfaces*. Schriftenreihe Geotechnik, Springer, Switzerland.
- Saint-Venant, A.J.C. Barré de (1871). *Théorie du mouvement non permanent des eaux, avec application aux crues des rivières et à l'introduction de marées dans leurs lits*. *Comptes Rendus de l'Académie des Sciences* 73:147–154 and 237–240. (in French)
- Sanchez, W., Bender, C., and Porcher, J.M. (2014). Wild gudgeons (*Gobio gobio*) from French rivers are contaminated by microplastics: Preliminary study and first evidence. *Environmental Research* 128: 98-100.
- Sanford, L.P., and Halka, J.P. (1993). Assessing the paradigm of mutually exclusive erosion and deposition of mud, with examples from upper Chesapeake Bay. *Marine Geology* 37–57.
- Sargent, R.G. (2013). Verification and validation of simulation models. *Journal of Simulation* 7: 12–24.
- Sassi, M.G., Hoitink, A.J.F., and Vermeulen, B. (2012). Impact of sound attenuation by suspended sediment on ADCP backscatter calibrations. *Water Resources Research* 48(9):W09520.
- Schaelchli, U. (1993). *Die Kolmation von Fließgewässersohlen: Prozesse und Berechnungsgrundlagen*. Doctoral thesis, ETH Zürich, Zürich, Switzerland. (in German)
- Schaelchli, U. (2002). *Kolmation - Methoden zur Erkennung und Bewertung*. EAWAG - Eidgenössische Anstalt für Wasserversorgung, Abwasserreinigung und Gewässerschutz (EAWAG), Zürich, Switzerland.
- Schäfer Rodrigues Silva, A., Noack, M., Schlabing, D., and Wieprecht, S. (2018). A data-driven fuzzy approach to simulate the critical shear stress of mixed cohesive/non-cohesive sediments. *Journal of Soils and Sediments* 18:3070–3081.
- Scherer, Ch., Weber, A., Stock, F., Vurusic, S., Egerci, H., Kochleus, Ch., Arendt, N., Foeldi, C., Dierkes, G., Wagner, M., Brennholt, N., and Reifferscheid, G. (2020). Comparative assessment of microplastics in water and sediment of a large European river. *Science of The Total Environment* 738:139866.
- Scheuerlein, H. (1990). *Removal of sediment deposits in reservoirs by means of flushing*. Proceedings: International Conference on Water Resources in Mountainous Regions, Symp. 3: Impact of Artificial Reservoirs on Hydrological Equilibrium, Lausanne, Switzerland.
- Schleiss, A., De Cesare, G., and Jenzer Althaus, J. (2010). Verlandung der Stauseen gefährdet dienachhaltige Nutzung der Wasserkraft. *WasserEnergie Luft* 102(1):31-40.
- Schlichting, H. (1979). *Boundary layer theory*. McGraw-Hill Book Company, New York, United States of America.
- Schneider, J., Badura, H., and Harb, G. (2012a). *Encyclopedia of Lakes & Reservoirs, chapter Turbidity Currents in Reservoirs*, pages 820 – 826. Springer, The Netherlands.

- Schneider, J., Hegglin, R., Meier, S., Turowski, J., Nitsche, M., and Rickenmann, D. (2010). *Studying sediment transport in mountain rivers by mobile and stationary RFID antennas*. Proceedings: 5th International Conference on Fluvial Hydraulics, River flow 2010, Braunschweig, Germany.
- Schneider, J., Turowski, J., Rickenmann, D., Hegglin, R., Arrigo, S., Mao, L., and Kirchner J. (2014). Scaling relationships between bed load volumes, transport distances, and stream power in steep mountain channels. *Journal of Geophysical Research Earth Surface* 119(3): 533–549.
- Schneider, J.M., Rickenmann, D., Turowski, J., Schmid, B., and Kirchner, J.W. (2016). Bed load transport in a very steep mountain stream (Riedbach, Switzerland): Measurement and prediction. *Water Resources Research* 52(12):9522–9541.
- Schoklitsch, A. (1935). *Stauraumverlandung und Kolkabwehr*. Springer Verlag, Vienna, Austria. (in German)
- Schuetz, M. (2020). *Potree - WebGL point cloud viewer for large datasets*. [online] Available at: <https://github.com/potree/potree> [Accessed 2021-04-19].
- Schünemann, M., and Kühl, H. (1991). *A device for erosion-measurements on naturally formed, muddy sediments: The EROMES-System*. GKSS Report GKSS 91/E/18, Geesthacht, Germany.
- Schwarzenbach, R.P., Escher, B.I., Fenner, K., Hofstetter, T.B., Johnson, C.A., von Gunten, U., and Wehrli, B. (2006). The challenge of micropollutants in aquatic systems. *Science* 313(5790):1072-1077.
- Scoffin, T.P. (1968). An underwater flume. *Journal of Sedimentary Petrology* 38:244-246.
- Sedicon AS (2013). *Reference project 2013: SediCon Dredgefor Banja reservoir, Albania*. [online] Available at: <https://sedicon.no/wp-content/uploads/2017/09/2015-Banja-Albania-Dredge-new.pdf>. [Accessed 2020-06-01].
- Seitz, L., Haas, C., Noack, M., and Wieprecht, S. (2018). From picture to porosity of river bed material using Structure-from-Motion with Multi-View-Stereo. *Geomorphology* 306:80–89.
- Seitz, L., Lenz, I., Noack, M., Wieprecht S., and Haas, C. (2019). Kolmation - Eine unterschätzte Größe in der Gewässerbewertung? *Wasserwirtschaft* 109:41-46 (in German).
- Seitz, L., Noack, M., Haun, S., Reindl, R., Senn, G., and Schletterer, M. (2017). *Analysing sediment characteristics of the alpine River Brixentaler Ache (Austria) including in-situ measurements of dissolved oxygen*. Proceedings: 13th International Symposium on River Sedimentation, Stuttgart, Germany. Published by CRC Press, London, United Kingdom.
- Shan, J., and Toth, Ch.K. (2018). *Topographic Laser Ranging and Scanning: Principles and Processing*. 2nd Edition, CRC Press, Boca Raton, United States of America.
- Shen, G., Yuan, J., and Phanikumar, M. (2020). Direct numerical simulations of turbulence and hyporheic mixing near sediment–water interfaces. *Journal of Fluid Mechanics* 892: A20.
- Shields, A. (1936). *Use of dimensional analysis and turbulence research for sediment transport*. Preussen Research Laboratory for Water and Marine Constructions, Publication no. 26, Berlin, Germany.
- Shoarinezhad, V., Wieprecht, S., and Haun, S. (2020a). Comparison of Local and Global Optimization Methods for Calibration of a 3D Morphodynamic Model of a Curved Channel. *Water* 12:1333.

- Shoarinezhad, V., Wieprecht, S., Kantoush, S., and Haun, S. (2021). *The geometry effect of shallow reservoirs on the sedimentation pattern: numerical analysis of lozenge- and hexagon-shaped reservoirs*. Proceedings: 6th IAHR European Congress, Warsaw, Poland.
- Simons, D.B., and Richardson, E.V. (1966). *Resistance to Flow in Alluvial Channels*, U.S. Geological Survey, Professional Paper 422-J, United States of America.
- Singal, S.P. (ed.) (1997). *Acoustic Remote Sensing Applications*. Lecture Notes in Earth Sciences, 69, Springer, Berlin, Germany.
- Smagorinsky, J. (1963). General Circulation Experiments with the Primitive Equations. *Monthly Weather Review* 91(3):99–164.
- Smoluchowski, M. (1916). Three lectures on diffusion, Brownian molecular motion and coagulation of colloid particles. *Zeitschrift für Physik* 17:557–585. (in German)
- Soulsby, R. (1983). *The bottom boundary layer of shelf seas*. Physical Oceanography of Coastal and Shelf Seas. Elsevier, Amsterdam. The Netherlands.
- Spalart, P., and Allmaras, S. (1992). *A one-equation turbulence model for aerodynamic flows*. Proceedings: 30th Aerospace Sciences Meeting and Exhibit, AIAA, Reno, United states of America.
- Stelczer, K. (1981). Bed Load Transport –theory and practice. *Water Resources Publication* 30-70.
- Stoesser, T. (2010). Physically Realistic Roughness Closure Scheme to Simulate Turbulent Channel Flow over Rough Beds within the Framework of LES. *Journal of Hydraulic Engineering* 136:812–819.
- Stoesser, T., and Nikora, V. (2008). Flow structure over square bars at intermediate submergence: Large-eddy simulation study of bar spacing effect. *Acta Geophysica* 56(3):876–893.
- Stoesser, T., Braun, C., Garcia-Villalba, M., and Rodi, W. (2008). Turbulence structures in flow over two dimensional dunes. *Journal of Hydraulic Engineering* 134(1):42–55.
- Stokes, G.G. (1851). On the effect of the internal friction of fluids on the motion of pendulums. *Cambridge Philosophical Society* 9: 8–106.
- Strand, B. (1994). Summation by Parts for Finite Difference Approximations for d/dx . *Journal of Computational Physics* 110:47-67.
- Stubbs, A., Stoesser, T., and Bockelmann-Evans, B. (2018). Developing an Approximation of a Natural, Rough Gravel Riverbed Both Physically and Numerically. *Geosciences* 8:449.
- Sumi, T. (2000). *Future perspective of dam reservoir sediment management*. Proceedings: Int. Workshop on Reservoir Sedimentation management.
- Sumi, T. (2006). *Reservoir sediment management measures and necessary instrumentation technologies to support them*. Proceedings: 6th Japan-Taiwan Joint Seminar on Natural Hazard Mitigation, Kyoto, Japan.
- Sumi, T. (2008). *Evaluation of Efficiency of Reservoir Sediment Flushing in Kurobe River*. Proceedings: 4th International Conference on Scour and Erosion 2008, Tokyo, Japan.
- Sumi, T., and Kantoush, S. (2011). *Sediment management strategies for sustainable reservoirs*. Proceedings: XX ICOLD Annual meeting, dams and reservoirs under changing challenges, Lucerne, Switzerland.

- Sumi, T., Okano, M., and Takata, Y. (2004). *Reservoir sedimentation management with bypass tunnels in Japan*. Proceedings: 9th International Symposium on River Sedimentation, Yichang, China.
- Surana, K.A., Allu, S., Tenpas, P.W., and Reddy, J.N. (2007). k-version of finite element method in gas dynamics: higher-order global differentiability numerical solutions. *International Journal for Numerical Methods in Engineering* 69(6):1109–1157.
- Sutherland, T., Lane, P., Amos, C., and Downing, J. (2000). The calibration of optical backscatter sensors for suspended sediment of varying darkness levels. *Marine Geology* 162:587–597.
- Syvitski J.P.M., Vörösmarty C.J., Kettner A.J., and Green, P. (2005). Impact of humans on the flux of terrestrial sediment to the global coastal ocean. *Science* 308:376.
- Taylor, T.S. (2020). *Introduction to Laser Science and Engineering*. First Edition, CRC Press, Boca Raton, United States of America.
- Tebaldi, C., Hayhoe, K., Arblaster, J.M., and Meehl, G.A. (2006). Going to the extremes; An intercomparison of model-simulated historical and future changes in extreme events. *Climatic Change* 79:185-211.
- Thevenot, M.M., Prickett, T.L., and Kraus, N.C. (1992). *Tylers Beach, Virginia, Dredged Material Plume Monitoring Project 27 September to 4 October 1991*. Technical Report DRP-92-7, U.S. Army Corps of Engineers, United States of America.
- Thompson, C.E.L., and Amos, C.L. (2002). The impact of mobile disarticulated shells of *Cerastoderma edulis* on the abrasion of a cohesive substrate. *Estuaries* 25(2):204-214.
- Thompson, R.C., Olsen, Y., Mitchell, R.P., Davis, A., Rowland, S.J., John, A.W., McGonigle, D., and Russell, A.E. (2004). Lost at sea: where is all the plastic? *Science* 304(5672):838–838.
- Thornberry-Ehrlich, T.L. (2020). *River Systems and Fluvial Landforms*. Colorado State University. [online] Available at: <https://www.nps.gov/subjects/geology/fluvial-landforms.htm> [Accessed 2021-03-27].
- Thorne, P. D. (1986). Laboratory and marine measurements on the acoustic detection of sediment transport. *Journal of the Acoustical Society of America* 80:899–910.
- Tolhurst, T.J., Black, K.S., Paterson, D.M., Mitchener, H.J. Termaat, G.R., and Shayler, S.A. (2000). A comparison and measurement standardisation of four in situ devices for de-termining the erosion shear stress of intertidal sediments. *Continental Shelf Research* 20:1397-1418.
- Toniolo, H., Parker, G., and Voller, V. (2007). Role of Poned Turbidity Currents in Reservoir Trap Efficiency. *Journal of Hydraulic Engineering* 2007:579–595.
- Topping, D.J., Rubin, D.M., Wright, S.A., and Melis, T.S. (2011). *Field evaluation of the error arising from inadequate time averaging in the standard use of depth-integrating suspended-sediment samplers*. Professional Paper 1774, USGS, Reston, VA, 95, United States of America.
- Tremblay, A., Varfalvy, L. Roehm, Ch., and Garneau, M. (2005). *Greenhouse Gas Emissions — Fluxes and Processes. Hydroelectric Reservoirs and Natural Environments*. Springer-Verlag Berlin Heidelberg, Germany.
- Tritton, D.J. (1988). *Physical Fluid Dynamics*. Oxford University Press, NewYork, United States of America.

- Troy, T.J., Wood, E.F., and Sheffield, J. (2008). An efficient calibration method for continental-scale land surface modeling: Efficient calibration for large-scale land surface modeling. *Water Resources Research* 44(9).
- Tsai, C.-H., and Lick, W. (1986). A portable device for measuring sediment resuspension. *Journal of Great Lakes and Research* 12(4):314-321.
- U.S. Army Corps of Engineers (1998). *SAM Hydraulic Design Package for Channels*. User's Manual. Vicksburg, MS., United States of America.
- U.S. Army Corps of Engineers (2016). *HEC-RAS River Analysis System*. Hydraulic Reference Manual Version 5.0, U.S. Army Corps of Engineers, Institute for Water Resources Hydrologic Engineering Center, United States of America.
- Ullman, S. (1979). The interpretation of structure from motion. *Proceedings of the Royal Society of London* 203(1153):405–426.
- Umeda, M., Yokoyama, K., and Ishikawa, T. (2006). Observation and Simulation of Floodwater Intrusion and Sedimentation in the Shichikashuku Reservoir. *Journal of Hydraulic Engineering* 132(9): 881–891.
- United Nations (2017). *World Population Prospects - Data Booklet - 2017 Revision*. New York: United Nations, United States of America.
- Urban, G., Fütterer, V., Fritz, H., Reif, H., Wunsch, W., and Ried, E. (2006). *80 Jahre Schwarzenbachwerk*. Wissenswertes über und rund um das Rudolf-Fettweis-Werk der EnBW. (in German)
- Urlick, R.J. (1983). *Principles of Underwater Sound*. Third Edition, McGraw-Hill, New York, United States of America.
- USBR (2006). *Erosion and Sedimentation Manual*. U.S. Department of the Interior Bureau of Reclamation Technical Service Center Sedimentation and River Hydraulics Group Denver, Colorado, United States of America.
- Van Cauwenberghe, L., Devriese, L., Galgani, F., Johan, R., and Janssen, C.R. (2015). Microplastics in sediments: A review of techniques, occurrence and effects. *Marine Environmental Research* 111:5–17
- Van Rijn L. C. (1984b) Sediment transport. Part II: suspended load transport. *Journal of Hydraulic Engineering* 110(11):1613–41.
- Van Rijn, L. (1993). *Principles of Sediment Transport in Rivers, Estuaries and Coastal Seas*. Aqua Publications, The Netherlands.
- Van Rijn, L.C. (1984a). Sediment Transport. Part I: Bed load transport. *Journal of Hydraulic Engineering* 110(10):1431–1456.
- Van Rijn, L.C. (1984b). Sediment Transport. Part II: Suspended load transport. *Journal of Hydraulic Engineering* 110(11):1613–1641.
- Van Rijn, L.C. (1984c). Sediment Transport. Part III: Bed forms and alluvial roughness. *Journal of Hydraulic Engineering* 110(12):1733–1754.
- Ven Te, Ch. (1959). *Open-channel hydraulics*. First Edition, McGraw-Hill, New, York, United States of America.

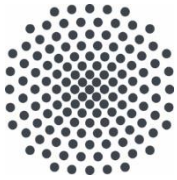
- Versteeg, H.K., and Malalasekera, W. (1995). *An introduction to Computational Fluid Dynamics, The Finite Volume Method*. Pearson Education Limited, Edinburgh, United Kingdom.
- Vetsch, D., Rousselot, P., and Fäh, R. (2011). Flussgebietsmodellierung mit der Simulationssoftware BASEMENT. *Wasser Energie Luft: 4/2011*, 313–319. (in German)
- Vetsch, D., Siviglia, A., Ehrbar, D., Facchini, M., Gerber, M., Kammerer, S., Peter, S., Vonwiller, L., Volz, C., Farshi, D., Mueller, R., Rousselot, P., Veprek, R., and Faeh, R. (2015). *System Manuals of BASEMENT, Version 2.5*. Laboratory of Hydraulics, Glaciology and Hydrology (VAW), ETH Zurich. Switzerland.
- Vidal, J.-P., Moisan, S., Faure, J.-B., and Dartus, D. (2005). Towards a reasoned 1D river model calibration. *Journal of Hydroinformatics* 7:91–104.
- Vidal, J.-P., Moisan, S., Faure, J.-B., and Dartus, D. (2007). River model calibration, from guidelines to operational support tools. *Environmental Modelling and Software* 22:1628–1640.
- Villaret, K. (2005). *User Manual Sisyphé Release 5.5. HP-76/05/009/A*. Department National Hydraulics and Environment Laboratory, Electricité de France, France.
- Violeau, D., Bourban, S., Cheviet, C., Markofsky, M., Petersen, O., Roberts, W., Spearman, J., Toorman, E., Vested, H.J., and Weilbee, H. (2002). *Numerical simulation of cohesive sediment transport: intercomparison of several numerical models*. In: *Fine Sediment Dynamics in the Marine Environment*, Volume 5, Elsevier Science, Amsterdam, The Netherlands.
- Vischer, D., Hager, W.H., Casanova, C., Joos, B., Lier, P., and Martini, O. (1997). *Bypass tunnels to prevent reservoir sedimentation*. Proceedings: 19th Congress of the International Commission on Large Dams (ICOLD), Florence, Italy.
- Vlasblom, W.J. (2005). *Cutter Suction Dredge*. [online] Available at: <http://www.dredging.org/documents/ceda/downloads/vlasblom3-the-cutter-suction-dredger.pdf>. [accessed: 2021-04-17].
- Vörösmarty, C.J., Meybeck, M., Fekete, B., and Sharma, K. (1997). *The potential impact of neo-Castorization on sediment transport by the global network of rivers*. Proceedings: Human Impact on Erosion and Sedimentation, Wallingford, United Kingdom.
- Vörösmarty, C.J., Meybeck, M., Fekete, B., Sharma, K., Green, P., and Syvitski, J.P.M. (2003). *Anthropogenic sediment retention: major global impact from registered river impoundments*. *Global and Planetary Change*, Vol. 39. Amsterdam, Elsevier Science, The Netherlands.
- Vreugdenhil, C.B. (1994). *Numerical Methods for Shallow Water Flow*. Kluwer Academic Publishers, Boston, United States of America.
- Walling, D.E., and Fang, D. (2003). Recent trends in the suspended sediment loads of the world's rivers, *Global and Planetary Change* 39(1–2):111-126.
- Walling, D.E. and Webb, B.W. (1983). *Patterns of sediment yield*. In Gregory, K.J. (ed.), *Background to palæohydrology*. Wiley, Chichester: 69–100.
- Walling, D.E., and Webb, B.W. (1996). *Erosion and Sediment Yield: Global and Regional Perspectives*. IAHS Publication, 236:3–19.
- Wanninger, L. (2020). *Introduction to Network RTK*. [online] Available at: www.wasoft.de. IAG Working Group 4.5.1. [accessed: 2020-10-06].

- Wasserwirtschaftsamt Weilheim (2009). *Der Sylvensteinspeicher*. Flyer. Dr. Tobias Lang, Wasserwirtschaftsamt Weilheim, Weilheim, Germany. (in German)
- Water and Disaster Management Bureau (2013). *Advanced technologies to upgrade Dams under Operation*. Ministry of Land, Infrastructure, Transport and Tourism. [online] Available at: http://www.wec.or.jp/image/130716_saiseigijutsu.pdf. [Accessed 2019-10-24].
- Water Technology (2018). *Grand Ethiopian Renaissance Dam Project, Benishangul-Gumuz*. [online] Available at: <http://www.water-technology.net/projects/grand-ethiopian-renaissance-dam-africa/> [Accessed 2018-03-05].
- Weichert R.B., Wahrheit-Lensing, A., Frings, R.M., Promny, M., and Vollmer, S. (2010). *Morphological characteristics of the river Rhine between Iffezheim and Bingen*. Proceedings: 5th International Conference on Fluvial Hydraulics, River flow 2010, Braunschweig, Germany.
- Wein, E. (2017). *EnBW zieht bei Atdorf den Stöpsel* [online] Available at: <https://www.stuttgarterzeitung.de/inhalt.aus-fuer-pumpspeicherwerk-enbw-zieht-bei-atdorf-den-stoepsel.80b2470a-28a1-4ff0-99cb-ee244a09c7c3.html> [Accessed 2018-03-21].
- Wen Shen, H. (1999). Flushing sediment through reservoirs. *Journal of Hydraulic Research* 37(6):743–757.
- White, R. (2001). *Evacuation of sediments from reservoirs*. Thomas Telford Publishing, United Kingdom.
- White, W., and Bettess, R. (1984). *The feasibility of flushing sediments through reservoirs*. Proceedings: Challenges in African Hydrology and Water Resources of the Harare Symposium, Harare, Simbawe.
- WHO and UNICEF (2017). *Progress on drinking water, sanitation and hygiene: 2017 update and SDG baselines*. Geneva: World Health Organization (WHO) and the United Nations Children’s Fund (UNICEF).
- WHOI (2020). *Grab Sampler (Van Veen)*. [online] Available at: <https://www.whoi.edu/what-we-do/explore/instruments/instruments-sensors-samplers/grab-sampler-van-veen/>. [accessed: 2020-10-04].
- Wiberg, P.L., and Smith, J.D. (1987). Calculations of the critical shear stress for motion of uniform and heterogeneous sediments, *Water Resources Research* 23:1471-1480.
- Widdows, J., Brinsley, M.D., Bowley, N., and Barret, C. (1998). A benthic annular flume for in situ measurement of suspension feeding/biodeposition rates and erosion potential of intertidal cohesive sediments. *Estuarine, Coastal and Shelf Science* 46: 27-38.
- Widdows, J., Friend, P.L., Bale, A.J., Brinsley, M.D., Pope, N.D., and Thompson, C.E.L. (2007). Inter-comparison between five devices for determining erodability of intertidal sediments. *Continental Shelf Research* 27:1174-1189.
- Wieprecht, S. (2001). *Entstehung und Verhalten von Transportkörpern*. In: Feststoffeintrag, Laufentwicklung und Transportprozesse in schiffbaren Flüssen, Bundesanstalt für Gewässerkunde. (in German)
- Wieprecht, S. and the CHARM-Team (2020). The “dirty secrets” of reservoirs. *ACADEMIA - The magazine of the Polish Academy of Sciences* 2(66):62-67.

- Wilcock, P.R., Kenworthy, S.T., and Crowe, J.C. (2001). Experimental study of the transport of mixed sand and gravel. *Water Resources Research* 37(12):3349-3358
- Wilcox, D.C. (2008). Formulation of the $k-\omega$ Turbulence Model Revisited. *AIAA Journal* 46:2823–2838.
- Winter, T.C. (1998). Relation of streams, lakes, and wetlands to groundwater flow systems. *Hydrogeology Journal* 7:28-45.
- Wischmeier, W. H., Johnson, C.B., and Cross, B.V. (1971). A soil erodibility nomograph for farmland and construction sites. *Journal of Soil and Water. Conservation* 26:189-193
- Witt, O., and Westrich, B. (2003). Quantification of erosion rates for undisturbed contaminated cohesive sediment cores by image analysis. *Hydrobiologia* 494:271–276.
- Wölz, J., Engwall, M., Maletz, S., Olsman Takner, H., van Bavel, B., Kammann, U., Klempt, M., Weber, R., Braunbeck, T., and Hollert H. (2008). Changes in toxicity and Ah receptor agonist activity of suspended particulate matter during flood events at the rivers Neckar and Rhine – a mass balance approach using in vitro methods and chemical analysis. *Environmental Science and Pollution Research* 15:536–53.
- Wu, W., Wang, S., and Jia, Y. (2000). Nonuniform sediment transport in alluvial rivers. *Journal of Hydraulic Research* 38(6):427–434.
- Wu., W. (2008). *Computational river dynamics*. Taylor & Francis, London, United Kingdom; New York, United States of America.
- Yalin, S. (1977). *Mechanics of Sediment Transport*. Second Edition, Pergamon Press, New York, United States of America.
- Yang, C. (1984). Unit Stream Power Equation for Gravel. *Journal of Hydraulic Division ASCE* 110:1783-1798.
- Yang, Y., Gao, S., Wang, Y.P., Jia, J. Xiong, J., and Zhou, L. (2019). Revisiting the problem of sediment motion threshold. *Continental Shelf Research* 187:103960.
- Yoon, Y.N. (1992). The state and the perspective of the direct sediment removal methods from reservoirs. *International Journal of Sediment Research* 7(2):99–116.
- Young, R.A. (1977). Seafume: A device for in-situ studies of threshold erosion velocity and erosional behaviour of undisturbed marine muds. *Marine Geology* 23:11-18.
- Yue, W., Lin, C.L., and Patel, V.C. (2006). Large-eddy simulation of turbulent flow over a fixed two-dimensional dune. *Journal of Hydraulic Engineering* 132(7):643–651.
- Zanke, U. (1982). *Grundlagen der Sedimentbewegung*. Springer Verlag Berlin, Heidelberg, Germany; New York, United States of America.
- Zarfl, C., Lumsdon, A.E., Berlekamp, J., Tydecks, L., and Tockner, K. (2015). A global boom in hydropower dam construction. *Aquatic Science* 77(161).
- Zhao, J., Zhao, X., Zhang, H., and Zhou, F. (2017). Shallow Water Measurements Using a Single Green Laser Corrected by Building a Near Water Surface Penetration Model. *Remote Sensing* 9(5):426.
- Zheng, M., Liao, Y., and He, J. (2014). Sediment Delivery Ratio of Single Flood Events and the Influencing Factors in a Headwater Basin of the Chinese Loess Plateau. *PLoS ONE* 9(11).

Ziegler, C.K., and Nisbet, B.S. (1995). Long-Term Simulation of Fine-Grained Sediment Transport in Large Reservoir. *Journal of Hydraulic Engineering* 121:773–781.

Zweckverband Wasserversorgung Kleine Kinzig (2018). *Technische Daten der WKK* [online] Available at: <http://www.zvwkk.de/unternehmen#technische-daten> [Accessed 2018-03-15]. (in German)



Institut für Wasser- und Umweltsystemmodellierung Universität Stuttgart

Pfaffenwaldring 61
70569 Stuttgart (Vaihingen)
Telefon (0711) 685 - 60156
Telefax (0711) 685 - 51073
E-Mail: iws@iws.uni-stuttgart.de
<http://www.iws.uni-stuttgart.de>

Direktoren

Prof. Dr. rer. nat. Dr.-Ing. András Bárdossy
Prof. Dr.-Ing. Rainer Helmig
Prof. Dr.-Ing. Wolfgang Nowak
Prof. Dr.-Ing. Silke Wieprecht

Vorstand (Stand 21.07.2022)

Prof. Dr. rer. nat. Dr.-Ing. A. Bárdossy
Prof. Dr.-Ing. R. Helmig
Prof. Dr.-Ing. W. Nowak
Prof. Dr.-Ing. S. Wieprecht
Prof. Dr. J.A. Sander Huisman
Jürgen Braun, PhD
apl. Prof. Dr.-Ing. H. Class
PD Dr.-Ing. Claus Haslauer
PD Stefan Haun, PhD
apl. Prof. Dr.-Ing. Sergey Oladyshkin
Dr. rer. nat. J. Seidel
Dr.-Ing. K. Terheiden

Emeriti

Prof. Dr.-Ing. habil. Dr.-Ing. E.h. Jürgen Giesecke
Prof. Dr.h.c. Dr.-Ing. E.h. Helmut Kobus, PhD

Lehrstuhl für Wasserbau und Wassermengenwirtschaft

Leiterin: Prof. Dr.-Ing. Silke Wieprecht
Stellv.: Dr.-Ing. Kristina Terheiden
Versuchsanstalt für Wasserbau
Leiter: PD Stefan Haun, PhD

Lehrstuhl für Hydromechanik und Hydrosystemmodellierung

Leiter: Prof. Dr.-Ing. Rainer Helmig
Stellv.: apl. Prof. Dr.-Ing. Holger Class

Lehrstuhl für Hydrologie und Geohydrologie

Leiter: Prof. Dr. rer. nat. Dr.-Ing. András Bárdossy
Stellv.: Dr. rer. nat. Jochen Seidel
Hydrogeophysik der Vadosen Zone
(mit Forschungszentrum Jülich)
Leiter: Prof. Dr. J.A. Sander Huisman

Lehrstuhl für Stochastische Simulation und Sicherheitsforschung für Hydrosysteme

Leiter: Prof. Dr.-Ing. Wolfgang Nowak
Stellv.: apl. Prof. Dr.-Ing. Sergey Oladyshkin

VEGAS, Versuchseinrichtung zur Grundwasser- und Altlastensanierung

Leiter: Jürgen Braun, PhD
PD Dr.-Ing. Claus Haslauer

Verzeichnis der Mitteilungshefte

- 1 Röhnisch, Arthur: *Die Bemühungen um eine Wasserbauliche Versuchsanstalt an der Technischen Hochschule Stuttgart*, und Fattah Abouleid, Abdel: *Beitrag zur Berechnung einer in lockeren Sand gerammten, zweifach verankerten Spundwand*, 1963
- 2 Marotz, Günter: *Beitrag zur Frage der Standfestigkeit von dichten Asphaltbelägen im Großwasserbau*, 1964
- 3 Gurr, Siegfried: *Beitrag zur Berechnung zusammengesetzter ebener Flächentragwerke unter besonderer Berücksichtigung ebener Stauwände, mit Hilfe von Randwert- und Lastwertmatrizen*, 1965
- 4 Plica, Peter: *Ein Beitrag zur Anwendung von Schalenkonstruktionen im Stahlwasserbau*, und Petrikat, Kurt: *Möglichkeiten und Grenzen des wasserbaulichen Versuchswesens*, 1966

- 5 Plate, Erich: *Beitrag zur Bestimmung der Windgeschwindigkeitsverteilung in der durch eine Wand gestörten bodennahen Luftschicht*, und Röhnisch, Arthur; Marotz, Günter: *Neue Baustoffe und Bauausführungen für den Schutz der Böschungen und der Sohle von Kanälen, Flüssen und Häfen; Gesteungskosten und jeweilige Vorteile*, sowie Unny, T.E.: *Schwingungsuntersuchungen am Kegelstrahlschieber*, 1967
- 6 Seiler, Erich: *Die Ermittlung des Anlagenwertes der bundeseigenen Binnenschiffahrtsstraßen und Talsperren und des Anteils der Binnenschifffahrt an diesem Wert*, 1967
- 7 *Sonderheft anlässlich des 65. Geburtstages von Prof. Arthur Röhnisch mit Beiträgen von* Benk, Dieter; Breitling, J.; Gurr, Siegfried; Haberhauer, Robert; Honekamp, Hermann; Kuz, Klaus Dieter; Marotz, Günter; Mayer-Vorfelder, Hans-Jörg; Miller, Rudolf; Plate, Erich J.; Radomski, Helge; Schwarz, Helmut; Vollmer, Ernst; Wildenhahn, Eberhard; 1967
- 8 Jumikis, Alfred: *Beitrag zur experimentellen Untersuchung des Wassernachschubs in einem gefrierenden Boden und die Beurteilung der Ergebnisse*, 1968
- 9 Marotz, Günter: *Technische Grundlagen einer Wasserspeicherung im natürlichen Untergrund*, 1968
- 10 Radomski, Helge: *Untersuchungen über den Einfluß der Querschnittsform wellenförmiger Spundwände auf die statischen und rammtechnischen Eigenschaften*, 1968
- 11 Schwarz, Helmut: *Die Grenztragfähigkeit des Baugrundes bei Einwirkung vertikal gezogener Ankerplatten als zweidimensionales Bruchproblem*, 1969
- 12 Erbel, Klaus: *Ein Beitrag zur Untersuchung der Metamorphose von Mittelgebirgsschneedecken unter besonderer Berücksichtigung eines Verfahrens zur Bestimmung der thermischen Schneequalität*, 1969
- 13 Westhaus, Karl-Heinz: *Der Strukturwandel in der Binnenschifffahrt und sein Einfluß auf den Ausbau der Binnenschiffskanäle*, 1969
- 14 Mayer-Vorfelder, Hans-Jörg: *Ein Beitrag zur Berechnung des Erdwiderstandes unter Ansatz der logarithmischen Spirale als Gleitflächenfunktion*, 1970
- 15 Schulz, Manfred: *Berechnung des räumlichen Erddruckes auf die Wandung kreiszylindrischer Körper*, 1970
- 16 Mobasseri, Manoutschehr: *Die Rippenstützmauer. Konstruktion und Grenzen ihrer Standsicherheit*, 1970
- 17 Benk, Dieter: *Ein Beitrag zum Betrieb und zur Bemessung von Hochwasserrückhaltebecken*, 1970
- 18 Gàl, Attila: *Bestimmung der mitschwingenden Wassermasse bei überströmten Fischbauchklappen mit kreiszylindrischem Staublech*, 1971, vergriffen
- 19 Kuz, Klaus Dieter: *Ein Beitrag zur Frage des Einsetzens von Kavitationserscheinungen in einer Düsenströmung bei Berücksichtigung der im Wasser gelösten Gase*, 1971, vergriffen
- 20 Schaak, Hartmut: *Verteilleitungen von Wasserkraftanlagen*, 1971
- 21 *Sonderheft zur Eröffnung der neuen Versuchsanstalt des Instituts für Wasserbau der Universität Stuttgart mit Beiträgen von* Brombach, Hansjörg; Dirksen, Wolfram; Gàl, Attila; Gerlach, Reinhard; Giesecke, Jürgen; Holthoff, Franz-Josef; Kuz, Klaus Dieter; Marotz, Günter; Minor, Hans-Erwin; Petrikat, Kurt; Röhnisch, Arthur; Rueff, Helge; Schwarz, Helmut; Vollmer, Ernst; Wildenhahn, Eberhard; 1972
- 22 Wang, Chung-su: *Ein Beitrag zur Berechnung der Schwingungen an Kegelstrahlschiebern*, 1972
- 23 Mayer-Vorfelder, Hans-Jörg: *Erdwiderstandsbeiwerte nach dem Ohde-Variationsverfahren*, 1972
- 24 Minor, Hans-Erwin: *Beitrag zur Bestimmung der Schwingungsanfachungsfunktionen überströmter Stauklappen*, 1972, vergriffen

- 25 Brombach, Hansjörg: *Untersuchung strömungsmechanischer Elemente (Fluidik) und die Möglichkeit der Anwendung von Wirbelkammerelementen im Wasserbau*, 1972, vergriffen
- 26 Wildenhahn, Eberhard: *Beitrag zur Berechnung von Horizontalfilterbrunnen*, 1972
- 27 Steinlein, Helmut: *Die Eliminierung der Schwebstoffe aus Flußwasser zum Zweck der unterirdischen Wasserspeicherung, gezeigt am Beispiel der Iller*, 1972
- 28 Holthoff, Franz Josef: *Die Überwindung großer Hubhöhen in der Binnenschifffahrt durch Schwimmerhebwerke*, 1973
- 29 Röder, Karl: *Einwirkungen aus Baugrundbewegungen auf trog- und kastenförmige Konstruktionen des Wasser- und Tunnelbaues*, 1973
- 30 Kretschmer, Heinz: *Die Bemessung von Bogenstaumauern in Abhängigkeit von der Talform*, 1973
- 31 Honekamp, Hermann: *Beitrag zur Berechnung der Montage von Unterwasserpipelines*, 1973
- 32 Giesecke, Jürgen: *Die Wirbelkammertriode als neuartiges Steuerorgan im Wasserbau*, und Brombach, Hansjörg: *Entwicklung, Bauformen, Wirkungsweise und Steuereigenschaften von Wirbelkammerverstärkern*, 1974
- 33 Rueff, Helge: *Untersuchung der schwingungserregenden Kräfte an zwei hintereinander angeordneten Tiefschützen unter besonderer Berücksichtigung von Kavitation*, 1974
- 34 Röhnisch, Arthur: *Einpreßversuche mit Zementmörtel für Spannbeton - Vergleich der Ergebnisse von Modellversuchen mit Ausführungen in Hüllwellrohren*, 1975
- 35 *Sonderheft anlässlich des 65. Geburtstages von Prof. Dr.-Ing. Kurt Petrikat mit Beiträgen von:* Brombach, Hansjörg; Erbel, Klaus; Flinspach, Dieter; Fischer jr., Richard; Gàl, Attila; Gerlach, Reinhard; Giesecke, Jürgen; Haberhauer, Robert; Hafner Edzard; Hausenblas, Bernhard; Horlacher, Hans-Burkhard; Hutarew, Andreas; Knoll, Manfred; Krummet, Ralph; Marotz, Günter; Merkle, Theodor; Miller, Christoph; Minor, Hans-Erwin; Neumayer, Hans; Rao, Syamala; Rath, Paul; Rueff, Helge; Ruppert, Jürgen; Schwarz, Wolfgang; Topal-Gökceli, Mehmet; Vollmer, Ernst; Wang, Chung-su; Weber, Hans-Georg; 1975
- 36 Berger, Jochum: *Beitrag zur Berechnung des Spannungszustandes in rotationssymmetrisch belasteten Kugelschalen veränderlicher Wandstärke unter Gas- und Flüssigkeitsdruck durch Integration schwach singulärer Differentialgleichungen*, 1975
- 37 Dirksen, Wolfram: *Berechnung instationärer Abflußvorgänge in gestauten Gerinnen mittels Differenzenverfahren und die Anwendung auf Hochwasserrückhaltebecken*, 1976
- 38 Horlacher, Hans-Burkhard: *Berechnung instationärer Temperatur- und Wärmespannungsfelder in langen mehrschichtigen Hohlzylindern*, 1976
- 39 Hafner, Edzard: *Untersuchung der hydrodynamischen Kräfte auf Baukörper im Tiefwasserbereich des Meeres*, 1977, ISBN 3-921694-39-6
- 40 Ruppert, Jürgen: *Über den Axialwirbelkammerverstärker für den Einsatz im Wasserbau*, 1977, ISBN 3-921694-40-X
- 41 Hutarew, Andreas: *Beitrag zur Beeinflußbarkeit des Sauerstoffgehalts in Fließgewässern an Abstürzen und Wehren*, 1977, ISBN 3-921694-41-8, vergriffen
- 42 Miller, Christoph: *Ein Beitrag zur Bestimmung der schwingungserregenden Kräfte an unterströmten Wehren*, 1977, ISBN 3-921694-42-6
- 43 Schwarz, Wolfgang: *Druckstoßberechnung unter Berücksichtigung der Radial- und Längsverschiebungen der Rohrwandung*, 1978, ISBN 3-921694-43-4
- 44 Kinzelbach, Wolfgang: *Numerische Untersuchungen über den optimalen Einsatz variabler Kühlsysteme einer Kraftwerkskette am Beispiel Oberrhein*, 1978, ISBN 3-921694-44-2
- 45 Barczewski, Baldur: *Neue Meßmethoden für Wasser-Luftgemische und deren Anwendung auf zweiphasige Auftriebsstrahlen*, 1979, ISBN 3-921694-45-0

- 46 Neumayer, Hans: *Untersuchung der Strömungsvorgänge in radialen Wirbelkammerverstärkern*, 1979, ISBN 3-921694-46-9
- 47 Elalfy, Youssef-Elhassan: *Untersuchung der Strömungsvorgänge in Wirbelkammerdiolen und -drosseln*, 1979, ISBN 3-921694-47-7
- 48 Brombach, Hansjörg: *Automatisierung der Bewirtschaftung von Wasserspeichern*, 1981, ISBN 3-921694-48-5
- 49 Geldner, Peter: *Deterministische und stochastische Methoden zur Bestimmung der Selbstdichtung von Gewässern*, 1981, ISBN 3-921694-49-3, vergriffen
- 50 Mehlhorn, Hans: *Temperaturveränderungen im Grundwasser durch Brauchwassereinleitungen*, 1982, ISBN 3-921694-50-7, vergriffen
- 51 Hafner, Edzard: *Rohrleitungen und Behälter im Meer*, 1983, ISBN 3-921694-51-5
- 52 Rinnert, Bernd: *Hydrodynamische Dispersion in porösen Medien: Einfluß von Dichteunterschieden auf die Vertikalvermischung in horizontaler Strömung*, 1983, ISBN 3-921694-52-3, vergriffen
- 53 Lindner, Wulf: *Steuerung von Grundwasserentnahmen unter Einhaltung ökologischer Kriterien*, 1983, ISBN 3-921694-53-1, vergriffen
- 54 Herr, Michael; Herzer, Jörg; Kinzelbach, Wolfgang; Kobus, Helmut; Rinnert, Bernd: *Methoden zur rechnerischen Erfassung und hydraulischen Sanierung von Grundwasserkontaminationen*, 1983, ISBN 3-921694-54-X
- 55 Schmitt, Paul: *Wege zur Automatisierung der Niederschlagsermittlung*, 1984, ISBN 3-921694-55-8, vergriffen
- 56 Müller, Peter: *Transport und selektive Sedimentation von Schwebstoffen bei gestautem Abfluß*, 1985, ISBN 3-921694-56-6
- 57 El-Qawasmeh, Fuad: *Möglichkeiten und Grenzen der Tropfbewässerung unter besonderer Berücksichtigung der Verstopfungsanfälligkeit der Tropfelemente*, 1985, ISBN 3-921694-57-4, vergriffen
- 58 Kirchenbaur, Klaus: *Mikroprozessorgesteuerte Erfassung instationärer Druckfelder am Beispiel seegangsbelasteter Baukörper*, 1985, ISBN 3-921694-58-2
- 59 Kobus, Helmut (Hrsg.): *Modellierung des großräumigen Wärme- und Schadstofftransports im Grundwasser*, Tätigkeitsbericht 1984/85 (DFG-Forschergruppe an den Universitäten Hohenheim, Karlsruhe und Stuttgart), 1985, ISBN 3-921694-59-0, vergriffen
- 60 Spitz, Karlheinz: *Dispersion in porösen Medien: Einfluß von Inhomogenitäten und Dichteunterschieden*, 1985, ISBN 3-921694-60-4, vergriffen
- 61 Kobus, Helmut: *An Introduction to Air-Water Flows in Hydraulics*, 1985, ISBN 3-921694-61-2
- 62 Kaleris, Vassilios: *Erfassung des Austausches von Oberflächen- und Grundwasser in horizontalebene Grundwassermodellen*, 1986, ISBN 3-921694-62-0
- 63 Herr, Michael: *Grundlagen der hydraulischen Sanierung verunreinigter Porengrundwasserleiter*, 1987, ISBN 3-921694-63-9
- 64 Marx, Walter: *Berechnung von Temperatur und Spannung in Massenbeton infolge Hydratation*, 1987, ISBN 3-921694-64-7
- 65 Koschitzky, Hans-Peter: *Dimensionierungskonzept für Sohlbelüfter in Schußrinnen zur Vermeidung von Kavitationsschäden*, 1987, ISBN 3-921694-65-5
- 66 Kobus, Helmut (Hrsg.): *Modellierung des großräumigen Wärme- und Schadstofftransports im Grundwasser*, Tätigkeitsbericht 1986/87 (DFG-Forschergruppe an den Universitäten Hohenheim, Karlsruhe und Stuttgart) 1987, ISBN 3-921694-66-3
- 67 Söll, Thomas: *Berechnungsverfahren zur Abschätzung anthropogener Temperaturanomalien im Grundwasser*, 1988, ISBN 3-921694-67-1
- 68 Dittrich, Andreas; Westrich, Bernd: *Bodenseeufererosion, Bestandsaufnahme und Bewertung*, 1988, ISBN 3-921694-68-X, vergriffen

- 69 Huwe, Bernd; van der Ploeg, Rienk R.: *Modelle zur Simulation des Stickstoffhaushaltes von Standorten mit unterschiedlicher landwirtschaftlicher Nutzung*, 1988, ISBN 3-921694-69-8, vergriffen
- 70 Stephan, Karl: *Integration elliptischer Funktionen*, 1988, ISBN 3-921694-70-1
- 71 Kobus, Helmut; Zilliox, Lothaire (Hrsg.): *Nitratbelastung des Grundwassers, Auswirkungen der Landwirtschaft auf die Grundwasser- und Rohwasserbeschaffenheit und Maßnahmen zum Schutz des Grundwassers*. Vorträge des deutsch-französischen Kolloquiums am 6. Oktober 1988, Universitäten Stuttgart und Louis Pasteur Strasbourg (Vorträge in deutsch oder französisch, Kurzfassungen zweisprachig), 1988, ISBN 3-921694-71-X
- 72 Soyeaux, Renald: *Unterströmung von Stauanlagen auf klüftigem Untergrund unter Berücksichtigung laminarer und turbulenter Fließzustände*, 1991, ISBN 3-921694-72-8
- 73 Kohane, Roberto: *Berechnungsmethoden für Hochwasserabfluß in Fließgewässern mit überströmten Vorländern*, 1991, ISBN 3-921694-73-6
- 74 Hassinger, Reinhard: *Beitrag zur Hydraulik und Bemessung von Blocksteinrampen in flexibler Bauweise*, 1991, ISBN 3-921694-74-4, vergriffen
- 75 Schäfer, Gerhard: *Einfluß von Schichtenstrukturen und lokalen Einlagerungen auf die Längsdispersion in Porengrundwasserleitern*, 1991, ISBN 3-921694-75-2
- 76 Giesecke, Jürgen: *Vorträge, Wasserwirtschaft in stark besiedelten Regionen; Umweltforschung mit Schwerpunkt Wasserwirtschaft*, 1991, ISBN 3-921694-76-0
- 77 Huwe, Bernd: *Deterministische und stochastische Ansätze zur Modellierung des Stickstoffhaushalts landwirtschaftlich genutzter Flächen auf unterschiedlichem Skalenniveau*, 1992, ISBN 3-921694-77-9, vergriffen
- 78 Rommel, Michael: *Verwendung von Kluftdaten zur realitätsnahen Generierung von Kluftnetzen mit anschließender laminar-turbulenter Strömungsberechnung*, 1993, ISBN 3-92 1694-78-7
- 79 Marschall, Paul: *Die Ermittlung lokaler Stofffrachten im Grundwasser mit Hilfe von Einbohrloch-Meßverfahren*, 1993, ISBN 3-921694-79-5, vergriffen
- 80 Ptak, Thomas: *Stofftransport in heterogenen Porenaquiferen: Felduntersuchungen und stochastische Modellierung*, 1993, ISBN 3-921694-80-9, vergriffen
- 81 Haakh, Frieder: *Transientes Strömungsverhalten in Wirbelkammern*, 1993, ISBN 3-921694-81-7
- 82 Kobus, Helmut; Cirpka, Olaf; Barczewski, Baldur; Koschitzky, Hans-Peter: *Versuchseinrichtung zur Grundwasser- und Altlastensanierung VEGAS, Konzeption und Programmrahmen*, 1993, ISBN 3-921694-82-5
- 83 Zang, Weidong: *Optimaler Echtzeit-Betrieb eines Speichers mit aktueller Abflußregenerierung*, 1994, ISBN 3-921694-83-3, vergriffen
- 84 Franke, Hans-Jörg: *Stochastische Modellierung eines flächenhaften Stoffeintrages und Transports in Grundwasser am Beispiel der Pflanzenschutzmittelproblematik*, 1995, ISBN 3-921694-84-1
- 85 Lang, Ulrich: *Simulation regionaler Strömungs- und Transportvorgänge in Karstaquiferen mit Hilfe des Doppelkontinuum-Ansatzes: Methodenentwicklung und Parameteridentifikation*, 1995, ISBN 3-921694-85-X, vergriffen
- 86 Helmig, Rainer: *Einführung in die Numerischen Methoden der Hydromechanik*, 1996, ISBN 3-921694-86-8, vergriffen
- 87 Cirpka, Olaf: *CONTRACT: A Numerical Tool for Contaminant Transport and Chemical Transformations - Theory and Program Documentation* -, 1996, ISBN 3-921694-87-6
- 88 Haberlandt, Uwe: *Stochastische Synthese und Regionalisierung des Niederschlages für Schmutzfrachtberechnungen*, 1996, ISBN 3-921694-88-4
- 89 Croisé, Jean: *Extraktion von flüchtigen Chemikalien aus natürlichen Lockergesteinen mittels erzwungener Luftströmung*, 1996, ISBN 3-921694-89-2, vergriffen

- 90 Jorde, Klaus: *Ökologisch begründete, dynamische Mindestwasserregelungen bei Ausleitungskraftwerken*, 1997, ISBN 3-921694-90-6, vergriffen
- 91 Helmig, Rainer: *Gekoppelte Strömungs- und Transportprozesse im Untergrund - Ein Beitrag zur Hydrosystemmodellierung-*, 1998, ISBN 3-921694-91-4, vergriffen
- 92 Emmert, Martin: *Numerische Modellierung nichtisothermer Gas-Wasser Systeme in porösen Medien*, 1997, ISBN 3-921694-92-2
- 93 Kern, Ulrich: *Transport von Schweb- und Schadstoffen in staugeregelten Fließgewässern am Beispiel des Neckars*, 1997, ISBN 3-921694-93-0, vergriffen
- 94 Förster, Georg: *Druckstoßdämpfung durch große Luftblasen in Hochpunkten von Rohrleitungen* 1997, ISBN 3-921694-94-9
- 95 Cirpka, Olaf: *Numerische Methoden zur Simulation des reaktiven Mehrkomponententransports im Grundwasser*, 1997, ISBN 3-921694-95-7, vergriffen
- 96 Färber, Arne: *Wärmetransport in der ungesättigten Bodenzone: Entwicklung einer thermischen In-situ-Sanierungstechnologie*, 1997, ISBN 3-921694-96-5
- 97 Betz, Christoph: *Wasserdampfdestillation von Schadstoffen im porösen Medium: Entwicklung einer thermischen In-situ-Sanierungstechnologie*, 1998, SBN 3-921694-97-3
- 98 Xu, Yichun: *Numerical Modeling of Suspended Sediment Transport in Rivers*, 1998, ISBN 3-921694-98-1, vergriffen
- 99 Wüst, Wolfgang: *Geochemische Untersuchungen zur Sanierung CKW-kontaminierter Aquifere mit Fe(0)-Reaktionswänden*, 2000, ISBN 3-933761-02-2
- 100 Sheta, Hussam: *Simulation von Mehrphasenvorgängen in porösen Medien unter Einbeziehung von Hysterese-Effekten*, 2000, ISBN 3-933761-03-4
- 101 Ayros, Edwin: *Regionalisierung extremer Abflüsse auf der Grundlage statistischer Verfahren*, 2000, ISBN 3-933761-04-2, vergriffen
- 102 Huber, Ralf: *Compositional Multiphase Flow and Transport in Heterogeneous Porous Media*, 2000, ISBN 3-933761-05-0
- 103 Braun, Christopherus: *Ein Upscaling-Verfahren für Mehrphasenströmungen in porösen Medien*, 2000, ISBN 3-933761-06-9
- 104 Hofmann, Bernd: *Entwicklung eines rechnergestützten Managementsystems zur Beurteilung von Grundwasserschadensfällen*, 2000, ISBN 3-933761-07-7
- 105 Class, Holger: *Theorie und numerische Modellierung nichtisothermer Mehrphasenprozesse in NAPL-kontaminierten porösen Medien*, 2001, ISBN 3-933761-08-5
- 106 Schmidt, Reinhard: *Wasserdampf- und Heißluftinjektion zur thermischen Sanierung kontaminierter Standorte*, 2001, ISBN 3-933761-09-3
- 107 Josef, Reinhold: *Schadstoffextraktion mit hydraulischen Sanierungsverfahren unter Anwendung von grenzflächenaktiven Stoffen*, 2001, ISBN 3-933761-10-7
- 108 Schneider, Matthias: *Habitat- und Abflussmodellierung für Fließgewässer mit unscharfen Berechnungsansätzen*, 2001, ISBN 3-933761-11-5
- 109 Rathgeb, Andreas: *Hydrodynamische Bemessungsgrundlagen für Lockerdeckwerke an überströmbaren Erddämmen*, 2001, ISBN 3-933761-12-3
- 110 Lang, Stefan: *Parallele numerische Simulation instationärer Probleme mit adaptiven Methoden auf unstrukturierten Gittern*, 2001, ISBN 3-933761-13-1
- 111 Appt, Jochen; Stumpp Simone: *Die Bodensee-Messkampagne 2001, IWS/CWR Lake Constance Measurement Program 2001*, 2002, ISBN 3-933761-14-X
- 112 Heimerl, Stephan: *Systematische Beurteilung von Wasserkraftprojekten*, 2002, ISBN 3-933761-15-8, vergriffen
- 113 Iqbal, Amin: *On the Management and Salinity Control of Drip Irrigation*, 2002, ISBN 3-933761-16-6
- 114 Silberhorn-Hemminger, Annette: *Modellierung von Kluftaquifersystemen: Geostatistische Analyse und deterministisch-stochastische Kluftgenerierung*, 2002, ISBN 3-933761-17-4

- 115 Winkler, Angela: *Prozesse des Wärme- und Stofftransports bei der In-situ-Sanierung mit festen Wärmequellen*, 2003, ISBN 3-933761-18-2
- 116 Marx, Walter: *Wasserkraft, Bewässerung, Umwelt - Planungs- und Bewertungsschwerpunkte der Wasserbewirtschaftung*, 2003, ISBN 3-933761-19-0
- 117 Hinkelmann, Reinhard: *Efficient Numerical Methods and Information-Processing Techniques in Environment Water*, 2003, ISBN 3-933761-20-4
- 118 Samaniego-Eguiguren, Luis Eduardo: *Hydrological Consequences of Land Use / Land Cover and Climatic Changes in Mesoscale Catchments*, 2003, ISBN 3-933761-21-2
- 119 Neunhäuserer, Lina: *Diskretisierungsansätze zur Modellierung von Strömungs- und Transportprozessen in geklüftet-porösen Medien*, 2003, ISBN 3-933761-22-0
- 120 Paul, Maren: *Simulation of Two-Phase Flow in Heterogeneous Porous Media with Adaptive Methods*, 2003, ISBN 3-933761-23-9
- 121 Ehret, Uwe: *Rainfall and Flood Nowcasting in Small Catchments using Weather Radar*, 2003, ISBN 3-933761-24-7
- 122 Haag, Ingo: *Der Sauerstoffhaushalt staugeregelter Flüsse am Beispiel des Neckars - Analysen, Experimente, Simulationen -*, 2003, ISBN 3-933761-25-5
- 123 Appt, Jochen: *Analysis of Basin-Scale Internal Waves in Upper Lake Constance*, 2003, ISBN 3-933761-26-3
- 124 Hrsg.: Schrenk, Volker; Batereau, Katrin; Barczewski, Baldur; Weber, Karolin und Koschitzky, Hans-Peter: *Symposium Ressource Fläche und VEGAS - Statuskolloquium 2003, 30. September und 1. Oktober 2003*, 2003, ISBN 3-933761-27-1
- 125 Omar Khalil Ouda: *Optimisation of Agricultural Water Use: A Decision Support System for the Gaza Strip*, 2003, ISBN 3-933761-28-0
- 126 Batereau, Katrin: *Sensorbasierte Bodenluftmessung zur Vor-Ort-Erkundung von Schadensherden im Untergrund*, 2004, ISBN 3-933761-29-8
- 127 Witt, Oliver: *Erosionsstabilität von Gewässersedimenten mit Auswirkung auf den Stofftransport bei Hochwasser am Beispiel ausgewählter Stauhaltungen des Oberrheins*, 2004, ISBN 3-933761-30-1
- 128 Jakobs, Hartmut: *Simulation nicht-isothermer Gas-Wasser-Prozesse in komplexen Kluft-Matrix-Systemen*, 2004, ISBN 3-933761-31-X
- 129 Li, Chen-Chien: *Deterministisch-stochastisches Berechnungskonzept zur Beurteilung der Auswirkungen erosiver Hochwasserereignisse in Flusstauhaltungen*, 2004, ISBN 3-933761-32-8
- 130 Reichenberger, Volker; Helmig, Rainer; Jakobs, Hartmut; Bastian, Peter; Niessner, Jennifer: *Complex Gas-Water Processes in Discrete Fracture-Matrix Systems: Up-scaling, Mass-Conservative Discretization and Efficient Multilevel Solution*, 2004, ISBN 3-933761-33-6
- 131 Hrsg.: Barczewski, Baldur; Koschitzky, Hans-Peter; Weber, Karolin; Wege, Ralf: *VEGAS - Statuskolloquium 2004*, Tagungsband zur Veranstaltung am 05. Oktober 2004 an der Universität Stuttgart, Campus Stuttgart-Vaihingen, 2004, ISBN 3-933761-34-4
- 132 Asie, Kemal Jabir: *Finite Volume Models for Multiphase Multicomponent Flow through Porous Media*. 2005, ISBN 3-933761-35-2
- 133 Jacoub, George: *Development of a 2-D Numerical Module for Particulate Contaminant Transport in Flood Retention Reservoirs and Impounded Rivers*, 2004, ISBN 3-933761-36-0
- 134 Nowak, Wolfgang: *Geostatistical Methods for the Identification of Flow and Transport Parameters in the Subsurface*, 2005, ISBN 3-933761-37-9
- 135 Süß, Mia: *Analysis of the influence of structures and boundaries on flow and transport processes in fractured porous media*, 2005, ISBN 3-933761-38-7
- 136 Jose, Surabhin Chackiath: *Experimental Investigations on Longitudinal Dispersive Mixing in Heterogeneous Aquifers*, 2005, ISBN: 3-933761-39-5

- 137 Filiz, Fulya: *Linking Large-Scale Meteorological Conditions to Floods in Mesoscale Catchments*, 2005, ISBN 3-933761-40-9
- 138 Qin, Minghao: *Wirklichkeitsnahe und recheneffiziente Ermittlung von Temperatur und Spannungen bei großen RCC-Staumauern*, 2005, ISBN 3-933761-41-7
- 139 Kobayashi, Kenichiro: *Optimization Methods for Multiphase Systems in the Subsurface - Application to Methane Migration in Coal Mining Areas*, 2005, ISBN 3-933761-42-5
- 140 Rahman, Md. Arifur: *Experimental Investigations on Transverse Dispersive Mixing in Heterogeneous Porous Media*, 2005, ISBN 3-933761-43-3
- 141 Schrenk, Volker: *Ökobilanzen zur Bewertung von Altlastensanierungsmaßnahmen*, 2005, ISBN 3-933761-44-1
- 142 Hundecha, Hirpa Yeshewatesfa: *Regionalization of Parameters of a Conceptual Rainfall-Runoff Model*, 2005, ISBN: 3-933761-45-X
- 143 Wege, Ralf: *Untersuchungs- und Überwachungsmethoden für die Beurteilung natürlicher Selbstreinigungsprozesse im Grundwasser*, 2005, ISBN 3-933761-46-8
- 144 Breiting, Thomas: *Techniken und Methoden der Hydroinformatik - Modellierung von komplexen Hydrosystemen im Untergrund*, 2006, ISBN 3-933761-47-6
- 145 Hrsg.: Braun, Jürgen; Koschitzky, Hans-Peter; Müller, Martin: *Ressource Untergrund: 10 Jahre VEGAS: Forschung und Technologieentwicklung zum Schutz von Grundwasser und Boden*, Tagungsband zur Veranstaltung am 28. und 29. September 2005 an der Universität Stuttgart, Campus Stuttgart-Vaihingen, 2005, ISBN 3-933761-48-4
- 146 Rojanschi, Vlad: *Abflusskonzentration in mesoskaligen Einzugsgebieten unter Berücksichtigung des Sickerraumes*, 2006, ISBN 3-933761-49-2
- 147 Winkler, Nina Simone: *Optimierung der Steuerung von Hochwasserrückhaltebeckensystemen*, 2006, ISBN 3-933761-50-6
- 148 Wolf, Jens: *Räumlich differenzierte Modellierung der Grundwasserströmung alluvialer Aquifere für mesoskalige Einzugsgebiete*, 2006, ISBN: 3-933761-51-4
- 149 Kohler, Beate: *Externe Effekte der Laufwasserkraftnutzung*, 2006, ISBN 3-933761-52-2
- 150 Hrsg.: Braun, Jürgen; Koschitzky, Hans-Peter; Stuhmann, Matthias: *VEGAS-Statuskolloquium 2006*, Tagungsband zur Veranstaltung am 28. September 2006 an der Universität Stuttgart, Campus Stuttgart-Vaihingen, 2006, ISBN 3-933761-53-0
- 151 Niessner, Jennifer: *Multi-Scale Modeling of Multi-Phase - Multi-Component Processes in Heterogeneous Porous Media*, 2006, ISBN 3-933761-54-9
- 152 Fischer, Markus: *Beanspruchung eingeeerdeter Rohrleitungen infolge Austrocknung bindiger Böden*, 2006, ISBN 3-933761-55-7
- 153 Schneck, Alexander: *Optimierung der Grundwasserbewirtschaftung unter Berücksichtigung der Belange der Wasserversorgung, der Landwirtschaft und des Naturschutzes*, 2006, ISBN 3-933761-56-5
- 154 Das, Tapash: *The Impact of Spatial Variability of Precipitation on the Predictive Uncertainty of Hydrological Models*, 2006, ISBN 3-33761-57-3
- 155 Bielinski, Andreas: *Numerical Simulation of CO₂ sequestration in geological formations*, 2007, ISBN 3-933761-58-1
- 156 Mödinger, Jens: *Entwicklung eines Bewertungs- und Entscheidungsunterstützungssystems für eine nachhaltige regionale Grundwasserbewirtschaftung*, 2006, ISBN 3-933761-60-3
- 157 Manthey, Sabine: *Two-phase flow processes with dynamic effects in porous media - parameter estimation and simulation*, 2007, ISBN 3-933761-61-1
- 158 Pozos Estrada, Oscar: *Investigation on the Effects of Entrained Air in Pipelines*, 2007, ISBN 3-933761-62-X
- 159 Ochs, Steffen Oliver: *Steam injection into saturated porous media – process analysis including experimental and numerical investigations*, 2007, ISBN 3-933761-63-8

- 160 Marx, Andreas: *Einsatz gekoppelter Modelle und Wetterradar zur Abschätzung von Niederschlagsintensitäten und zur Abflussvorhersage*, 2007, ISBN 3-933761-64-6
- 161 Hartmann, Gabriele Maria: *Investigation of Evapotranspiration Concepts in Hydrological Modelling for Climate Change Impact Assessment*, 2007, ISBN 3-933761-65-4
- 162 Kebede Gurmessa, Tesfaye: *Numerical Investigation on Flow and Transport Characteristics to Improve Long-Term Simulation of Reservoir Sedimentation*, 2007, ISBN 3-933761-66-2
- 163 Trifković, Aleksandar: *Multi-objective and Risk-based Modelling Methodology for Planning, Design and Operation of Water Supply Systems*, 2007, ISBN 3-933761-67-0
- 164 Göttinger, Jens: *Distributed Conceptual Hydrological Modelling - Simulation of Climate, Land Use Change Impact and Uncertainty Analysis*, 2007, ISBN 3-933761-68-9
- 165 Hrsg.: Braun, Jürgen; Koschitzky, Hans-Peter; Stuhmann, Matthias: *VEGAS – Kolloquium 2007*, Tagungsband zur Veranstaltung am 26. September 2007 an der Universität Stuttgart, Campus Stuttgart-Vaihingen, 2007, ISBN 3-933761-69-7
- 166 Freeman, Beau: *Modernization Criteria Assessment for Water Resources Planning; Klamath Irrigation Project, U.S.*, 2008, ISBN 3-933761-70-0
- 167 Dreher, Thomas: *Selektive Sedimentation von Feinstschwebstoffen in Wechselwirkung mit wandnahen turbulenten Strömungsbedingungen*, 2008, ISBN 3-933761-71-9
- 168 Yang, Wei: *Discrete-Continuous Downscaling Model for Generating Daily Precipitation Time Series*, 2008, ISBN 3-933761-72-7
- 169 Kopecki, Ianina: *Calculational Approach to FST-Hemispheres for Multiparametrical Benthos Habitat Modelling*, 2008, ISBN 3-933761-73-5
- 170 Brommundt, Jürgen: *Stochastische Generierung räumlich zusammenhängender Niederschlagszeitreihen*, 2008, ISBN 3-933761-74-3
- 171 Papafotiou, Alexandros: *Numerical Investigations of the Role of Hysteresis in Heterogeneous Two-Phase Flow Systems*, 2008, ISBN 3-933761-75-1
- 172 He, Yi: *Application of a Non-Parametric Classification Scheme to Catchment Hydrology*, 2008, ISBN 978-3-933761-76-7
- 173 Wagner, Sven: *Water Balance in a Poorly Gauged Basin in West Africa Using Atmospheric Modelling and Remote Sensing Information*, 2008, ISBN 978-3-933761-77-4
- 174 Hrsg.: Braun, Jürgen; Koschitzky, Hans-Peter; Stuhmann, Matthias; Schrenk, Volker: *VEGAS-Kolloquium 2008 Ressource Fläche III*, Tagungsband zur Veranstaltung am 01. Oktober 2008 an der Universität Stuttgart, Campus Stuttgart-Vaihingen, 2008, ISBN 978-3-933761-78-1
- 175 Patil, Sachin: *Regionalization of an Event Based Nash Cascade Model for Flood Predictions in Ungauged Basins*, 2008, ISBN 978-3-933761-79-8
- 176 Assteerawatt, Anongnart: *Flow and Transport Modelling of Fractured Aquifers based on a Geostatistical Approach*, 2008, ISBN 978-3-933761-80-4
- 177 Karnahl, Joachim Alexander: *2D numerische Modellierung von multifraktionalem Schwebstoff- und Schadstofftransport in Flüssen*, 2008, ISBN 978-3-933761-81-1
- 178 Hiester, Uwe: *Technologieentwicklung zur In-situ-Sanierung der ungesättigten Bodenzone mit festen Wärmequellen*, 2009, ISBN 978-3-933761-82-8
- 179 Laux, Patrick: *Statistical Modeling of Precipitation for Agricultural Planning in the Volta Basin of West Africa*, 2009, ISBN 978-3-933761-83-5
- 180 Ehsan, Saqib: *Evaluation of Life Safety Risks Related to Severe Flooding*, 2009, ISBN 978-3-933761-84-2
- 181 Prohaska, Sandra: *Development and Application of a 1D Multi-Strip Fine Sediment Transport Model for Regulated Rivers*, 2009, ISBN 978-3-933761-85-9
- 182 Kopp, Andreas: *Evaluation of CO₂ Injection Processes in Geological Formations for Site Screening*, 2009, ISBN 978-3-933761-86-6
- 183 Ebigbo, Anozie: *Modelling of biofilm growth and its influence on CO₂ and water (two-phase) flow in porous media*, 2009, ISBN 978-3-933761-87-3

- 184 Freiboth, Sandra: *A phenomenological model for the numerical simulation of multiphase multicomponent processes considering structural alterations of porous media*, 2009, ISBN 978-3-933761-88-0
- 185 Zöllner, Frank: *Implementierung und Anwendung netzfreier Methoden im Konstruktiven Wasserbau und in der Hydromechanik*, 2009, ISBN 978-3-933761-89-7
- 186 Vasin, Milos: *Influence of the soil structure and property contrast on flow and transport in the unsaturated zone*, 2010, ISBN 978-3-933761-90-3
- 187 Li, Jing: *Application of Copulas as a New Geostatistical Tool*, 2010, ISBN 978-3-933761-91-0
- 188 AghaKouchak, Amir: *Simulation of Remotely Sensed Rainfall Fields Using Copulas*, 2010, ISBN 978-3-933761-92-7
- 189 Thapa, Pawan Kumar: *Physically-based spatially distributed rainfall runoff modelling for soil erosion estimation*, 2010, ISBN 978-3-933761-93-4
- 190 Wurms, Sven: *Numerische Modellierung der Sedimentationsprozesse in Retentionsanlagen zur Steuerung von Stoffströmen bei extremen Hochwasserabflussereignissen*, 2011, ISBN 978-3-933761-94-1
- 191 Merkel, Uwe: *Unsicherheitsanalyse hydraulischer Einwirkungen auf Hochwasserschutzdeiche und Steigerung der Leistungsfähigkeit durch adaptive Strömungsmodellierung*, 2011, ISBN 978-3-933761-95-8
- 192 Fritz, Jochen: *A Decoupled Model for Compositional Non-Isothermal Multiphase Flow in Porous Media and Multiphysics Approaches for Two-Phase Flow*, 2010, ISBN 978-3-933761-96-5
- 193 Weber, Karolin (Hrsg.): *12. Treffen junger WissenschaftlerInnen an Wasserbauinstituten*, 2010, ISBN 978-3-933761-97-2
- 194 Bliedernicht, Jan-Geert: *Probability Forecasts of Daily Areal Precipitation for Small River Basins*, 2011, ISBN 978-3-933761-98-9
- 195 Hrsg.: Koschitzky, Hans-Peter; Braun, Jürgen: *VEGAS-Kolloquium 2010 In-situ-Sanie- rung - Stand und Entwicklung Nano und ISCO -*, Tagungsband zur Veranstaltung am 07. Oktober 2010 an der Universität Stuttgart, Campus Stuttgart-Vaihingen, 2010, ISBN 978-3-933761-99-6
- 196 Gafurov, Abror: *Water Balance Modeling Using Remote Sensing Information - Focus on Central Asia*, 2010, ISBN 978-3-942036-00-9
- 197 Mackenberg, Sylvia: *Die Quellstärke in der Sickerwasserprognose: Möglichkeiten und Grenzen von Labor- und Freilanduntersuchungen*, 2010, ISBN 978-3-942036-01-6
- 198 Singh, Shailesh Kumar: *Robust Parameter Estimation in Gauged and Ungauged Basins*, 2010, ISBN 978-3-942036-02-3
- 199 Doğan, Mehmet Onur: *Coupling of porous media flow with pipe flow*, 2011, ISBN 978-3-942036-03-0
- 200 Liu, Min: *Study of Topographic Effects on Hydrological Patterns and the Implication on Hydrological Modeling and Data Interpolation*, 2011, ISBN 978-3-942036-04-7
- 201 Geleta, Habtamu Itefa: *Watershed Sediment Yield Modeling for Data Scarce Areas*, 2011, ISBN 978-3-942036-05-4
- 202 Franke, Jörg: *Einfluss der Überwachung auf die Versagenswahrscheinlichkeit von Stau- stufen*, 2011, ISBN 978-3-942036-06-1
- 203 Bakimchandra, Oinam: *Integrated Fuzzy-GIS approach for assessing regional soil ero- sion risks*, 2011, ISBN 978-3-942036-07-8
- 204 Alam, Muhammad Mahboob: *Statistical Downscaling of Extremes of Precipitation in Mesoscale Catchments from Different RCMs and Their Effects on Local Hydrology*, 2011, ISBN 978-3-942036-08-5

- 205 Hrsg.: Koschitzky, Hans-Peter; Braun, Jürgen: *VEGAS-Kolloquium 2011 Flache Geothermie - Perspektiven und Risiken*, Tagungsband zur Veranstaltung am 06. Oktober 2011 an der Universität Stuttgart, Campus Stuttgart-Vaihingen, 2011, ISBN 978-3-933761-09-2
- 206 Haslauer, Claus: *Analysis of Real-World Spatial Dependence of Subsurface Hydraulic Properties Using Copulas with a Focus on Solute Transport Behaviour*, 2011, ISBN 978-3-942036-10-8
- 207 Dung, Nguyen Viet: *Multi-objective automatic calibration of hydrodynamic models – development of the concept and an application in the Mekong Delta*, 2011, ISBN 978-3-942036-11-5
- 208 Hung, Nguyen Nghia: *Sediment dynamics in the floodplain of the Mekong Delta, Vietnam*, 2011, ISBN 978-3-942036-12-2
- 209 Kuhlmann, Anna: *Influence of soil structure and root water uptake on flow in the unsaturated zone*, 2012, ISBN 978-3-942036-13-9
- 210 Tuhtan, Jeffrey Andrew: *Including the Second Law Inequality in Aquatic Ecodynamics: A Modeling Approach for Alpine Rivers Impacted by Hydropeaking*, 2012, ISBN 978-3-942036-14-6
- 211 Tolossa, Habtamu: *Sediment Transport Computation Using a Data-Driven Adaptive Neuro-Fuzzy Modelling Approach*, 2012, ISBN 978-3-942036-15-3
- 212 Tatomir, Alexandru-Bodgan: *From Discrete to Continuum Concepts of Flow in Fractured Porous Media*, 2012, ISBN 978-3-942036-16-0
- 213 Erbertseder, Karin: *A Multi-Scale Model for Describing Cancer-Therapeutic Transport in the Human Lung*, 2012, ISBN 978-3-942036-17-7
- 214 Noack, Markus: *Modelling Approach for Interstitial Sediment Dynamics and Reproduction of Gravel Spawning Fish*, 2012, ISBN 978-3-942036-18-4
- 215 De Boer, Cjstmir Volkert: *Transport of Nano Sized Zero Valent Iron Colloids during Injection into the Subsurface*, 2012, ISBN 978-3-942036-19-1
- 216 Pfaff, Thomas: *Processing and Analysis of Weather Radar Data for Use in Hydrology*, 2013, ISBN 978-3-942036-20-7
- 217 Lebreuz, Hans-Henning: *Addressing the Input Uncertainty for Hydrological Modeling by a New Geostatistical Method*, 2013, ISBN 978-3-942036-21-4
- 218 Darcis, Melanie Yvonne: *Coupling Models of Different Complexity for the Simulation of CO₂ Storage in Deep Saline Aquifers*, 2013, ISBN 978-3-942036-22-1
- 219 Beck, Ferdinand: *Generation of Spatially Correlated Synthetic Rainfall Time Series in High Temporal Resolution - A Data Driven Approach*, 2013, ISBN 978-3-942036-23-8
- 220 Guthke, Philipp: *Non-multi-Gaussian spatial structures: Process-driven natural genesis, manifestation, modeling approaches, and influences on dependent processes*, 2013, ISBN 978-3-942036-24-5
- 221 Walter, Lena: *Uncertainty studies and risk assessment for CO₂ storage in geological formations*, 2013, ISBN 978-3-942036-25-2
- 222 Wolff, Markus: *Multi-scale modeling of two-phase flow in porous media including capillary pressure effects*, 2013, ISBN 978-3-942036-26-9
- 223 Mosthaf, Klaus Roland: *Modeling and analysis of coupled porous-medium and free flow with application to evaporation processes*, 2014, ISBN 978-3-942036-27-6
- 224 Leube, Philipp Christoph: *Methods for Physically-Based Model Reduction in Time: Analysis, Comparison of Methods and Application*, 2013, ISBN 978-3-942036-28-3
- 225 Rodríguez Fernández, Jhan Ignacio: *High Order Interactions among environmental variables: Diagnostics and initial steps towards modeling*, 2013, ISBN 978-3-942036-29-0
- 226 Eder, Maria Magdalena: *Climate Sensitivity of a Large Lake*, 2013, ISBN 978-3-942036-30-6

- 227 Greiner, Philipp: *Alkoholinjektion zur In-situ-Sanierung von CKW Schadensherden in Grundwasserleitern: Charakterisierung der relevanten Prozesse auf unterschiedlichen Skalen*, 2014, ISBN 978-3-942036-31-3
- 228 Lauser, Andreas: *Theory and Numerical Applications of Compositional Multi-Phase Flow in Porous Media*, 2014, ISBN 978-3-942036-32-0
- 229 Enzenhöfer, Rainer: *Risk Quantification and Management in Water Production and Supply Systems*, 2014, ISBN 978-3-942036-33-7
- 230 Faigle, Benjamin: *Adaptive modelling of compositional multi-phase flow with capillary pressure*, 2014, ISBN 978-3-942036-34-4
- 231 Oladyshkin, Sergey: *Efficient modeling of environmental systems in the face of complexity and uncertainty*, 2014, ISBN 978-3-942036-35-1
- 232 Sugimoto, Takayuki: *Copula based Stochastic Analysis of Discharge Time Series*, 2014, ISBN 978-3-942036-36-8
- 233 Koch, Jonas: *Simulation, Identification and Characterization of Contaminant Source Architectures in the Subsurface*, 2014, ISBN 978-3-942036-37-5
- 234 Zhang, Jin: *Investigations on Urban River Regulation and Ecological Rehabilitation Measures, Case of Shenzhen in China*, 2014, ISBN 978-3-942036-38-2
- 235 Siebel, Rüdiger: *Experimentelle Untersuchungen zur hydrodynamischen Belastung und Standsicherheit von Deckwerken an überströmbaren Erddämmen*, 2014, ISBN 978-3-942036-39-9
- 236 Baber, Katherina: *Coupling free flow and flow in porous media in biological and technical applications: From a simple to a complex interface description*, 2014, ISBN 978-3-942036-40-5
- 237 Nuske, Klaus Philipp: *Beyond Local Equilibrium — Relaxing local equilibrium assumptions in multiphase flow in porous media*, 2014, ISBN 978-3-942036-41-2
- 238 Geiges, Andreas: *Efficient concepts for optimal experimental design in nonlinear environmental systems*, 2014, ISBN 978-3-942036-42-9
- 239 Schwenck, Nicolas: *An XFEM-Based Model for Fluid Flow in Fractured Porous Media*, 2014, ISBN 978-3-942036-43-6
- 240 Chamorro Chávez, Alejandro: *Stochastic and hydrological modelling for climate change prediction in the Lima region, Peru*, 2015, ISBN 978-3-942036-44-3
- 241 Yulizar: *Investigation of Changes in Hydro-Meteorological Time Series Using a Depth-Based Approach*, 2015, ISBN 978-3-942036-45-0
- 242 Kretschmer, Nicole: *Impacts of the existing water allocation scheme on the Limarí watershed – Chile, an integrative approach*, 2015, ISBN 978-3-942036-46-7
- 243 Kramer, Matthias: *Luftbedarf von Freistrahlturbinen im Gegendruckbetrieb*, 2015, ISBN 978-3-942036-47-4
- 244 Hommel, Johannes: *Modeling biogeochemical and mass transport processes in the subsurface: Investigation of microbially induced calcite precipitation*, 2016, ISBN 978-3-942036-48-1
- 245 Germer, Kai: *Wasserinfiltration in die ungesättigte Zone eines makroporösen Hanges und deren Einfluss auf die Hangstabilität*, 2016, ISBN 978-3-942036-49-8
- 246 Hörning, Sebastian: *Process-oriented modeling of spatial random fields using copulas*, 2016, ISBN 978-3-942036-50-4
- 247 Jambhekar, Vishal: *Numerical modeling and analysis of evaporative salinization in a coupled free-flow porous-media system*, 2016, ISBN 978-3-942036-51-1
- 248 Huang, Yingchun: *Study on the spatial and temporal transferability of conceptual hydrological models*, 2016, ISBN 978-3-942036-52-8
- 249 Kleinknecht, Simon Matthias: *Migration and retention of a heavy NAPL vapor and remediation of the unsaturated zone*, 2016, ISBN 978-3-942036-53-5

- 250 Kwakye, Stephen Oppong: *Study on the effects of climate change on the hydrology of the West African sub-region*, 2016, ISBN 978-3-942036-54-2
- 251 Kissinger, Alexander: *Basin-Scale Site Screening and Investigation of Possible Impacts of CO₂ Storage on Subsurface Hydrosystems*, 2016, ISBN 978-3-942036-55-9
- 252 Müller, Thomas: *Generation of a Realistic Temporal Structure of Synthetic Precipitation Time Series for Sewer Applications*, 2017, ISBN 978-3-942036-56-6
- 253 Grüninger, Christoph: *Numerical Coupling of Navier-Stokes and Darcy Flow for Soil-Water Evaporation*, 2017, ISBN 978-3-942036-57-3
- 254 Suroso: *Asymmetric Dependence Based Spatial Copula Models: Empirical Investigations and Consequences on Precipitation Fields*, 2017, ISBN 978-3-942036-58-0
- 255 Müller, Thomas; Mosthaf, Tobias; Gunzenhauser, Sarah; Seidel, Jochen; Bárdossy, András: *Grundlagenbericht Niederschlags-Simulator (NiedSim3)*, 2017, ISBN 978-3-942036-59-7
- 256 Mosthaf, Tobias: *New Concepts for Regionalizing Temporal Distributions of Precipitation and for its Application in Spatial Rainfall Simulation*, 2017, ISBN 978-3-942036-60-3
- 257 Fenrich, Eva Katrin: *Entwicklung eines ökologisch-ökonomischen Vernetzungsmodells für Wasserkraftanlagen und Mehrzweckspeicher*, 2018, ISBN 978-3-942036-61-0
- 258 Schmidt, Holger: *Microbial stabilization of lotic fine sediments*, 2018, ISBN 978-3-942036-62-7
- 259 Fetzer, Thomas: *Coupled Free and Porous-Medium Flow Processes Affected by Turbulence and Roughness – Models, Concepts and Analysis*, 2018, ISBN 978-3-942036-63-4
- 260 Schröder, Hans Christoph: *Large-scale High Head Pico Hydropower Potential Assessment*, 2018, ISBN 978-3-942036-64-1
- 261 Bode, Felix: *Early-Warning Monitoring Systems for Improved Drinking Water Resource Protection*, 2018, ISBN 978-3-942036-65-8
- 262 Gebler, Tobias: *Statistische Auswertung von simulierten Talsperrenüberwachungsdaten zur Identifikation von Schadensprozessen an Gewichtsstaumauern*, 2018, ISBN 978-3-942036-66-5
- 263 Harten, Matthias von: *Analyse des Zuppinger-Wasserrades – Hydraulische Optimierungen unter Berücksichtigung ökologischer Aspekte*, 2018, ISBN 978-3-942036-67-2
- 264 Yan, Jieru: *Nonlinear estimation of short time precipitation using weather radar and surface observations*, 2018, ISBN 978-3-942036-68-9
- 265 Beck, Martin: *Conceptual approaches for the analysis of coupled hydraulic and geomechanical processes*, 2019, ISBN 978-3-942036-69-6
- 266 Haas, Jannik: *Optimal planning of hydropower and energy storage technologies for fully renewable power systems*, 2019, ISBN 978-3-942036-70-2
- 267 Schneider, Martin: *Nonlinear Finite Volume Schemes for Complex Flow Processes and Challenging Grids*, 2019, ISBN 978-3-942036-71-9
- 268 Most, Sebastian Christopher: *Analysis and Simulation of Anomalous Transport in Porous Media*, 2019, ISBN 978-3-942036-72-6
- 269 Buchta, Rocco: *Entwicklung eines Ziel- und Bewertungssystems zur Schaffung nachhaltiger naturnaher Strukturen in großen sandgeprägten Flüssen des norddeutschen Tieflandes*, 2019, ISBN 978-3-942036-73-3
- 270 Thom, Moritz: *Towards a Better Understanding of the Biostabilization Mechanisms of Sediment Beds*, 2019, ISBN 978-3-942036-74-0
- 271 Stolz, Daniel: *Die Nullspannungstemperatur in Gewichtsstaumauern unter Berücksichtigung der Festigkeitsentwicklung des Betons*, 2019, ISBN 978-3-942036-75-7
- 272 Rodriguez Pretelin, Abelardo: *Integrating transient flow conditions into groundwater well protection*, 2020, ISBN: 978-3-942036-76-4

- 273 Weishaupt, Kilian: *Model Concepts for Coupling Free Flow with Porous Medium Flow at the Pore-Network Scale: From Single-Phase Flow to Compositional Non-Isothermal Two-Phase Flow*, 2020, ISBN: 978-3-942036-77-1
- 274 Koch, Timo: *Mixed-dimension models for flow and transport processes in porous media with embedded tubular network systems*, 2020, ISBN: 978-3-942036-78-8
- 275 Gläser, Dennis: *Discrete fracture modeling of multi-phase flow and deformation in fractured poroelastic media*, 2020, ISBN: 978-3-942036-79-5
- 276 Seitz, Lydia: *Development of new methods to apply a multi-parameter approach – A first step towards the determination of colmation*, 2020, ISBN: 978-3-942036-80-1
- 277 Ebrahim Bakhshipour, Amin: *Optimizing hybrid decentralized systems for sustainable ur-ban drainage infrastructures planning*, 2021, ISBN: 978-3-942036-81-8
- 278 Seitz, Gabriele: *Modeling Fixed-Bed Reactors for Thermochemical Heat Storage with the Reaction System $\text{CaO}/\text{Ca}(\text{OH})_2$* , 2021, ISBN: 978-3-942036-82-5
- 279 Emmert, Simon: *Developing and Calibrating a Numerical Model for Microbially Enhanced Coal-Bed Methane Production*, 2021, ISBN: 978-3-942036-83-2
- 280 Heck, Katharina Klara: *Modelling and analysis of multicomponent transport at the interface between free- and porous-medium flow - influenced by radiation and roughness*, 2021, ISBN: 978-3-942036-84-9
- 281 Ackermann, Sina: *A multi-scale approach for drop/porous-medium interaction*, 2021, ISBN: 978-3-942036-85-6
- 282 Beckers, Felix: *Investigations on Functional Relationships between Cohesive Sediment Erosion and Sediment Characteristics*, 2021, ISBN: 978-3-942036-86-3
- 283 Schlabing, Dirk: *Generating Weather for Climate Impact Assessment on Lakes*, 2021, ISBN: 978-3-942036-87-0
- 284 Becker, Beatrix: *Efficient multiscale multiphysics models accounting for reversible flow at various subsurface energy storage sites*, 2021, ISBN: 978-3-942036-88-7
- 285 Reuschen, Sebastian: *Bayesian Inversion and Model Selection of Heterogeneities in Geo-statistical Subsurface Modeling*, 2021, ISBN: 978-3-942036-89-4
- 286 Michalkowski, Cynthia: *Modeling water transport at the interface between porous GDL and gas distributor of a PEM fuel cell cathode*, 2022, ISBN: 978-3-942036-90-0
- 287 Koca, Kaan: *Advanced experimental methods for investigating flow-biofilm-sediment interactions*, 2022, ISBN: 978-3-942036-91-7
- 288 Modiri, Ehsan: *Clustering simultaneous occurrences of extreme floods in the Neckar catchment*, 2022, ISBN: 978-3-942036-92-4
- 289 Mayar, Mohammad Assem: *High-resolution spatio-temporal measurements of the colmation phenomenon under laboratory conditions*, 2022, ISBN: 978-3-942036-93-1
- 290 Schäfer Rodrigues Silva, Aline: *Quantifying and Visualizing Model Similarities for Multi-Model Methods*, 2022, ISBN: 978-3-942036-94-8
- 291 Moreno Leiva, Simón: *Optimal planning of water and renewable energy systems for copper production processes with sector coupling and demand flexibility*, 2022, ISBN 978-3-942036-95-5
- 292 Schönau, Steffen: *Modellierung von Bodenerosion und Sedimentausttrag bei Hochwasserereignissen am Beispiel des Einzugsgebiets der Rems*, 2022, ISBN 978-3-942036-96-2
- 293 Glatz, Kumiko: *Upscaling of Nanoparticle Transport in Porous Media*, 2022, ISBN 978-3-942036-97-9
- 294 Pavia Santolamazza, Daniela: *Event-based flood estimation using a random forest algorithm for the regionalization in small catchments*, 2022, ISBN 978-3-942036-98-6
- 295 Haun, Stefan: *Advanced Methods for a Sustainable Sediment Management of Reservoirs*, 2022, ISBN 978-3-942036-99-3

Die Mitteilungshefte ab der Nr. 134 (Jg. 2005) stehen als pdf-Datei über die Homepage des Instituts: www.iws.uni-stuttgart.de zur Verfügung.

ISSN 0343-1150